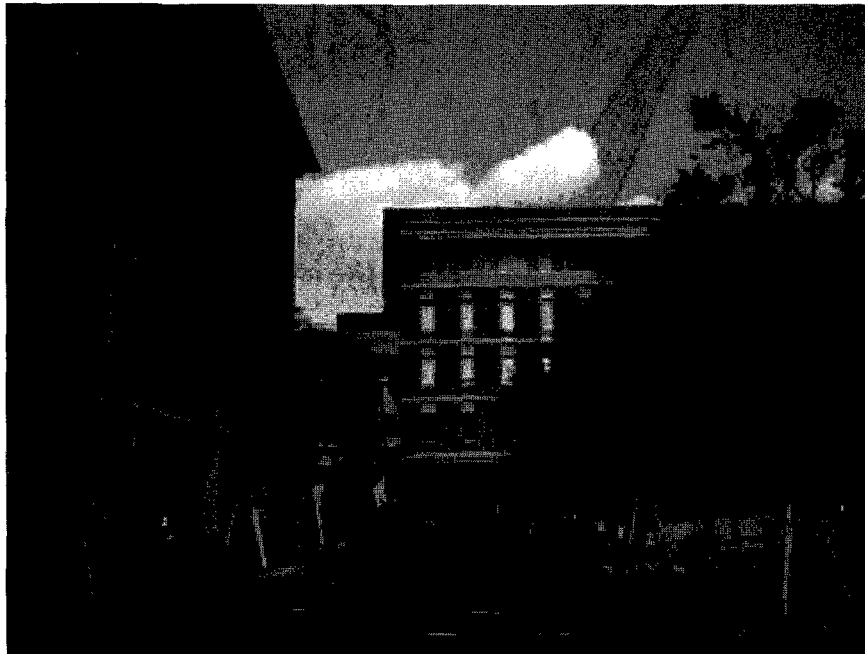


Abstract
The 38th Fullerene-Nanotubes General Symposium

第38回フラーレン・ナノチューブ
総合シンポジウム

講演要旨集

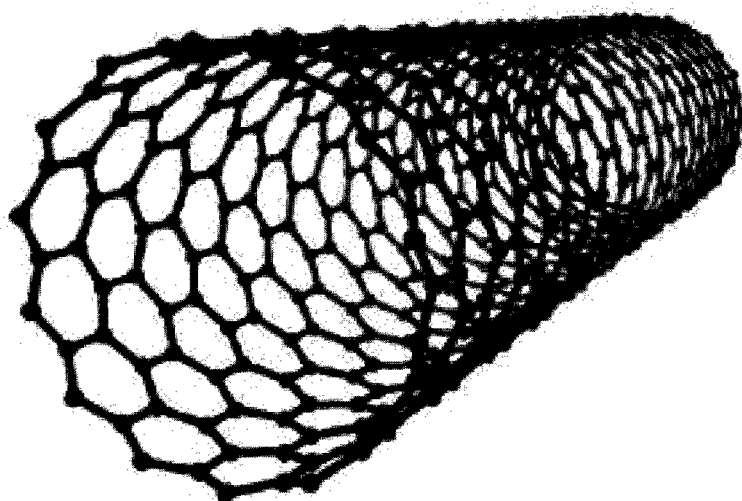


March 2-4, 2010, Nagoya, Aichi
平成22年3月2日～4日 名城大学

The Fullerenes and Nanotubes Research Society
フラーレン・ナノチューブ学会

Single-Walled Nanotubes by CoMoCAT[®] process

www.sigma-aldrich.com/nano-jp



SWeNT[®] CG 100

704113-250MG ¥23,900 704113-1G ¥66,300

SWeNT[®] SG 65

704148-250MG ¥33,000 704148-1G ¥100,000

SWeNT[®] SG 76

704121-250MG ¥33,000 704121-1G ¥100,000

SWeNT and CoMoCAT is a registered trademark of SouthWest NanoTechnologies, Inc.

SIGMA-ALDRICH[®]

シグマ アルドリッチ ジャパン株式会社

〒140-0002 東京都品川区東品川2-2-24
天王洲セントラルタワー4階

■製品に関するお問い合わせは、弊社テクニカルサポートへ
TEL : 03-5796-7330 FAX : 03-5796-7335
E-mail : sialjpts@sial.com

■在庫照会・ご注文方法に関するお問い合わせは、弊社カスタマーサービスへ
TEL : 03-5796-7320 FAX : 03-5796-7325
E-mail : sialjpcs@sial.com

<http://www.sigma-aldrich.com/japan>

Abstract
The 38th Fullerene-Nanotubes General Symposium

第 38 回 フラーレン・ナノチューブ
総合シンポジウム

講演要旨集

The Fullerenes and Nanotubes Research Society

The Chemical Society of Japan

The Japan Society of Applied Physics

The Physical Society of Japan

The Electrochemical Society of Japan

The Society of Polymer Science, Japan

主催：フラーレン・ナノチューブ学会

共催：日本化学会

協賛：日本物理学会・応用物理学会・電気化学会・高分子学会

Date: March 2nd(Tue)–4th(Thu), 2010

Place: Meijo University

1-501 Shiogamaguchi, Tempaku-ku, Nagoya 468-8502

TEL: 052-832-1151

Presentation: Special Lecture (25 min presentation, 5min discussion)

General Lecture (10 min presentation, 5min discussion)

Poster Preview (1 min presentation, no discussion)

日時：平成 22 年 3 月 2 日(火)～4 日(木)

場所：名城大学

〒468-8502 愛知県名古屋市天白区塩釜口 1-501

TEL：052-832-1151

発表時間：特別講演 (発表 25 分・質疑応答 5 分)

一般講演 (発表 10 分・質疑応答 5 分)

ポスタープレビュー (発表 1 分・質疑応答 なし)

展示団体御芳名(アイウエオ順、敬称略)

IOP英国物理学会出版局
アイクストロン(株)
(株)イデアルスター
コスモ・バイオ(株)
シグマアルドリッチジャパン(株)
(株)島津製作所
(株)シンキー
(株)セントラル科学貿易
(株)ダルトン
ナカライテスク(株)
日本カンタム・デザイン(株)
日本電計(株)
日本電子(株)
日本分析工業(株)
日本ベル(株)
(株)堀場製作所
(株)名城ナノカーボン
レニショー(株)

広告掲載団体御芳名(アイウエオ順、敬称略)

アイクストロン(株)
(株)ATR
エクセルソフト(株)
(株)岡村製作所
(株)カーク
コスモ・バイオ(株)
(株)三洋商事
シグマアルドリッチジャパン(株)
(株)島津製作所
スペクトラ・フィジックス(株)
(株)セントラル科学貿易
東洋炭素(株)
ナカライテスク(株)
日本カンタム・デザイン(株)
日本電子(株)
日本分光(株)
日本分析工業(株)
(有)菱田商店
日立工機(株)
ブルカー・ダルトニクス(株)
フロンティアカーボン(株)
(株)マシナックス
理科研(株)
レニショー(株)
(株)UBE科学分析センター
(株)ユニソク

Contents

Time Table	i
Chairperson	iii
Program	Japanese	iv
	English	xvi
Abstracts	Special lecture	1
	General lecture	7
	Poster preview	49
Author Index	173

目次

早見表	i
座長一覧	iii
プログラム	和文	iv
	英文	xvi
講演予稿	特別講演	1
	一般講演	7
	ポスター発表	49
発表索引	173

プログラム早見表

各項目敬称略

	3月2日(火)	3月3日(水)	3月4日(木)	
9:00	特別講演1(大澤 映二) 9:00~9:30	特別講演3(村田 靖次郎) 9:00~9:30	特別講演5(秋庭 英治) 9:00~9:30	9:00
9:30	一般講演4件 (ナノチューブの物性) 9:30~10:30	一般講演4件 (フラーレンの機能と応用) 9:30~10:30	一般講演4件 (ナノチューブの生成と精製) 9:30~10:30	9:30
10:30	休憩 10:30~10:45			10:30
10:45	一般講演4件 (ナノチューブの物性) 10:45~11:45	一般講演4件 (フラーレンの機能と応用) 10:45~11:45	一般講演2件 (ナノチューブの生成と精製) 10:45~11:30	10:45
11:45	昼食 11:45~13:00		一般講演5件 (グラフェン) 11:30~12:30	11:15
13:00	一般講演5件 (ナノチューブの応用) 13:00~14:15	授賞式 13:00~13:45	昼食 12:30~13:45	12:30
14:15	休憩 14:15~14:30	特別講演4(Haeseong Lee) 13:45~14:15	特別講演6(日浦 英文) 13:45~14:15	13:45
14:30	特別講演2(増野 匡彦) 14:30~15:00	一般講演4件 (ハイブリットカーボン) 14:15~15:15	ポスタープレビュー 1分×41件 14:15~15:00	14:15
15:45	一般講演3件 (ナノチューブの応用) 15:00~15:45	休憩 15:15~15:30	ポスターセッション 15:00~16:20	15:00
15:45	ポスタープレビュー 1分×41件 15:45~16:30	一般講演3件 (ハイブリットカーボン) 15:30~16:15		16:20
16:30	ポスターセッション 16:30~17:50	ポスタープレビュー 1分×42件 16:15~17:00		
17:50		ポスターセッション 17:00~18:20		

3月2日(火)
チュートリアル 103講義室
15:00~16:30
講師 齋藤 理一郎先生
東北大学大学院理学研究科
教授

18:30~懇親会

特別講演 発表25分 質疑5分
一般講演 発表10分 質疑5分
ポスタープレビュー

発表1分 質疑なし

TIME TABLE

	Tue. Mar. 2	Wed. Mar. 3	Thu. Mar. 4	
9:00	Special Lecture (E. Osawa) 9:00~9:30	Special Lecture (Y. Murata) 9:00~9:30	Special Lecture (E. Akiba) 9:00~9:30	9:00
9:30	General Lecture[4] (Properties of Nanotubes) 9:30~10:30	General Lecture[4] (Function and Applications of Fullerenes) 9:30~10:30	General Lecture[4] (Formation and Purification of Nanotubes) 9:30~10:30	9:30
10:30	Break 10:30~10:45			10:30
10:45	General Lecture[4] (Properties of Nanotubes) 10:45~11:45	General Lecture[4] (Function and Applications of Fullerenes) 10:45~11:45	General Lecture[2] (Formation and Purification of Nanotubes) 10:45~11:15	10:45
11:45	Lunch 11:45~13:00		General Lecture[5] (Graphene) 11:15~12:30	11:15
13:00	General Lecture[5] (Applications of Nanotubes) 13:00~14:15	Awards Ceremony 13:00~13:45	Lunch 12:30~13:45	12:30
14:15	Break 14:15~14:30	Special Lecture (H. Lee) 13:45~14:15	Special Lecture (H. Hiura) 13:45~14:15	13:45
14:30	Special Lecture (T. Masuno) 14:30~15:00	General Lecture[4] (Hybrid Carbon) 14:15~15:15	Poster Preview 1min × [41] 14:15~15:00	14:15
15:45	General Lecture[3] (Applications of Nanotubes) 15:00~15:45	Break 15:15~15:30	Poster Session 15:00~16:20	15:00
15:45	Poster Preview 1min × [41] 15:45~16:30	General Lecture[3] (Hybrid Carbon) 15:30~16:15		16:20
16:30	Poster Session 16:30~17:50	Poster Preview 1min × [42] 16:15~17:00		16:20
17:50		Poster Session 17:00~18:20		

18:30~ Banquet

Tue. Mar. 2
Tutorial Room103
15:00~16:30
Prof. Riichiro Saito

Special Lectures: 25min Presentation, 5min Discussion
 General Lectures: 10min Presentation, 5min Discussion
 Poster Previews: 1min Presentation, No Discussion

座長一覧

3月2日(火)

(敬称略)

	時 間	座 長
特 別 講 演(大澤)	9:00 ~ 9:30	篠原 久典
一 般 講 演	9:30 ~ 10:30	斎藤 毅
一 般 講 演	10:45 ~ 11:45	松田 一成
一 般 講 演	13:00 ~ 14:15	大野 雄高
特 別 講 演(増野)	14:30 ~ 15:00	村田 靖次郎
一 般 講 演	15:00 ~ 15:45	佐野 正人
ポスターレビュー	15:45 ~ 16:25	田中 丈士
ポスターセッション	16:25 ~ 17:45	宮田 耕充

3月3日(水)

	時 間	座 長
特 別 講 演(村田)	9:00 ~ 9:30	阿知波 洋次
一 般 講 演	9:30 ~ 10:30	兒玉 健
一 般 講 演	10:45 ~ 11:45	岡崎 俊也
特 別 講 演(Lee)	13:45 ~ 14:15	大澤 映二
一 般 講 演	14:15 ~ 15:15	菅井 俊樹
一 般 講 演	15:30 ~ 16:15	小澤 理樹
ポスターレビュー	16:15 ~ 16:55	前田 優
ポスターセッション	16:55 ~ 18:15	藤ヶ谷 剛彦

3月4日(木)

	時 間	座 長
特 別 講 演(秋庭)	9:00 ~ 9:30	中山 喜萬
一 般 講 演	9:30 ~ 10:30	湯田坂 雅子
一 般 講 演	10:45 ~ 11:15	北浦 良
一 般 講 演	11:15 ~ 12:30	齋藤 理一郎
特 別 講 演(日浦)	13:45 ~ 14:15	宮本 良之
ポスターレビュー	14:15 ~ 14:55	小塩 明
ポスターセッション	14:55 ~ 16:15	岸 直希

3月2日(火)

特別講演 発表25分・質疑応答5分
一般講演 発表10分・質疑応答5分
ポスタープレビュー 発表1分・質疑応答なし

特別講演 (9:00-9:30)

- 1S-1 ナノダイヤモンド研究開発はどこまで進んだか? 1
○大澤映二

一般講演 (9:30-10:30)

ナノチューブの物性

- 1-1 ホールドープされた単層カーボンナノチューブにおける励起子ダイナミクス 7
○松田一成、宮内雄平、坂下健郎、金光義彦
- 1-2 PFOでラップされた単層カーボンナノチューブペーパーの発光ダイナミクス 8
○小山剛史、宮田耕充、浅田有紀、篠原久典、片浦弘道、中村新男
- 1-3 コヒーレントフォノンによるカーボンナノチューブの環境効果の観測 9
○加藤景子、高木大輔、小林慶裕、日比野浩樹、石澤淳、小栗克弥、後藤秀樹、中野秀俊
- 1-4 高バイアス印加によるカーボンナノチューブからの短波長エレクトロルミネッセンス 10
○牧英之、鈴木哲、日比野訓士、小林慶裕、佐藤徹哉

☆☆☆☆☆☆ 休憩 (10:30-10:45) ☆☆☆☆☆☆

一般講演 (10:45-11:45)

ナノチューブの物性

- 1-5 パルス磁場勾配核磁気共鳴法によるCNT分散液中の束縛Tween80分子の観察 11
○加藤晴久、中村文子、水野耕平、島田学、高橋かより、衣笠晋一
- 1-6 金属ナノダイマーギャップにおける単一単層カーボンナノチューブの表面増強ラマン散乱計測 12
○保田諭、高瀬舞、米田啓一郎、奈良正伸、並河英紀、村越敬
- 1-7 アルミニウムクラスター吸着による単層カーボンナノチューブのE11、E22バンドギャップ変調 13
○高木祥光、岡田晋
- 1-8 光吸収分光法を用いた単層カーボンナノチューブの精密評価におけるバックグラウンド補正の重要性 14
○斎藤毅、大森滋和、丹下将克、ピカウシユクラ、岡崎俊也、湯村守雄、飯島澄男

☆☆☆☆☆☆ 昼食 (11:45-13:00) ☆☆☆☆☆☆

一般講演 (13:00-14:15)

ナノチューブの応用

- 1-9 パターン化自己組織化単分子膜によるカーボンナノチューブの位置選択的吸着と薄膜トランジスタへの応用 15
○藤井俊治郎、田中丈士、三成剛生、塚越一仁、片浦弘道
- 1-10 プラズマCVD成長単層カーボンナノチューブを用いた高性能薄膜トランジスタの創製と動作機構の解明 16
○黒田峻介、加藤俊顕、金子俊郎、畠山力三
- 1-11 カーボンナノチューブのドナーアクセプタヘテロ接合有機太陽電池への導入効果 17
○カリタゴラップ、脇田紘一、梅野正義
- 1-12 ボトムアップアプローチによるカーボンナノチューブ燃料電池触媒の構築と性能 18
○藤ヶ谷剛彦、松本和也、中嶋直敏
- 1-13 多層カーボンナノチューブの電界放出特性の劣化モード 19
○市橋鋭也、中村文滋、弓削亮太、小坂真由美、當山清彦

3月2日(火)

☆☆☆☆☆☆ 休憩 (14:15-14:30) ☆☆☆☆☆☆

特別講演 (14:30-15:00)

- 1S-2 フラーレン類の生体応用 2
○増野匡彦、中村茂夫

一般講演 (15:00-15:45)

ナノチューブの応用

- 1-14 HRTEM observation of a crystalline-cluster phase inside ionic liquids freestanding on CNT super-thin films 20
○Shimou Chen, Keita Kobayashi, Ryo Kitaura, Yasumitsu Miyata, Kazu Suenaga, Hisanori Shinohara
- 1-15 カーボンナノチューブでコーティングされたシリカゲルの作製とクロマトグラフィーへの応用 21
○ユジョンテ、藤ヶ谷剛彦、中嶋直敏
- 1-16 垂直配向多層カーボンナノチューブと金薄膜の表面活性化接合 22
○藤野真久、須賀唯知、曾我育生、近藤大雄、石月義克、岩井大介、水越正孝

ポスタープレビュー (15:45-16:30)

ポスターセッション (16:30-17:50)

ナノチューブの物性

- 1P-1 窒素ドーピング型カーボンナノチューブのエネルギー論と電子状態 49
○藤本義隆、齋藤晋
- 1P-2 ラマン分光を用いた垂直配向単層カーボンナノチューブ膜の熱伝導特性の測定について 50
○石川桂、千足昇平、Theerapol Thurakitserree、堀琢磨、Rong Xiang、渡辺誠、塩見淳一郎、丸山茂夫
- 1P-3 金属表面に吸着したカーボンナノチューブの変形と電荷移動 51
○長谷川正之、西館数芽
- 1P-4 カーボンナノチューブに物理吸着した分子に対する IRおよびラマンスペクトル強度の遮蔽効果 52
○西村好史、Stephan Irle
- 1P-5 Effect of adsorption of benzene on field electron emission from a carbon nanotube 53
○Akkawat Ruammitree, Hailong HU, Hitoshi Nakahara, Yahachi Saito
- 1P-6 ビンゲル反応により修飾された単層カーボンナノチューブに対する理論的考察 54
○川端栄佑、笛野博之、田中一義、梅山有和、今堀博
- 1P-7 Vibrational spectra and excited state calculation of polyynes@SWNTs 55
○Md. Mahbul Haque, Riichiro Saito
- 1P-8 Simple dielectric constant function for the environment effects on the exciton energies of single-wall carbon nanotubes 56
○Ahmad R. T. Nugraha, Riichiro Saito, Kentaro Sato, Paulo T. Araujo, Ado Jorio
- 1P-9 半導体単層カーボンナノチューブのラマン共鳴窓に対するエキシトン効果 57
○朴珍成、佐藤健太郎、齋藤理一郎
- 1P-10 電気化学ドーピングによる金属型・半導体型単層カーボンナノチューブ薄膜の色制御 58
○守屋理恵子、柳和宏、鈴木拓也、内藤泰久、片浦弘道、松田和之、真庭豊
- 1P-11 ナノチューブの共鳴ラマンとフォトルミネッセンス強度における励起子効果 59
○佐藤健太郎、齋藤理一郎、丸山茂夫
- 1P-12 Structure separation of single-walled carbon nanotubes by agarose gel 60
○Huaping Liu, Ye Feng, 田中丈士、片浦弘道

3月2日(火)

1P-13	有限長ジグザグ炭素ナノチューブのグラフ理論的研究 ○溝口則幸	61
1P-14	マイクロ波プラズマCVD法によるボロンドープカーボンナノチューブの合成と物性評価 ○渡邊徹、津田俊輔、山口尚秀、高野義彦	62
1P-15	螺旋度を変化させた各種カーボンナノチューブの電子構造とエネルギー論 ○加藤幸一郎、斎藤晋	63
1P-16	ラマン分光法によるHiPcoナノチューブのレーザー照射と過熱の評価 ○袴塚麻里、姜東哲、小島謙一、橘勝	64
1P-17	カーボンナノチューブ界面での酸化還元種の電子移動反応速度の評価 ○富永昌人、山口裕之	65
1P-18	単原子吸着したカーボンナノチューブの自己無撞着計算 ○細谷直樹、草部浩一	66
ナノチューブの応用		
1P-19	SWNT/高分子ゲル複合体中におけるSWNT表面上での小分子の刺激応答性吸着および脱離 ○森本達郎、藤ヶ谷剛彦、中嶋直敏	67
1P-20	キャップ層導入によるポリマー/単層カーボンナノチューブ正孔輸送層を用いた有機薄膜太陽電池の特性改善 ○岸直希、加藤慎也、斎藤毅、伊東大輝、林靖彦、曾我哲夫、神保孝志	68
1P-21	側壁修飾したCNTによるPVA/CNTコンポジットの強度向上 ○関戸大、内海浩希、大宮浩之、山崎太平、熊谷進、北村啓、竹内久人、大野正富	69
1P-22	垂直配向カーボンナノチューブ薄膜で構成されたマイクロリアクターの開発 ○木之下博、山川陽、大前伸夫	70
1P-23	エタノール熱分解による水素生成と炭素固定に関する研究 ○垣見洋輔、中原仁、安坂幸師、齋藤弥八	71
1P-24	SPMカンチレバー先端でのCo, Ni, Pd粒子内包CNTの作製 ○クラーク・イアン・トーマス、吉村雅満	72
1P-25	ポリベンズイミダゾール被覆カーボンナノチューブの炭素化とその酸素還元特性 ○内海剛志、藤ヶ谷剛彦、中嶋直敏	73
1P-26	自転・公転混合技術を用いて作製されたカーボンナノチューブ・ゴムコンポジットの電気特性 ○酒井歩、土屋好司、古川猛夫、矢島博文	74
1P-27	単層カーボンナノチューブのパターン成長法による薄膜トランジスタの作製 ○相川慎也、項榮、エリックエイナルソン、千足昇平、塩見淳一郎、西川英一、丸山茂夫	75
1P-28	Microcontact Printing of Organic Molecules and Carbon Nanotubes ○Jan Mehlich, Bart Jan Ravoo, Hisanori Shinohara	76
炭素ナノ粒子		
1P-29	アルコールアーク放電法による銅ナノワイヤー内包カーボンナノチューブと多面体グラファイト粒子の形成 ○小塩明、山本誠、祇園和輝、小海文夫	77
1P-30	泡状ナノ炭素の強磁性に対する高温アニーリングの影響 ○浅野洋仁、飯島澄男、坂東俊治	78
1P-31	自転・公転混練技術によって作製された炭素材料/ポリマーコンポジットの電気特性 ○塩谷亮、土屋好司、古川猛夫、矢島博文	79

3月2日(火)

1P-32	20 Torr He下で生成したフラーレン煤の迅速熱処理による LaC_2 内包多層カーボンナノカプセルの生成 ○山本和典、赤阪健	80
若手奨励賞候補者		
1P-33	長さ分離したカーボンナノチューブを用いた薄膜トランジスタの特性評価 ○浅田有紀、宮田耕充、塩澤一成、大野雄高、北浦良、菅井俊樹、水谷孝、篠原久典	81
1P-34	金触媒使用プラズマCVDにおける水素反応を利用した単層カーボンナノチューブの直径制御 ○ゴラネビスゾーレ、加藤 俊顕、金子 俊郎、畠山 力三	82
1P-35	可溶性ポリベンゾオキサゾール前駆体を用いた単層カーボンナノチューブの可溶化の溶媒依存性 ○福丸貴弘、藤ヶ谷剛彦、中嶋直敏	83
1P-36	$\text{La@C}_{82}\text{Cp}^*$ 二量体の構造解析 ○佐藤悟、前田優、二川秀史、溝呂木直美、土屋敬広、赤阪健、Zdenek Slanina、永瀬茂	84
1P-37	DFTB/MD法を用いた高温下における開端修飾カーボンナノチューブ閉端化シミュレーション ○原裕訓、Stephan Irle	85
1P-38	カーボンナノチューブワイヤの電気伝導率向上 ○島津智寛、Milan Siry、桶結憲二、大島久純	86
1P-39	透過電子顕微鏡法による金とカーボンナノチューブの接合その場観察 ○荻田基志、安坂幸師、齋藤弥八	87
1P-40	金属カーバイド内包フラーレン $\text{Sc}_2\text{C}_2@\text{C}_{80}$ カルベン誘導体の異性化 ○栗原広樹、山崎裕子、二川秀史、溝呂木直美、土屋敬広、永瀬茂、赤阪健	88
1P-41	炭素同位体からなる孤立単層カーボンナノチューブにおける G^+ バンドの線幅 ○趙沛、項榮、佐藤健太郎、エリック エイナルソン、丸山茂夫	89

3月3日(水)

特別講演 発表25分・質疑応答5分
一般講演 発表10分・質疑応答5分
ポスタープレビュー 発表1分・質疑応答なし

特別講演 (9:00-9:30)

- 2S-3 小分子内包フラーレンの有機合成 3
○村田靖次郎

一般講演 (9:30-10:30)

フラーレンの機能と応用

- 2-1 液々界面におけるフラーレンの電子アクセプターの挙動 23
○林亜実, 高橋英志, 田路和幸
- 2-2 シラシクロプロパンによる $\text{La}_2@C_{80}$ のカルボシリル化反応 24
○美野輪まり, 山田道夫, 加固昌寛, 土屋敬広, 溝呂木直美, 赤阪健, 永瀬茂
- 2-3 $C_{3v}\text{-M}_2@C_{82}$ と $C_{3v}\text{-(MC)}_2@C_{82}$ (M= Er, Lu, Tm)の紫外光電子スペクトル 25
○宮崎隆文, 青木雄祐, 徳本頌治, 隅井良平, 沖本治哉, 梅本久, 伊藤靖浩, 泉乃里子, 篠原久典, 日野照純
- 2-4 リチウム内包[60]フラーレンの単離 26
○岡田洋史, 酒井健, 小野吉弘, 河地和彦, 表研次, 笠間泰彦, 横尾邦義, 小野昭一, 青柳忍, 西堀英治, 澤博, 北浦良, 篠原久典, 石川真介, 小室貴士, 飛田博実

☆☆☆☆☆☆ 休憩 (10:30-10:45) ☆☆☆☆☆☆

一般講演 (10:45-11:45)

フラーレンの機能と応用

- 2-5 フラーレン-アルミニウムポルフィリン分子の光誘起電荷分離に基づく光電池の構築 27
○伊藤攻, アツラ サンダナヤカ, 羽曾部卓, パラシャント パドトリ, アルト イスト
- 2-6 パーフルオロアルキル基を有する両親媒性フラーレンからなる水溶性フルオラスベシクルの性質 28
○本間達也, 原野幸治, 磯部寛之, 中村栄一
- 2-7 UV光照射フラーレンナノウイスキーの電気伝導特性とESR 29
○土井達也, 小山恭平, 青木伸之, 落合勇一
- 2-8 fcc A_3C_{60} および $A15 A_3C_{60}$ における電子格子相互作用と超伝導 30
○是常隆, 斎藤晋

☆☆☆☆☆☆ 昼食 (11:45-13:00) ☆☆☆☆☆☆

授賞式 (13:00-13:45)

特別講演 (13:45-14:15)

- 2S-4 Standardization on carbon nanotubes 4
○Haeseong Lee

一般講演 (14:15-15:15)

ハイブリットカーボン

- 2-9 プラズマ制御による窒素内包フラーレンの多量合成 31
○宮長淳, 金子俊郎, 石田裕康, 畠山力三
- 2-10 アザフラーレン内包単層カーボンナノチューブの電子状態 32
○八木創, 徳本 頌治, 善木 将嗣, 財満 壮晋, 宮崎 隆文, 日野 照純, Nikos Tagmatarchis, 飯泉 陽子, 岡崎 俊也

3月3日(水)

- 2-11 カーボンナノチューブ内部空間におけるスズおよび鉛の結晶成長の阻害 33
○小林慶太、末永和知、斎藤毅、飯島澄男
- 2-12 ポタシウムドーパ六方晶窒化ホウ素 34
○岡田晋、大谷実

☆☆☆☆☆☆ 休憩 (15:15-15:30) ☆☆☆☆☆☆

一般講演 (15:30-16:15)

ハイブリットカーボン

- 2-13 CVD法で作製したナノチューブ-ナノホーン複合体の電界電子放出源への応用 35
○弓削 亮太、宮脇 仁、黒島 貞則、市橋 鋭也、吉武 務、大川 哲也、青木 康、飯島 澄男、湯田坂 雅子
- 2-14 ポリイン炭素鎖の生成過程における同位体混合 36
○若林知成、才川真央、和田資子
- 2-15 イオントラップ気相移動度法の開発 37
○澤西慶彦、菅井俊樹

ポスタープレビュー (16:15-17:00)

ポスターセッション (17:00-18:20)

フラーレンの機能と応用

- 2P-1 プラズマスパッタ生成ニッケルイオン照射によるニッケル内包フラーレン合成 90
○馬越達也、石田裕康、金子俊郎、島山力三
- 2P-2 Nature of chemical bonding in endohedral di-metallofullerenes and their carbides: $M_2(C_2)@C_{2n}$ (M=Y, La, Er, Lu; 2n=82 and 80) 91
○Jian Wang,、Stephan Irlle
- 2P-3 $[Li@C_{60}]$ +塩の精製とキャラクタリゼーション 92
○酒井健、岡田洋史、小野吉弘、河地和彦、表研次、笠間泰彦、横尾邦義、小野昭一、小室貴士、飛田博実
- 2P-4 $Li@C_{60}$ カチオンが配位したイリジウム錯体の合成と構造 93
○渡邊孝仁、小室貴士、岡田洋史、酒井健、小野吉弘、笠間泰彦、飛田博実
- 2P-5 $Gd@C_{82}$ derivatives based MRI contrast agents 94
○張錦英、宮田耕充、篠原久典
- 2P-6 一電子還元された $Li^+@C_{60}$ の分光学的研究 95
○秋山公男、岡田洋史、酒井健、小野吉弘、笠間泰彦、飛田博実
- 2P-7 12相交流アークプラズマによる金属の内包 96
○松浦次雄、真木教雄
- 2P-8 Sc_2 または Sc_2C_2 金属内包フラーレン $Sc_2(C_2)@C_{82}$ の電子状態に関するDFTとDFTBの比較 97
○西本佳央、イレ ステファン
- 2P-9 Computed Structures and Relative Stabilities of $Dy_2@C_{100}$ 98
○T. Yang, X. Zhao
- 2P-10 C_{60} に内包されたLiイオンの電子密度分布解析による直接観測 99
○青柳忍、西堀英治、北浦良、岡田洋史、酒井健、小野吉弘、笠間泰彦、飛田博実、篠原久典、澤博
- 2P-11 ベンゼン可燃における、フラーレン生成のReaxFFシミュレーション 100
○銭虎軍、ヅイン アデリヴァン、サハ ビスワジテ、諸熊奎治、イレ ステファン

3月3日(水)

2P-12	ベンゼン架橋フラーレン二量体の合成と評価 ○伊藤靖浩、Jamie H. Warner、Maria del Carmen Gimenez-Lopez、Kyriakos Porfyraakis、 Andrei N. Khlobystov、G. Andrew D. Briggs	101
2P-13	ポリ水酸化フラーレン塩 ○上野裕、菅井俊樹、森山広思	102
2P-14	電子供与基を有するフラーレン十重付加体:その光物性および二重膜の光電気化学特性 ○一木孝彦、松尾豊、中村栄一	103
2P-15	Structure of Thin Polymerized C ₆₀ Coatings Formed by Electron-Beam Dispersion with Additional Electric Field Assistance ○Ihar Razanau、三重野哲、Viktor Kazachenko	104
2P-16	表面処理された基板上の電極間に直接成長したC ₆₀ 結晶 ○加藤翔太、栗原浩平、飯尾靖也、岩田展幸、山本寛	105
2P-17	Na-H-C ₆₀ 化合物の構造と電子状態 ○大波英幸、緒方啓典	106
2P-18	MgドープC ₆₀ 膜の成膜温度上昇による構造変化 ○西誠治、名取雅人、小島信晃、山口真史	107
2P-19	金属ドープフラーレンポリマーの電子状態 ○千葉奨、岡田晋	108
ハイブリットカーボン		
2P-20	マイクロ波プラズマ化学気相成長カーボンナノウォールの水素エッチング効果 ○鈴木誠也、吉村雅満	109
2P-21	高分解能透過型電子顕微鏡による単分子観察の為の注意点 ○新見佳子、越野雅至、中村栄一、末永和知	110
2P-22	希土類-黒鉛層間化合物の磁気特性 ○平郡諭、小林本忠	111
2P-23	触媒担持カーボンナノコイルの酸化反応における黒鉛化処理の有無の比較 ○川畑貴博、横田真志、瀧本幸太郎、池田峻、須田善行、滝川浩史、桶真一郎、植仁志、梅田良人、 清水一樹	112
2P-24	光応答カーボンナノチューブ細胞培養基板の開発 ○佐田貴生、藤ヶ谷剛彦、中嶋直敏	113
ポリイン		
2P-25	n-ヘキサンとn-デカンへの高強度フェムト秒レーザー照射によるポリイン分子の合成 佐藤祐旭、○兒玉健、城丸春夫、Joseph H. Sanderson、藤野竜也、和田資子、若林知成、阿知波洋次	114
2P-26	リサイクリングHPLCにおけるN@C ₆₀ の光学的検出 ○吉川愛里、若林知成	115
2P-27	シアノポリインの生成過程における同位体混合 ○オ川真央、若林知成	116
2P-28	ポリイン・ヨウ素錯体C ₁₀ H ₂ -I ₆ の構造モデル ○和田資子、槐靖範、加藤立久、若林知成	117
2P-29	ポリイン分子鎖の単層カーボンナノチューブ内における構築 ○手柴雅臣、吉本重理沙、若林知成	118

3月3日(水)

- 2P-30 準安定 C_4H^- , C_6H^- の検出と寿命測定 119
松本淳、後藤基、座間優、間嶋拓也、田沼肇、東俊行、○城丸春夫、阿知波洋次

ナノホーン

- 2P-31 マグネタイト担持カーボンナノホーン 120
入江路子、宮脇仁、飯島澄男、○湯田坂雅子
- 2P-32 サイズの異なるナノホーンのマウス生体内分布 121
○張民芳、山口貴氏、飯島澄男、湯田坂雅子
- 2P-33 開孔カーボンナノホーンの生体内分布 122
宮脇仁、張民芳、飯島澄男、○湯田坂雅子

若手奨励賞候補者

- 2P-34 添加剤フリーでの単層カーボンナノチューブ・ミリメータ成長 123
○長谷川 馨、野田 優
- 2P-35 金属型・半導体型単層カーボンナノチューブパッキーペーパーの電気伝導特性 124
○鶴戸口浩樹、柳和宏、鷺谷智、大島勇吾、竹延大志、片浦弘道、松田和之、真庭豊
- 2P-36 CVD法による瞬間冷却を用いた単層グラフェン合成 125
○加門慶一、宮田耕充、北浦良、篠原久典
- 2P-37 孤立化した半導体単層カーボンナノチューブを用いた薄膜トランジスタ 126
○塩澤一成、浅田有紀、宮田耕充、北浦良、大野雄高、水谷孝、篠原久典
- 2P-38 発光・電気伝導の同時測定によるカーボンナノチューブからの励起子・自由キャリア電界発光観測 127
○若原弘行、牧英之、佐藤徹哉、鈴木哲
- 2P-39 パルス通電加熱によるCNTフィールドエミッタの瞬間実装 128
○関口康太郎、古市考次、白鳥洋介、杉目恒志、野田優
- 2P-40 マクロファージ様細胞を用いたフラーレンナノウィスカーの生分解性評価 129
○ぬで島真一、宮澤薫一、奥田順子、谷口彰良
- 2P-41 金属フタロシアニン担持カーボンナノチューブの燃料電池用カソードへの応用 130
○八尾勉、橋新剛、玉置純
- 2P-42 実験的に決定したHiPco & CoMoCAT SWNTの電子準位 131
○平兮康彦、田中泰彦、新留康郎、中嶋直敏

3月4日(木)

特別講演 発表25分・質疑応答5分
一般講演 発表10分・質疑応答5分
ポスタープレビュー 発表1分・質疑応答なし

特別講演 (9:00-9:30)

- 3S-5 カーボンナノチューブのコーティングによる導電繊維「CNTEC」の開発と安全性に関する課題 5
○秋庭英治

一般講演 (9:30-10:30)

ナノチューブの生成と精製

- 3-1 カーボンナノチューブの核生成の過程による初期段階: アセチレン重合の密度汎関数強力結合分子動力学シミュレーションと Fe_{38} 粒子の上で架橋処理すること 38
○王穎、太田靖人、銭虎軍、諸熊奎治、イレステファン
- 3-2 Gas-phase and On-surface Decomposition of Ethanol in Alcohol CCVD 39
○項 榮、侯 博、エイナルソン エリック、塩見 淳一郎、丸山 茂夫
- 3-3 エタノールを用いた垂直配向単層カーボンナノチューブのミリメートル成長 40
○杉目恒志、野田優
- 3-4 カーボンナノチューブのカイラリティー制御 41
○井上亮人、鶴岡泰広、兒玉健、岡崎俊也、阿知波洋次

☆☆☆☆☆☆ 休憩 (10:30-10:45) ☆☆☆☆☆☆

一般講演 (10:45-12:30)

ナノチューブの生成と精製

- 3-5 R-cut水晶基板上における単層カーボンナノチューブの水平配向成長 42
○岡部寛人、千足昇平、塩見淳一郎、佐藤忠、河野修一、寺澤正己、丸山茂夫
- 3-6 分散剤の疎水性と静電的相互作用がカーボンナノチューブ分散に与える影響 43
片倉伸、○佐野正人

グラフェン

- 3-7 低温酸化によるグラフェン"バッファー層"の π バンド復元 44
○種田智、Fenton R. McFeely, James B. Hannon, Rudolf M. Tromp, Zhihong Chen, Yanning Sun, Damon B. Farmer and John J. Yurkas
- 3-8 Ni(111)上グラフェンナリボンにおける磁性 45
○澤田啓介、石井史之、斎藤峯雄
- 3-9 電場によるグラファイト薄膜の磁性制御 46
○大谷実、越野幹人、高木祥光、岡田晋
- 3-10 曲率を持つグラフェンの磁性およびゲスト吸着効果 47
○高井和之、鈴木豪、榎敏明、西原洋知、京谷隆
- 3-11 グラフェントランジスタ特性の電極幅依存性 48
○野内亮、齊藤達也、谷垣勝己

☆☆☆☆☆☆ 昼食 (12:30-13:45) ☆☆☆☆☆☆

3月4日(木)

特別講演 (13:45-14:15)

3S-6 グラフェン研究の過去と将来展望の概略
○日浦英文

6

ポスタープレビュー (14:15-15:00)

ポスターセッション (15:00-16:20)

内包ナノチューブ

- 3P-1 Synthesis and Electrical Transport Properties of $C_{69}N$ Azafullerenes Encapsulated Single-Walled Carbon Nanotubes 132
○李永峰, 金子俊郎, 畠山力三,
- 3P-2 高分解能透過型電子顕微鏡による単層カーボンナノチューブ中のKClナノ結晶 133
○廣瀬香里, 劉崢, 斎藤毅, 末永和知
- 3P-3 強磁性金属内包カーボンナノチューブの磁気特性 134
○松井悠祐, 久田大二郎, 金子哲也, 市川雄基, 佐藤英樹, 藤原裕司, 畑浩一

ナノチューブの生成と精製

- 3P-4 ZigZag構造カーボンナノチューブの成長と光学特性 135
○阿知波洋次, 井上亮人, 大西侑気, 児玉健, 岡崎俊也
- 3P-5 擬連続流動層法によるカーボンナノチューブの大量合成 136
○金東榮, 杉目 恒志, 長谷川 馨, 大沢 利男, 野田 優
- 3P-6 ダイヤモンド微粒子触媒を用いた単層カーボンナノチューブの直径制御 137
○千足 昇平, 平松 典大, 高木 大輔, 本間 芳和, 丸山 茂夫
- 3P-7 高真空アルコールガスソース法を用いた $Al_2O_3/Co/Al_2O_3$ 多層触媒上のSWNT成長 138
○水谷芳裕, 佐藤一徳, 丸山隆浩, 成塚重弥
- 3P-8 エキシマレーザによるCoMoCATナノチューブのカイラリティ分布変化 139
○橋本賢樹, 真木教雄, 芦原将彰, 松浦次雄
- 3P-9 エアロゾルアシストCVD法による金属的な単層カーボンナノチューブの収率制御 140
○小池晋也, 坂東俊治, 安藤義則
- 3P-10 単層カーボンナノチューブの電気化学的切断手法の進展 141
○大森滋和, 斎藤毅, シュクラビカウ, 湯村守雄, 飯島澄男
- 3P-11 アルコール化学気相成長法によるカーボンナノチューブ合成におけるバッファー層の影響 142
○松岡佑樹, 吉村雅満
- 3P-12 窒素雰囲気中アーク放電法で作製した孤立分散単層カーボンナノチューブの精製 143
○水澤崇志, 鈴木信三, 岡崎俊也, 阿知波洋次
- 3P-13 グラフェン上水分子の吸着: 局在基底による密度汎関数法の計算精度 144
○大淵真理
- 3P-14 SWNT Nucleation, Growth and Healing: Insights from Density-Functional Tight-Binding Molecular Dynamics Simulations 145
○Alister J. Page, Stephan Irle, 諸熊奎治
- 3P-15 Sn/Fe触媒担持多孔質材料を用いた細線カーボンナノコイルのCVD製造 146
○瀧本幸太郎, 横田真志, リムシュリン, 須田善行, 滝川浩史, 植仁志, 清水一樹, 梅田良人
- 3P-16 密度勾配法で高純度半導体型カーボンナノチューブの分離 147
○Ye Feng, Yasumitsu Miyata, Shunjiro Fujii, Kiyoto Matsuishi, Hiromichi Kataura

3月4日(木)

3P-17	カーボンナノチューブ垂直配向膜の高速成長のための触媒と担体 ○野村桂甫、長谷川馨、野田優	148
3P-18	フェロセンとアセチレン・メタン原料を用いた単層カーボンナノチューブの気相合成 ○石塚洋行、佐藤佳邦、大沢利男、野田優	149
3P-19	炭素源分解が単層カーボンナノチューブ合成に与える影響についての実験とシミュレーション ○侯博、項榮、Erik Einarsson、塩見淳一郎、三好明、丸山茂夫	150
3P-20	自由電子レーザを成長中照射した単層カーボンナノチューブの複数励起波長によるラマン解析 ○境恵二郎、石塚大祐、園村拓也、竹下弘毅、金木邦英、矢島博文、岩田展幸、山本寛	151
3P-21	サブマリン式基板加熱によるカーボンナノチューブ合成法の開発 ○横井裕之、百田寛、岩本知広	152
3P-22	低圧CVD法によるカーボンナノチューブ成長における触媒酸化の効果 ○南智之、澤口大樹、佐藤英樹、畑浩一	153
3P-23	単層カーボンナノチューブ直径に対する触媒還元条件の影響 ○ティエラポン トウラキットセーリー、エリック エイナルソン、項榮、千足昇平、塩見淳一郎、丸山茂夫	154
3P-24	プラズマCVD法によるカーボンナノチューブの低温合成 ○三宅雅人、飯島徹、Kenneth Teo、Nalin Rupesinghe、堀川和徳、小沼賢二郎、阿部勝義、佐藤正之、林靖彦	155
3P-25	アガロースゲルを用いた金属・半導体単層カーボンナノチューブの分離のための界面活性剤の探索 ○田中丈士、卜部泰子、片浦弘道	156
3P-26	ジメチルエーテルを炭素源とした垂直配向単層カーボンナノチューブ膜のCVD合成 ○井ノ上泰輝、岡部寛人、侯博、千足昇平、渡辺誠、塩見淳一郎、丸山茂夫	157
3P-27	ゲル分離と密度勾配遠心分離を組み合わせた単層カーボンナノチューブの選別 ○西出大亮、劉華平、田中丈士、片浦弘道	158
3P-28	室温・CO ₂ レーザ蒸発法による単層カーボンナノチューブの生成 山口貴司、中西亮、北浦良、坂東俊二、湯田坂雅子、篠原久典、飯島澄男、	159
グラフェン		
3P-29	Carbon Spiral Helix, a Novel Nanoarchitecture Derived from Monovacancy Defects in Graphene ○Lili Liu, Xingfa Gao, Shigeru Nagase, Stephan Irlé	160
3P-30	DFT計算によるグラフェン上の吸着子の安定性 ○中田謙吾、石井晃	161
3P-31	剥離法によるグラフェンの作製と評価 ○松山慶一郎、前田哲平、岩田展幸、山本寛	162
3P-32	グラフェンフレーク上に層状成長したグラフェン薄膜のラマンスペクトル ○根岸良太、平野博紀、小林慶裕、大野恭秀、前橋兼三、松本和彦	163
若手奨励賞候補者		
3P-33	フラーレン二重膜ベシクルの光修飾と水透過性の制御 ○成田明光、原野幸治、中村栄一	164
3P-34	金属原子内包カーボンナノチューブの透明導電性薄膜への応用 ○崔大憲、北浦良、宮田耕充、篠原久典	165

3月4日(木)

- | | | |
|-------|---|-----|
| 3P-35 | 燃料電池用多層カーボンナノチューブの成長制御
○喜多村慎也、山本リカ、橋新剛、玉置純 | 166 |
| 3P-36 | 高い電子受容性を有する[60]フラーレン二付加体の合成
○アラストS.リヤー、小久保研、Hao Geng、Hsing-Lin Wang、大島巧、Long Y. Chiang | 167 |
| 3P-37 | ドーピングされたナノチューブヘテロ構造の電子輸送特性
○櫻井誠大、斎藤晋 | 168 |
| 3P-38 | 非水溶性低度水酸化フラーレンの簡便合成とそのナノ粒子特性
○小林直記、小久保研、大島巧 | 169 |
| 3P-39 | 単一単層カーボンナノチューブの局所光励起と反応制御
○高瀬 舞、並河 英紀、保田 諭、村越 敬 | 170 |
| 3P-40 | 酸化チタン内包MWNTsの調製
○池之子英洋、橋新剛、玉置純 | 171 |
| 3P-41 | 外部電界印加によるカーボンナノチューブフォトルミネッセンスのシュタルク効果
○河合佑治、牧英之、佐藤徹哉 | 172 |

Tuesday, March 2nd

Special Lectures: 25 min (Presentation) + 5 min (Discussion)
General Lectures: 10 min (Presentation) + 5 min (Discussion)
Poster Previews: 1 min (Presentation), No Discussion

Special Lecture (9:00-9:30)

- 1S-1 Recent Developments in Nanodiamond Research 1
○Eiji Osawa

General Lecture (9:30-10:30)

Properties of Nanotubes

- 1-1 Exciton Dynamics in Hole-Doped Single-Walled Carbon Nanotubes 7
○Kazunari Matsuda, Yuhei Miyauchi, Takero Sakashita, and Yoshihiko Kanemitsu
- 1-2 Photoluminescence Kinetics in PFO-Wrapped SWNT Papers 8
○Takeshi Koyama, Yasumitsu Miyata, Yuki Asada, Hisanori Shinohara, Hiromichi Kataura, Arao Nakamura
- 1-3 Environment Effects on Bundled Carbon Nanotubes Detected by Coherent Phonons 9
○Keiko Kato, Daisuke Takagi, Yoshihiro Kobayashi, Hiroki Hibino, Atsushi Ishizawa, Katsuya Oguri, Hideki Gotoh, Hidetoshi Nakano
- 1-4 Short wavelength electroluminescence from single-walled carbon nanotubes with high bias voltage 10
○Hideyuki Maki, Satoru Suzuki, Norihito Hibino, Yoshihiro Kobayashi, Tetsuya Sato

☆☆☆☆☆☆ Coffee Break (10:30-10:45) ☆☆☆☆☆☆

General Lecture (10:45-11:45)

Properties of Nanotubes

- 1-5 Observation of Bound Tween80 Surfactant Molecules on Carbon Nanotubes in an Aqueous Solution using Pulsed Field Gradient Nuclear Magnetic Resonance Method 11
○Haruhisa Kato, Ayako Nakamura, Kohei Mizuno, Manabu Shimada, Kayori Takahashi, Sinichi Kinugasa
- 1-6 Surface-Enhanced Raman Scattering from an Isolated Single-Walled Carbon Nanotube at the Gap of Metal Nanodimer 12
○Satoshi Yasuda, Mai Takase, Keiichiro Komeda, Masanobu Nara, Kei Murakoshi
- 1-7 E_{11} and E_{22} Bandgap Modulation of Semiconducting Single-Walled Carbon Nanotube by Adsorbing 13
○Yoshiteru Takagi, Susumu Okada
- 1-8 The fundamental importance of background analysis in precise characterization of single-wall carbon nanotubes by optical absorption spectroscopy 14
○Takeshi Saito, Shigekazu Ohmori, Masayoshi Tange, Bikau Shukla, Toshiya Okazaki, Motoo Yumura, Sumio Iijima

☆☆☆☆☆☆ Lunch Time (11:45-13:00) ☆☆☆☆☆☆

General Lecture (13:00-14:15)

Applications of Nanotubes

- 1-9 Site-selective deposition of single-wall carbon nanotube film using patterned self-assembled monolayer and its application to thin-film transistors 15
○Shunjiro Fujii, Takeshi Tanaka, Takeo Minari, Kazuhito Tsukagoshi, Hiromichi Kataura
- 1-10 Fabrication of high-performance thin film transistor with plasma CVD grown single-walled carbon nanotubes and elucidation of its working mechanism 16
○Shunsuke Kuroda, Toshiaki Kato, Toshiro Kaneko, Rikizo Hatakeyama

Tuesday, March 2nd

- 1-11 Incorporating of carbon nanotubes in donor-acceptor based heterojunction solar cells 17
○Golap Kalita, Koichi Wakita and Masayoshi Umeno
- 1-12 Bottom-up assembly of carbon nanotubes electrocatalyst for polymer electrolyte fuel cell 18
○Tsuyohiko Fujigaya, Kazuya Matsumoto, Naotoshi Nakashima
- 1-13 Morphology Change of Multi-Walled Carbon Nanotube Field Emitters Studied by In-Situ Transmission Electron Microscopy 19
○Toshinari Ichihashi, Fumishige Nakamura, Ryota Yuge, Mayumi Kosaka, Kiyohiko Toyama

☆☆☆☆☆☆ Coffee Break (14:15-14:30) ☆☆☆☆☆☆

Special Lecture (14:30-15:00)

- 1S-2 Biological Application of Fullerene Derivatives 2
○Tadahiko Mashino, Shigeo Nakamura

General Lecture (15:00-15:45)

Applications of Nanotubes

- 1-14 HRTEM observation of a crystalline-cluster phase inside ionic liquids freestanding on CNT super-thin films 20
○Shimou Chen, Keita Kobayashi, Ryo Kitaura, Yasumitsu Miyata, Kazu Suenaga, Hisanori Shinohara
- 1-15 Preparation of silica gel microparticles coated by pristine carbon nanotubes for the liquid chromatography stationary phase 21
○JongTae Yoo, Tsuyohiko Fujigaya, Naotoshi Nakashima
- 1-16 Surface Activated Bonding between Au layer and Vertically Aligned Multiwalled Carbon Nanotubes 22
○Masahisa Fujino, Tadatomo Suga, Ikuo Soga, Daiyu Kondo, Yoshikatsu Ishizuki, Taisuke Iwai, Masataka Mizukoshi

Poster Preview (15:45-16:30)

Poster Session (16:30-17:50)

Properties of Nanotubes

- 1P-1 Energetics and Electronic structure of Nitrogen-doped Carbon Nanotube 49
○Yoshitaka Fujimoto, Susumu Saito
- 1P-2 Thermal conduction property measurements of vertically-aligned single-walled carbon nanotube film by utilizing Raman spectrum 50
○Kei Ishikawa, Shohei Chiashi, Theerapol Thurakitserree, Takuma Hori, Rong Xiang, Makoto Watanabe, Junichiro Shiomi, Shigeo Maruyama
- 1P-3 Deformation and charge transfer of the single-walled carbon nanotube adsorbed on the metallic surfaces 51
○Masayuki Hasegawa, Kazume Nishidate
- 1P-4 IR and Raman Stealth Effect for Molecules Absorbed on Single-Walled Carbon Nanotubes 52
○Yoshifumi Nishimura, Stephan Irle
- 1P-5 Effect of adsorption of benzene on field electron emission from a carbon nanotube 53
○Akkawat Ruammitree, Hailong Hu, Hitoshi Nakahara, Yahachi Saito
- 1P-6 Theoretical Investigation on Single-Walled Carbon Nanotubes Functionalized by Bingel Reaction 54
○Eisuke Kawabata, Hiroyuki Fueno, Kazuyoshi Tanaka, Tomokazu Umeyama, Hiroshi Imahori
- 1P-7 Vibrational spectra and excited state calculation of polyynes@SWNTs 55
○Md. Mahbulul Haque, Riichiro Saito

Tuesday, March 2nd

1P-8	Simple dielectric constant function for the environment effects on the exciton energies of single-wall carbon nanotubes ○Ahmad R. T. Nugraha, Riichiro Saito, Kentaro Sato, Paulo T. Araujo, Ado Jorio	56
1P-9	What is the exciton effect in the Raman resonance window of semiconducting single wall carbon nanotubes? ○Jin Sung Park, Kentaro Sato, Riichiro Saito	57
1P-10	Control of colors of thin films of metallic and semiconducting single-wall carbon nanotube by electrochemical doping ○Rieko Moriya, Kazuhiro Yanagi, Takuya Suzuki, Yasuhisa Naitoh, Hiromichi Kataura, Kazuyuki Matsuda, Yutaka Maniwa	58
1P-11	Exciton environmental effects of resonance Raman and photoluminescence intensity of single wall carbon nanotubes ○Kentaro Sato, Riichiro Saito, Shigeo Maruyama	59
1P-12	Structure separation of single-walled carbon nanotubes by agarose gel ○Huaping Liu, Ye Feng, Takeshi Tanaka, Hiromich Kataura	60
1P-13	Graph-Theoretical Study of Finite Length Zigzag Carbon Nanotubes ○Noriyuki Mizoguchi	61
1P-14	Physical properties of boron-doped Carbon nanotube grown by Microwave Plasma CVD method ○Tohru Watanabe, Shunsuke Tsuda, Takahide Yamaguchi, Yoshihiko Takano	62
1P-15	Energetics and Electronic Structures of Twisted Carbon Nanotubes ○Koichiro Kato, Susumu Saito	63
1P-16	Effects of laser irradiation and heating on HiPco nanotubes probed by Raman spectroscopy ○Mari Hakamatsuka, Dongchul Kang, Kenichi Kojima, Masaru Tachibana	64
1P-17	Evaluation of Electron Transfer Reaction Rate of Redox Species at Carbon Nanotube Interface ○Masato Tominaga, Hiroyuki Yamaguchi	65
1P-18	Self-consistent calculation of single atom adsorption on a carbon nanotube ○Naoki Hosoya, Koichi Kusakabe	66
Applications of Nanotubes		
1P-19	Stimuli responsive adsorption and desorption of small molecules on SWNTs surfaces in SWNT/polymer gel composite. ○Tatsuro Morimoto, Tsuyohiko Fujigaya, Naotoshi Nakashima	67
1P-20	Performance Enhancement of Organic Solar Cells with Polymer-SWCNT Composite Hole Transport Layer by Inserting Thin Cap Layer ○Naoki Kishi, Shinya Kato, Takeshi Saito, Daiki Ito, Yasuhiko Hayashi, Tetsuo Soga, Takashi Jimbo	68
1P-21	Mechanical Strength Improvement of PVA/CNT Composites by Sidewall Functionalization of CNT ○Masaru Sekido, Kouki Utsumi, Hiroyuki Ohmiya, Taihei Yamazaki, Susumu Kumagai, Hiroshi Kitamura, Hisato Takeuchi, Masatomi Ohno	69
1P-22	Development of microreactors consisting of vertically aligned carbon nanotube films ○Hiroshi Kinoshita, Akira Yamakawa, Nobuo Ohmae	70
1P-23	Production of hydrogen and fixation of carbon by thermal decomposition of ethanol ○Yosuke Kakimi, Hitoshi Nakahara, Koji Asaka, Yahachi Saito	71
1P-24	Scalable Fabrication of Co-, Ni-, and Pd-Nanoparticle-Containing CNTs on SPM Probe Apices ○Ian Thomas Clark, Masamichi Yoshimura	72
1P-25	Carbonization of polybenzimidazole-wrapped carbon nanotubes and their oxygen reduction activity ○Takeshi Uchinoumi, Tsuyohiko Fujigaya, Naotoshi Nakashima	73

Tuesday, March 2nd

- 1P-26 Electrical Properties of Carbon Nanotubes / Rubber Composites Prepared with Rotation / Revolution Mixing Technique 74
○Ayumu Sakai, Koji Tsuchiya, Takeo Furukawa and Hirofumi Yajima
- 1P-27 One-step Fabrication of Single-Walled Carbon Nanotubes Thin Film Transistor by Patterned Growth Technique 75
○Shinya Aikawa, Rong Xiang, Erik Einarsson, Shohei Chiashi, Junichiro Shiomi, Eiichi Nishikawa, Shigeo Maruyama
- 1P-28 Microcontact Printing of Organic Molecules and Carbon Nanotubes 76
○Jan Mehlich, Bart Jan Ravoo, Hisanori Shinohara

Carbon nanoparticles

- 1P-29 Formation of Copper Nanowire-filled Carbon Nanotubes and Polyhedral Graphite Particles by Alcohol Arc 77
○Akira Koshio, Makoto Yamamoto, Kazuki Gion, Fumio Kokai
- 1P-30 Effect of high temperature annealing on the ferromagnetism of carbon nanofoam 78
○Hirohito Asano, Sumio Iijima, Shunji Bandow
- 1P-31 Electric Properties of Carbon Materials / Polymer Composites Prepared with Rotation / Revolution Kneading Technique 79
○Ryo Shiotani, Koji Tsuchiya, Takeo Furukawa, Hirofumi Yajima
- 1P-32 Formation of LaC₂ containing multi-shell carbon nanocapsules by rapid heat treatment of La fullerene soot synthesized at 20 Torr He 80
○Kazunori Yamamoto, Takeshi Akasaka

Candidates for the Young Scientist Poster Award

- 1P-33 Characterization of lengthsorted DNA-wrapped carbon nanotube thin film transistors 81
○Yuki Asada, Yasumitsu Miyata, Kazunari Shiozawa, Yutaka Ohno, Ryo Kitauara, Toshiki Sugai, Tkashi Mizutani, Hisanori Shinohara
- 1P-34 Diameter Tuning of Single-Walled Carbon Nanotubes through H₂ Reaction in Au-Catalyzed Plasma CVD 82
○Zohreh Ghorannevis, Toshiaki Kato, Toshiro Kaneko, Rikizo Hatakeyama
- 1P-35 Solvent dependency for solubilization of single-walled carbon nanotubes using soluble polybenzoxazoles precursor 83
○Takahiro Fukumaru, Tsuyohiko Fujigaya, Naotoshi Nakashima
- 1P-36 Structural Characterization of La@C₈₂Cp* Dimer 84
○Satoru Sato, Yutaka Maeda, Hidefumi Nikawa, Naomi Mizorogi, Takahiro Tsuchiya, Takeshi Akasaka, Zdenek Slanina, Shigeru Nagase
- 1P-37 DFTB/MD simulations of functionalized open-ended SWCNTs annealing under high-T 85
○Hironori Hara, Stephan Irle
- 1P-38 Electrical Conductivity Improvement of Carbon Nanotube Wire 86
○Tomohiro Shimazu, Milan Siry, Kenji Okeyui, Hisayoshi Oshima
- 1P-39 In-situ transmission electron microscopy of structural change of the contact between gold and a carbon nanotube 87
○Motoyuki Karita, Koji Asaka, Yahachi Saito
- 1P-40 Isomerization of a Carbene Derivative of Metal Carbide Endofullerene Sc₂C₂@C₈₀ 88
○Hiroki Kurihara, Yuko Yamazaki, Hidefumi Nikawa, Naomi Mizorogi, Takahiro Tsuchiya, Shigeru Nagase, Takeshi Akasaka
- 1P-41 Linewidth of Raman G⁺-Band Features of Individual Single-Walled Carbon Nanotubes from Isotopic 89
○Pei Zhao, Rong Xiang, Kentaro Sato, Erik Einarsson, Shigeo Maruyama

Wednesday, March 3rd

Special Lectures : 25 min (Presentation) + 5 min (Discussion)

General Lectures : 10 min (Presentation) + 5 min (Discussion)

Poster Previews: 1 min (Presentation), No Discussion

Special Lecture (9:00-9:30)

- 2S-3 Organic Synthesis of Endofullerenes Encapsulating a Small Molecule 3
○Yasujirou Murata

General Lecture (9:30-10:30)

Function and Applications of Fullerenes

- 2-1 Behavior of fullerenes as electron acceptor at the liquid-liquid interface 23
○Tsugumi Hayashi, Hideyuki Takahashi, Kazuyuki Tohji
- 2-2 Carbosilylation of $\text{La}_2@C_{80}$ with Silacyclopropane 24
○Mari Minowa, Michio Yamada, Masahiro Kako, Takahiro Tsuchiya, Naomi Mizorogi, Takeshi Akasaka, Shigeru Nagase
- 2-3 Ultraviolet photoelectron spectra of $C_{3v}\text{-M}_2@C_{82}$ and $C_{3v}\text{-(MC)}_2@C_{82}$ (M= Er, Lu, Tm) 25
○Takafumi Miyazaki, Yusuke Aoki, Youji Tokumoto, Ryohei Sumii, Haruya Okimoto, Hisashi Umemoto, Yasuhiro Ito, Noriko Izumi, Hisanori Shinohara, Shojun Hino
- 2-4 Isolation of Lithium Endohedral [60]fullerene 26
○Hiroshi Okada, Takeshi Sakai, Yoshihiro Ono, Kazuhiko Kawachi, Kenji Omote, Yasuhiko Kasama, Kuniyoshi Yokoo, Shoichi Ono, Shinobu Aoyagi, Eiji Nishibori, Hiroshi Sawa, Ryo Kitaura, Hisanori Shinohara, Shinsuke Ishikawa, Takashi Komuro, Hiromi Tobita

☆☆☆☆☆☆ Coffee Break (10:30-10:45) ☆☆☆☆☆☆

General Lecture (10:45-11:45)

Fullerene solids and Chemistry of Fullerenes

- 2-5 Photovoltaic Cell based on Photoinduced Charge Separation of Fullerene-Aluminum(III) Porphyrin Molecular Systems 27
○Osamu Ito, Atula D. S. Sandanayaka, Taku Hasobe, Prashanth K. Poddutoori, Art van der Est
- 2-6 Properties of Water-soluble Fluorous Vesicle Formed from Perfluoroalkylated Fullerene Amphiphile 28
○Tatsuya Homma, Koji Harano, Hiroyuki Isobe, Eiichi Nakamura
- 2-7 Electron transport property and ESR measurement of UV light irradiated fullerene nano whisker 29
○Tatsuya Doi, Kyouhei Koyama, Nobuyuki Aoki, Yuichi Ochiai
- 2-8 Electron-phonon couplings and superconductivity in fcc and $A_{15}A_3C_{60}$ 30
○Takashi Koretsune, Susumu Saito

☆☆☆☆☆☆ Lunch Time (11:45-13:00) ☆☆☆☆☆☆

Awards Ceremony (13:00-13:45)

Special Lecture (13:45-14:15)

- 2S-4 Standardization on carbon nanotubes 4
○Haeseong Lee

General Lecture (14:15-15:15)

Nanowires

- 2-9 High-Yield Synthesis of Nitrogen Endohedral Fullerenes by Plasma Control 31
○Sunao Miyanaga, Toshiro Kaneko, Hirosasu Ishida, Rikizo Hatakeyama

Wednesday, March 3rd

- 2-10 The electronic structure of azafullerene encapsulated single-walled carbon nanotubes 32
○H.Yagi, Y.Tokumoto, M. Zenki, T.Zaima, T.Miyazaki, S.Hino, N.Tagmatarchis, Y.Iizumi, T.Okazaki
- 2-11 Prevention of Crystal Growth of Tin and Lead in Confined Nanospace of Carbon Nanotubes 33
○Keita Kobayashi, Kazu Suenaga, Takeshi Saito, Sumio Iijima
- 2-12 Metallic layered compound: Potassium-intercalated hexagonal boron nitride 34
○Susumu Okada, Minoru Otani

☆☆☆☆☆ Coffee Break (15:15-15:30) ☆☆☆☆☆

General Lecture (15:30-16:15)

Graphene and Carbon Nanoparticles

- 2-13 Highly-Efficient Field Emission from Carbon Nanotube-Nanohorn Hybrids Prepared by Chemical Vapor Deposition 35
○Ryota Yuge, Jin Miyawaki, Sadanori, Kuroshima, Toshinari Ichihashi, Tsutomu Yoshitake, Tetsuya Ohkawa, Yasushi Aoki, Sumio Iijima, Masako Yudasaka
- 2-14 Isotope Scrambling in the Formation of Polyene Carbon Chains 36
○Tomonari Wakabayashi, Mao Saikawa, Yoriko Wada
- 2-15 Development of Ion Trap Ion Mobility Measurements 37
○Yoshihiko Sawanishi, Toshiki Sugai

Poster Preview (16:15-17:00)

Poster Session (17:00-18:20)

Function and Applications of Fullerenes

- 2P-1 Nickel-Atom Endohedral Fullerenes Synthesized by Irradiation of Nickel Ions Generated by Plasma Sputtering 90
○Tatsuya Umakoshi, Hiroyasu Ishida, Toshiro Kaneko, and Rikizou Hatakeyama
- 2P-2 Nature of chemical bonding in endohedral di-metallofullerenes and their carbides: $M_2(C_2)@C_{2n}$ (M=Y, La, Er, Lu; 2n=82 and 80) 91
○Jian Wang, Stephan Irle
- 2P-3 Purification and Characterization of $[Li@C_{60}]^+$ salts 92
○Takeshi Sakai, Hiroshi Okada, Yoshihiro Ono, Kazuhiko Kawachi, Kenji Omote, Yasuhiko Kasama, Kuniyoshi Yokoo, Shoichi Ono, Takashi Komuro, Hiromi Tobita
- 2P-4 Synthetic and Structural Studies on an Iridium Complex of the $Li@C_{60}$ Cation 93
○Takahito Watanabe, Takashi Komuro, Hiroshi Okada, Takeshi Sakai, Yoshihiro Ono, Yasuhiko Kasama, Hiromi Tobita
- 2P-5 $Gd@C_{82}$ derivatives based MRI contrast agents 94
○Jinying Zhang, Yasumitsu Miyata, and Hisanori Shinohara
- 2P-6 Spectroscopic Characterization of Singly Reduced $Li^+@C_{60}$ 95
○Kimio Akiyama, Hiroshi Okada, Takeshi Sakai, Yoshihiro Ono, Yasuhiko Kasama, Hiromi Tobita
- 2P-7 Encapsulation of metals by arc plasma reactor with twelve-phase alternating current discharge 96
○Tsugio Matsuura, Norio Maki
- 2P-8 Electronic Properties of Di-Scandium and Di-Scandium Carbide Endohedral Fullerenes 97
 $S_{c2}(C_2)@C_{82}$: Comparison Between DFT and DFTB
○Yoshio Nishimoto, Stephan Irle

Wednesday, March 3rd

2P-9	Computed Structures and Relative Stabilities of Dy ₂ @C ₁₀₀ ○T. Yang, X. Zhao	98
2P-10	Direct observation of a Li cation inside C ₆₀ by the charge density analysis ○Shinobu Aoyagi, Eiji Nishibori, Ryo Kitaoura, Hiroshi Okada, Takeshi Sakai, Yoshihiro Ono, Yasuhiko Kasama, Hiromi Tobita, Hisanori Shinohara, Hiroshi Sawa	99
2P-11	ReaxFF Simulation of Fullerene Formation in Benzene Combustions ○Hu-Jun Qian, Adri van Duin, Biswajit Saha, Keiji Morokuma, Stephan Irle	100
2P-12	Synthesis and Characterization of Benzene-bridged Fullerene Dimers ○Yasuhiro Ito, Jamie H. Warner, Maria del Carmen Gimenez-Lopez, Kyriakos Porfyarakis, Andrei N. Khlobystov, G. Andrew D. Briggs	101
2P-13	Polyhydroxylated Fullerene Salts ○Hiroshi Ueno, Toshiki Sugai, Hiroshi Moriyama	102
2P-14	Loading Pentapod Deca(organo)[60]fullerenes with Electron Donors: From Photophysics to Photoelectrochemical Bilayers ○Takahiko Ichiki, Yutaka Matsuo, Eiichi Nakamura	103
2P-15	Structure of Thin Polymerized C ₆₀ Coatings Formed by Electron-Beam Dispersion with Additional Electric Field Assistance ○Ihar Razanau, Tetsu Mieno, Viktor Kazachenko	104
2P-16	C ₆₀ Crystal Growth Directly between Electrodes on the Surface Treated Substrate ○Shota Kato, Kohei Kurihara, Yasunari Iio, Nobuyuki Iwata, Hiroshi Yamamoto	105
2P-17	Structure and electronic properties of Na-H-C ₆₀ compounds ○Hideyuki Ohnami, Hironori Ogata	106
2P-18	Structural change of Mg-doped C ₆₀ films along with growth temperature increasing ○Seiji Nishi, Masato Natori, Nobuaki Kojima, Masafumi Yamaguchi	107
2P-19	Electronic Structure of Metal-Doped C ₆₀ Polymers ○Tasuku Chiba, Susumu Okada	108
Hybrid Carbon		
2P-20	Hydrogen Etching Effect of CNW Prepared in Microwave Plasma Enhanced Chemical Vapor Deposition ○Seiya Suzuki, Yoshimura Masamichi	109
2P-21	Notices for single molecular imaging by HR-TEM ○Yoshiko Niimi, Masanori Koshino, Eiichi Nakamura, Kazutomo Suenaga	110
2P-22	Magnetic Properties of Rare Earth Metal Graphite Intercalation Compounds ○Satoshi Heguri, Mototada Kobayashi	111
2P-23	Comparison of combustion between catalyst-supported carbon nanocoil and graphitized carbon nanocoil ○Takahiro Kawabata, Masashi Yokota, Kotaro Takimoto, Takashi Ikeda, Yoshiyuki Suda, Hirofumi Takikawa, Shinichiro Oke, Hitoshi Ue, Yoshito Umeda, Kazuki Shimizu	112
2P-24	Development of optical responsive carbon nanotubes cell cultured substrate ○Takao Sada, Tsuyohiko Fujigaya, Naotoshi Nakashima	113
Polyynes		
2P-25	Synthesis of Polyynes Molecules from n-Hexane and n-Decane by Irradiation of Intense Femtosecond Laser Pulses Yuki Sato, ○Takeshi Kodama, Haruo Shiromaru, Joseph H. Sanderson, Tatsuya Fujino, Yoriko Wada, Tomonari Wakabayashi, Yohji Achiba	114

Wednesday, March 3rd

2P-26	Optical Detection of N@C ₆₀ upon Recycling HPLC ○Airi Yoshikawa, Tomonari Wakabayashi	115
2P-27	Isotope Scrambling in the Formation of Cyanopolyynes ○Mao Saikawa, Tomonari Wakabayashi	116
2P-28	A Model Structure for the Polyene-Iodine Complex C ₁₀ H ₂ -I ₆ ○Yoriko Wada, Yasunori Kai, Tatsuhisa Kato, Tomonari Wakabayashi	117
2P-29	Assembling Molecular Polyene Chains in Single-Wall Carbon Nanotubes ○Masashi Teshiba, Arisa Yoshimoto, Tomonari Wakabayashi	118
2P-30	Detection and lifetime measurements of C ₄ H- and C ₆ H- metastables Jun Matsumoto, Motoshi Goto, Yu Zama, Takuya Majima, Hajime Tanuma, Toshiyuki Azuma, ○Haruo Shiromaru, Yohji Achiba	119

Nanohorns

2P-31	Magnetite-Loaded Carbon Nanohorns Michiko Irie, Jin Miyawaki, Sumio Iijima and ○Masako Yudasaka	120
2P-32	In Vivo Study of SWNHs with Different Sizes on Biodistribution ○Minfang Zhang, Takashi Yamaguchi, Sumio Iijima, Masako Yudasaka	121
2P-33	Biodistribution of Hole-Opened Carbon Nanohorns Jin Miyawaki, Minfang zhang, Sumio Iijima and ○Masako Yudasaka	122

Candidates for the Young Scientist Poster Award

2P-34	Water-free, rapid growth of millimeter-tall single-walled carbon nanotube ○Kei Hasegawa, Suguru Noda	123
2P-35	Crossover from weak localization to exponential localization in conduction of metallic and semiconducting single-wall carbon nanotube buckypaper ○Hiroyuki Udoguchi, Kazuhiro Yanagi, Satoshi Sagitani, Yugo Oshima, Taishi Takenobu, Hiromichi Kataura, Kazuyuki Matsuda, Yutaka Maniwa	124
2P-36	Uniform single-layer graphene synthesis using flash-cooling CVD ○Keiichi kamon, Yasumitsu Miyata, Ryo Kitaura, Hisanori Shinohara	125
2P-37	Thin film transistors using unbundled pure semiconducting single-wall carbon nanotubes ○Kazunari Shiozawa, Yuki Asada, Yasumitsu Miyata, Ryo Kitaura, Yutaka Ohno, Takashi Mizutani, Hisanori Shinohara	126
2P-38	Exciton and free carrier electroluminescence from a SWNT observed through simultaneous measurements of electrical conductivity and emission spectra ○Hiroyuki Wakahara, Hideyuki Maki, Tetsuya Sato, Satoru Suzuki	127
2P-39	Instant Implementation of CNT field emitter arrays by pulse current heating ○Kotaro Sekiguchi, Koji Furuichi, Yosuke Shiratori, Hisashi Sugime, Suguru Noda	128
2P-40	Biodegradation Assessment of Fullerene Nanowhiskers using Macrophage-like Cells ○Shin-ichi Nudajima, Kun'ichi Miyazawa, Junko Okuda-Shimazaki and Akiyoshi Taniguchi	129
2P-41	Preparation of Metallophthalocyanine loaded Multi-walled Carbon Nanotubes for Fuel Cell Cathode ○Tsutomu Yao, Takeshi Hashishin, Jun Tamaki	130
2P-42	Experimentally Determined Electronic States of Isolated (n,m) HiPco & CoMoCAT Single-Walled Carbon ○Yasuhiko Hirana, Yasuhiko Tanaka, Yasuro Niidome, Naotoshi Nakashima	131

Thursday, March 4th

Special Lectures : 25 min (Presentation) + 5 min (Discussion)
General Lectures : 10 min (Presentation) + 5 min (Discussion)
Poster Previews : 1 min (Presentation), No Discussion

Special Lecture (9:00-9:30)

- 3S-5 CNT Coated Conductive Fiber “CNTEC”- Development, Applications and Risk Assessment - 5
○Eiji Akiba

General Lecture (9:30-10:30)

Formation and Purification of Nanotubes

- 3-1 Early Stages in the Nucleation Process of Carbon Nanotubes: Density-Functional Tight-Binding Molecular Dynamics Simulations of Acetylene Polymerization and Cross-Linking on an Fe₃S₄ Particle 38
○Ying Wang, Yasuhito Ohta, HuJun Qian, Keiji Morokuma, Stephan Irle
- 3-2 Gas-phase and On-surface Decomposition of Ethanol in Alcohol CCVD 39
○Rong Xiang, Bo Hou, Erik Einarsson, Junichiro Shiomi, Shigeo Maruyama
- 3-3 Millimeter-tall single-walled carbon nanotube forests grown from ethanol 40
○Hisashi Sugime, Suguru Noda
- 3-4 Chirality selective production of carbon nanotubes in He/N₂ mixed gas 41
○Akihito Inoue, Yasuhiro Tsuruoka, Takeshi Kodama, Toshiya Okazaki, Yohji Achiba

☆☆☆☆☆☆ Coffee Break (10:30-10:45) ☆☆☆☆☆☆

General Lecture (10:45-12:30)

Formation and Purification of Nanotubes

- 3-5 Horizontally Aligned SWNT Growth on R-cut Crystal Quartz 42
○Hiroto Okabe, Shohei Chiashi, Junichiro Shiomi, Tadashi Sato, Shouichi Kono, Masami Terasawa, Shigeo Maruyama
- 3-6 Interplay of Hydrophobic and Electrostatic Interactions between Dispersants and Single-walled Carbon Nanotubes in Water 43
Shin Katakura, ○Masahito Sano

Graphene

- 3-7 Restoration of π -bands on the graphene “buffer layer” on SiC(0001) by low temperature oxidation 44
○Satoshi Oida, Fenton R. McFeely, James B. Hannon, Rudolf M. Tromp, Zhihong Chen, Yanning Sun, Damon B. Farmer and John J. Yurkas
- 3-8 Magnetism in Graphene Nanoribbons on Ni(111) 45
○Keisuke Sawada, Fumiyuki Ishii, Mineo Saito
- 3-9 Phase control on Magnetic State of Graphite Thin Films by Electric Field 46
○Minoru Otani, Mikito Koshino, Yoshiteru Takagi, Susumu Okada
- 3-10 Magnetism of Curved-Graphene and its Guest adsorption systems 47
○Kazuyuki Takai, Tuyoshi Suzuki, Toshiaki Enoki, Hiroto Nishihara, Takashi Kyotani
- 3-11 Electrode-Width Dependence of Transistor Properties of Graphene 48
○Ryo Nouchi, Tatsuya Saito, Katsumi Tanigaki

☆☆☆☆☆☆ Lunch Time (12:30-13:45) ☆☆☆☆☆☆

Thursday, March 4th

Special Lecture (13:45-14:15)

- 3S-6 A Brief Retrospective and Perspective of Graphene Research 6
○Hidefumi Hiura

Poster Preview (14:15-15:00)

Poster Session (15:00-16:20)

Endohedral Nanotubes

- 3P-1 Synthesis and Electrical Transport Properties of $C_{69}N$ Azafullerenes Encapsulated Single-Walled Carbon 132
○Yongfeng Li, Toshiro Kaneko, Rikizo Hatakeyama
- 3P-2 HR-TEM of KCl nano-crystals in single-walled carbon nanotubes 133
○Kaori Takai Hirose, Zheng Liu, Takeshi Saito, Kazu Suenaga
- 3P-3 Magnetic properties of carbon nanotubes filled with ferromagnetic metal 134
○Yusuke Matsui, Daijiro Hisada, Tetsuya Kaneko, Yuki Ichikawa, Hideki Sato, Yuji Fujiwara, Koichi Hata

Formation and Purification of Nanotubes

- 3P-4 A zigzag carbon nanotube: Growth and optical properties 135
○Yohji Achiba, Akihito Inoue, Yuuki Onishi, Takeshi Kodama, Toshiya Okazaki
- 3P-5 Mass-Production of Carbon Nanotubes by Semi-Continuous Fluidized-Bed 136
○Dong Young Kim, Hisashi Sugime, Kei Hasegawa, Toshio Osawa, Suguru Noda
- 3P-6 Diameter Control of SWNTs by Nano-diamond Catalyst 137
○Shohei Chiashi, Norihiro Hiramatsu, Daisuke Takagi, Yoshikazu Homma, Shigeo Maruyama
- 3P-7 SWNT Growth on $Al_2O_3/Co/Al_2O_3$ Multilayer Catalyst using Alcohol Gas Source Method in High Vacuum 138
○Yoshihiro Mizutani, Kuninori Sato, Takahiro Maruyama, Shigeo Naritsuka
- 3P-8 Change in Chirality Distribution of CoMoCAT Nanotubes Using Excimer Laser 139
○Masaki Hashimoto, Norio Maki, Masaaki Ashihara, Tsugio Matsuura
- 3P-9 Controllable yield of metallic single-walled carbon nanotubes by aerosol-assisted chemical vapor deposition 140
○Shinya Koike, Shunji Bandow, Yoshinori Ando
- 3P-10 Progress in the electrochemical cutting method of single-wall carbon nanotubes 141
○Shigekazu Ohmori, Takeshi Saito, Bikau Shukla, Motoo Yumura and Sumio Iijima
- 3P-11 Effect of Buffer Layers on the Synthesis of Carbon Nanotubes by Alcohol Catalytic Chemical Vapor 142
○Yuki Matsuoka, Masamichi Yoshimura
- 3P-12 Purification of mono-dispersed single-walled carbon nanotubes made with arc-burning technique in 143
nitrogen atmosphere
○Takashi Mizusawa, Shinzo Suzuki, Toshiya Okazaki, Yohji Achiba
- 3P-13 Adsorption of a Water Molecule on Graphene: Accuracy of Density Functional Methods with Localized 144
Orbitals
○Mari Ohfuchi
- 3P-14 SWNT Nucleation, Growth and Healing: Insights from Density-Functional Tight-Binding Molecular 145
Dynamics Simulations
○Alister J. Page, Stephan Irlé, Keiji Morokuma

Thursday, March 4th

3P-15	CVD Fabrication of Thin Carbon Nanocoil with Sn/Fe Catalyst on Mesoporous Particles ○Kotaro Takimoto, Masashi Yokota, Lim Siew Ling, Yoshiyuki Suda, Hirofumi Takikawa, Hitoshi Ue, Kazuki Shimizu, Yoshito Umeda	146
3P-16	High-purity semiconducting single-wall carbon nanotubes separation by density gradient ultracentrifugation ○Ye Feng, Yasumitsu Miyata, Shunjiro Fujii, Kiyoto Matsuishi, Hiromichi Kataura	147
3P-17	Catalysts and supports for rapid growth of vertically-aligned CNTs ○Keisuke Nomura, Kei Hasegawa, Suguru Noda	148
3P-18	Gas-phase synthesis of SWCNTs using ferrocene and C ₂ H ₂ /CH ₄ feedstocks ○Youkou Ishitsuka, Yoshikuni Sato, Toshio Osawa, Suguru Noda	149
3P-19	Experimental and numerical study on the effect of carbon feedstock decomposition on CVD synthesis of single-walled carbon nanotubes ○Bo Hou, Rong Xiang, Erik Einarsson, Junichiro shiomi, Akira Miyoshi, Shigeo Maruyama	150
3P-20	Raman Analysis with Multi Excitation Laser of Single-Walled Carbon Nanotubes Grown with Free Electron Laser Irradiation during Growth ○Keijiro Sakai, Daisuke Ishiduka, Takuya Somonura, Hiroki Takeshita, Kunihide Kaneki, Hirofumi Yajima, Nobuyuki Iwata, Hiroshi Yamamoto	151
3P-21	Synthesis of Carbon Nanotubes by a “Submarine”-style Substrate Heating Method ○Hiroyuki Yokoi, Hiroshi Momota, Tomohiro Iwamoto	152
3P-22	Effect of Catalyst Oxidation on Carbon Nanotube Growth by Low Pressure Chemical Vapor Deposition ○Tomoyuki Minami, Daiki Sawaguchi, Hideki Sato, Koichi Hata	153
3P-23	Influence of catalyst reduction conditions on single-walled carbon nanotube diameter ○Theerapol Thurakitsee, Erik Einarsson, Rong Xiang, Shohei Chiashi, Junichiro Shiomi, Shigeo Maruyama	154
3P-24	Low-temperature preparation of Carbon Nanotubes by Plasma Enhanced Chemical Vapor Deposition ○Masato Miyake, Toru Iijima, Kenneth Teo, Nalin Rupesinghe, Kazunori Horikawa, Kenjiro Onuma, Katsuyoshi Abe, Masayuki Satoh and Yasuhiko Hayashi	155
3P-25	Screening of Surfactants for Metallic/semiconducting Separation of Single-Wall Carbon Nanotubes Using Agarose Gel ○Takeshi Tanaka, Yasuko Urabe, Hiromichi Kataura	156
3P-26	CVD Growth of Vertically Aligned SWNT Films Using Dimethyl Ether as the Carbon Source ○Taiki Inoue, Hiroto Okabe, Bo Hou, Shohei Chiashi, Makoto Watanabe, Junichiro Shiomi, Shigeo Maruyama	157
3P-27	Sorting of Single-Wall Carbon Nanotubes combined by Gel-Separation and Density-Gradient Ultracentrifugation ○Daisuke Nishide, Huaping Liu, Takeshi Tanaka, Hiromichi Kataura	158
3P-28	Preparation of single wall carbon nanotubes by CO ₂ laser ablation method at room temperature ○Takashi Yamaguchi, Ryo Nakanishi, Ryo Kitaura, Shunji Bandow, Masako Yudasaka, Hisanori Shinohara, Sumio Iijima	159
Graphene		
3P-29	Carbon Spiral Helix, a Novel Nanoarchitecture Derived from Monovacancy Defects in Graphene ○Lili Liu, Xingfa Gao, Shigeru Nagase, Stephan Irle	160
3P-30	DFT investigation of stability of adatom adsorption on graphene ○Kengo Nakada, Akira Ishii	161

Thursday, March 4th

3P-31	Preparation and Evaluation of Graphene by Cleavage Method ○Keiichirou Matsuyama, Teppei Maeda, Nobuyuki Iwata, Hiroshi Yamamoto	162
3P-32	Raman spectroscopy of few-layer graphene grown on graphene flakes ○Ryota Negishi, Hiroki Hirano, Yoshihiro Kobayashi, Yasuhide Ohno, Kenzo Maehashi, Kazuhiko Matsumoto	163
Candidates for the Young Scientist Poster Award		
3P-33	Photomodification of Fullerene Bilayer Vesicles and Control of their Membrane Permeability to Water ○Akimitsu Narita, Koji Harano, Eiichi Nakamura	164
3P-34	Fabrication of transparent conductive films using carbon nanotubes encapsulating metal-nanowires ○Daeheon Choi, Ryo Kitaura, Yasumitsu Miyata, Hisanori Shinohara	165
3P-35	Growth control of Multi-Walled Carbon Nanotubes for fuel cell ○Shinya Kitamura, Rika Yamamoto, Takeshi Hashishin, Jun Tamaki	166
3P-36	Synthesis of Highly Electron Accepting [60]Fullerene Bisadduct ○Riyah S. Arastoo, Ken Kokubo, Hao Geng, Hsing-Lin Wang, Takumi Oshima, Long Y. Chiang	167
3P-37	Electronic transport properties of doped nanotube heterostructure ○Masahiro Sakurai, Susumu Saito	168
3P-38	Facile Synthesis of Water-Insoluble Lowly Hydroxylated Fullerenol and its Nanoparticle Property ○Naoki Kobayashi, Ken Kokubo, Takumi Oshima	169
3P-39	Highly Localized Photoelectrochemical Reaction of an Isolated Single-Walled Carbon Nanotube at Metal ○Mai Takase, Hideki Nabika, Satoshi Yasuda, Kei Murakoshi	170
3P-40	Preparation of TiO ₂ -filled MWNTs ○Hidechiro Ikenoko, Takeshi Hashishin, Jun Tamaki	171
3P-41	Stark effect of SWNT photoluminescence induced by external electric field ○Yuji Kawai, Hideyuki Maki, Tetsuya Sato	172

特別講演
Special Lecture

1S - 1 ~ 1S - 2

2S - 3 ~ 2S - 4

3S - 5 ~ 3S - 6

Recent Developments in Nanodiamond Research

Eiji Ōsawa

*NanoCarbon Research Institute, AREC, Faculty of Textile Science & Technology,
Shinshu University, 3-15-1 Tokita, Ueda, Nagano 386-8567, Japan*

My last review on this topic was printed in 2008[1], but the rapid progress in this area made the review already obsolete. The most remarkable step achieved during this period is the systematic calculations by Barnard of the geometrical and electronic structure on the models of our 5-nm diamond [2]. She found that these diamond particles are not just very small pieces of diamond crystals but have a well-defined core-shell structure with graphitic shells, which caused novel permanent polarization to occur and prominent surface charges appear on the facets. A new type of inter-particle interaction through coherent and incoherent interfacial Coulombic forces was presented. Long-enigmatic behaviors of dispersed 5-nm diamond particles like the high solubility in water and stability of the colloid solution without surfactants are understood [3].

In consonance with the theoretical perspectives, a new principle called ‘*number effect*’ emerged for 5-nm diamond particles, and probably applies in other smaller nanoparticles as well. As our diamond is extremely small, only a tiny weight involves surprisingly large number of individual particles, each of which behaves as independent platform of action. The principle, which is obvious but has been neglected so far, will be illustrated by unexpected lubrication capability of aqueous nanodiamond colloid. A number of promising applications being developed are based on the number principle: highly successful refill for mechanical pencil dispersed with only 0.01wt% of nanodiamond in graphite, a non-capsule type of drug delivery system for anti-cancer drugs [4], additives for complex plating of metal films, and a few others.

A new interpretation on the gross quasi-spherical shapes of 5-nm diamond particles will be given with their transformation pathways map.

[1] Ōsawa, E. *Pure & Appl. Chem.* **2008**, *80*, 1365-1379. [2] Barnard, A. *J. Mater. Chem.* **2007**, *17*, 4811; **2008**, *18*, 4038. [3] Ōsawa, E. *et al.*, *Diam. Rel. Mater.* **2009**, *18*, 904. [4] Zhang, X.-Q. *et al.* *ACS Nano* **2009**, 10.1021/nn900865g.

Corresponding Author: Eiji Ōsawa, TEL:+81-268-75-8381, FAX: +81-268-75-8551, E-mail: OsawaEiji@aol.com.

Biological Application of Fullerene Derivatives

Tadahiko Mashino, Shigeo Nakamura

Department of Pharmaceutical Sciences, Faculty of Pharmacy, Keio University,
Tokyo, 105-8512, Japan

Recently, biological activities of fullerene derivatives related to the unique chemical properties attract a great deal of attention. We have synthesized some types of water-soluble fullerene derivatives and have investigated their biological effects.

Antioxidant and anti-inflammatory activities of anionic fullerene derivatives

Anionic malonic acid-type fullerene derivative (**1**) showed antioxidant activities such as quenching of superoxide and relief from growth inhibition of *E. coli* by paraquat. Then, we investigated inhibition of NF κ B transcriptional activation by this fullerene derivative. These derivatives significantly attenuated tumor necrosis factor α -induced expression of inflammatory chemokine (CCL2/MCP-1). This result suggests that fullerene is potent lead compound against inflammatory diseases.

Antiproliferative effect of cationic fullerene derivatives: Generation of reactive oxygen species (ROS)

Cationic dimethylpyrrolidinium derivative (**2**) induced apoptosis and showed an antiproliferative effect on human leukemic cell line (HL-60). This derivative inhibited respiratory chain by ROS production. Fullerene derivative **2** also increased DCF fluorescence intensity, the marker of intracellular oxidative stress. Pretreatment with α -tocopherol reduced **2**-induced cell death and DCF fluorescence intensity, respectively. These results suggest that cationic fullerene derivative **2** increases intracellular ROS level.

Inhibition of HIV-reverse transcriptase (HIV-RT) by proline-type fullerene derivatives

Proline-type derivative (**3**) showed a very strong activity on HIV-RT inhibition and had no cytotoxicity. IC₅₀ value of **3** was lower about two orders than nevirapine, a clinically-used anti-HIV drug. We consider that **3** is able to bind HIV-RT more strongly because of its high hydrophobicity. Sulfonium-type derivative (**4**) had hepatitis C virus-RNA polymerase inhibition activity.

These activities depend on the properties of the fullerene core, while the substituents on the fullerene core control and modify the biological activities of fullerene derivatives. Our data show that the fullerene derivatives are good candidates for medicine.

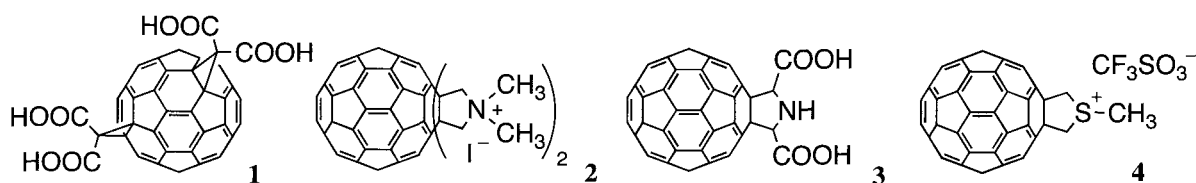


Fig. Fullerene derivatives

Corresponding Author: Tadahiko Mashino

Tel: +81-3-5400-2694, Fax: +81-3-5400-2691, E-mail: mashino-td@pha.keio.ac.jp

Organic Synthesis of Endofullerenes Encapsulating a Small Molecule

Yasujiro Murata

Institute for Chemical Research, Kyoto University, Uji, Kyoto 611-0011, Japan

Endohedral fullerenes are so far produced by arc-discharge method using metal-doped graphite, high-pressure/high-temperature treatment with noble gases, and ion implantation with nitrogen, phosphorus, and lithium. These methods are generally conducted under high-energy conditions,¹ so it is difficult to apply for encapsulation of a small molecule such as H₂ and H₂O owing to high reactivity toward fullerenes under these conditions.

The molecular surgical approach, involving creation of an orifice on the empty fullerene cage, insertion of a small guest through the orifice, and closure of the orifice with retention of the guest, is a promising method to synthesize yet-unknown endohedral fullerenes and their derivatives. Several open-cage fullerene derivatives have been reported so far, which can encapsulate He, H₂, H₂O, CH₄, NH₃, and CO.² However, examples of closure of the orifice are still limited to the synthesis of H₂@C₆₀, H₂@C₇₀, and (H₂)₂@C₇₀ from the open-cage fullerenes having a 13-membered ring orifice.^{3,4} In order to realize endohedral fullerenes encapsulating a small molecule which is larger than H₂, creation as well as restoration of a larger orifice are needed. Herein we report our approach to synthesize endohedral C₆₀ encapsulating a small molecule by means of organic synthesis under mild conditions.

- (1) T. Akasaka and S. Nagase, *Endofullerenes: A new family of carbon clusters*, Kluwer Academic Publishers, Dordrecht, The Netherlands, 2002.
- (2) For recent reviews, (a) M. Murata, Y. Murata and K. Komatsu, *Chem. Commun.*, **2008**, 6083. (b) G. C. Vougioukalakis, M. M. Roubelakis, M. Orfanopoulos, *Chem. Soc. Rev.*, **2010**, DOI: 10.1039/b913766a.
- (3) (a) K. Komatsu, M. Murata and Y. Murata, *Science*, **2005**, 307, 238. (b) M. Murata, Y. Murata and K. Komatsu, *J. Am. Chem. Soc.*, **2006**, 128, 8024.
- (4) M. Murata, S. Maeda, Y. Morinaka, Y. Murata and K. Komatsu, *J. Am. Chem. Soc.*, **2008**, 130, 15800.

Corresponding Author: Yasujiro Murata

E-mail: yasujiro@scl.kyoto-u.ac.jp, Tel: +81-774-38-3172, Fax: +81-774-38-3178

Standardization on carbon nanotubesHaeseong Lee ^{1*} and Ha-Jin Lee²

¹ *Department of Nanomaterials Engineering, Jeonju University, 1200 Hyojadong 3ga
Wansangu, Jeonju 560-759 Republic of Korea*

² *Jeonju Center of Korea Basic Science Institute, 664-14 Dukjin-Dong 1Ga, Jeonju 561-756
Republic of Korea*

When carbon nanotubes (CNTs) were introduced in 1991, the public were fascinated by their possible applications in many industry fields. However, no sooner had scientific knowledge been accumulated than technical bottleneck was appeared. Generally there exist two main problems, which obstruct practical applications of CNTs, such as dispersion and inhomogeneity in regard of electrical conductivity. In spite of these drawbacks, there have made many efforts how to apply this noble nanomaterial for practical usage and how to accelerate its industrialization. One of these efforts is standardization of CNTs.

In this presentation we are going to report our attempts to formulate an international standard which can categorize CNT products in terms of electrical property. Our standardization activity has been being discussed in IEC TC 113 and ISO TC229 since in 2007 under the title of “Technical Specification for the Electrical Characterization of Carbon Nanotubes (CNTs) Using 4-Probe Measurement”(Project number : PT62607). This specification contains two parts such as sample preparation and measurement methods. If this technical specification is completed, CNT manufacturers can use this standard method to evaluate their products and include the result in MSDS. More detail information on this project and discussion so far made in ISO TC229 and IEC TC113 will be introduced and further discussed.

For reference,

IEC : International Electrotechnical Commission

ISO : International Organization for Standardization

TC : Technical Committee

Corresponding Author : Haeseong Lee

E-mail : haeseong@jj.ac.kr

Tel : 082-19-240-4059

Fax : 082-63-220-2056

**CNT Coated Conductive Fiber “CNTEC”
- Development, Applications and Risk Assessment -**

○Eiji Akiba¹, Bunshi Fugetsu², Masaaki Hachiya³

¹*KURARAY LIVING Co., Ltd. Umeda Kita-ku, Osaka 530-8611, Japan*

²*CNT-Laboratory, Graduate School of Environmental Science,
Hokkaido University, Sapporo 060-0810, Japan*

³*Chakyu Dyeing Co., Ltd., Ichinomiya-City, Aichi 494-0001, Japan*

Carbon Nano-tubes (CNT) has excellent electrical conductive, heat conductive, and mechanical properties. So far, various applications have ever been tried, but because of CNT's aggregation behavior, it has been still not enough to utilize CNT's excellent properties. Recently, we have developed electrical conductive fiber “CNTEC”, CNT network is formed on the surface of the fiber, by the collaboration of the tubular level CNT dispersion technology¹⁾ and the precise coating technology to fiber using this dispersion²⁾.

The main features of “CNTEC” are adjustable electrical resistance at particular levels, stable electrical resistance, full face conductivity, high durability, soft touch tactile, light weight and compact. Utilizing these futures, we have developed antistatic fabrics, a brush of printer, an electrical conductive “Vectran”, a fabric heater and a sensor for living body. Especially, in comparison with common heater, “CNTEC” fabric heater performs thin, light-weight, high durability and full-face heating properties.

Moreover, because of some reports about the toxicity of CNT, many people have worried about the risk of the dropped CNT from CNT-using product. In order to build up social receptivity of “CNTEC” products, we are promoting the risk assessment of “CNTEC” products by the safety evaluation in the viewpoint of life-cycle assessment.

[1] 「Disassembling Single-walled Carbon Nanotube Bundles by Dipole/Dipole Electrostatic Interactions」
Bunshi Fugetsu, Wenhai Han, Chemistry Letters Vol.34, No9, 1218 (2005)

[2] Carbon 47 (2009) 527-544 Bunshi Fugetsu, Eiji Akiba, Masaaki Hachiya, Morinobu Endo

Corresponding Author: Eiji Akiba

E-mail: eiji_akiba@kuraray.co.jp

Tel: +81-6-6348-9365, Fax: +81-6-6348-9960

A Brief Retrospective and Perspective of Graphene Research

○Hidefumi Hiura^{1,2}, Hisao Miyazaki^{2,3} and Kazuhito Tsukagoshi^{2,3}

¹*Nano Electronics Research Laboratories, NEC Corporation, Tsukuba 305-8501, Japan*

²*International Center for Materials Nanoarchitectonics (MANA),*

National Institute for Materials Science (NIMS), Tsukuba 305-0044, Japan

³*CREST, Japan Science and Technology Agency, Kawaguchi, Saitama 332-0012, Japan*

Graphene is described by more fascinating keywords than we can count, for examples, ultra-thin crystal, “quantum critical” perfect fluid, hyper-relativistic electron gas, super-speed semiconductor, ultimate two-dimensional material and the most extreme material. Although an exaggerated image, if any, should be stripped away from graphene, almost all of the favorable remarks about graphene are well confirmed by the experimental and theoretical evidence. So far, scientific papers about graphene are increasing in number year after year as shown in Figure 1. This tendency is particularly prominent in the past half decade. As is evident, the rapid rise is due to the emergence of a single article reported by Novoselov *et al.* in 2004 [1]. Without doubt, their remarkable and beautiful results of the field effect in graphene have inspired not a few researchers to pay much attention to graphene. It could be more important for the rise of graphene that their preparation method of graphene from bulk graphite, namely, so-called Scotch-tape technique, is so simple to reproduce it.

In general, it is believed to be very obvious that the first experimental contribution to graphene research was carried out by Novoselov *et al.* [1]. Nonetheless, it is not so simple to draw a conclusion. Looking back in the past, Mizushima, Fujibayashi and Shiki released a brief note entitled “Electric resistivity and Hall coefficient of very thin graphite crystals” in 1971 [2]. Because the word of graphene was not invented at that time, they described graphitic flakes exfoliated from kish graphite as very thin graphite crystals. They obtained graphitic samples as thin as ~10nm by the cellophane-tape technique. Intriguingly, both Mizushima *et al.* and Novoselov *et al.* used a blue tape to peel graphite mechanically. Some people might say that graphitic samples by Mizushima *et al.* are too thick to regard them as graphene, however, a few layers of graphene nanoribbons were observed by AFM before 1995 [3] prior to the first report of Novoselov *et al.* [1].

In conjunction with the progress of graphene research, the future applications of graphene will be presented in our talk.

Acknowledgement: This work is partially supported by Japan Science and Technology Agency (JST).

[1] K. S. Novoselov, A. K. Geim, S. V. Morozov, D. Jiang, Y. Zhang, S. V. Dubonos, I. V. Grigorieva & A. A. Firsov, *Science* **306**, 666 (2004). [2] S. Mizushima, Y. Fujibayashi & K. Shiki, *J. Phys. Soc. Japan* **30**, 299 (1971). [3] T. W. Ebbesen & H. Hiura., *Adv. Mater.* **7(6)**, 582 (1995).

Corresponding Author: H. Hiura

Tel: +81-29-860-4872, FAX: +81-29-860-4706 (NIMS), E-mail: h-hiura@bq.jp.nec.com

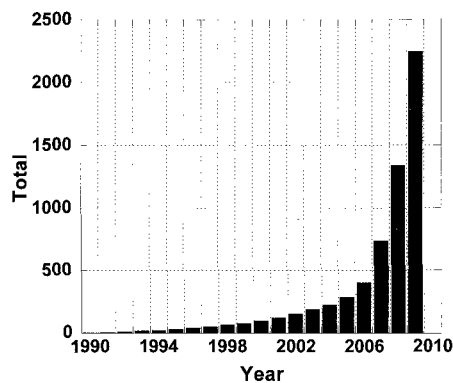


Figure 1. Total number of papers about graphene. The counting was done by searching a database (Scitation & SPIN, AIP) by the keyword of graphene.

一般講演
General Lecture

1-1 ~ 1-16

2-1 ~ 2-15

3-1 ~ 3-11

Exciton Dynamics in Hole-Doped Single-Walled Carbon Nanotubes

○Kazunari Matsuda, Yuhei Miyauchi, Takero Sakashita, and Yoshihiko Kanemitsu

Institute for Chemical Research, Kyoto University, Uji, Kyoto 611-0011, Japan

The optical properties of single-walled carbon nanotubes (SWNTs) have been the subject of intense investigation for their fundamental physics interest. The optically generated electron-hole pairs in SWNTs form stable excitons due to the strong Coulomb interactions, and the exciton dynamics determine the optical properties [1-3]. The optical properties are sensitive to the doped carriers. However, the understanding of the optical properties and exciton dynamics in the doped SWNTs are not fully understood. We studied on the optical properties and exciton dynamics of hole-doped SWNTs [3]. The photoluminescence (PL) spectra were measured as functions of the hole dopant (tetrafluorotetracyano-*p*-quinodimethane: F₄TCNQ) concentration [4]. The PL intensities for all chiral indices decrease with increasing F₄TCNQ concentration. We also measured the PL decay of hole-doped SWNTs using the femtosecond excitation correlation spectroscopy to understand the exciton decay dynamics relating to the PL intensity change. The PL decay times become shorter with increasing the F₄TCNQ concentration. Since the PL lifetimes are much shorter than the radiative exciton lifetimes in SWNTs [2], the PL lifetimes are primarily determined by nonradiative exciton decay processes. The decrease of the PL lifetime indicates that additional nonradiative decay paths are introduced by the doped holes. The nonradiative exciton relaxation can be explained by phonon-assisted indirect ionization processes in the hole-doped SWNTs [3,5].

References:

- [1] H. Hirori, K. Matsuda, Y. Miyauchi, S. Maruyama, and Y. Kanemitsu, *Phys. Rev. Lett.* 97, (2006) 257401.
- [2] Y. Miyauchi, H. Hirori, K. Matsuda, and Y. Kanemitsu, *Phys. Rev. B* 80, (2009) 081410 (R).
- [3] K. Matsuda, Y. Miyauchi, T. Sakashita, and Y. Kanemitsu, *Phys. Rev. B* in press.
- [4] N. Izard, S. Kazaoui, K. Hata, T. Okazaki, T. Saito, S. Iijima, and N. Minami, *Appl. Phys. Lett.* 92, (2008) 243112.
- [5] V. Perebeinos and P. Avouris, *Phys. Rev. Lett.* 101, (2008) 057401.

Corresponding Author: Kazunari Matsuda

Tel: +81-774-38-4515, Fax +81-774-38-4515, E-mail: matsuda@scl.kyoto-u.ac.jp

Photoluminescence Kinetics in PFO-Wrapped SWNT Papers

OT. Koyama¹, Y. Miyata², Y. Asada², H. Shinohara², H. Kataura³, and A. Nakamura¹

¹*Department of Applied Physics, Nagoya University, Nagoya 464-8603, Japan*

²*Department of Chemistry, Nagoya University, Nagoya 464-8602, Japan*

³*Nanotechnology Research Institute (NRI), AIST, Ibaraki 305-8562, Japan*

Organic conjugated polymers have attracted much attention for selective solubilization of carbon nanotubes. One of the well-known polymers is poly(9,9-dioctylfluorenyl-2,7-diyl) (PFO) [1]. PFO-wrapped single-walled carbon nanotubes (SWNTs) in toluene exhibit strong luminescence even at low tube concentrations. Toward future applications to luminescence materials, the polymer-wrapped SWNTs are preferable because of the solid form.

In this work, we investigate photoluminescence properties in a paper form of PFO-wrapped HiPco SWNTs. Figure 1 shows a photoluminescence emission (PLE) map in the sample. The PLE map involves fingerprints indicating luminescence from SWNTs with chiralities of (7,5), (7,6), (8,6), (8,7), and (9,7). The sample exhibits a relatively strong luminescence compared with film samples of surfactant-encapsulated SWNTs. The strong luminescence suggests substantial residuals of solubilized SWNTs due to a strong wrapping by PFO. Some other fingerprints are also involved (indicated by arrows) and suggest exciton energy transfer from wide to narrow gap SWNTs, e.g., from (7,5) and (7,6) tubes to (8,6), (8,7), and (9,7) tubes.

Figure 2 shows luminescence decay kinetics in SWNTs with the five chiralities shown above together with (9,8), (10,8), and (10,9). The decay curves are well fitted to double exponential functions. The time constants of the fast component are approximately the same value of $<\sim 1$ ps in all the curves, and this component is originated from the bundled SWNTs. The time constant of the slow component increases with increase of chiral index: 2 ps in (7,5) tubes and 10 ps in (10,9) tubes. Such behavior will be discussed considering exciton energy transfer to narrower gap SWNTs.

[1] A. Nish *et al.*, *Nat. Nanotechnol.* **2**, 640 (2007).

Corresponding Author: Takeshi Koyama

TEL: +81-52-789-4452, FAX: +81-52-789-5316,

E-mail: koyama@nuap.nagoya-u.ac.jp

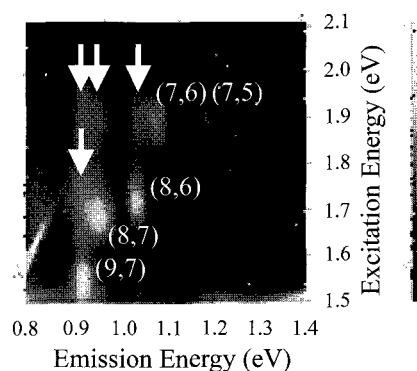


Fig. 1 PLE map.

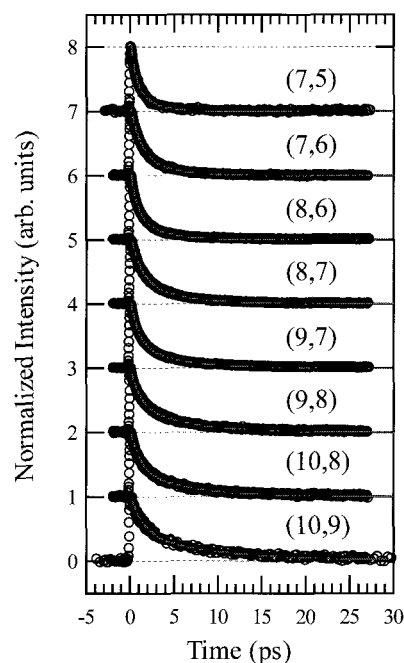


Fig. 2 Luminescence decay kinetics.

Environment Effects on Bundled Carbon Nanotubes Detected by Coherent Phonons

○Keiko Kato, Daisuke Takagi, Yoshihiro Kobayashi*, Hiroki Hibino, Atsushi Ishizawa, Katsuya Oguri, Hideki Gotoh, and Hidetoshi Nakano

NTT Basic Research Laboratories, Atsugi, Kanagawa, 243-0198, Japan

Carbon nanotubes (CNTs) are sensitively affected by environments around CNTs. Environment effects on CNTs have been widely investigated by Raman spectroscopy[1]. For bundled CNTs, however, it is difficult to probe environment effects by Raman spectrum since macroscopic forms of CNTs completely lose intrinsic properties of individual CNTs[2]. As an alternative way to Raman measurements, real-time observations of phonons, that is, coherent phonons have potential to detect environment effects on CNTs since coherent lattice vibrations would be dephased with disturbance from environment around CNTs. In this presentation, we report effects of aggregation of bundled CNTs on coherent phonons, induced with a drop of ethanol.

Time-resolved reflectivity was measured with 10-fs laser pulse with a center wavelength of 780 nm. Samples were CVD-grown bundled single-walled carbon nanotubes (SWCNT) on a glass-substrate. Time-resolved reflectivity of SWCNTs is analyzed with Fourier Transform (FT) (dotted line in Fig. 1(a)). It is found that coherent phonons of radial breathing mode (RBM), G-mode, and D-mode are observed. With a drop of ethanol on SWCNTs, coherent-phonon amplitudes of RBM and G-mode increase (gray line in Fig. 1(a)). However, no change is observed with Raman measurements (Fig. 1(b)). The present results indicate that coherent phonons can detect aggregation of CNTs by ethanol, which cannot be detected by conventional Raman measurements.

[1] D. A. Heller *et al.*, *J. Phys. Chem. B.* **108**, 6905 (2004).

[2] D. N. Futaba *et al.*, *Nature Mat.* **5**, 987 (2006).

*: Present address: Osaka Univ., Osaka, 565-0871, Japan

Corresponding Author: Keiko Kato

TEL: +81-46-240-3441, FAX: +81-46-270-2361, E-mail: kkato@will.brl.ntt.co.jp

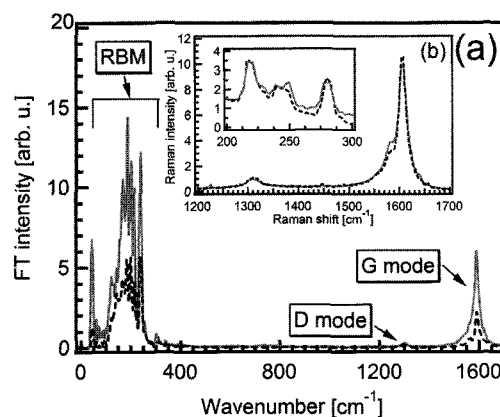


Fig. 1(a) FT spectrum of the time-resolved reflectivity of SWCNTs (b) Raman spectrum of SWCNTs. Inset shows the spectrum for RBM. Black dotted and gray solid lines correspond to the data taken before and after a drop of ethanol, respectively.

Short wavelength electroluminescence from single-walled carbon nanotubes with high bias voltage

Hideyuki Maki¹, Satoru Suzuki², Norihito Hibino^{1,2}, Yoshihiro Kobayashi² and Tetsuya Sato¹

¹*Department of Applied Physics and Physico-Informatics, Faculty of Science and Technology, Keio University, Hiyoshi, Yokohama 223-8522, Japan*

²*NTT Basic Research Laboratories, Nippon Telegraph and Telephone Corporation, Morinosato-Wakamiya, Atsugi 243-0198, Japan*

Carbon nanotube field-effect transistor (CNFET) is expected to be utilized for a light emitting device because an electroluminescence (EL) is demonstrated in CNFETs with ambipolar and unipolar characteristics by applying a bias voltage. In the EL, however, only the long wavelength ($\lambda > \sim 1500$ nm) has been reported due to the difficulty of the electrical excitation of the wide band-gap SWNT. In this study, we obtained the short wavelength EL by applying high bias voltage. The high bias voltage increases the accelerating field defined by the voltage drop, and make it possible to increase the impact excitation rate in the wide band-gap SWNTs. However, SWNTs are easy to be electrically broken by applying high bias voltage due to current induced oxidation. In this study, we constructed the EL measurement system, in which the electrical and EL measurement can be carried out in high vacuum to prevent current induced oxidation. In addition, we used carbon nanotubes lying on the substrate i.e., unsuspended carbon nanotubes to dissipate heat at high bias voltage.

The typical EL spectra from the p-type unipolar device as a function of the bias voltage V_{ds} at $V_g = -20$ V is shown in Fig. 1(a). The short wavelength EL emission at ~ 1170 nm (~ 1.06 eV) is clearly observed at $V_{ds} > 11$ V. The V_{ds} dependence of the current and the EL intensity is shown in Fig. 1(b). At $V_{ds} > 11$ V, the EL intensity is rapidly increased with increasing V_{ds} . By comparison between the EL and the current result in Fig. 1(b), the EL intensity exhibits exponential dependence on the current [Fig. 1(b), inset]. In the impact excitation mechanism, the emission intensity should be proportional to the impact excitation rate $\exp(-\varepsilon_{th}/\varepsilon)$, where ε is the electric field and ε_{th} is the threshold electrical field for impact excitation. Because ε_{th} becomes large for a wide band-gap nanotube, high electric field ε is necessary to obtain the short wavelength EL emission. In our experiment, we have obtained the short wavelength EL emission from a CNFET by applying high bias voltage, which causes an increase of electric field in a nanotube.

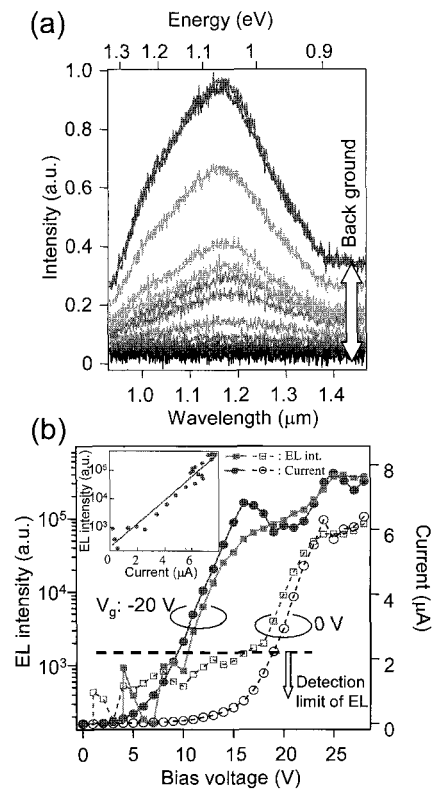


Fig. 1. (a) EL spectra as a function of the bias voltage V_{ds} at $V_g = -20$ V. (b) V_{ds} dependence of the current and the EL intensity at $V_g = 0$ and -20 V (inset: EL intensity v.s. current).

Corresponding Author: Hideyuki Maki

E-mail: maki@appi.keio.ac.jp,

Tel: +81-45-566-1643, FAX: +81-566-1587

Observation of Bound Tween80 Surfactant Molecules on Carbon Nanotubes in an Aqueous Solution using Pulsed Field Gradient Nuclear Magnetic Resonance Method

○Haruhisa Kato¹, Ayako Nakamura¹, Kohei Mizuno², Manabu Shimada³, Kayori Takahashi¹, and Sinichi Kinugasa¹

¹ *Polymer Standards Section Japan (PSSJ), National Metrology Institute of Japan (NMIJ), National Institute of Advanced Industrial Science and Technology (AIST), Tsukuba, 305-8565 Japan*

² *Thermophysical Properties Section, National Metrology Institute of Japan (NMIJ), AIST, Tsukuba, 305-8563 Japan*

³ *Department of Chemical Engineering, Graduate School of Engineering, Hiroshima University, Higashi-Hiroshima 739-8527, Japan.*

The pulsed field gradient nuclear magnetic resonance (PFG-NMR) method was used to characterize Tween80 molecular surfactants in a stable single-walled carbon nanotube (SWCNT) aqueous dispersion. The slow diffusion of Tween80 surfactant molecules in the aqueous dispersion was directly observed using PFG-NMR. The fast diffusion component of Tween80 was assigned to bulk Tween80 molecules and the slowly diffusing Tween80 molecules were attributed to the strongly adsorbed molecules on the SWCNTs in the aqueous solution. The calculated amount of the bound Tween80 molecules was approximately 12 % of the total amount of Tween80 molecules in the aqueous dispersion, contributing to the stability of the CNT aqueous dispersion.

This study is the first investigation of the amount of bound surfactant on CNT molecules using PFG-NMR method without any treatment of the SWCNT dispersion to our knowledge. This study has an importance to investigate the amount of bound surfactant molecules on CNT in the field of human toxicity assessment of CNTs. This study also plays an important role in producing a new application of CNT in research of functional materials.

[1] H. Kato, K. Mizuno, M. Shimada, A. Nakamura, K. Takahashi, K. Hata, and S. Kinugasa, *Carbon*, **2009**, 47, 3434.

Corresponding Author: Haruhisa Kato

TEL: +81 (0)29 861 4895, FAX: +81 (0)29 861 4618, E-mail: h-kato@aist.go.jp

Surface-Enhanced Raman Scattering from an Isolated Single-Walled Carbon Nanotube at the Gap of Metal Nanodimer

○Satoshi Yasuda, Mai Takase, Keiichiro Komeda, Masanobu Nara,
Hideki Nabika and Kei Murakoshi

Division of Chemistry, Graduate School of Science, Hokkaido University, Sapporo 060-0810, Japan

Understanding of vibrational, chemical and electronic properties of a single SWNT has become major objectives in recent research [1]. In particular, surface-enhanced Raman Scattering (SERS) measurement, which results in the localized surface plasmon resonance at the vicinity of metal surface allows us more sensitive characterization of a single SWNT. Although SERS measurements have demonstrated for individual SWNTs deposited on rough metal surface and decorated with nano metal particles [2], there are difficulties in measuring highly-sensitive and reproducible SERS spectra of a single SWNT due to the poorly optimization of position, size and orientation of metal structures. Recently, using angle-resolved nanosphere lithography technique (AR-NSL), we have succeeded in optimizing the position and the structure of metal nanodimer arrays for obtaining maximal surface plasmon resonance and consequently the intense SERS [3]. In this study, the well-defined Au nanodimer arrays with the SERS active (Fig. 1(a) and (b)) were employed for measuring highly sensitive SERS spectra of a single SWNT. Highly dispersed SWNT/SDS solution was dropped onto the substrate with Au nanodimer arrays, and SERS measurement was performed. We observed highly-intense SERS spectra (Fig. 1(c)) and single RBM peak with narrow FWHM (e.g. 5 and 3 cm^{-1} for each metallic and semiconducting tube). This result strongly indicates that measured SWNT is a single which is located between the nano-metal dimer. Notably, this method allows us to evaluate intermediate frequency modes (IFMs) of a single SWNT, which are difficult to observe at normal resonance Raman measurements. We found that certain IFMs increases drastically with the increase of the local defect density of the structure as well as D band, suggesting that IFMs serve to identification of defects and chemical reaction monitoring.

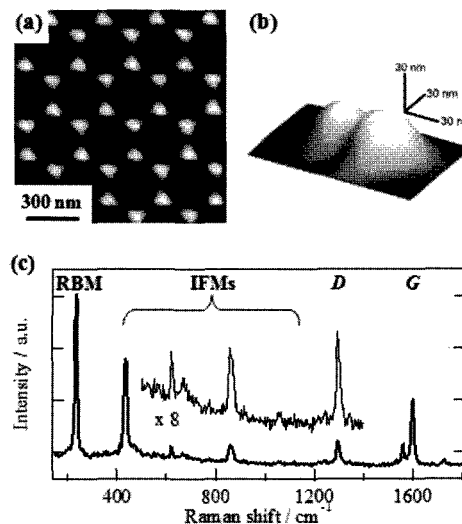


Fig. 1. (a) AFM 2-D and (b) 3-D images of Au nano-dimer arrays. (c) SERS spectra of a single semiconducting (11, 3) SWNT ($\omega_{\text{RBM}} = 234 \text{ cm}^{-1}$, $d = 1.0 \text{ nm}$) under 785 nm excitation.

[1] S. Yasuda, T. Hiraoka, D. N. Futaba, M. Yumura, K. Hata, *Nano Lett.* **9**, 769-773 (2009).

[2] T. Yano, P. Verma, Y. Saito, T. Ichimura, S. Kawata, *Nat. Photonics* **3**, 473-477 (2009)

[3] (a) Y. Sawai, B. Takimoto, H. Nabika, K. Ajito, K. Murakoshi, *J. Am. Chem. Soc.*, **129**, 1658-1662 (2007), (b) M. Takase, S. Yoshitaka, H. Nabika, K. Murakoshi, *Trans. Mater. Res. Soc. Jpn.*, **32**, 409-412 (2007)

Corresponding Author: Satoshi Yasuda,

TEL & FAX: +81-(0)11-706-4811, E-mail: satoshi-yasuda@sci.hokudai.ac.jp

E_{11} and E_{22} Bandgap Modulation of Semiconducting Single -Walled Carbon Nanotube by Adsorbing Aluminium Clusters

Yoshiteru Takagi^{1,2} and Susumu Okada^{1,2}

¹Center for Computational Sciences and Graduate School of Pure and Applied Science,
University of Tsukuba, Tsukuba 305-8577, Japan

²CREST, Japan Science and Technology Agency, CREST, 5 Sanbancho, Chiyoda-ku, Tokyo
102-0075, Japan

Since the hybrid structure of carbon nanotube and other materials are essential in the electronic devices, it is important to understand the fundamental issues of optical properties of CNT-complexes with the conventional materials. We investigate electronic structures of a semiconducting zigzag SWCNT absorbed by an Al atom or small Al clusters by the first principle calculations. Our calculations reveal that hybridization between SWCNT and an Al atom is too weak to lead substantial modulation on the electronic structures of an isolated SWCNT. Thus, we easily assign E_{11} and E_{22} band gap of SWCNT/Al complexes. However, the Al atom adsorbed on SWCNTs induces systematic shift of the optical gap: E_{11} bandgap is wider and E_{22} bandgap is narrower for (11,0), (14,0), and (17,0) SWCNT upon the adsorption [Fig. 1(c)]. In sharp contrast, E_{11} bandgap is narrower and E_{22} bandgap is wider for (10,0), (13,0), and (16,0) upon adsorption [Fig. 1(d)]. We will discuss the origin of the systematic shift of energy gap, and also show the electronic structures of SWCNT with small Al clusters.

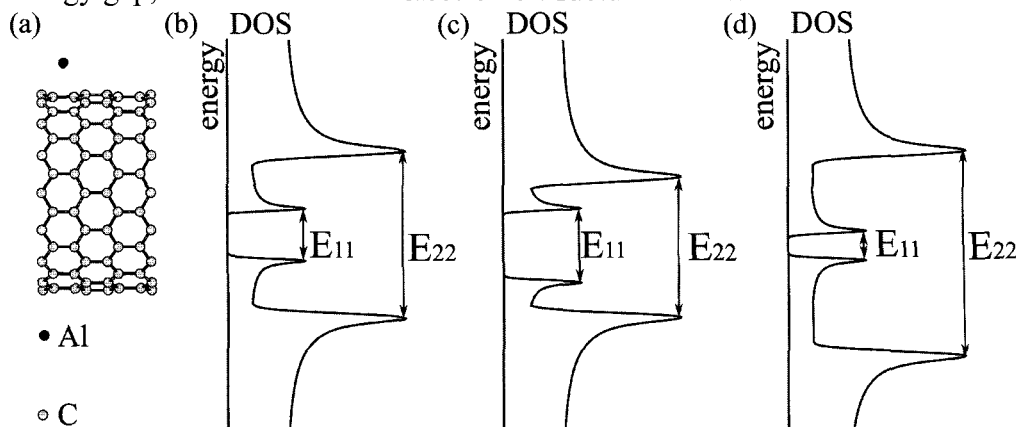


Fig.1 (a) A structural model of SWCNT absorbed by an Al atom. Schematic pictures of E_{11} and E_{22} band gap for (b) isolated zigzag SWCNT (c) an Al adsorbed (11,0), (14,0), and (17,0) SWCNT (d) an Al adsorbed (10,0), (13,0), and (16,0).

Corresponding Author: Yoshiteru Takagi

E-mail: ytakagi@comas.frsc.tsukuba.ac.jp, TEL: +81-29-853-5600(8233), FAX:+81-29-853-5924

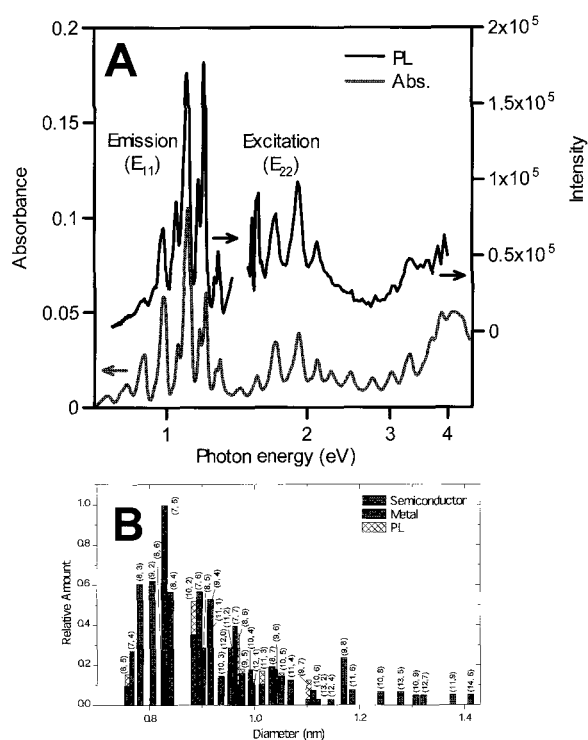
The Fundamental Importance of Background Analysis in Precise Characterization of Single-wall Carbon Nanotubes by Optical Absorption Spectroscopy

○Takeshi Saito^{1,2}, Shigekazu Ohmori¹, Masayoshi Tange¹, Bikau Shukla¹, Toshiya Okazaki^{1,2},
Motoo Yumura¹ and Sumio Iijima¹

¹*Nanotube Research Center, National Institute of Advanced Industrial Science and
Technology (AIST), Tsukuba 305-8565, Japan*

²*PRESTO, Japan Science and Technology Agency,
Kawaguchi 332-0012, Japan*

For precise characterizations of SWCNTs by optical absorption spectroscopy, the background extinction originated from precipitable impurities and SWCNTs' bundles has been experimentally determined by interval centrifugation and difference spectrum (IC-DS) technique. The baseline correction using the lineshape of obtained background extinction revealed the actual absorption spectrum of absolutely de-bundled SWCNTs with detailed features. The chirality distribution including both semiconductive and metallic SWCNTs was evaluated by deconvoluting the corrected absorption spectrum into multiple Lorentzian lines, that was well consistent with the result of photoluminescence (PL) mapping measurements as shown in Fig. 1. The baseline correction by IC-DS technique provides a useful analysis method for characterizing SWCNTs, complement/ alternative to the similar analysis done by PL spectroscopy. This work has been partially supported by New Energy and Industrial Technology Development Organization (NEDO) project.



Corresponding Author : Takeshi Saito
E-mail : takeshi-saito@aist.go.jp
Tel: +81-29-861-6276, Fax: +81-29-861-4413

Site-selective deposition of single-wall carbon nanotube film using patterned self-assembled monolayer and its application to thin-film transistors

○Shunjiro Fujii¹, Takeshi Tanaka¹, Takeo Minari², Kazuhito Tsukagoshi^{2,3},
Hiromichi Kataura^{1,3}

¹*Nanotechnology Research Institute, National Institute of Advanced Industrial Science and Technologies (AIST), Tsukuba, Ibaraki 305-8562, Japan*

²*International Center for Materials Nanoarchitectonics, NIMS, Tsukuba 305-0044, Japan*

³*JST, CREST, Kawaguchi 330-0012, Japan*

Semiconducting Thin-film transistors (TFTs) using single-wall carbon nanotubes (SWCNTs) have attracted a great deal of attention for their possible use in transparent, flexible, high-speed, and high-current electronics. Recently, we achieved performance enhancement of solution-processed TFTs by using semiconductor-enriched SWCNTs (s-SWCNTs) separated by agarose gel [1,2]. However, for a realization of integrated circuits by solution processes, appropriate fabrication technique for patterning SWCNT films in designed geometry is required. In this work, we performed a site-selective deposition of SWCNT film by patterning self-assembled monolayers (SAMs) of octadecyltrichlorosilane (OTS) on SiO₂/Si surface.

The OTS-SAM was patterned by UV light and then partly replaced by the SAM of 3-aminopropyltriethoxysilane (APTES). Due to the different affinity with each SAM, drop-cast s-SWCNT solution was selectively placed onto the area covered with APTES, resulting in a selective adsorption of SWCNTs on the channel region as shown in the AFM images (Fig. 1). TFTs were fabricated from the patterned s-SWCNT films with top-contact and back-gate geometry. Detailed fabrication procedure and device characteristics will be discussed.

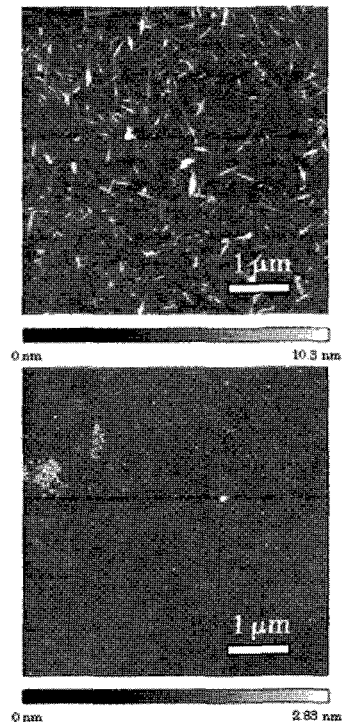


Fig.1 AFM images of SiO₂/Si substrate :
regions covered with (a) APTES and (b) OTS.

References:

- [1] T. Tanaka et al., *Nano Lett.* **9** (2009) 1668
[2] S. Fujii et al., *Appl. Phys. Express* **1** (2009) 114001

Corresponding Author: Hiromichi Kataura

E-mail: h-kataura@aist.go.jp, **Tel:** +81-29-861-2551, **Fax:** +81-29-861-2786

Fabrication of high performance thin film transistor with plasma CVD grown single-walled carbon nanotubes and elucidation of its working mechanism

○S. Kuroda, T. Kato, T. Kaneko, and R. Hatakeyama

Department of Electronic Engineering, Tohoku University, Sendai 980-8579, Japan

Since single-walled carbon nanotubes (SWNTs) have great and unique electrical properties, development of high performance SWNTs field effect transistor (SWNTs-FET) is expected to be a critical component of next-generation nano electronics. On purpose to realize the high performance SWNTs-FET, it is necessary to selectively utilize semiconducting SWNTs as a channel of FET. Although several groups reported the preferential growth of semiconducting SWNTs by plasma CVD [1, 2], the detailed mechanism for this phenomenon still remains to be clarified. Based on this background, we investigate electrical transport properties of thin film SWNTs-FET as a function of diameter distribution of SWNTs grown by diffusion plasma CVD [3].

The SWNTs production is carried out on a Co 0.2 nm/SiO₂ 300 nm/Si substrate. SWNTs-FETs are fabricated by forming source and drain electrodes (Pd) on the top of SWNTs films using photo-lithography technique. Figure 1 represents Raman spectra of SWNTs synthesized at different growth temperature (T) = 600, 700, 800 °C. The SWNTs main diameter tends to increase with an increase in the growth temperature. Figure 2 shows the concentration of working device as a function of main tube diameter. Note that we count the devices which show on/off ratio more than 5 as a working device. SWNTs-FET consists of large diameter SWNTs is found to show good performance compared with other devices made by relatively small diameter tubes. This could be explained by the difference of the reactivity in each SWNTs, which strongly depends on the tube diameter and metallicity.

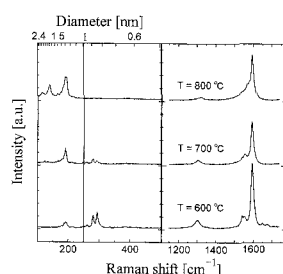


Fig. 1: Raman spectra of SWNTs grown at different growth temperature.

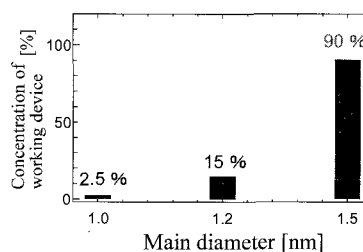


Fig. 2: Concentration of the working devices as a function of tube diameter.

[1] Y. Li, D. Mann, M. Rolandi, W. Kim, A. Ural, S. Hung, A. Javey, J. Cao, D. Wang, E. Yenilmez, Q. Wang, J. F. Gibbons, Y. Nishi, and H. Dai, *Nano Lett.* **4**, 317, (2004).

[2] L. Qu, F. Du and L. Dai, *Nano Lett.* **8**, 2682 (2008).

[3] T. Kato and R. Hatakeyama, *J. Am. Chem. Soc.* **130**, 8101 (2008).

Corresponding Author: Shunsuke. Kuroda

TEL: +81-22-795-7046, FAX: +81-22-263-9225, E-mail: kuroda@plasma.ecei.tohoku.ac.jp

Incorporating of carbon nanotubes in donor-acceptor based heterojunction solar cells

***Golap Kalita, Koichi Wakita and Masayoshi Umeno**

Chubu University, Department of Electrical and Electronics Engineering,

1200 Matsumoto-Cho. Kasugai-shi, Aichi 487-8501, Japan

E-mail: golapkalita@yahoo.co.in

Incorporation of carbon nanotubes (CNTs) in the active layer of donor-acceptor based solar cells and thereby significantly enhanced device performance has been demonstrated. The enhanced device performance with introduction of CNTs is attributed to better hole transportation and large surface area for exciton dissociation in the active layer. We have introduced different modified CNTs for organic solar cells application. Work function of MWNTs is in the range of 4.5~5.1 eV, which is close to valance band of polymer; it signifies possible hole transportation through MWNTs in the active layer.

Here, we present fabrication of bulk heterojunction solar cells based on poly (3-hexylthiophene) (P3HT) and fullerene derivative (PCBM) incorporating functionalized CNTs. Enhanced device performance was achieved for P3HT:PCBM solar cells incorporating a certain amount of CNTs in the active layer. P3HT:PCBM bulk heterojunction solar cells were fabricated with a thin layer of TiO_x between the active layer and top electrode as a hole blocking layer. Fabricated device with the structure ITO/PEDOT:PSS/CNTs+P3HT:PCBM/ TiO_x /Al shows short circuit current density (J_{sc}), open circuit voltage (V_{oc}), fill factor (FF) and conversion efficiency as 10.52 mA/cm², 0.50 V, 42 % and 2.2 %, respectively. The TiO_x layer also acts as a barrier for shorting and shunting in the device, caused by the presence of metallic CNTs. In the fabricated device, CNTs provide efficient charge transportation path and the TiO_x layer acts as an electron selective layer.

References:

1. G. Kalita, M. Masahiro, W. Koichi and M. Umeno, Solid State Electronics, in press (2010).
2. G. Kalita, H.R. Aryal, S. Adhikari, K. Wakita and M. Umeno, J. Nanosci. Nanotechnol. 10, 1-5, (2010).
3. G. Kalita, H.R. Aryal, S. Adhikari, R. Afre, T. Soga, M. Sharon, K. Wakita and M. Umeno, Jour. Phys. D: Appl Phys., 42, 115104, (2009).
4. G. Kalita, S. Adhikari H.R. Aryal, M. Umeno, R. Afre, T. Soga and M. Sharon, Appl. Phys. Lett. 92, 063508, (2008).
5. G. Kalita, S. Adhikari H.R. Aryal, M. Umeno, R. Afre, T. Soga and M. Sharon, Appl. Phys. Lett. 92, 123508, (2008).

Bottom-up assembly of carbon nanotubes electrocatalyst for polymer electrolyte fuel cell

○Tsuyohiko Fujigaya¹, Kazuya Matsumoto², Naotoshi Nakashima^{1,2}

¹*Department of Applied Chemistry, Graduate School of Engineering
Kyushu University, Fukuoka, Japan*

²*JST-CREST, 5 Sanbancho, Chiyoda-ku, Tokyo 102-0075, Japan*

Abstract: Polybenzimidazole (**PBI**: Fig. 1) is widely known as a promising candidate for electrolyte membrane of polymer electrolyte fuel cell (PEFC) operating under dry condition. On the other hand, carbon nanotubes

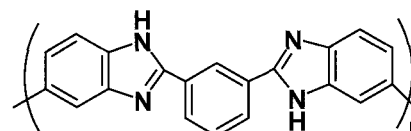
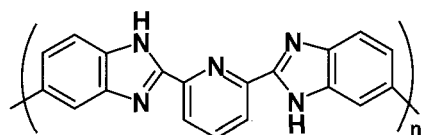


Fig. 1 Polybenzimidazole (**PBI**).

(CNTs) have been emerged as a better carbon support material than conventional material such as carbon black. We have reported the **PBI** is adsorbed onto the surface of CNTs and acts as the good solubilizer [1]. By taking advantage of stable wrapping of **PBI** on CNTs, we utilized this composite as a novel carbon supporting materials for loading the metal catalyst such as platinum (Pt). As the result, the **PBI**-wrapped CNTs show better efficiency of Pt loading than that of pristine CNTs due to the coordination between Pt ion and **PBI**. Furthermore, the obtained electrocatalyst (CNT/**PBI**/Pt) shows excellent Pt utilization



efficiency mainly due to the formation of ideal interfacial structure constructed by the CNTs, **PBI** and Pt [2]. However, we also noticed the electrochemically active area (ECSA) was gradually decreased during long time operations caused by the aggregation of the Pt.

In this study, we replaced **PBI** to pyridine-containing PBI (**PyPBI**: Fig. 2), which have a wider operating temperature than **PBI** for the new electrocatalyst (denote as CNT/**PyPBI**/Pt) and found similar electrocatalyst formation (Fig. 3)[3]. Detail studies in oxygen reduction, methanol oxidation for CNT/**PyPBI**/Pt and results will be explained in the presentation.

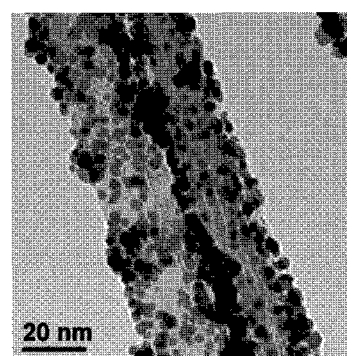


Fig. 3 TEM image for the CNT/**PyPBI**/Pt.

- References:** [1] M. Okamoto, T. Fujigaya, N. Nakashima, *Adv. Funct. Mater.* **2008**, 18, 1776-1782
[2] M. Okamoto, T. Fujigaya, N. Nakashima, *Small* **2009**, 5, 735-740.
[3] T. Fujigaya, M. Okamoto, N. Nakashima *Carbon* 2009, 47, 3227-3232.

Corresponding Author: Naotoshi Nakashima

E-mail: nakashima-tcm@mail.cstm.kyushu-u.ac.jp

Tel&Fax: +81-92-802-2840

Morphology Change of Multi-Walled Carbon Nanotube Field Emitters Studied by in-situ Transmission Electron Microscopy

○T. Ichihashi¹, F. Nakamura², R. Yuge¹, M. Kosaka¹, K. Toyama¹

¹*Nanoelectronics Research Laboratories, NEC Corporation, Tsukuba 305-8501, Japan*

²*National Metrology Institute of Japan, AIST, Tsukuba 305-8563, Japan*

Carbon nanotubes (CNTs) have promising properties such as small tip radius, high aspect ratio and toughness for field emission electron sources. It is important for its application to know the stability and the life of the CNT emitters. We studied the stability of field emission current and morphology by in-situ transmission electron microscopy.

CNTs used in this study are multi-walled CNTs produced by chemical vapor deposition method. CNT emitter was fixed on the STM tip by electron beam induced deposition. The STM tip was settled on TEM-STM holder (Nanofactory Instruments AB) and measured I-V curves.

Correlation between F-N current and CNT morphology were shown in figure 1. The shape of the CNT emitter was changed when the emission current was jumped. We observed two modes of the evaporation of carbon atoms from the top of the CNT emitter, one was from outside and the other was inside of the CNT.

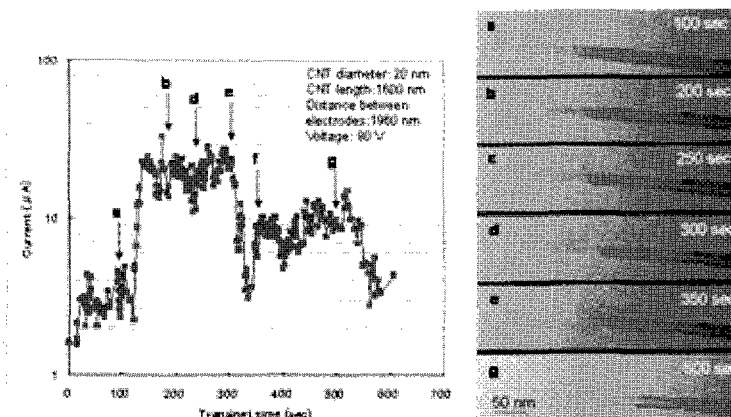


Fig.1 Correlation between F-N current and MWCNT morphology

Corresponding Author: Toshinari Ichihashi¹, Fumishige Nakamura²

¹**E-mail:** t-ichihashi@ap.jp.nec.com **Tel&Fax:** +81-29-850-1134, +81-29-856-6137

²**E-mail:** fumishige-nakamura@aist.go.jp **Tel&Fax:** +81-29-861-4166, +81-29-861-4039

HRTEM observation of a crystalline-cluster phase inside ionic liquids freestanding on CNT super-thin films

Shimou Chen¹, Keita Kobayashi², Ryo Kitaura¹, Yasumitsu Miyata¹, Kazu Suenaga²,
Hisanori Shinohara¹

¹ *Department of Chemistry and Institute for Advanced Research, Nagoya University, Nagoya, 464-8602, Japan;*

² *Nanotube Research Center, National Institute of Advanced Industrial Science and Technology, Tsukuba 305-8565, Japan*

Insight into the microstructure of bulk liquids is essential for understanding the macroscopic properties of liquids and chemical reaction processes in solution. The recent advances in high-resolution spectroscopy together with the first-principle calculations have revealed an intriguing feature of liquids: the co-existence of crystalline-cluster and liquid phases at nanometer-scale¹⁻². However, the direct observation of such crystalline clusters has been extremely difficult and has not yet been realized since usual molecular liquids are extremely frangible, instantaneous² and especially volatile, which has precluded any high-resolution spectroscopy under high-vacuum conditions.

Ionic liquids have received intense worldwide scrutiny as environmentally friendly solvents because of their low-vapor-pressure characteristics. Similar to water and other molecular liquids, recent scattering experiments and simulation works also suggested the existence of micro-heterogeneous structure in ionic liquids³. Likewise, there is still no direct evidence on this point. Here we report the first observation of a crystalline-cluster phase inside an imidazolium-based room-temperature ionic liquid by high-resolution transmission electron microscopy (HRTEM), with the aid of a special carbon nanotube grid incorporating nanosized-holes which can support a freestanding monolayer ionic liquid film. Since the freestanding liquid film may be regarded as one intact building block for the bulk liquid, we can anticipate that the present investigation is an important starting point for more sophisticated structural studies on the microstructure of liquidus materials.

[1] Ludwig, R. *Angew. Chem. Int. Ed.* 40, 1808–1827 (2001).

[2] Smith, J. D. et al. *Proc. Natl. Acad. Sci. USA* 102, 14171–14174 (2005).

[3] Del Pópolo, M. G., Kohanoff, J., Lynden-Bell, R. M. Pinilla, C.. *Acc. Chem. Res.* 2007, 40, 1156–1164

Acknowledgements We thank Professors K. Jiang and S. Fan for providing special CNT-TEM grids.

Corresponding Author: Hisanori Shinohara

TEL: +81-52-789-2482, FAX: +81-52-789-1169, E-mail: noris@nagoya-u.a.jp

Preparation of silica gel microparticles coated by pristine carbon nanotubes for the liquid chromatography stationary phase

○JongTae Yoo¹, Tsuyohiko Fujigaya¹, and Naotoshi Nakashima^{1,2}

¹*Department of Applied Chemistry, Graduate School of Engineering, Kyushu University, 744 Motoooka, Fukuoka 819-0395, Japan*

²*Japan Science and Technology Agency, CREST, 5 Sanbancho, Chiyoda-ku, Tokyo, 102-0075, Japan*

Carbon nanotubes (CNTs) have unique π -rich, hydrophobic and curvature surfaces. There, interfacial interactions of CNTs with molecules have been the focus of interests in the aspect from solubilization of CNTs through physisorption [1] and many applications. However, no systematic investigations for the degree of interactions have been carried out due the lack of evaluation methodology. In this situation, the chromatography-based analysis using CNTs as a stationary phase provides precise as well as higher throughput method. We succeeded the first non-covalent coating of the silica gel with pristine SWNTs and the utilization of the gel for liquid chromatography stationary phase.

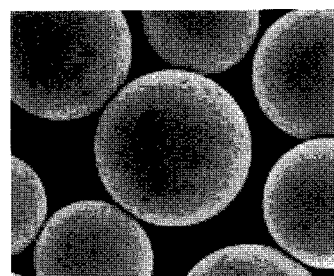


Fig. 1. SEM image of the SWNT/NH₂-silica.

Figure 1 shows silica gel microparticles coated with SWNT monolayer (denote as SWNT/NH₂-silica) prepared by the simple mixing of pristine SWNTs dispersed in the 1-methyl-2-pyrrolidinone (NMP) with the amine-functionalized silica gel. We fabricated the HPLC column packed with the SWNT/NH₂-silica (denote as SWNT/NH₂-column) and NH₂-silica (denote as NH₂-column) as well. SWNT/NH₂-column gave longer retention time (11.2 min) than that of NH₂-column (3.7 min) for the same solute, which clearly indicate SWNTs on the gel served as an affinity-based stationary phase due to the stronger interaction between SWNTs and porphyrin than NH₂ group and porphyrin.

We believe that SWNT/NH₂-column provide the promising opportunity for the systematic studies using wide range of molecules to achieve the deep understanding of the degree of interaction between CNTs and molecules.

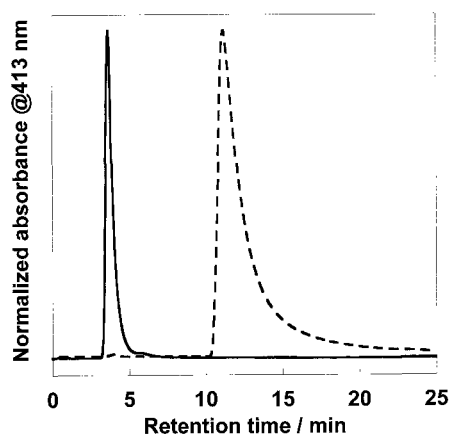


Fig. 2. Chromatogram of porphyrin derivative obtained from NH₂-column (solid line) and SWNT/NH₂-column (dotted line).

[1] (a) N. Nakashima, T. Fujigaya, *Chem. Lett.*, **36**, 692. (2007).

(b) T. Fujigaya, N. Nakashima, *Polymer J.*, **40**, 577. (2008).

Corresponding Author: Naotoshi Nakashima

E-mail: nakashima-tcm@mail.cstm.kyushu-u.ac.jp

Tel & Fax: +81-92-802-2842

Surface Activated Bonding between Au layer and Vertically Aligned Multiwalled Carbon Nanotubes

OMasahisa Fujino¹, Tadatomo Suga¹, Ikuo Soga², Daiyu Kondo², Yoshikatsu Ishizuki², Taisuke Iwai² and Masataka Mizukoshi²

¹*Department of Precision Engineering, The University of Tokyo, Tokyo 113-8656, Japan*
²*FUJITSU Laboratories Ltd. and FUJITSU Ltd., Kanagawa 243-0197, Japan*

Instead of copper, carbon nanotubes (CNTs), especially Multi-walled Carbon Nanotubes (MWNTs) are expected application of via structure in high-density integrate circuits. But the interconnection between CNTs and metal substrate are still electrically high resistance, such as about $0.22 \Omega/\mu\text{m}^2$ per MWNT via that was fabricated by metal sputtering deposition on them [1]. Therefore, in order to reduce the contact resistance, we suggested direct bonding between CNTs and metal by surface activated bonding (SAB) method, that the surface of bonding materials is sputter etched by Ar fast atom beam (FAB) [2].

In this research, vertically aligned MWNTs and Au layer (50nm thickness) were bonded by SAB method. Vertically aligned MWNTs were grown by acetylene-CVD with Fe catalysis. The formed MWNTs were with 1-2 nm diameter, 150-200 μm length. MWNTs chips were designed to measure the resistance of a 200 μm diameter MWNTs vias and contact between Au layer and them by 4-point method. Au layer on Si was deposited by plasma sputter. A pair of MWNTs chip and Au layer substrate was set to a bonding jig, and it was installed to vacuum chamber. At first, MWNTs chip was annealed with an infrared heater, then both chip and substrate were FAB processed with 1.5kV-15mA, and at last, they were bonded with some load. As a result, MWNTs-Au bonding was succeeded on condition that MWNTs were annealed over 650°C, Au layer and MWNTs were FAB processed longer than 300 sec, and bonding pressure was larger than 0.17 MPa (Fig.1), and the average resistance of one MWNT

via was 130 k Ω . Furthermore, when the bonding pressure was 0.7 MPa, the average resistance of one was 16 Ω .

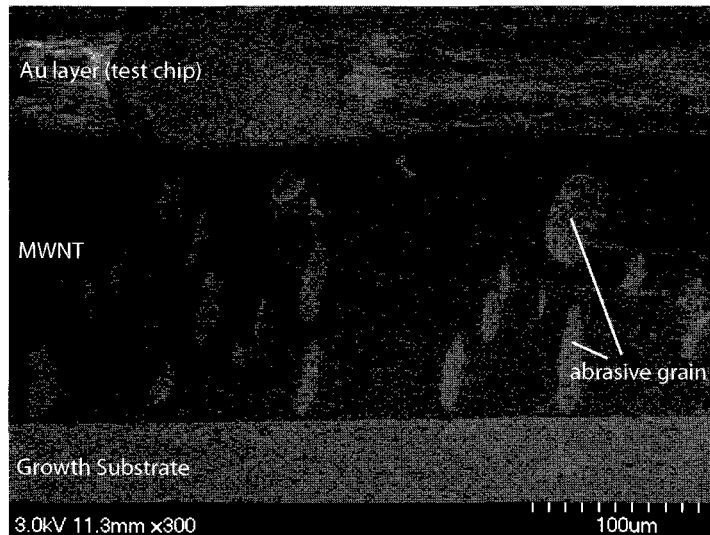


Figure 1 A cross-sectional image of vertical aligned MWNTs and Au layer.

[1] M. Nihei, D. Kondo, A. Kawabata, S. Sato, H. Shioya, M. Sakaue, T. Iwai, M. Ohfuti, and Y. Awano, *Proc. Interconnect Technology Conference 2005*, 234 (2005)

[2] H. Takagi, R. Maeda, N. Hosoda and T. Suga, *Appl. Phys. Lett.*, **74**, 2387 (1999)

Corresponding Author: Masahisa Fujino

TEL: +81-3-5842-6495, FAX: +81-3-5842-6485, E-mail: fujino.masahisa@su.t.u-tokyo.ac.jp

2-1

Behavior of fullerenes as electron acceptor at the liquid-liquid interface

○Hayashi Tsugumi¹, Hideyuki Takahashi¹, Kazuyuki Tohji¹

1. Graduate School of Environmental Studies, Tohoku University, Sendai 980-8579

Electrochemical studies of fullerenes have much attention because of its specific behavior. Haddon et.,al and Hawkins et.,al were calculated its molecular orbital^[1,2], and there are several reports concerning on the electrochemical detection of C₆₀ and also C₇₀ by utilizing cyclic voltammetry method^[3-5]. These researches demonstrated that C₆₀ could be able to accept at least six electrons to form C₆₀⁶⁻. In this study, the idea based on the electrochemical nature of fullerenes was introduced into the development of collection method for several ion species, such as poly sulfide ion (S₂²⁻) and Fe²⁺ from aqueous solution.

Fullerene/toluene solutions were mixed with S₂²⁻ or Fe²⁺ ion/aqueous solutions. After agitation, synthesized materials were collected and well washed with distilled water.

In the case of S₂²⁻, the color of the aqueous phase was changed from yellow to transparent. During every treatment, white precipitates were produced in the aqueous phase, while black crystals were formed after 4th treatment. XRD results indicated that former was elemental sulfur, and later was fullerene-sulfur compounds. Thus, it considered that electron of S₂²⁻ ions were moved to fullerenes to form S⁰. By 5th times treatment, *c.a.* 675 S₂²⁻ ions per one fullerene were successfully collected from the aqueous solution. On the other hand, the transparency of the aqueous phase contained the Fe²⁺ ion was decreased and precipitates were synthesized. Results of TEM-electron diffraction analysis indicated that precipitates was Fe(OH)₃. Thus, it considered that Fe²⁺ ions were oxidized to Fe³⁺ by the reaction with fullerene at the interface between aqueous solution and organic solvent.

In both experiments, no ion species were reduced in aqueous solution, excepted S₂²⁻ and Fe²⁺. From these results, it is plausible that fullerenes acted as electron acceptor.

[1] R.C. Haddon, L.E. Brus and K. RAGHAVACHARI, *Chem. Phys. Lett.*, 125, 459-464 (1986)

[2] J.M. Hawkins, *Chem. Phys. Lett.*, 122, 421-424 (1985)

[3] R.E.Haufler, J. Conceicao, L. P. F. Chibante et al, *J. Phys. Chem.*, 94 8634-8636 (1990)

[4] P. M. Allemand, A. Koch and F. Wudl, *J. Am. Chem. Soc.*, 113, 1050-1051 (1991)

[5] D. Dubois, K. M. Kadish, S. Flanagan, R. E. Haufler et al, *J. Am. Chem. Soc.*, 113, 4364 (1991)

Corresponding Author: Tsugumi Hayashi

E-mail: tsugumi@bucky1.kankyo.tohoku.ac.jp

Tel: +81-22-795-3871

Carbosilylation of $\text{La}_2@C_{80}$ with Silacyclopropane

○ Mari Minowa,¹ Michio Yamada,¹ Masahiro Kako,² Takahiro Tsuchiya,¹
Naomi Mizorogi,¹ Takeshi Akasaka,¹ Shigeru Nagase³

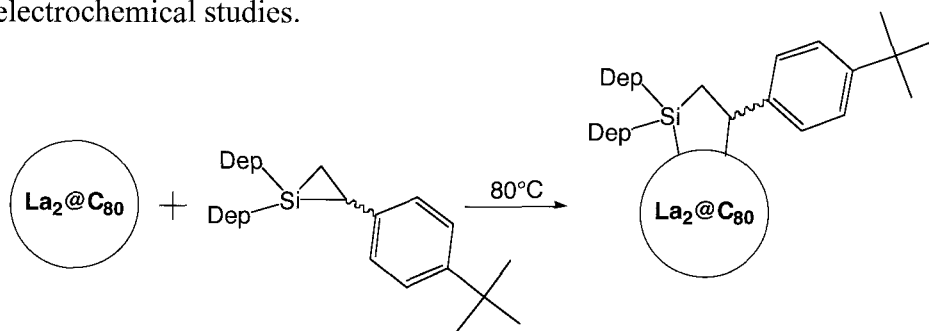
¹Center for Tsukuba Advanced Research Alliance, University of Tsukuba,
Tsukuba, Ibaraki 305-8577, Japan

²Department of Applied Physics and Chemistry, University of Electro-Communications,
Chofu, Tokyo 182-8585, Japan

³Department of Theoretical Studies, Institute for Molecular Science, Okazaki,
Aichi 444-8585, Japan

Abstract:

Endohedral metallofullerenes have fascinating structural and electronic properties, which are derived from the electron transfer from the encapsulated metal atoms to the carbon cage.¹ We have examined the chemical modification of fullerenes with organosilicon compounds. In this context, it is expected that combination of organosilicon compounds with endohedral metallofullerenes can provide a new class of fullerene-organosilicon hybrids. However, chemical modifications of endohedral metallofullerenes with organosilicon compounds have been limited to bissilylation so far.² Here, we report for the first time the carbosilylation of $\text{La}_2@C_{80}$ with silacyclopropane, in which two regioisomers of carbosilylated $\text{La}_2@C_{80}$ were obtained and isolated. The structures and electronic properties were determined by NMR, XRD and electrochemical studies.



References: (1) a) *Endofullerenes: A New Family of Carbon Clusters*; Akasaka, T., Nagase, S., Eds.; Kluwer, Dordrecht, the Netherlands, 2002. b) Yamada, M. et al. *Acc. Chem. Res.* **2010**, in press. c) Yamada, M. et al. *Pure Appl. Chem.* **2010**, accepted.

(2) a) Akasaka, T. et al. *Nature* **1995**, 374, 600–601, b) Yamada, M. et al. *J. Phys. Chem. B* **2005**, 109, 6049–6051. c) Iiduka, Y. et al. *J. Am. Chem. Soc.* **2005**, 127, 9956–9957. d) Yamada, M. et al. *J. Am. Chem. Soc.* **2005**, 127, 14570–14571. e) Wakahara, T. et al. *J. Am. Chem. Soc.* **2006**, 128, 9919–9925.

Corresponding Author: Takeshi Akasaka

E-mail: akasaka@tara.tsukuba.ac.jp

Tel&Fax: 029-853-6409

Ultraviolet photoelectron spectra of $C_{3v}\text{-M}_2@C_{82}$ and $C_{3v}\text{-(MC)}_2@C_{82}$ (M= Er, Lu, Tm)

○Takafumi Miyazaki¹, Yusuke Aoki¹, Youji Tokumoto¹, Ryohei Sumii², Haruya Okimoto³,
Hisashi Umemoto³, Yasuhiro Ito³, Noriko Izumi³, Hisanori Shinohara³, Shojun Hino¹

¹ Graduate School of Science and Engineering, Ehime University

² Institute for Molecular Science

³ Graduate School of Science, Nagoya University

The valence band electronic structure of C_{82} endohedral fullerenes containing multiple atoms was studied by ultraviolet photoelectron spectroscopy. Ultraviolet photoelectron spectra (UPS) of $C_{3v}\text{-Tm}_2C_2@C_{82}$ were measured at $h\nu=20\sim60\text{ eV}$ and discussed in conjunction with the difference among them.

Figure 1 shows the UPS of $M_2@C_{82}$ and $(MC)_2@C_{82}$ (M= Er, Lu, Tm) obtained with $h\nu = 40\text{ eV}$ irradiation. These endohedral fullerenes have the same C_{3v} symmetry. The spectral onset of these endohedral fullerenes is around $0.8 \sim 0.9\text{ eV}$. Although the entrapped elements differ, the UPS are similar. Except for two structures at about 9 eV and 12 eV of the UPS of Lu entrapped endohedral fullerenes, the UPS of deeper binding energy region (BE $>5\text{ eV}$) are almost identical. Close inspection of the UPS reveals minute difference at upper valence band region ($0 \sim 4\text{ eV}$). Principally, four structures labeled A - D are observed more or less at the same binding energy region, but the intensity of structures B and D is different; when the entrapped species are metal atoms and carbon atoms (metal carbide), these structures are more enhanced in comparison with those of only metal atoms entrapped endohedral fullerenes. This difference might be due to entrapped C_2 clusters. Theoretical treatment including entrapped species is required to investigate the effect of C_2 cluster to the electronic structure of endohedral fullerenes.

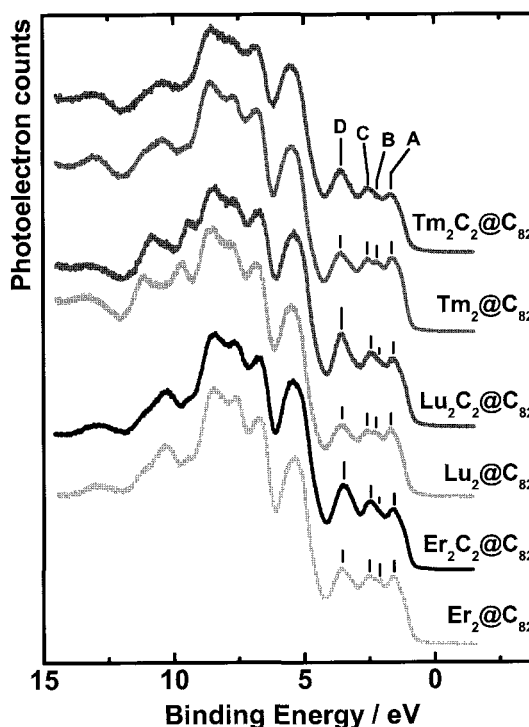


Figure 1 The UPS comparison of $C_{3v}\text{-M}_2@C_{82}$ and $C_{3v}\text{-(MC)}_2@C_{82}$

Corresponding Author: S. Hino, E-mail: hino@eng.ehime-u.ac.jp, phone: 089-927-9924

Isolation of Lithium Endohedral [60]fullerene

○Hiroshi Okada¹, Takeshi Sakai¹, Yoshihiro Ono¹, Kazuhiko Kawachi¹, Kenji Omote¹,
Yasuhiko Kasama¹, Kuniyoshi Yokoo¹, Shoichi Ono¹, Shinobu Aoyagi², Eiji Nishibori²,
Hiroshi Sawa², Ryo Kitaura³, Hisanori Shinohara³,
Shinsuke Ishikawa⁴, Takashi Komuro⁴, and Hiromi Tobita⁴

¹*ideal star Inc., ICR Bldg, 6-6-3 Minamiyoshinari, Aoba-ku, Sendai 989-3204, Japan*

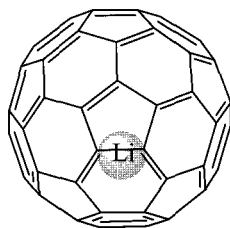
²*Department of Applied Physics, Nagoya University, Nagoya 464-8603, Japan*

³*Department of Chemistry and Institute for Advanced Research, Nagoya University,
Nagoya 464-8602, Japan*

⁴*Department of Chemistry, Graduate School of Science, Tohoku University,
Sendai 980-8578, Japan*

Among C_{60} and higher fullerenes, C_{60} is undoubtedly the most interesting molecule due to its availability in large quantity and its completely spherical structure. From these advantages, C_{60} has been applied to the construction of organic photovoltaic devices [1] and field effect transistors [2]. C_{60} -based metallofullerenes encapsulating metal atoms inside a C_{60} cage are also promising materials for application to electronic devices, because we are able to modify their physical and chemical properties extensively without changing the exterior structure of the C_{60} cage. However, isolation and structural determination of the C_{60} -based metallofullerenes have not been reported.

We recently succeeded in the efficient synthesis of lithium endohedral [60]fullerene ($Li@C_{60}$) by plasma shower method [3]. But the isolation of $Li@C_{60}$ was extremely difficult due to its strong attractive interaction with empty C_{60} in the product mixture [4]. Therefore, we tried to oxidize only $Li@C_{60}$ in the products to weaken the interaction, and achieved the complete isolation of the salt of $[Li@C_{60}]^+$ ion. Its endohedral structure was confirmed by a single crystal synchrotron radiation x-ray diffraction. Thus, $[Li@C_{60}]^+$ is the first structurally characterized metal endohedral [60]fullerene.



[1] Y. Matsuo et al., *J. Am. Chem. Soc.*, **131**, 16048 (2009).

[2] Y. Kubozono, *Appl. Phys. Lett.*, **93**, 033316 (2008).

[3] H. Okada et al., *The 33rd Fullerene-Nanotubes General Symposium*, **1P-13** (2007).

[4] T. Sakai et al., *The 34th Fullerene-Nanotubes General Symposium*, **2P-33** (2008).

Corresponding Author: Yasuhiko Kasama

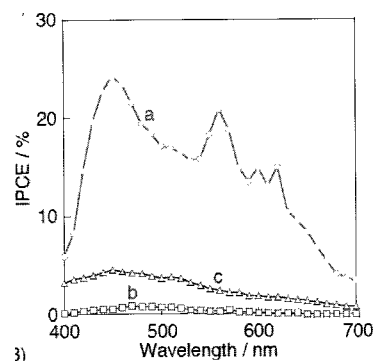
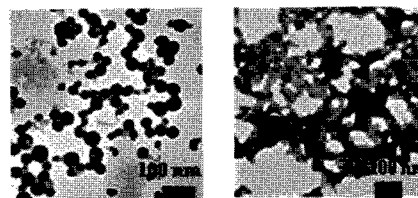
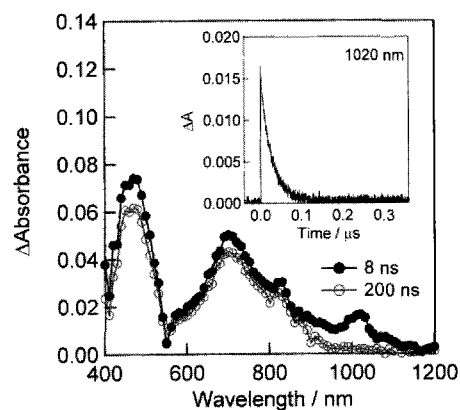
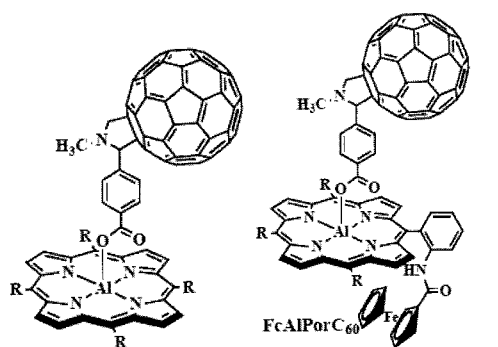
TEL: +81-22-303-7336, FAX: +81-22-303-7339, E-mail: idealstar@idealstar-net.com

Photovoltaic Cell based on Photoinduced Charge Separation of Fullerene–Aluminum(III) Porphyrin Molecular Systems

○O. Ito,^a A. S. D. Sandanayaka,^b T. Hasobe,^{b,c} P. K. Poddutoori,^d A. van der Est^d

^aNIMS, Tsukuba, Japan, ^bJAIST, Nomi, Japan, ^cPRESTO (JST), Kawaguchi, Japan, ^dDepartment of Chemistry, Brock University, Canada.

Photovoltaic cells are constructed employing newly designed fullerene-aluminum(III) porphyrin dyad (AlPor-C₆₀) and the ferrocene appended triad (Fc-AlPor-C₆₀). As shown in right scheme, fullerene unit (C₆₀) is bound axially to one side of the aluminum(III) porphyrin (AlPor) via a benzoate spacer and ferrocene (Fc) is attached via an amide linkage to one of the four phenyl groups in the meso positions of the AlPor ring. Time resolved optical and TREPR data show that photoexcitation of the porphyrin dyad results in efficient electron transfer from the excited singlet state of the AlPor to C₆₀ producing the charge-separated state such as AlPor^{•+}-C₆₀^{•-} (1020 nm, and triplet absorptions at 480 and 700 nm in right spectra). The lifetime of AlPor^{•+}-C₆₀^{•-} is evaluated to be 39 ns at RT in *o*-dichlorobenzene. In the case of Fc-AlPor-C₆₀, the subsequent hole transfer from AlPor^{•+} to Fc gives rise to Fc^{•+}-AlPor-C₆₀^{•-} (lifetime = 17 ns). Photovoltaic cells are constructed on the OTE/SnO₂ electrode casting AlPor-C₆₀ and Fc-AlPor-C₆₀. TEM images show the channel formations among AlPor-C₆₀ molecules (left TEM) and Fc-AlPor-C₆₀ molecules on OTE/SnO₂ (right TEM), quite favorable for photovoltaic performance. Photocurrent measurements show that both dyad and the triad show good photovoltaic performance in the whole visible light region with maxima of IPCE=25% for (a) OTE/SnO₂/(AlPorC₆₀)_n, (b) OTE/SnO₂/(AlPor)_n and (c) OTE/SnO₂/(C₆₀)_n at 450 nm, while IPCE=20% for OTE/SnO₂/Fc-AlPor-C₆₀. These IPCE values reflect the lifetimes of the radical pairs.



References: F. D'Souza, O. Ito, *Chem. Commun. Feature Article*, **2009**, 4913. T. Hasobe, *Phys. Chem. Chem. Phys. Review*, **12**, **2010**, 44.

Corresponding Author: Osamu Ito,

E-mail: ito@tagen.tohoku.ac.jp Tel & Fax 022-376-5970

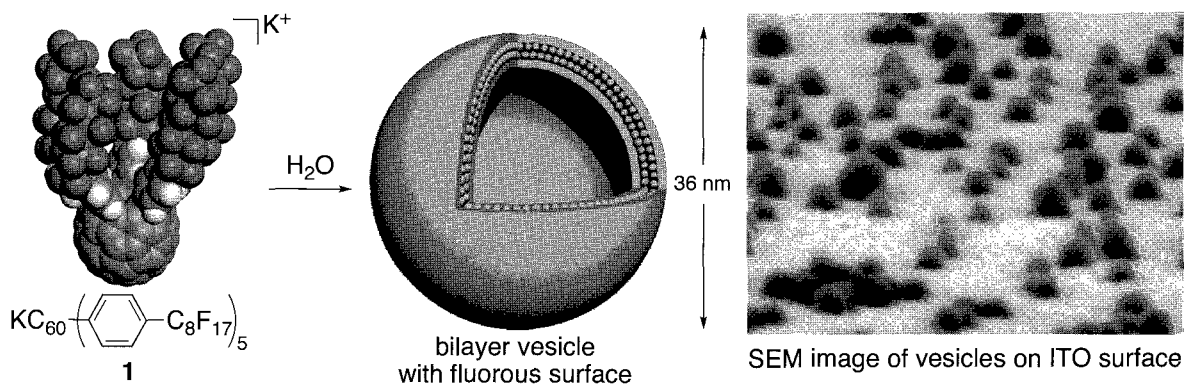
Properties of Water-soluble Fluorous Vesicle Formed from Perfluoroalkylated Fullerene Amphiphile

○Tatsuya Homma, Koji Harano, Hiroyuki Isobe[†], Eiichi Nakamura

*Department of Chemistry and ERATO (JST),
The University of Tokyo, Hongo, Bunkyo-ku, Tokyo 113-0033, Japan*

A lipid molecule has a polar head/nonpolar aliphatic tail structural motif, and, in water, forms a bilayer vesicle, in which the polar heads are exposed to the aqueous environment and the aliphatic tails cluster together to form the core of the bilayer membrane. The lipid vesicle is mechanically labile because of the polymorphic behavior of the aliphatic chains. Although the polar head/nonpolar tail motif is universally accepted, the question may arise whether such a binary motif is mandatory for vesicle formation in aqueous media.

In this study, we found a fluorous fullerene anion **1** that features a non-polar/polar/non-polar ternary motif, spontaneously forms an average 36-nm-diameter vesicle in water that exposes its nonpolar fluorous chains to the aqueous environment. Unlike a lipid vesicle that easily loses its structural integrity when removed from an aqueous solution, the present vesicle is very robust and retains its spherical shape even on a solid substrate under high vacuum, and hence it looks like a nanometer-size hollow Teflon ball. In contrast, this vesicle, tightly yet noncovalently binds fluorous molecules on its surface in water. When the vesicle solution is coated and dried on a hydrophilic surface, it becomes water-insoluble and makes the surface as water-repelling as Teflon surface. The vesicles are well dispersed on ITO surface just by spin-coating method, because of the low surface energy of perfluoroalkyl group on vesicle surface.



[†] Present address: *Department of Chemistry, Tohoku University, Aoba-ku, Sendai 980-8578, Japan*

Reference: Homma, T.; Harano, K.; Isobe, H.; Nakamura, E. *Angew. Chem. Int. Ed.* in press

Corresponding Author: Eiichi Nakamura, **Tel&Fax:** 03-5841-4369, **E-mail:** nakamura@chem.s.u-tokyo.ac.jp

This work is supported by the Global COE Program for Chemistry Innovation

Electron Transport Property and ESR Measurement of UV Light Irradiated Fullerene Nano Whisker

○Tatsuya Doi, Kyouhei Koyama, Nobuyuki Aoki and Yuichi Ochiai

Graduate School of Advanced Integrated Science, Chiba University, Chiba 263-8522, Japan

Abstract: Fullerene has been expected to near future applications for high performance n-type organic field effect transistor (FET). However, the intractableness of performing in atmosphere has been prevented the fullerene from applying to electronic devices. Since the first report in 1993 [1], several trials, such as polymerization due to photo irradiation, have been proposed [2]. In case of UV irradiated thin film of C₆₀, we could observe FET performance in atmosphere [3].

Our UV irradiated polymerization has been performed in a fine crystalline nano whisker consisting of C₆₀ molecules {Fullerene Nano Whisker (FNW)} fabricated by using liquid-liquid interfacial precipitation method [4] in the system of C₆₀ saturated *m*-xylene and isopropyl alcohol. In a UV irradiation FNW field effect transistor shows a n-type characteristics in atmosphere as indicated in Fig. 1. The ESR results have been obtained in the temperature dependence of g value and half width which of ESR measurement in the UV irradiated FNWs. Those results are different from pristine FNW as shown in Fig. 2a and Fig. 2b. Transport with a conduction electron can be suggested in a case of the UV irradiated FNW.

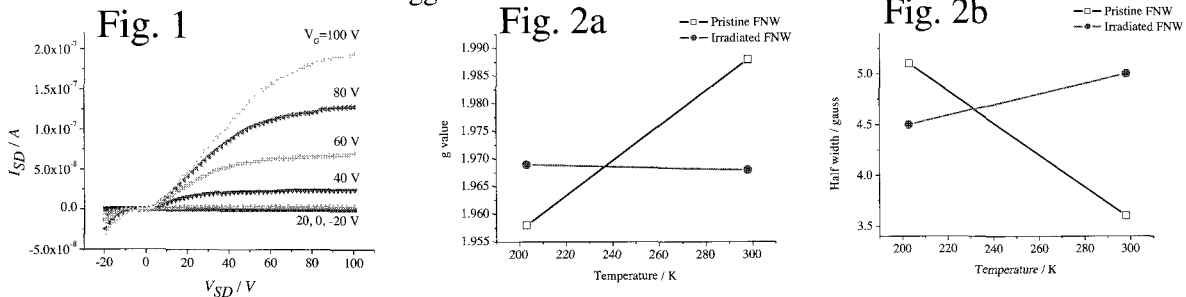


Fig. 1; The IV characteristics of UV irradiated FNW-FET in vacuum, Fig. 2a; The temperature dependence of the g value, and Fig. 2b; The half width obtained by ESR measurement

References:

- [1] A. M. Rao, P. Zhou, K.-A. Wang, G. T. Hager, J. M. Holden, Y. Wang, W.-T. Lee, X.-X. Bi, P. C. Eklund, D. S. Cornett, D. S. Duncan, and I. J. Amster: *Science* **259** (1993) 955.
- [2] H. Yamawaki, M. Yoshida, Y. Kakudate, S. Usuda, H. Yokoi, S. Fujiwara, K. Aoki, R. Ruoff, R. Malhotra, and D. Lorents: *J. Phys. Chem.* **97** (1993) 11161.
- [3] Y. Chiba, S. -R. Chen, H. Tsuji, M. Ueno, N. Aoki, and Y. Ochiai: *J. Phys. Conf. Ser.* **159** (2009) 012017.
- [4] K. Miyazawa, Y. Kuwasaki, A. Obayasi, and M. Kuwabara: *J. Mater. Res.* **17** (2002) 83.

Corresponding Author: Yuichi Ochiai

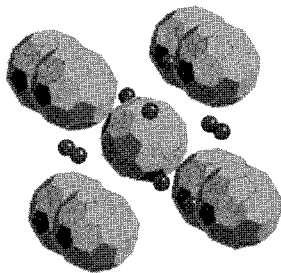
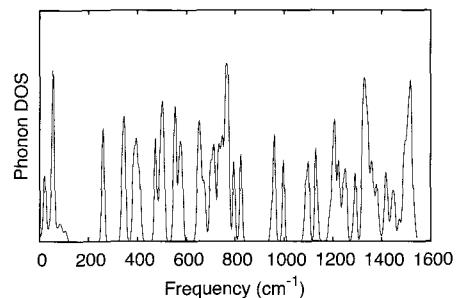
E-mail: ochiai@faculty.chiba-u.jp, **Tel:** +81-43-290-3428

Electron-phonon couplings and superconductivity in fcc and A15 A_3C_{60}

○Takashi Koretsune and Susumu Saito

*Department of Physics, Tokyo Institute of Technology
Oh-Okayama, Meguro-ku, Tokyo 152-8551, Japan*

Since the discovery of superconductivity in alkali-doped fcc C_{60} compounds[1], there have been numerous theoretical and experimental studies, leading to a qualitative understanding of the mechanism of superconductivity via electron-phonon coupling. In the theoretical viewpoint, however, there still remain problems such as a quantitative prediction of transition temperature and the effect of Coulomb interaction. Recent discovery of bulk A15 Cs_3C_{60} [2] renewed attention on these problems since it has the highest transition temperature in C_{60} compounds and the superconducting phase is next to antiferromagnetic-insulating phase. To clarify these problems, we study the electron-phonon couplings of fcc and A15 A_3C_{60} using first-principles method based on the density functional theory. To improve the previous studies, we perform accurate calculations of phonon dispersion and electron-phonon coupling including momentum dependence and lattice symmetry. Furthermore, to estimate the superconducting transition temperature, we use Eliashberg equation instead of McMillan's formula. It is found that the Eliashberg equation gives a quantitative improvement and that the obtained transition temperatures are reasonable compared to the experiments. We will also discuss the effect of Coulomb interaction.

Fig. 1 Structure of A15 Cs_3C_{60} Fig. 2 Phonon Density of states of A15 Cs_3C_{60}

References:

- [1] A. F. Hebard *et al.* Nature **350** (1991) 600.
[2] A. Y. Ganin *et al.* Nature mat. **7** (2008) 367

Corresponding Author: Takashi Koretsune

E-mail: koretune@stat.phys.titech.ac.jp

High-Yield Synthesis of Nitrogen Endohedral Fullerenes by Plasma Control

○S. Miyanaga, T. Kaneko, H. Ishida, and R. Hatakeyama

Department of Electronic Engineering, Tohoku University, Sendai 980-8579, Japan

Although many works related to the properties of a nitrogen atom endohedral fullerene ($N@C_{60}$) are reported [1, 2], the synthesis of $N@C_{60}$ with high yield has not yet been realized. $N@C_{60}$ has been produced by several plasma methods [3], however the purity ($10^{-3} \sim 10^{-2}$ %) and amount (~ 100 ng) of $N@C_{60}$ are still low. Therefore, the purpose of this research is to elucidate a formation mechanism of $N@C_{60}$ in order to improve the yield.

The schematic of experimental apparatus is shown in Ref.[4]. The nitrogen plasma is generated by applying an RF power with a frequency of 13.56 MHz to a spiral-shaped RF antenna and controlled by the applied RF power P_{RF} , a nitrogen gas pressure P_{N_2} , a substrate potential V_{sub} , a potential V_g of a mesh grid which is set up in the area between the RF antenna and the substrate. The upper and lower sides of the grid are defined as “plasma production area” and “process area”, respectively. In this research, we newly equip an end plate near the substrate. The plasma potentials in the plasma production area and the process area are controlled by V_g and the end plate potential V_{ep} , respectively, and the potential difference formed between these areas produces an electron beam which effectively ionizes nitrogen molecules in the process area. C_{60} is sublimated from an oven and deposited on the substrate, where the sublimation rate of C_{60} R_{subli} is possible to be changed. The nitrogen plasma is continuously irradiated to C_{60} on the substrate. The C_{60} compound including $N@C_{60}$ deposited on the substrate is analyzed by electron spin resonance (ESR) and UV-vis absorption spectroscopy to calculate the purity.

Figure 1 shows a dependence of the amount and purity of $N@C_{60}$ on V_{ep} . It is found that the amount and purity increase under the condition that V_{ep} is larger than 0 V. Since the potential in the process area is observed to rise with increasing V_{ep} , the ion irradiation energy toward C_{60} on the substrate becomes large, resulting in the high purity. The amount of $N@C_{60}$ is over 3 μ g, which is realized by large V_{ep} and high $R_{subli} > 200$ mg/h.

Consequently, we have succeeded in clarifying the experimental conditions for the high-yield synthesis of $N@C_{60}$.

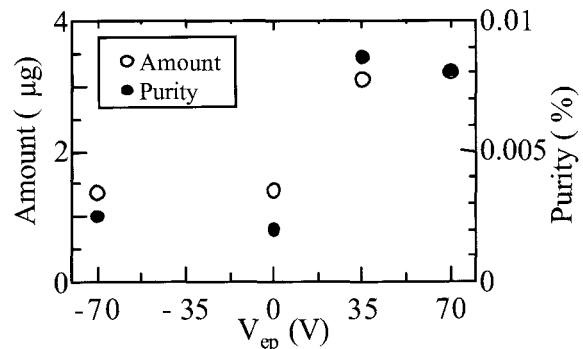


Fig. 1: Dependence of the amount and purity of $N@C_{60}$ on V_{ep} . $P_{RF} = 500$ W, $P_{N_2} = 0.8$ Pa, $V_g = -100$ V, $V_{sub} = -100$ V, $R_{subli} = 280$ mg/h.

- [1] M. Waiblinger *et al.*, Phys. Rev. B, **64**, 159901 (2001).
- [2] S. C. Benjamin *et al.*, J. Phys. Condens. Matter, **18**, S867 (2006).
- [3] T. Kaneko *et al.*, Phys. Plasmas, **14**, 110705 (2007).
- [4] S.Nishigaki *et al.*, Abstract of the 32nd Fullerene-Nanotubes General Symposium, 155 (2007).

Corresponding Author: Toshiro Kaneko

TEL: +81-22-795-7046, FAX: +81-22-263-9225, E-mail: kaneko@ecei.tohoku.ac.jp

The electronic structure of azafullerene encapsulated single-walled carbon nanotubes

○H. Yagi¹, Y. Tokumoto¹, M. Zenki¹, T. Zaima¹, T. Miyazaki¹,
S. Hino¹, N. Tagmatarchis², Y. Iizumi³, T. Okazaki^{3,4}

¹Graduate School of Science and Engineering, Ehime University, Matsuyama 790-8577

²Theoretical and Physical Chemistry Institute, Athens 116 35, Greece

³Nanotube Research Center, AIST, Tsukuba 305-8565

⁴PRESTO, JST, 4-1-8 Honcho, Kawaguchi 332-0012

Single walled carbon nanotubes (SWCNTs) encapsulating fullerenes, so called fullerene peapods, have attracted considerable interests as candidates for the new nano-electronic materials. Field effect transistor (FET) devices using fullerene peapods as channels are reported to show various transport properties depending on the encapsulated fullerenes[1]. C₅₉N@SWCNT was the first fullerene peapods that exhibited n-type FET characteristics[2]. As it has not been clear whether this finding is the result of the electron donating property of entrapped C₅₉N or the change of the work function, we measured ultraviolet photoelectron spectra to elucidate the electronic structure of C₅₉N@SWCNT. The work function of C₅₉N@SWCNT, which can be estimated from the secondary electron cutoff, is almost the same as that of SWCNT. Figure 1 shows the spectra of C₅₉N@SWCNT and SWCNT. There are several structures in the spectrum of C₅₉N@SWCNT which are not observed in that of SWCNT. Figure 1 also shows the spectrum of C₅₉N peas obtained by subtracting the spectrum of SWCNT from that of C₅₉N@SWCNT, together with the spectrum of a (C₅₉N)₂ thin film. The spectra of C₅₉N pea and (C₅₉N)₂ are analogous, which might indicate that C₅₉N molecules are entrapped in the SWCNTs in a form of dimer. Spectral shift should be noted; the C₅₉N pea spectrum is shifted about 0.1 eV toward lower binding energy compared to that of (C₅₉N)₂. This might suggest charge transfer from C₅₉N to SWCNTs.

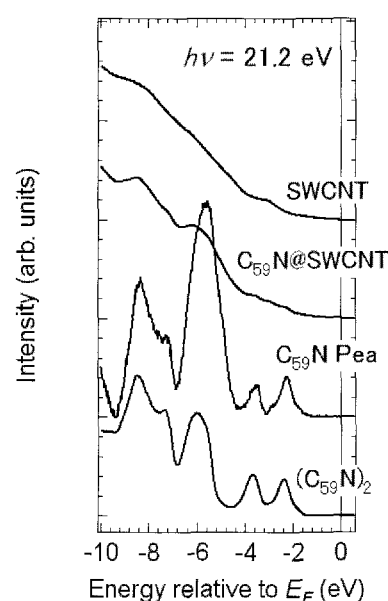


Fig. 1. The UPS of SWCNT, C₅₉N@SWCNT, C₅₉N pea and (C₅₉N)₂.

[1] T. Shimada *et al.*, *Physica E*, **21**, 1089 (2004).

[2] T. Kaneko *et al.*, *J. Am. Chem. Soc.*, **130**, 2714 (2008).

Corresponding Author: S. Hino

Tel : +81-89-927-9924, E-mail: hino@eng.ehime-u.ac.jp

Prevention of Crystal Growth of Tin and Lead in Confined Nanospace of Carbon Nanotubes

○Keita Kobayashi¹, Kazu Suenaga¹, Takeshi Saito^{1,2}, Sumio Iijima¹

¹*Research Center for Advanced Carbon Materials, National Institute of Advanced Industrial Science and Technology (AIST), Tsukuba 305-8565, Japan*

²*PRESTO, Japan Science and Technology (JST) Kawaguchi 332-0012, Japan*

Nano-materials confined within the inner space of carbon nanotubes (CNTs) are known to exhibit unusual behavior that differs from that of bulk materials; thus, extensive research has been carried out on the encapsulation of various molecules in the inner space of SWCNTs in order to produce novel low-dimensional nano-materials [1-5].

In this study, we report that crystal growth of Sn and Pb are prevented by confinement of molten Sn and Pb within the inner space of CNTs. Sn and Pb were heat-treated at 723 K in vacuo (10^{-4} Pa) with end-opened CNTs to be encapsulated within inner space of CNTs by capillary action of molten Sn and Pb. The structure of Sn and Pb encapsulated within the inner space of CNTs were observed by high resolution transmission electron microscopy (HRTEM). The HRTEM observation suggests that the structure of Sn and Pb can be assumed to amorphous structures with fluidity at room temperature. Based on these results and thermo-dynamic calculation, we consider that the nucleation of crystal growth of Sn and Pb cannot progress within confined nanospace of CNTs.

References

- [1] J. Sloan, A. I. Kirkland, J. L. Hutchison, M. L. H. Green, M. L. H, *Chem. Commun.*, 1319 (2002).
- [2] Y Maniwa, H Kataura, M. Abe, S. Suzuki, Y. Achiba, H. Kira, K. Matsuda, *J. Phys. Soc. Jpn.*, **71**, 2863 (2002)
- [3] R. Carter, J. Sloan, A. I. Kirkland, R. R. Meyer, P. J. D. Lindan, G. Lin, M. L. H. Green, A. Vlandas, J. L. Hutchison, and J. Harding, *Phys. Rev. Lett.*, **96**, 215501 (2006).
- [4] L. Guan, K.Suenaga, Z. Shi, Z. Gu, S. Iijima, *Nano Lett.*, **7**, 1532 (2007).
- [5] K. Kobayashi, K. Suenaga, T. Saito, H. Shinohara, S. Iijima, *Adv. Mater.*, Submitted.

Corresponding Author: Keita Kobayashi

TEL: +81-29-861-5694, **FAX:** +81-29-861-4806, **E-mail:** kobayashi-z@aist.go.jp

Metallic layered compound: Potassium-intercalated hexagonal boron nitride

Susumu Okada^{1,3} and Minoru Otani^{2,3}

¹*Graduate School of Pure and Applied Sciences, Center for Computational Sciences, University of Tsukuba, Tennodai, Tsukuba 305-8577, Japan*

²*Research Institute for Computational Sciences, National Institute of Advanced Industrial Science and Technology (AIST), Tsukuba 305-8568, Japan*

³*Japan Science and Technology Agency, CREST, 5 Sanbancho, Chiyoda-ku, Tokyo 102-0075, Japan*

Graphite has occupied an important position in low-dimensional sciences and surface sciences for many years because of its layered structure, which comprises perfectly planar hexagonal networks of carbon atoms. This layered structure serve as a host material for the intercalation of various atoms and molecules into the two-dimensional interlayer spaces that are several angstroms thick. These complexes are called graphite intercalation compounds (GICs), and some are known to exhibit superconductivity under appropriate conditions. In early theoretical work and a recent angle-resolved photoemission spectroscopy (ARPES) experiment showed that the peculiar electron state floating from the atomic layers (NFE state) substantially contributes to the electronic properties near the Fermi level of metal-doped GICs. Hexagonal boron nitride (h-BN) is another prototypical layered material and possesses a hexagonal network consisting of B and N atoms. Due to the chemical difference between B and N atoms, h-BN is an insulator with a large energy gap. However, the large interlayer spacing caused by its layered structure also leads to the NFE state, as for graphite. Thus, in the present study, we explore the possibility of potassium-intercalated h-BN compounds and elucidate its electronic properties.

Our first-principle, total-energy calculations of K-intercalated h-BN clarify that the compound is stable in energy and is exothermic upon formation. Furthermore, the electronic structure near the Fermi energy of the compound exhibits characteristics similar to those of metal-doped GIC. In particular, we find a clear isotropic Fermi surface around the Γ point in K-intercalated h-BN.

Corresponding Author: Susumu Okada, sokada@comas.frsc.tsukuba.ac.jp

Highly-Efficient Field Emission from Carbon Nanotube-Nanohorn Hybrids Prepared by Chemical Vapor Deposition

○Ryota Yuge¹, Jin Miyawaki^{2,†}, Sadanori Kuroshima¹, Toshinari Ichihashi¹, Tsutomu Yoshitake¹, Tetsuya Ohkawa³, Yasushi Aoki³, Sumio Iijima^{1,2,4,5}, and Masako Yudasaka^{2,5}

¹*Nano Electronics Research Laboratories, NEC Corporation, 34 Miyukigaoka, Tsukuba 305-8501, Japan*

²*SORST, Japan Science and Technology Agency, Yaesu-Dori Building 6F, 3-4-15 Nihonbashi, Chuo-ku, Tokyo 103-0027, Japan*

³*Research and Development Department, NEC Lighting, Ltd., 3-1 Nichiden, Minakuchi, Koga, 528-8501, Japan*

⁴*Meijo University, 1-501 Shiogamaguchi, Tenpaku-ku, Nagoya, 468-8502, Japan*

⁵*Nanotube Research Center, National Institute of Advanced Science and Technology (AIST), Central 5, 1-1-1 Higashi, Tsukuba, 305-8565, Japan*

[†]*Current address: Institute for materials chemistry and engineering, Kyushu University*

It is reported that the carbon nanotube (CNTs) is one of the best cold cathode emitters for field emission display (FED) and field emission lamp (FEL) [1-2] due to their large aspect ratio, high mechanical strength, and high electrical conductivity. For the manufacture of highly efficient field emission (FE) devices, we synthesized single-wall carbon nanotube (SWNT) on catalyst-supported single-wall carbon nanohorn (SWNH). This hybridized material (NTNH) had both promising FE properties of SWNTs and high-dispersion properties of SWNHs.

We incorporated Fe acetate into SWNHs, heat-treated them, and obtained Fe oxide nano-particles attached to the tips of SWNHs (Fe@NHox). Using Fe@NHox as the catalyst, SWNTs were grown by ethanol-CVD technique. TEM observation and Raman spectra showed that the diameters of the SWNTs were 1~1.7 nm. We also found that FE flat lamps of NTNH showed lower FE emission threshold and more homogeneous illumination than those made by using HiPco SWNTs or the mixture of HiPco SWNT and SWNHs. The major advantage of NTNHs is that the bundle thickness of SWNTs in the device formation processes was avoided because SWNTs were rooted on the bulky aggregates of SWNHs, leading to the high dispersion in the composites. Therefore, we expect that NTNH will be a promising electrode material for FE application. The details are shown in the presentation.

Reference:

[1] A. G. Rinzler et al. *Science*, **296**, 1550 (1995).

[2] J. M. Bonard et al. *Appl. Phys. Lett.*, **78**, 2775(2001).

Corresponding Author: R. Yuge and M. Yudasaka

TEL: +81-29-850-1566, FAX: +81-29-856-6137

E-mail: r-yuge@bk.jp.nec.com, m-yudasaka@aist.go.jp

Isotope Scrambling in the Formation of Polyynes Carbon Chains

○Tomonari Wakabayashi*, Mao Saikawa, and Yoriko Wada

Department of Chemistry, Kinki University, Higashi-Osaka 577-8502, Japan

Linear carbon chain molecules are major ingredients in high-temperature carbon vapor. Among others, end-capped polyynes with alternating triple- and single-bonds are relatively stable against polymerization and accessible under ambient conditions. Hydrogen-capped polyynes, $\text{H}(\text{C}\equiv\text{C})_n\text{H}$, are known for major products upon ablation of carbon particles in organic solvents with nanosecond laser pulses [1]. Formation of cyanopolyynes, $\text{H}(\text{C}\equiv\text{C})_n\text{C}\equiv\text{N}$, are also reported from ablation in acetonitrile. It might be reasonable to consider that vaporization of carbon clusters from carbon particules is followed by termination of their ends with hydrogen atoms or cyano groups from solvent molecules [2]. However, detailed mechanism for the formation of carbon chains is not well understood. Recent experiment using femtosecond laser pulses clearly showed that polyynes are formed from liquid hydrocarbons without carbon powder [3]. This observation indicates that carbon atoms in solvent molecules also contribute as building blocks for carbon chains.

We studied three polyynes, HC_7N , HC_9N and C_{10}H_2 , by NMR spectroscopy. In order to distinguish the origin of carbon nuclei, i.e., particle or solvent, we employed ^{13}C -enriched carbon powder (~96%) for nanosecond laser ablation in acetonitrile of natural isotopic abundance (1.01%). As a result, many “isomers” having different isotopic sequences within a carbon chain, namely *isotopomers*, were formed indeed. For HC_7N and HC_9N , substantial fraction of molecules contain ^{13}C isotope in its cyano group, $-\text{C}\equiv\text{N}$. The elimination of a cyano group from an intact solvent molecule is not the only scheme for termination leading to cyanopolyynes. Furthermore, ^{12}C isotopes are found frequently within the carbon chain in both cases for polyynes and cyanopolyynes. The concentration of ^{13}C isotope was fairly diluted in the polyynone carbon chains. The carbonaceous contribution from solvents spans from ~25% to ~50% depending on the number of laser shots from 10^4 to 10^5 pulses. We report our experimental results and analysis in detail and discuss on the formation mechanism for the polyynone carbon chains under the experimental conditions.

[1] M. Tsuji et al. Chem. Phys. Lett. **355**, 101 (2002).

[2] J. R. Heath et al. J. Am. Chem. Soc. **109**, 359 (1987).

[3] Y. Sato et al. Carbon, in press.

Corresponding Author: Tomonari Wakabayashi

E-mail: wakaba@chem.kindai.ac.jp

Tel. 06-6730-5880 (ex. 4101) / FAX 06-6723-2721

Development of Ion Trap Mobility Measurements

Yoshihiko Sawanishi and Toshiki Sugai

Department of Chemistry, Toho University, Miyama 2-2-1 Funabashi, 274-8510, Japan

Ion mobility/mass measurements have been utilized for nano carbon materials[1]. The high sensitivity and high throughputs for mixed and unstable materials have lots of advantages to clarify the new structures and the production processes. However, the measurement requires high pressure buffer gas which leads to ion dilution and other experimental difficulties. To overcome these problems we have developed an ion trap[2] and have succeeded to perform the mobility measurements on charged droplets.

Figure 1 shows the scheme of the measurement system. The ion trap is consist of stacked ring electrodes and an RF and LF power supplies. The RF and LF power supplies produced the radio frequency field (20 kHz, 600 Vpp) to trap the droplets and the low frequency field (2~5 Hz, 10 Vpp) to move the droplets in the trap for the mobility measurements, respectively. The charged droplets were produced and introduced in the trap by the atomizer with high DC potential (10 kV) and were detected by a microscope with a laser irradiation.

The droplets were trapped in the center of the ring electrodes with the modulation by the LF power supply. The movement is shown as the arrow in Fig. 1. The amplitude of the modulation is roughly proportional to the inverse of the frequency of the LF power supply showing that the droplet cannot moves so much at higher frequency condition since the period for the movement reduced inversely as the frequency increases. The movement continued for about 2 hours showing the potential high sensitivity and high accuracy of the measurements.

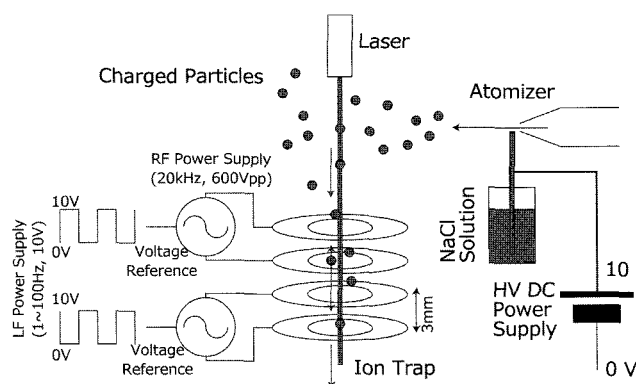


Fig.1 Ion Trap

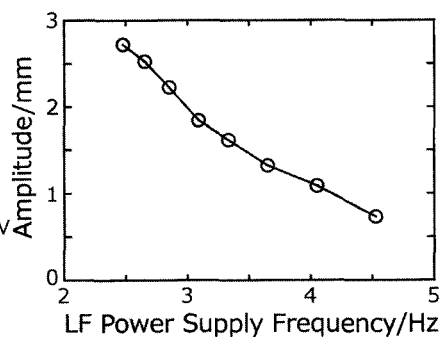


Fig. 2 Amplitude vs. Modulation

[1] T. Sugai *et al.*, *J. Am. Chem. Soc.* **123**, 6427 (2001).

[2] A.V. Tolmachev *et al.*, *Int. J. Mass Spec.* **203**, 31 (2000).

Early Stages in the Nucleation Process of Carbon Nanotubes: Density-Functional Tight-Binding Molecular Dynamics Simulations of Acetylene Polymerization and Cross-Linking on an Fe₃₈ Particle

○Ying Wang,¹ Yasuhito Ohta,² HuJun Qian,¹ Keiji Morokuma³ and Stephan Irle¹

¹*Institute for Advanced Research and Department of Chemistry, Nagoya University, Nagoya 464-8602, Japan*

²*Department of Chemistry Faculty of Science, Nara Women University, Nara 630-8506, Japan*

³*Fukui Institute for Fundamental Chemistry, Kyoto University, Kyoto, 606-8103, Japan*

Carbon nanotubes (CNTs) have been the focus of great scientific interest. There are many methods for CNT synthesis. When comparing these methods, the CVD method has several technological advantages, while the exact role of metal catalysts is still unknown. Since Fe substrate is known to be highly effective for the CNT growth in the CVD process and C₂H₂ is the major decomposition product from hydrocarbon, we apply quantum chemical molecular dynamics (QM/MD) simulation based on the density-functional tight-binding (DFTB) method to investigate self assembly of carbon nanotubes from acetylene on Fe₃₈. Here, we report polymerization and cross-linking as a first step towards CNT nucleation.

We found during acetylene supply simulations, that some C₂H₂ transfer H to Fe to form C₂H_x. Subsequently, these more reactive species initiate polymerization reactions. During extended carbon diffusion simulations following supply, five or six-membered rings were formed, indicating cross-linking of polyacetylene-like chains.



Fig. 1: The results of carbon supply simulation and carbon diffusion simulation for trajectory A.

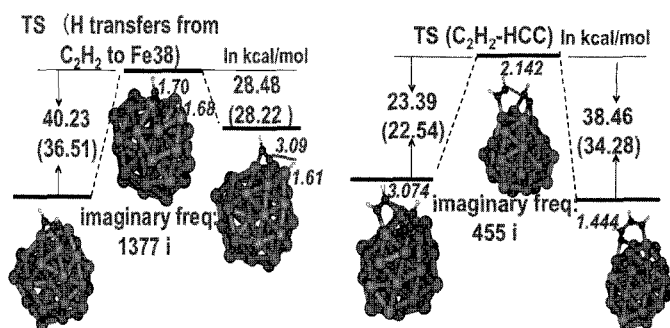


Fig. 2: The PECs for reactions of C-H broken and C-C connection. The values in parenthesis are included ZPE correction.

Accompanying our QM/MD simulations, the barrier heights for four kinds of reactions of H transfer, C-C bond breaking, H₂ abstraction, and C-C polymerization were investigated at the DFTB level.

Corresponding Author: Stephan Irle and K. J. Morokuma

TEL:+81-52-747-6397, FAX:+81-52-788-6151 E-mail: sirle@iar.nagoya-u.a.jp, keiji.morokuma@emory.edu

Gas-phase and On-surface Decomposition of Ethanol in Alcohol CCVD

○Rong Xiang, Bo Hou, Erik Einarsson, Junichiro Shiomi, Shigeo Maruyama

Department of Mechanical Engineering, the University of Tokyo

The gas phase decomposition of ethanol was previously calculated by CHEMKIN and measured by FTIR. It was confirmed that ethanol decomposes quickly (into C₂H₄, C₂H₂ and etc.) in a typical alcohol catalytic chemical vapor deposition (ACCVD). Since C₂H₄ and C₂H₂ are much more active than ethanol in producing SWNTs, we questioned whether all SWNTs were yielded from C₂H₄ and C₂H₂ through indirect pathways in ACCVD. The isotope experiments revealed #1 carbon and #2 carbon behave differently in the reaction, which convinced us asymmetric molecules like ethanol are also growing SWNTs in ACCVD.¹

Our recent data show the inequivalent contribution of two carbon atoms in an ethanol molecule (indicated by G-band position in Figure 1) varies with CVD parameters. When CVD temperature increases, the shift of G-band to a lower wavenumber directly reflects the ethanol decomposes more, which is expected to occur. However, it is unexpected that the addition of Mo also makes a big difference (Table 1). This elucidates, other than simply immobilizing Co on the substrate,² Mo also promotes the ethanol decomposition that happens on the surface of catalyst particles. This may explain why addition of Mo increases the yield of SWNT grown. A model will be proposed to discuss the difference between gas-phase and on-surface decomposition in determining the quality of produced SWNTs.³

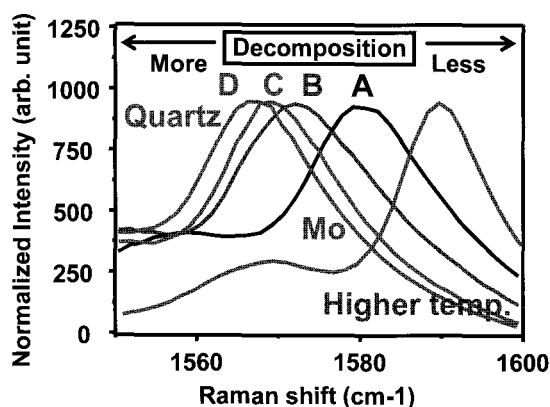


Figure 1: Raman spectra of SWNTs grown from 1-C₁₃ ethanol at various CVD conditions. A shift to the lower wavenumber indicates that ethanol decomposes more before forming SWNTs. (CVD condition of A, B, C and D are listed in Table 1)

Catalyst	750°C	850°C
CoS	1579.5 (A)	1571.9 (B)
CoFeS	1579.5	1571.9
CoFeZeo	1579.5	1568.9
CoMoS	1573.4	1568.9 (C)
CoMoQuartz	x	1566 (D)

Table 1: G band peak position of SWNTs grown from 1-C₁₃ ethanol at various CVD conditions, showing the inequivalent contribution of two carbon atoms in an ethanol molecule may be altered by temperature, Mo addition and substrate.

References:

1. R. Xiang, E. Einarsson, J. Okawa, Y. Miyauchi, S. Maruyama, *J. Phys. Chem. C* 2009, 113, 7511.
2. M. Hu, Y. Murakami, M. Ogura, S. Maruyama, T. Okubo, *J. Catalysis* 2004, 225, 230.
3. R. Xiang, B. Hou, E. Einarsson, J. Shiomi, S. Maruyama, 2010, *in preparation*.

Corresponding Author: Shigeo Maruyama (maruyama@photon.t.u-tokyo.ac.jp)

Millimeter-tall single-walled carbon nanotube forests grown from ethanol

○Hisashi Sugime and Suguru Noda

Dept. of Chemical System Engineering, The University of Tokyo, Tokyo, 113-8656, Japan

In direct growth of SWCNTs on substrates by CVD methods, bimetallic catalysts and/or underlayers are frequently used to realize the growth of vertically aligned SWCNTs (VA-SWCNTs). To effectively grow VA-SWCNTs at a sub-millimeter length or even longer, aluminum oxide underlayer plays an important role when combined with a Fe catalyst in C_2H_4 -CVD [1-3], plasma-enhanced CVD from CH_4 [4], and C_2H_2 -CVD [5] or when combined with a Co catalyst in C_2H_5OH -CVD [6]. However, the effect of the aluminum oxide underlayer remains unclear and it is important to understand how the CVD and catalytic conditions affect the growth of the VA-SWCNTs.

In this study we investigated the use of both aluminum oxide and silicon oxide as underlayers for the Co catalyzed growth in C_2H_5OH -CVD using a combinatorial catalyst library which can realize varying nominal thicknesses of both Co and aluminum oxide on a single substrate [7]. Fig. (a) shows a schematic of the Co library and Fig. (b) shows photographs of the libraries taken during CNT growth at 850 °C and the relationship between the distance from the edge of the libraries and nominal thickness of Co (t_{Co}). We used Si substrates with a 50-nm-thick thermal oxide layer (SiO_2) and Al was deposited with the nominal thickness of 15 nm and was subsequently oxidized in air, resulting in the formation of aluminum oxide (Al_2O_3). During the CNT growth, the total gas flow rate was 150 sccm and the C_2H_5OH partial pressure was 4.0 kPa. Fig. (c) shows the growth curves of VA-CNTs at each value of t_{Co} . Thick Co catalytic layers (≥ 1.3 nm) produced (sub-)millimeter-tall multi-walled VA-CNTs on both the aluminum oxide and silicon oxide underlayers. However, thin Co catalytic layers (0.62 - 1.0 nm) produced (sub-)millimeter-tall VA-CNTs, which consisted mainly of single-walled CNTs, only on the aluminum oxide underlayers. Aluminum oxide therefore plays an essential role either in retaining the catalytic activity of small Co particles by inhibiting their coarsening or in enhancing their catalytic activity.

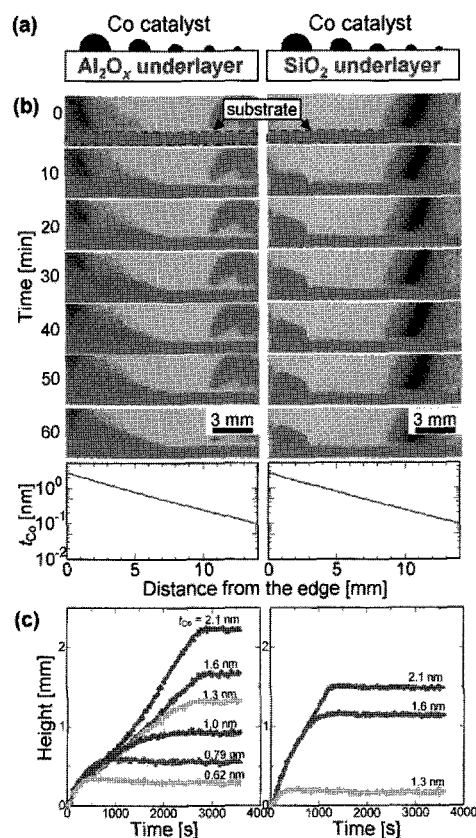


Fig. (a) A schematic of the catalyst library (b) photographs of substrates during CVD (initial substrates are shown with a dashed line) and relationship between distance from the edge of libraries and t_{Co} , and (c) growth curves of VA-CNTs at different t_{Co}

[1] K. Hata, et al., *Science* **306**, 1362 (2004). [2] S. Chakrabarti, et al., *J. Phys. Chem. C* **111**, 1929 (2007). [3] S. Noda, et al., *Jpn. J. Appl. Phys.* **46** L399 (2007). [4] G.F. Zhong, et al., *Jpn. J. Appl. Phys.* **44**, 1558 (2005). [5] G. Eres, et al., *J. Phys. Chem. B* **109**, 16684 (2005). [6] H. Ohno, et al., *Jpn. J. Appl. Phys.* **47**, 1956 (2008). [7] H. Sugime, et al., *Carbon* **47**, 234 (2009).

Corresponding Author: Suguru Noda TEL/FAX: +81-3-5841-7332, E-mail: noda@chemsys.t.u-tokyo.ac.jp

Chirality selective production of carbon nanotubes in HeN₂ mixed gas

○Akihito Inoue¹⁾, Yasuhiro Tsuruoka¹⁾, Takeshi Kodama¹⁾, Toshiya Okazaki²⁾
and Yohji Achiba¹⁾

1) Department of Chemistry, Tokyo Metropolitan University, Hachioji, Tokyo 192-0397 Japan

2) Advanced Industrial Science and Technology (AIST), Tsukuba 305-8565, Japan

Electronic structures of single-walled carbon nanotubes (SWNTs) significantly depend on the diameter and chirality of their tube structures. Therefore, the controlling diameter and chirality is of particularly importance for application of SWNTs to the field of nano-electronics, nano-optoelectronics as well as bio-electronics. In the earlier study, our research group has demonstrated that very narrow diameter distribution could be realized by the laser vaporization with Rh/Pd catalyst in N₂ gas atmosphere, in which the N₂ gas was thought to work efficiently as a cooling gas for the initially very hot laser ablated carbon materials. By optimizing the gas condition, we were able to produce the SWNT with highly enrichment of (6,5) chiral tube. However, the experimental gas condition such as pressure and pumping speed by which only (6,5) tube production as a single chiral species was realized was found to be extremely limited one. In order to overcome the difficulty in the production of large amounts of SWNT with a single chirality, in the present paper, we used HeN₂ mixed gas in the laser vaporization experiments and intended to clarify the role of cooling gas on the chirality distribution of SWNTs.

In the present work, we examined the chirality distribution of SWNTs by laser vaporization, by placing the emphases on the following two points; how the furnace temperature does work on the size and chirality distributions of SWNTs and how the mixed foreign gas of He and N₂ gives rise of changing the chirality distribution of SWNT.

Figure 1 shows absorption spectra of the tubes in SDBS/H₂O solution. The raw soot was prepared in HeN₂ mixed gas under the different furnace temperature. Detailed discussion on the growth process will be done in the symposium.

Corresponding Author Yohji Achiba

E-mail achiba-yohji@tmu.ac.jp **Tel & Fax** 042-677-2534

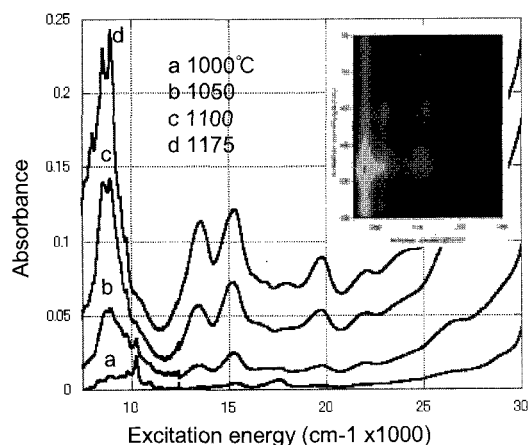


Fig1. Absorption spectra of SWNTs prepared at different furnace temperature a-d (1000-1175°C).

Inserted picture corresponds to 2D fluorescence mapping of sample a. Only 6,5 tube fluorescence was observed in this energy region.

Horizontally Aligned SWNT Growth on R-cut Crystal Quartz

○Hiroto Okabe¹, Shohei Chiashi¹, Junichiro Shiomi¹, Tadashi Sato²,
Shouichi Kono³, Masami Terasawa³, Shigeo Maruyama¹

¹*Department of Mechanical Engineering, The University of Tokyo, Tokyo 113-8656, Japan,*

²*KYOCERA Corporation,*

³*KYOCERA KINSEKI Corporation*

Single-walled carbon nanotubes (SWNTs) are one of the most promising materials for next generation electronics. One key issue towards the circuit integration is the control of horizontal alignment of SWNTs. In this course, recent works have shown that the crystal quartz substrates can be utilized to grow aligned SWNTs [1]. For this, ST-cut quartz is popularly used after high temperature annealing for a long time to re-crystallize the surface. However, ST-cut surface is still complicated since it is not natural crystal surface, despite the simplified pictures offered by theories [2]. Here, we report that it is possible to achieve well aligned SWNTs without the annealing process by using R-cut quartz, whose surface is one of the natural crystal surfaces. The alignment mechanism will be discussed in terms of quartz surface structures.

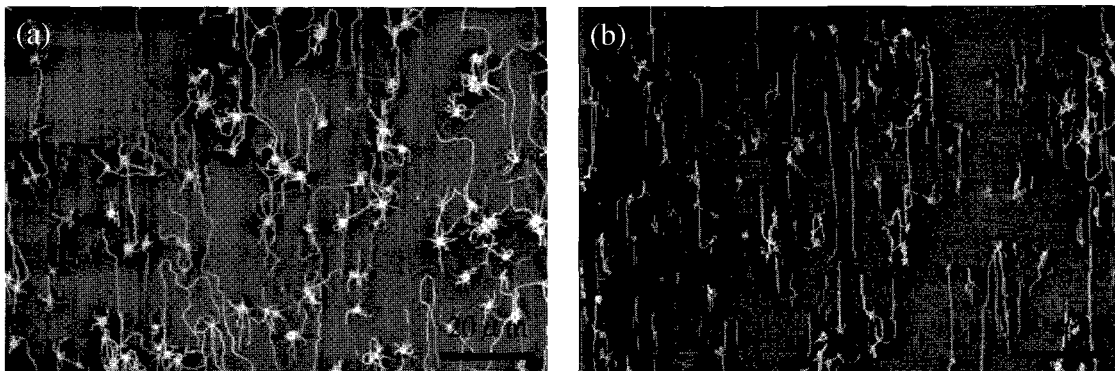


Fig. 1. SEM images of SWNTs grown without annealing,
on (a)ST-cut quartz and (b)R-cut quartz

[1] C. Kocabas *et al.*, *Small*, **1**, 1110 (2005)

[2] J. Xiao *et al.*, *Nano lett.*, **9**, 4311 (2009)

Corresponding Author: Shigeo Maruyama

TEL: +81-3-5841-6421, FAX: +81-3-5841-6408,

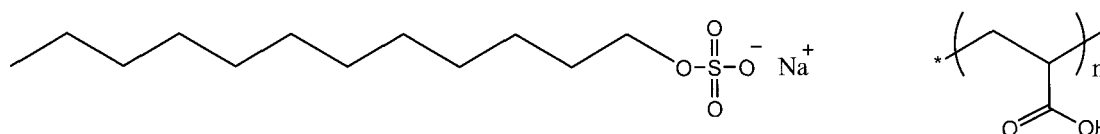
E-mail: maruyama@photon.t.u-tokyo.ac.jp

Interplay of Hydrophobic and Electrostatic Interactions between Dispersants and Single-walled Carbon Nanotubes in Water

Shin Katakura and Masahito Sano

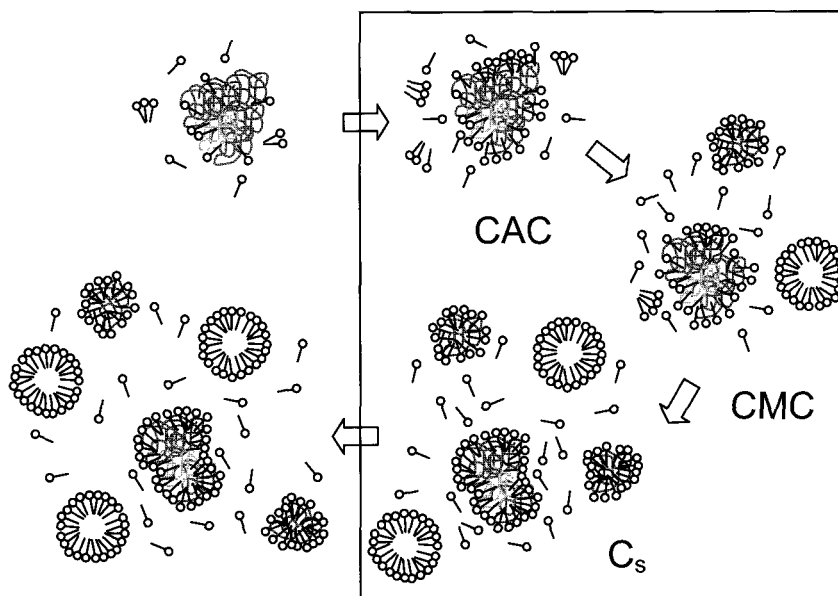
*Department of Polymer Science and Engineering, Yamagata University
Yonezawa, Yamagata 992-8510, Japan*

Dispersing single-walled carbon nanotubes (SWCNTs) in water is important for characterization of tube themselves as well as various applications. In some cases, dependences on metallicity or on chirality are observed, allowing different electronic tubes to separate. Typically, surfactants like sodium dodecyl sulfate (SDS) are often employed to improve wetting and polyelectrolytes are used to gain dispersion stability. Despite of its importance, hardly nothing is known about their interactions and structures on SWCNTs.



Among common polyelectrolytes, poly(acrylic acid) (PAA) is a special compound that exhibits hydrophobic interaction with SDS. At low pH where a majority of carboxylic groups is acid, several PAA chains form aggregates in water. It has been shown that alkyl chains of SDS bind to apolar segments of PAA through hydrophobic interaction above critical aggregation concentration (CAC). It continues to bind and free some PAA until saturation concentration (C_s) is reached. The interaction is thermodynamically favorable ($\Delta H < 0$, $\Delta S > 0$). At higher pH where more than 20% of carboxylic groups are ionized, strong electrostatic repulsion hinders hydrophobic interaction, making SDS and PAA behave independently.

The present study was undertaken to investigate the effects of these interactions between SDS and PAA on SWCNT dispersion. The dispersed amount of SWCNTs was found to depend on the SDS concentration in complicated way. At low pH, PAA binds to SWCNTs without SDS. Increasing the SDS concentration to above CAC promotes exchange adsorption by SDS, which proceeds inhomogeneously over the SWCNT surfaces.



Corresponding Author: Masahito Sano

TEL: +81-238-26-3072 E-mail: mass@yz.yamagata-u.ac.jp

Restoration of π -bands on the graphene “buffer layer” on SiC(0001) by low temperature oxidation

○Satoshi Oida, Fenton R. McFeely, James B. Hannon, Rudolf M. Tromp, Zhihong Chen, Yanning Sun, Damon B. Farmer and John J. Yurkas

IBM Research Division, T.J. Watson Research Center, Yorktown Heights, NY 10598, USA

Graphene, one, or a very few layers of graphite, has attracted many researchers because of its exotic properties¹. For compatibility with current fabricating processes, Si sublimation from SiC(0001) is attractive because wafer-sized graphene may be grown on a semi-insulating wafer. However, the first graphene layer is a non-conductive sheet, the so called “buffer layer”, due to the absence of π -bands caused by coupling to the SiC substrate². Furthermore, due to the SiC decomposition process, thick graphene growth can cause a rough surface, and this surface roughness considerably degrades the electronic properties. So modification of the buffer layer to restore the electronic properties of graphene would be beneficial. In our presentation, we demonstrate the restoration of π -bands on a graphene buffer layer by a simple oxidation process that produces a thin oxide layer between the graphene and the substrate.

The graphene buffer layer was synthesized by Si sublimation from SiC(0001) or by carbon CVD on SiC(0001). First, we note that the SiC substrate was patterned by FIB allowing multiple measurements from the same area of the surface. A dot-line in Fig.1 is an EELS spectrum taken on the as-grown sample surface in a LEEM chamber. No energy loss features are observed, as expected for the buffer layer with disrupted pi-bands. Then, the sample was introduced into an XPS chamber, and C 1s photoelectron spectra were obtained before and after oxidation (a dot- and a solid-line in Fig. 2). Compared to peaks in the spectrum taken on the non-oxidized sample, all peaks in the spectrum taken on the oxidized sample shifted toward lower binding energy, indicating a decoupling of buffer layer from SiC substrate. Furthermore, surface morphology did not change after oxidation. Next, the sample was re-introduced into the LEEM chamber and EELS spectrum was recorded from the same area (a solid-line in Fig. 1). The peak related to the graphene π -plasmon appears after the oxidation, indicating a restoration of π -bonds of the buffer layer. These results indicate semi-insulating buffer layer becomes *bona-fide* graphene without any surface modulations. We also measured conductance of before and after decoupled buffer layer and conductance increased by a factor of 10^4 .

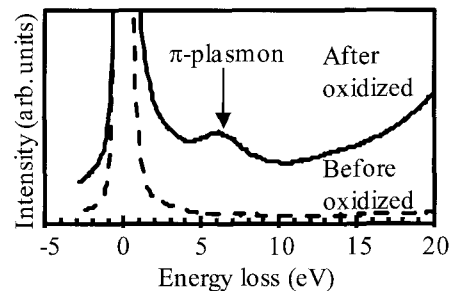


Fig.1 EELS spectra taken on the before or after oxidized sample surface.

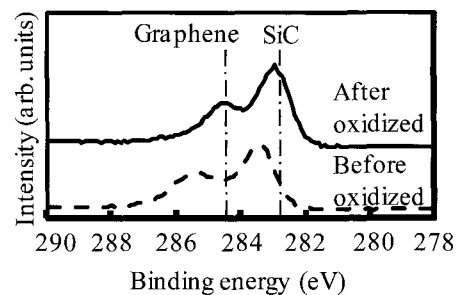


Fig.2 C 1s XPS spectra taken on the before or after oxidized sample surface.

¹K.S. Novoselov *et al.*, *Science*, **306**, 666 (2004).

²A. Mattausch and O. Pankratov, *Phys. Rev. Lett.*, **99** 076802 (2007).

Corresponding Author: Satoshi Oida

TEL: +1-914-945-1138, FAX: +1-914-945-2141, E-mail: soida@us.ibm.com

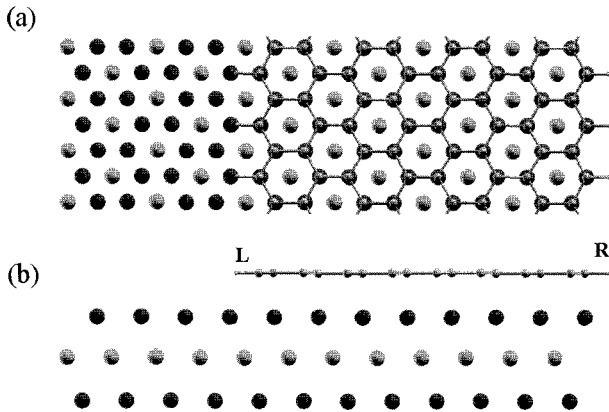
Magnetism in Graphene Nanoribbons on Ni(111)

○Keisuke Sawada, Fumiyuki Ishii and Mineo Saito

Division of Mathematical and Physical Science, Graduate School of Natural Science and Technology, Kanazawa University, Kakuma, Kanazawa 920-1192, Japan

Graphene is a candidate for spintronics materials[1, 2]. It is known that the flat-band ferromagnetism appears at the zigzag edges of graphene[3]. DFT calculation predicted that the magnetic ground state of zigzag graphene nanoribbon (ZGNR) is antiferromagnetic structure with anti-parallel ferromagnetic (FM) chains of both edges. Recently, we found that the FM state with parallel FM chains of both edges and noncollinear magnetic state with non-parallel FM chains of both edges can be achieved by carrier doping[4].

In this study, we clarify that the FM state also appears in the case of ZGNRs on Ni(111) (Fig. 1) by using first-principles calculations. We find that the magnetic moment of the edge C atom at the mono ZGNR on Ni(111) layer is very small due to the hybridization between π electron of the ZGNR and d electron of the first Ni layer (Table I). On the other hand, in the case of the bilayer ZGNR on Ni(111), the magnetic moment of the edge C atom at the top layer maintains and the FM state is the ground state. So the bilayer structure is favorable from the viewpoint of spintronics application.



Magnetic moment of edge C atoms (μ_B /atom)		
	ZGNR on Ni	isolated ZGNR
L	0.04	0.24
R	0.01	0.24

Fig. 1: Lattice structure of ZGNR on Ni(111). Top and side views are shown in (a) and (b), respectively.

Table I: Magnetic moment of edge C atoms.

- [1] Y. Son et al., *Nature* **444**, 347 (2006).
 [2] N. Tombros et al., *Nature* **448**, 571 (2007).
 [3] M. Fujita et al., *J. Phys. Soc. Jpn.* **65**, 1920 (1996).
 [4] K. Sawada et al., *Nano Lett.* **9**, 269 (2009).

Corresponding Author: Keisuke Sawada
 E-mail: sawada@cphys.s.kanazawa-u.ac.jp

Phase control on Magnetic State of Graphite Thin Films by Electric Field

○Minoru Otani^{1,4}, Mikito Koshino², Yoshiteru Takagi^{3,4}, and Susumu Okada^{3,4}

¹*Research Institute for Computational Sciences, National Institute of Advanced Industrial Science and Technology, Tsukuba 305-8568, Japan*

²*Department of Physics, Tokyo Institute of Technology, 2-12-1 Oh-okayama, Meguro-ku, Tokyo 152-8551, Japan*

³*Graduate School of Pure and Applied Sciences and Center for Computational Sciences, University of Tsukuba, 1-1-1 Tennodai, Tsukuba 305-8571, Japan*

⁴*Japan Science and Technology Agency, CREST, 5 Sanbancho, Chiyoda-ku, Tokyo 102-0075, Japan*

The recent synthesis of monolayer graphite (graphene) and graphene thin films have stimulated many theoretical and experimental studies on these materials. These works uncovered peculiar properties of graphite and graphene predicted by previous theory, and also showed novel unusual properties. Graphene is a material made of a hexagonal-symmetry carbon layer in which electron mobility along the layer is about ten times higher than that of the silicon. This characteristic property is resulting from the linear dispersion of the bands at the Fermi level. Besides the perfect two-dimensional graphene sheet, when graphene flaks or ribbons have edges with a zigzag shape, there is another peculiar electronic state at the Fermi level. This state is known as the edge state that is extended along the edge region with certain magnetic ordering: polarized electron spins are ferromagnetically aligned along each edge while antiferromagnetically coupled between two edges.

In the present work, based on the first-principle total-energy calculations, we demonstrate that the surface of the rhombohedral (ABC stacking) graphite layers show magnetic ordering at the surface region. The origin of the polarization is the flat-band states at the Fermi level. We also demonstrate the possibility of phase control on magnetic state of rhombohedral graphite layers by applying the external electric field normal to the layer. Our calculations clearly show that the rhombohedral graphite undergoes magnetic phase transition from ferrimagnetic to ferromagnetic states under the moderate electronic field. The present results give the possibility of applications of the graphite thin layers for a constituent material in spintornic devices with MOSFET structure.

Magnetism of Curved-Graphene and its Guest adsorption systems

○K. Takai^{1*}, T. Suzuki¹, T. Enoki¹, H. Nishihara², T. Kyotani²

¹*Department of Chemistry, Tokyo Institute of Technology, Tokyo 152-8551, Japan*

²*Institute of Multidisciplinary Research for Advanced Materials,
Tohoku University, Aoba-ku, Sendai, Miyagi, 980-8577, Japan*

The presence of a curvature gives additional functions to graphene, as well as the edge site, which gives a magnetic function to graphene-based host material in creating unconventional electronic and magnetic systems [1]. Here, we fabricate new graphene-based host materials with the curved nature, and investigate the magnetism of host-guest system based on them. An acetylene CVD with zeolite Y as a template is applied as a strategy for the fabrication of the arrayed nanographene host with a curvature. This results in the zeolite templated carbon (ZTC) after acid treatment, where the nanospace network composed of curved graphene sheet with the periodicity of 1.4 nm is present [2]. Non-guest-adsorbed ZTC is found to be paramagnetic host with a spin density of $\sim 1 \times 10^{20}$ / spin g⁻¹, which corresponds to the 1 spin per nanopore irrespective of the heat-treatment temperature. Potassium adsorbed ZTC exhibits an anomaly in the magnetic susceptibility around 16 K accompanied with a sudden increase in the ESR line width. In spite of no hysteresis in the case of non-adsorbed ZTC, the magnetization curve for K-ZTC shows hysteresis behavior at 2K, which becomes vanished at the temperature above 16 K. These suggest the onset of the magnetic order in the potassium clusters confined into nano space based on nanographene. On the other hand, bromine adsorption is found to be harmful for the nanospace network structure of ZTC, as it completely destroys the regularity of the structure and modify the ZTC host magnetism significantly.

References:

[1] K. Takai, S. Eto, M. Inaguma, T. Enoki, H. Ogata, M. Tokita and J. Watanabe, Phys. Rev. Lett. 98, 017203 (2007).

[2] T. Kyotani, T. Nagai, S. Inoue, and A. Tomita, Chem. Mater., 9, 609 (1997).

Corresponding Author: Kazuyuki TAKAI

E-mail: ktakai@chem.titech.ac.jp

Tel&Fax: +81-3-5734-2610, +81-3-5734-2242

Electrode-Width Dependence of Transistor Properties of Graphene

○Ryo Nouchi¹, Tatsuya Saito² and Katsumi Tanigaki^{1,2}

¹WPI-Advanced Institute for Materials Research, Tohoku University, Sendai 980-8577, Japan

²Graduate School of Science, Tohoku University, Sendai 980-8578, Japan

Graphene, one-atom-thick carbon sheet with a honeycomb structure, shows an extraordinary high mobility of charge carriers and is considered to be a major candidate for a future high-speed transistor material. Operation properties of electronic devices such as field-effect transistors (FETs) are known to be governed by the interfaces between a semiconductor channel and metallic electrodes. In the case of graphene FETs, metal contacts have been reported to affect the operation through charge transfer from electrodes to the

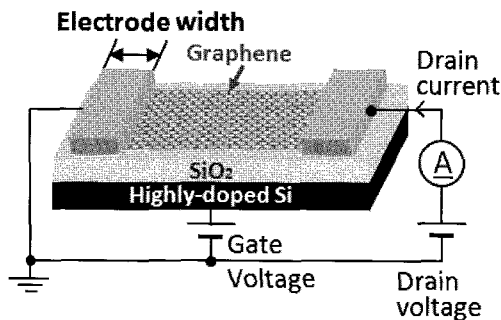


Fig.1 Schematic diagram of a graphene FET fabricated in this study.

Figure 2 shows transfer characteristics of graphene FETs with 0.8-, 2.4-, and 4.4- μm -wide Ni contacts. These results clearly display that wider contacts lead larger distortions. A general model of contact resistance, however, predicts that wider contacts result in smaller contact resistances and then smaller distortions. The contradiction between the model and the experimental results can be explained by the inhomogeneity of the actual interfaces.

graphene channel [1] and charge density pinning of graphene [2] at the metal-graphene interfaces. To the contrary, in the previous symposium, we have shown that distortions in transfer (drain current, I_D , versus gate voltage, V_G) characteristics of graphene FETs with ferromagnetic source/drain contacts [3] are attributable to metal-graphene interfaces *without* the charge density pinning (or with very weak pinning). In the present work, we examined graphene FETs which have Ni contacts with various electrode widths (Fig. 1) in order to gain further insights into the ferromagnet-graphene interface.

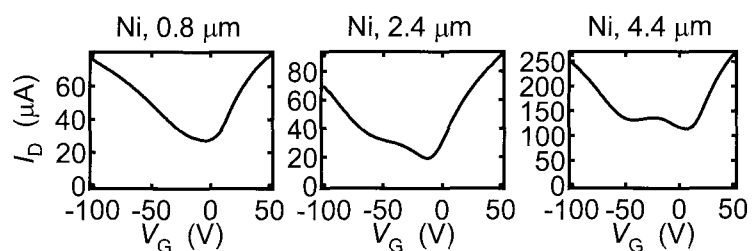


Fig.2 Transfer characteristics of graphene FETs with Ni source/drain electrodes. The contact widths are specified in the figure.

[1] G. Giovannetti, P. A. Khomyakov, G. Brocks, V. M. Karpan, J. van den Brink and P. J. Kelly, *Phys. Rev. Lett.* **101**, 026803 (2008).

[2] E. J. H. Lee, K. Balasubramanian, R. T. Weitz, M. Burghard and K. Kern, *Nat. nanotechnol.* **3**, 486 (2008).

[3] R. Nouchi, M. Shiraishi and Y. Suzuki, *Appl. Phys. Lett.* **93**, 152104 (2008).

Corresponding Author: Ryo Nouchi

TEL: +81-22-795-6468, FAX: +81-22-795-6470, E-mail: nouchi@sspns.phys.tohoku.ac.jp

ポスター発表
Poster Preview

1P-1 ~ 1P-41

2P-1 ~ 2P-42

3P-1 ~ 3P-41

Energetics and Electronic Structure of Nitrogen-doped Carbon Nanotube

○Yoshitaka Fujimoto and Susumu Saito

Department of Physics, Tokyo Institute of Technology, Tokyo 152-8551, Japan

Ever since the discovery of carbon nanotubes (CNTs) in 1991[1], carbon nanotubes have been studied extensively since they are expected to possess the potential applications in nanoelectronics devices such as a gas sensor, a field emission display and so on. In order to enhance the properties of the electron devices further, it is desired to understand relationship between the atomic and electronic structures, and control the electronic property of CNTs.

Nitrogen doping in CNTs is one of the most accessible means to tailor the electronic structures. Nitrogen-doped CNTs have been synthesized in several groups and x-ray photoelectron spectroscopy experiments have showed the existence of pyridine-type and substitution-type defects in CNTs[2,3].

We here investigate atomic and electronic structures, and energetics of the nitrogen-doped CNTs using the first-principles total-energy calculations within the framework of the density-functional theory. The pyridine-type [Fig. 1(a)] and substitution-type [Fig. 1(b)] configurations in CNTs are considered. In this presentation, the effects on diameter, chirality, and doping rate in the N-doped CNTs are discussed.

This work was partly supported by grants-in-aid from MEXT Japan through Global Center of Excellence Program of Nanoscience and Quantum Physics of Tokyo Institute of Technology.

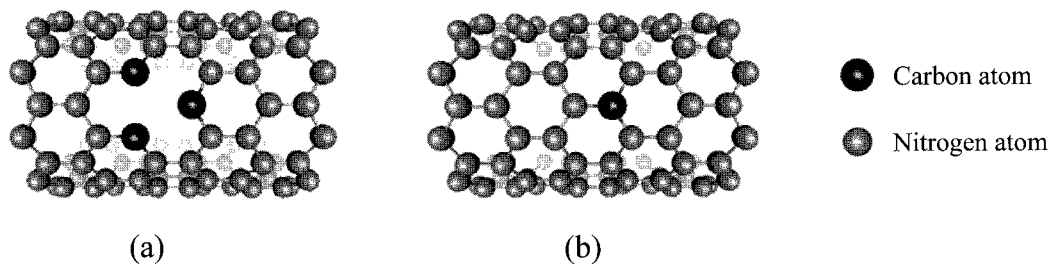


Fig. 1 Atomic structures of nitrogen-doped carbon nanotube with (a) pyridine-type defect and (b) substitution-type defect.

[1] S. Iijima, *Nature* **354**, 56 (1991).

[2] R. Czerw, M. Terrones, J. C. Charlier, X. Blasé, B. Foley, R. Kamalakaran, N. Grobert, H. Terrones, D. Tekleab, P. M. Ajayan, W. Blau, M. Ruhle, M. Ruhler, and D. L. Carroll, *Nano. Lett.* **1**, 457 (2001).

[3] W-C. Fang, *Nanotechnology* **19**, 165705 (2008).

Corresponding Author: Yoshitaka Fujimoto

TEL: +81-3-5734-2368, FAX: +81-3-5734-2368, E-mail: fujimoto@stat.phys.titech.ac.jp

Thermal conduction property measurements of vertically-aligned single-walled carbon nanotube film by utilizing Raman spectrum

○Kei Ishikawa, Shohei Chiashi, Theerapol Thurakitserree, Takuma Hori, Rong Xiang, Makoto Watanabe, Junichiro Shiomi, Shigeo Maruyama*

Department of Mechanical Engineering, The University of Tokyo, Tokyo 113-8656, Japan

We present two novel methodologies of measuring thermal conduction property of vertically-aligned single-walled carbon nanotubes (VA-SWNTs) grown by ACCVD method [1], both of them utilizing temperature dependence of the Raman spectrum obtained from SWNTs [2].

First methodology measures temperature gradient of the cross section of the VA-SWNT film (Fig. 1). Heat was generated at the heater, and was removed through Si. From the temperature measured at the both end of the film, the film thermal conductivity was deduced to be around $0.5 \text{ Wm}^{-1}\text{K}^{-1}$. Si also shows temperature dependence [3], from which thermal contact resistance between the film and the Si substrate was deduced to be around $8 \times 10^{-6} \text{ m}^2\text{KW}^{-1}$.

Second methodology utilizes the excitation laser of the Raman system, the absorption characteristics [4] and the strong anisotropy [5] of the VA-SWNT film (Fig. 2). Excitation laser power of the Raman system is absorbed and converted into heat mostly at the top part of the film. Assuming lateral heat conduction inside the film is small enough, we can say that heat is dominantly transported along SWNTs to Si. Since most of the Raman signal comes from the top part of the film, the measured temperature from Raman spectrum is from the top part of the film. From the measured temperature, the film thermal resistance plus the thermal contact resistance was deduced to be $10^{-5} \sim 10^{-6} \text{ m}^2\text{KW}^{-1}$.

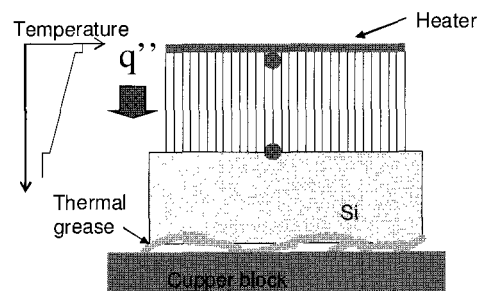


Fig. 1 Schematics of thermal conductivity / thermal contact resistance measurement by measuring temperature of the cross section

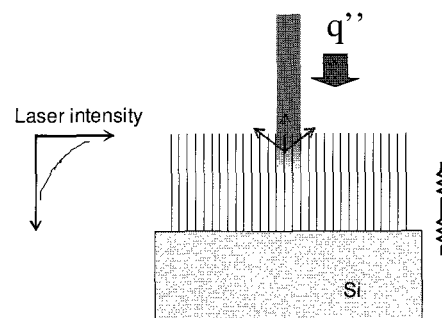


Fig. 2 Schematics of thermal conduction property measurement by excitation laser of the Raman system

[1] Y. Murakami *et al.*, *Chem. Phys. Lett.*, **385** (2004) 298.

[2] S. Chiashi *et al.*, *Jpn. J. Appl. Phys.*, **47** (2008) 2010.

[3] M. Balkanski *et al.*, *Phys. Rev. B*, **28** (1983) 1928.

[4] E. Einarsson *et al.*, *Carbon*, **46** (2008) 923.

[5] C. Lin *et al.*, *2nd Int. Conf. New Diam. Nano Carbons (NDNC 2008)*, (2008).

Corresponding Author: Shigeo Maruyama

Tel&Fax: +81-3-5800-6983, E-mail: maruyama@photon.t.u-tokyo.ac.jp

Deformation and transfer doping of a single-walled carbon nanotube adsorbed on the metallic substrates

Masayuki Hasegawa¹ and Kazume Nishidate²

¹*Faculty of Engineering, Iwate University, Morioka 020-8551, Japan*

²*Department of Electrical Engineering and Information Science, Iwate University, Morioka 020-8551, Japan*

We have examined the effects of radial deformation and transfer doping on the electronic properties of an armchair single-walled carbon nanotube (SWNT) adsorbed on the gold (Au) and silver (Ag) surfaces. Using a semiempirical method developed on the basis of the continuum elastic shell model [1], it is found that the radial deformation of SWNTs with $D < 21 \text{ \AA}$, where D is nanotube diameter, is reversible in the whole range of radial deformation. Whereas, large deformations of SWNTs with $D > 21 \text{ \AA}$ tend to be irreversible and a collapsed nanotube can be stabilized [2]. We have chosen the metallic armchair (21,21) SWNT with $D \approx 28.5 \text{ \AA}$ and confirmed by *ab initio* calculations that large deformation of this nanotube can actually be stabilized and the collapsed tube is a semiconductor with small band gap of $\sim 60 \text{ meV}$. The charge transfers of this nanotube, both circular and collapsed, adsorbed on the Au(100) and Ag(100) were investigated by large-scale *ab initio* calculations and a phenomenological model, which was developed on the basis of the rigid-band model. The model yields the Fermi-level shift of the nanotube adsorbed on the Au(100) surface in good agreement with the experiments [3, 4] and provides a useful insight into the transfer doping. On the other hand, the transfer doping virtually does not occur for the nanotube adsorbed on the Ag surface, not in agreement with the experiments with large uncertainty. The phenomenological model is also applied to the graphene adsorption on the metallic surfaces and is found to yield reasonable results for the transfer doping and to be useful in understanding the previous results [5], both experimental and theoretical.

- [1] M. Hasegawa and K. Nishidate, Phys. Rev. B **74**, 115401 (2006).
- [2] M. Hasegawa and K. Nishidate, e-J. Surf. Sci. Nanotech. **7**, 541 (2009).
- [3] J. W. G. Wildoer *et al.* Nature (London) **391**, 59 (1998).
- [4] C. E. Giusca, Y. Tison, and S. R. P. Silva, Phys. Rev. B **76**, 035429 (2007).
- [5] H.-J. Shin, S. Clair, Y. Kim, and M. Kawai, Appl. Phys. Lett. **93**, 233104 (2008).

Corresponding Author: Masayuki Hasegawa

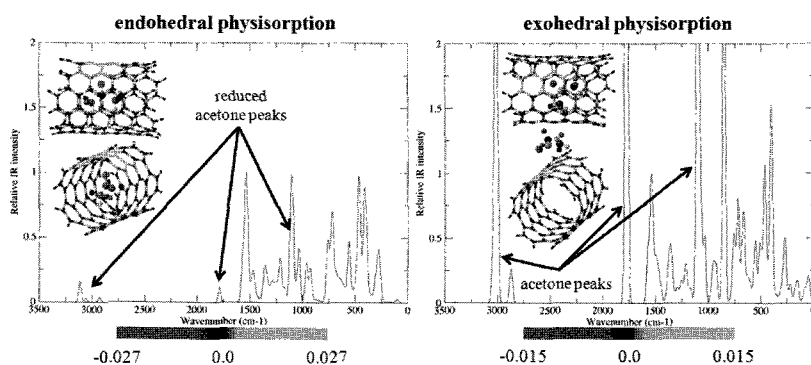
TEL: +81-19-621-6948, FAX: +81-19-661-6012, E-mail: hasegawa@iwate-u.ac.jp

IR and Raman Stealth Effect for Molecules Absorbed on Single-Walled Carbon Nanotubes

○Yoshifumi Nishimura, Stephan Irle

*Institute for Advanced Research and Department of Chemistry, Nagoya University,
Nagoya 464-8602, Japan*

Theoretical investigations on vibrational properties of large molecules containing hundreds of atoms such as carbon nanotubes (CNTs) have never been accomplished due to heavy computational costs when *ab initio* or density functional theory with dispersion correction (DFT-D) are employed. However, dispersion augmented self-consistent-charge density functional tight-binding (SCC-DFTB-D), where analytical second-order geometrical derivatives of the total energy are available, allows to simulate reliable IR and Raman spectra of nanoscale materials with DFT-D-like accuracy. Here, we applied this methodology to systems where molecules are physisorbed on single walled CNTs (SWCNTs). As an example, the IR spectra for the case of an acetone molecule physisorbed endo- and exohedrally on hydrogen-terminated, 10 Å long (6,5) SWCNT fragments are shown below. In agreement with combined temperature programmed desorption (TPD) and FTIR experimental studies it was observed that the intensities of endohedrally adsorbed acetone peaks are greatly reduced compared with those of the exohedrally adsorbed or free species. Since the integrated IR intensities are proportional to the change of molecular dipole moment during oscillations along the corresponding normal coordinates, it is important to consider the magnitude of the induced image dipoles on the highly polarizable SWCNT sidewalls for both cases. Induced Mulliken atomic charges and dynamic charge fluctuations during vibrations (which are directly proportional to the IR intensities) were visualized, and we clearly identified dielectric screening due to the SWCNT sidewalls, even though the model systems are of finite length and formally non-metallic. Although



Faraday shielding and dipole screening have already been reported for fullerenes and SWCNTs, this is the first time to theoretically predict and quantify the spectroscopic IR stealth effect of molecules encapsulated inside SWCNTs.

Corresponding Author: Stephan Irle

TEL: +81-52-747-6397, FAX: +81-52-788-6151, E-mail: sirle@iar.nagoya-u.ac.jp

Effect of adsorption of benzene on field electron emission from a carbon nanotube

Department of Quantum Engineering, Nagoya University
 Akkawat RUAMMAITREE, Hailong HU, Hitoshi NAKAHARA, Yahachi SAITO
 Email: akkawat@surf.nuqe.nagoya-u.ac.jp

1. Introduction

Carbon nanotubes (CNTs) are characterized by high aspect ratio, small radii of curvature at the tip, mechanical toughness and so on. CNTs have received considerable attention in the field of electron-beam technology. For field-electron sources, the CNT can continually emit electrons for a long period even in non-ultrahigh vacuum (non-UHV). Moreover, the current density of CNT can be increased when the CNT adsorbs hydrocarbon gas [1, 2]. In this report, the increase of emission current from a CNT was studied when benzene molecules were adsorbed on the surface of CNT.

2. Experimental

A piece of tungsten (W) wire was electrochemically etched by 2M sodium hydroxide (NaOH) to make a sharp tungsten tip. A multiwall CNT was mounted on the sharp W tip using a manipulator in a scanning electron microscope (SEM). A SEM image of the CNT emitter is shown in Fig.1. Then, the CNT emitter was put in a vacuum chamber for field emission microscope (FEM) and heated up to about 700 °C for 30 seconds to clean the surface before FEM observation. The background pressure of the FEM is 1.4×10^{-7} Pa. After introducing benzene, the measurement was conducted under the pressure of 1×10^{-5} Pa.

3. Results and Discussion

Fig.2 shows current-voltage (I - V) characteristics before and after introducing benzene gas. It is obvious that in the presence of benzene the emission current increased greatly. At the same time, the absolute value of slope in the Fowler-Nordheim plot decreased. Fig.3 shows FEM images for the CNT emitter. By comparison, the emission pattern size and shape did not change apparently after introducing benzene gas into the chamber. Therefore the emission area and field enhancement factor did not change significantly. From the Fowler-Nordheim equation, the remarkable increase in emission current could be attributed to the change in work function. Woods *et al.* calculated the total density of state of benzene-adsorbed single-wall CNT(8,0) and found that the Fermi energy and the highest occupied molecular orbital of CNT increase by the physisorbed derivatives [1]. It is the benzene molecules adsorbed on the emitter tip that decreases the work function and ionization potential, thus resulting in easier extraction of electrons from the CNT emitter.

4. conclusion

The effects of adsorbed benzene molecules on the field emission behaviors of a single CNT were studied. It was found that absorption of benzene molecules on the CNT surface can increase the emission current in I - V characteristic. This was attributed to the decrease in work function of the emitter caused by the benzene adsorbates.

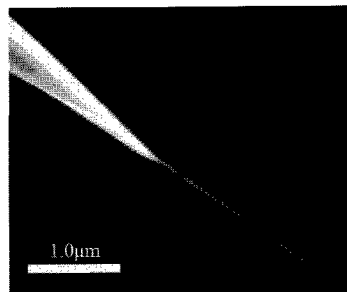


Fig. 1. SEM image of a CNT emitter.

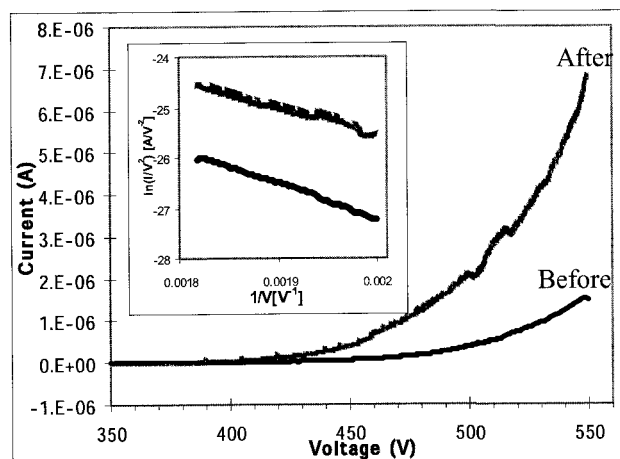


Fig. 2. I - V characteristics of emitter measured before and after introducing benzene molecules. Inset shows the Fowler-Nordheim plot.

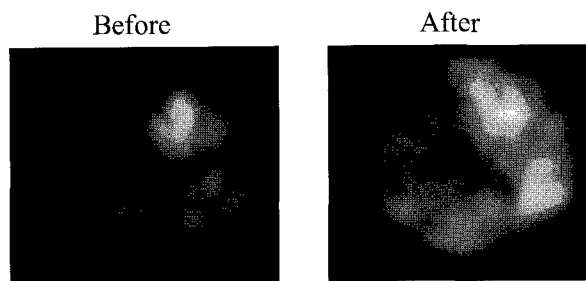


Fig. 3. FEM images before and after introducing benzene.

References:

- [1] L. M. Woods et al. Phys. Rev. B 75, 155415 (2007)
- [2] T. Yamashita, Master's thesis, Nagoya University (2009)

Theoretical Investigation on Single-Walled Carbon Nanotubes Functionalized by Bingel Reaction

○Eisuke Kawabata¹, Hiroyuki Fueno¹, Kazuyoshi Tanaka¹, Tomokazu Umeyama¹ and Hiroshi Imahori^{1,2}

¹Graduate School of Engineering, Kyoto University, Kyoto 615-8510, Japan

²Institute for Integrated Cell-Material Sciences, Kyoto University, Kyoto 615-8510, Japan

It is known that covalent modification at sidewall significantly alters the electronic properties of the pristine single-walled carbon nanotubes (SWCNTs). However, we recently revealed that the electronic structures of SWCNTs are largely retained after a significant degree of sidewall modification by the nucleophilic cycloaddition of enolate anion, namely Bingel reaction, by experimental investigations [1]. Here, we report the first theoretical study of the structural and electronic properties of SWCNTs functionalized by Bingel reaction based on density functional theory.

Computational calculations were performed at B3LYP level with the 3-21G basis set using the Gaussian 03 program package. We used fragments of an armchair (8,8) tube containing 140 carbon atoms as a typical model of pristine SWCNTs in this study. We also calculated the tube fragment functionalized by Bingel reaction with dimethylmalonate. There are two types of the binding configurations, in which the plane of the three-membered ring is perpendicular (denoted as Type 1) and slanted (Type 2) to the tube axis (Figure 1).

Figure 2 shows orbital energy diagrams of the (8,8) tube fragment functionalized with one dimethylmalonate (Type 1 and 2) as well as the pristine one. The binding configurations significantly influence the electronic structures. The orbital energies of Type 1 are retained very much after the sidewall functionalization by the Bingel reaction, whereas the addition reaction with Type 2 configuration clearly causes the splitting of orbitals. In addition, the similar calculation using a chiral (10,5) tube fragment also revealed that the electronic properties are preserved very much after the modification with perpendicular configurations. Accordingly, selective formation of cyclopropane ring relatively perpendicular to tube axis will rationalize the retention of the electronic properties of SWCNTs functionalized by the Bingel reaction.

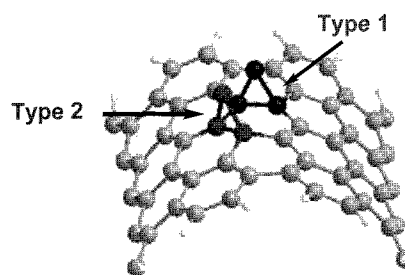


Figure 1. Binding configurations of dimethylmalonate attached to (8,8) SWCNTs.

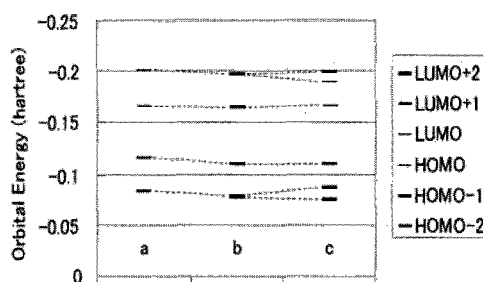


Figure 2. Orbital energy diagrams of the (8,8) tube fragments. (a) Pristine, (b) Type 1, and (c) Type 2.

Reference: [1] Umeyama, T.; Tezuka, N.; Fujita, M.; Matano, Y.; Takeda, N.; Murakoshi, K.; Yoshida, K.; Isoda, S.; Imahori, H. *J. Phys. Chem. C* **2007**, *111*, 9734.

Corresponding Author: Eisuke Kawabata

E-mail: kawabata.eisuke@t03.mbox.media.kyoto-u.ac.jp

Tel: +81-75-383-2568, Fax: +81-75-383-2571

Vibrational spectra and excited state calculation of polyynes@SWNTs

○ M. M. Haque, R. Saito

Department of Physics, Tohoku University, Sendai 980-8578, Japan

Early calculations by Longuet-Higgins and Burkitt (1952) and Hoffman (1966) concluded that polyynes (linear chain of even number of carbon atoms) are chemically bonded with alternatively single and triple bonds. Finite-size polyynes $\text{H}-(\text{C}\equiv\text{C})_n-\text{H}$ have been synthesized using several techniques by several experimental groups (Eastmond *et al.* 1972, Kloster-Jensen 1972 up to $n=12$, Masaharu Tsuji *et al.* up to $n=8-14$, Nishide *et al.* up to $n = 8-16$ etc.). However, polyynes is unstable in gaseous form but it has been observed that it is surprisingly stable (well above 300°C under dry-air conditions) inside carbon nanotubes. Nishide *et al.* [1,2] have confirmed the encapsulation of polyynes inside SWNTs by Raman spectroscopy and X-ray diffraction measurement. They studied Resonance Raman spectra for the systems $\text{C}_n\text{H}_2@\text{SWNTs}$ ($n=8,10,12$) and found the band in a region of $2000-2200\text{ cm}^{-1}$ which is due to the Raman active modes (σ_g in D_{oh}) of stretching vibrations of the linear carbon chain, namely the polyynic ‘‘P’’ band. The fine structure within the band is explained as due to the presence of more than two Raman active modes. Another weak band near around $\sim 3600\text{ cm}^{-1}$ is found which is the combination of vibrational transitions of the graphitic G and polyynic P band. Resonance Raman study of $\text{C}_n\text{H}_2@\text{SWNTs}$ [3] at different laser lines also showed that a strong enhancement of the polyynes Raman features is observed around 2.1 eV and this result is ascribed to dark electronic transitions of the linear carbon chains that is observed when they are trapped inside CNTs.

In this work we reproduce the Raman spectra for the system polyynes@SWNTs by using DFT (B3LYP) calculation using Gaussian basis (6-31G) sets. Our calculation also includes configuration interaction (CI) method to calculate the excited states energies of polyynes. As it has been reported that excitons exist in carbon nanotubes because of their high binding energies even at room temperature, in our calculation we examine the existence of exciton in the polyyn@SWNTs. Exciton binding energy in polyynes is comparatively higher than those on CNTs hence it could be expected that electronic transition through optical absorption can take place from CNTs to excited states of polyynes which would result a high intense of Raman signals. We also calculate the force constants associated with the IR and Raman active modes for polyynes.

[1] D. Nishide, H. Dohi, T. Wakabayashi, E. Nishibori, S. Aoyagi, M. Ishida, S. Kikuchi, R. Kitaura, T. Sugai, M. Sakata, H. Shinohara, *Chemical Physics Letter*, 428, 2006, 356-360

[2] D. Nishide, T. Wakabayashi, T. Sugai, R. Kitaura, H. Kataura, Y. Achiba, and H. Shinohara, *J. Phys. Chem. C* 2007, 11, 5178-5183

[3] L. M. Malard, D. Nishide, L.G. Dias, Rodrigo B. Capaz, A. P. Gomes, A. Jorio, C. A. Achete, R. Saito, Y. Achiba, H. Shinohara, and M. A. Pimenta, *Physical Review B*, 76, 233412 (2007)

Corresponding Author: Md. Mahbul Haque

TEL: +81-22-795-5719, FAX: +81-22-795-6447, E-mail: mmhaque@flex.phys.tohoku.ac.jp

Simple dielectric constant function for the environment effects on the exciton energies of single-wall carbon nanotubes

○ Ahmad R.T. Nugraha¹, Riichiro Saito¹, Kentaro Sato²,
Paulo T. Araujo³, Ado Jorio³

¹*Department of Physics, Tohoku University, Sendai 980-8578, Japan*

²*Department of Mechanical Engineering, University of Tokyo, Tokyo 113-8656, Japan*

³*Department of Physics, UFMG, Belo Horizonte 30123-970, Brazil*

The excitonic transition energies E_{ii} for a given single-wall carbon nanotube (SWNT), where $i = 1, 2, 3, \dots$ characterizes the transitions between the i -th valence and the i -th conduction band, are known to be strongly affected by the change of surrounding materials around the SWNT, which is known as the environmental effect [1,2]. The E_{ii} of SWNT measured in some different environments can now be reproduced consistently by considering a dielectric constant κ as a function of cutting line parameter p , nanotube diameter d_t and exciton size l_k^{-1} . In the previous calculation κ depends only on the nanotube diameter [3], thus the κ function has to be prepared for each E_{ii} and each metallicity of the nanotubes: metal, semiconductor type-I and type-II. By including the exciton size, the κ function is improved to work well for all samples considered here and also for dominant transitions observed in the experiments: E_{11}^S , E_{22}^S , E_{11}^M , E_{33}^S , E_{44}^S [4]. The dependence on surrounding materials can then be expressed by a constant parameter κ_{env} for each sample.

Using the κ function thus obtained, we calculate the shift of E_{ii} from $\kappa = 1$ (vacuum) for many samples. The calculated results are compared with (1) water-assisted CVD (supergrowth sample), (2) alcohol-assisted CVD + SDS, (3) HiPCO and (4) trench-suspended nanotubes with several different environments [5]. This work is expected to be a practical guide for experimentalists in constructing a general Kataura plot which is free from environmental effect.

- [1] C. Fantini, A. Jorio, M. S. Strano, M. S. Dresselhaus, M. A. Pimenta, *Phys. Rev. Lett.* 93, 147406 (2004).
- [2] Y. Ohno, S. Iwasaki, Y. Murakami, S. Kishimoto, S. Maruyama, T. Mizutani, *Phys. Rev. B* 73, 235427 (2006).
- [3] P. T. Araujo, A. Jorio, M.S. Dresselhaus, K. Sato, R. Saito, *Phys. Rev. Lett.* 103, 146802-1-4 (2009).
- [4] A.R.T. Nugraha, R. Saito, K. Sato, P. T. Araujo, A. Jorio, *unpublished*.
- [5] Y. Ohno, S. Iwasaki, Y. Murakami, S. Kishimoto, S. Maruyama, T. Mizutani, *arXiv:0704.1018* (2007)

Corresponding Author: A.R.T. Nugraha

TEL: +81-22-795-5719, FAX: +81-22-795-6447, E-mail: nugraha@flex.phys.tohoku.ac.jp

What is the exciton effect in the Raman resonance window of semiconducting single wall carbon nanotubes?

Jin Sung Park¹, Kentaro Sato², Riichiro Saito¹

¹*Department of Physics, Tohoku University, Sendai 980-8578, Japan*

²*Department of Mechanical Engineering, University of Tokyo, Tokyo 113-8656, Japan*

In the Raman excitation profile (RRP), that is Raman intensity as functions of excitation energy, an important parameter for evaluating the population of SWNTs is the Raman resonance window, γ , which is defined by an energy full width at half maximum in the RRP. In quantum mechanics, γ is obtained by the uncertainty relation for the lifetime of the exciton. A dominant origin of the lifetime of the exciton in the Raman scattering process is an inelastic scattering by emitting or absorbing phonons. In the previous paper, we have calculated the carrier lifetime by considering electron-phonon interaction and the Fermi golden rule [1]. In the case of semiconducting (S-) SWNT, the calculated γ values are in a good agreement with the experiment. However, some deviation between calculation and experiment appears in a different way for type I and II S-SWNTs in which type I and II S-SWNTs are defined, respectively, by $[\text{mod}(2n+m,3)=1]$ and $[\text{mod}(2n+m,3)=2]$ for a (n,m) SWNT. In fact, the experimental γ values for the type I S-SWNTs are smaller than the calculated ones while those for the type II S-SWNTs are larger than the calculated one. A possible reason for this deviation might come from the exciton effect which we did not consider in the previous calculation. For improving the deviation, we calculate the γ value by considering exciton-phonon interaction. The exciton-phonon matrix element for the electron scattering process can be obtained by the electron-phonon matrix element weighted by the exciton wave function coefficient [2] which depends on the chiral angle and diameter. In the previous calculation [2], we use a simple tight binding wavefunction for exciton-phonon interaction, but recently, the exciton-phonon interaction is calculated by extended tight binding method. We will report the new calculated γ values and compare with the recent precise measurement by single nanotube spectroscopy.

Reference:

- 1) J. S. Park, et al., Phys. Rev. B, 74, 165414, (2006)
- 2) J. Jiang, et al., Phys. Rev. B, 75, 035405, (2007)

*Email address: park@flex.phys.tohoku.ac.jp

Control of colors of thin films of metallic and semiconducting single-wall carbon nanotube by electrochemical doping

○ R.Moriya¹, K.Yanagi¹, T.Suzuki¹, Y.Naitou², H.Kataura^{2,3}, K.Matsuda¹,
Y.Maniwa^{2,3}

1. Department of Physics, Tokyo Metropolitan University

2. Nanotechnology Research Institute, National Institute of Advanced Industrial Science and Technology (AIST)

3. JST-CREST

Single-wall carbon nanotubes (SWCNTs) can exhibit colors depending on their chirality. For example, metallic SWCNTs with three different diameters, 0.9, 1.0, and 1.4 nm, have yellow, magenta, and cyan colors, respectively.¹ It is one of fascinating subjects to develop a technique to control the colors of SWCNTs for the following two reasons: (1) The colors of SWCNTs impede efficient photoexcitation on encapsulated molecules, thus the removal of the colors is crucial to understand the details of the optical properties of encapsulated molecules. (2) A method to tune the colors of nanotubes will open a door to color display devices using SWCNTs. One of approaches to change the color of SWCNTs is to dope electronic states of SWCNTs by electrochemical processes. A number of studies about electrochemical doping on SWCNTs has been reported.² However, most of the studies have focused on the change of optical absorption/emission of semiconducting SWCNTs in near infra-red region, and it is not clear whether it is possible to change the optical absorption bands of metallic (or semiconducting) SWCNTs in visible region. Therefore, this study was performed to clarify whether electrochemical doping can remove the color of SWCNTs. We prepared high-purity metallic and semiconducting SWCNTs with diameter of 1.4 nm by a density gradient method, and performed electrochemical doping on their thin films. Figure 1a shows the changes of the optical absorption spectrum of the metallic SWCNTs induced by electrochemical doping at different electrode potentials. The results clearly indicate that the absorption bands could be completely removed by this technique, and that it is possible to change the color of thin film by this process. This study was partially supported by Industrial Technology Research Grant Program in 2007 from NEDO and a Grant-in-Aid for Scientific Research on Innovative Areas (π -Space) from MEXT, Japan.

Reference: [1] Yanagi et al. Appl. Phys. Express 1 034003 (2008). [2] Kazaoui et al. (2001), Kavan et al. (2001), Okazaki et al. (2003), Tanaka et al., (2009)

Corresponding Author: K. Yanagi
E-mail: yanagi@phys.metro-u.ac.jp
Tel & Fax: 042-677-2494 (& 2483)

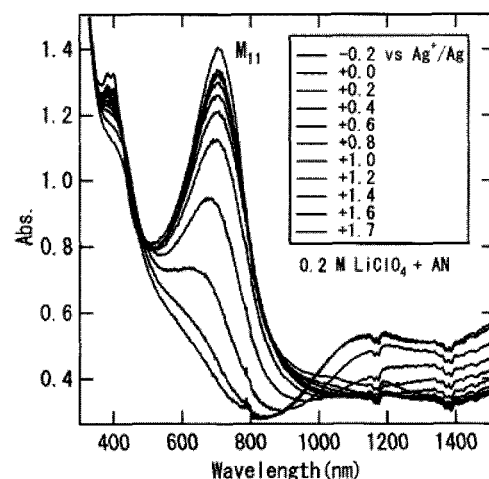


FIG1: Change of optical absorption spectrum of a thin film of metallic SWCNT induced by electrochemical doping at different electrode potentials.

Exciton environmental effects of resonance Raman and photoluminescence intensity of single wall carbon nanotubes

○Kentaro Sato¹, Riichiro Saito² and Shigeo Maruyama¹

¹*Department of Mechanical Engineering, The University of Tokyo,
7-3-1 Hongo, Bunkyo-ku, Tokyo 113-8656, Japan*

²*Department of Physics, Tohoku University, Aramaki, Aoba-ku, Sendai 980-8578, Japan*

Resonance Raman spectroscopy and photoluminescence (PL) have been used to investigate exciton physics of single wall carbon nanotubes (SWNTs). Experiments and theoretical studies have been demonstrated that resonance Raman and PL intensity depend on diameter, chirality and environment of SWNTs [1-4]. The excitonic effect in the presence of electron-hole and electron-electron interaction and the screening from the environment occurs to the change of the intensity and the optical transition energy of the PL and resonance Raman peaks. To investigate the excitonic effect in the PL and resonance Raman spectra, we need to consider and calculate the PL and resonance Raman intensity in the exciton picture.

In this paper we will discuss the excitonic effect of the PL and resonance Raman intensity, and the dependence of the PL and resonance Raman intensity on diameter and chirality. Here we use the exciton-phonon and exciton-photon matrix elements in the framework of the tight-binding scheme in order to calculate the PL and resonance Raman intensity in the exciton picture. The exciton energy and the exciton wave function coefficient of SWNTs are calculated by solving the Bethe-Salpeter equation in which the one particle energies are given by the tight-binding method [4-6]. The screening from environment and nanotubes itself is expressed by the dielectric constant. We also compare our calculation results with the experimental results.

References:

- [1] C. Fantini *et al.*, Chem. Phys. Lett. **473**, 96 (2009).
- [2] P. T. Araujo *et al.*, Phys. Rev. Lett. **103**, 146802 (2009).
- [3] Y. Oyama *et al.*, Carbon **44**, 873 (2006).
- [4] J. Jiang *et al.*, Phys. Rev. B **75**, 035407 (2007).
- [5] T. Ando, J. Phys. Soc. Jpn. **66**, 1066 (1997).
- [6] J. Jiang *et al.*, Phys. Rev. B **75**, 035405 (2007).

Corresponding Author: Kentaro Sato

Tel: +81-3-5841-6408, E-mail: kentaro@photon.t.u-tokyo.ac.jp

Structure separation of single-walled carbon nanotubes by agarose gelHuaping Liu^{1,2}, Ye Feng^{1,2,3}, Takeshi Tanaka¹, Hiromichi Kataura^{1,2*}¹Nanotechnology Research Institute, National Institute of Advanced Industrial Science and Technology (AIST), Tsukuba, Ibaraki 305-8562, Japan²Japan Science and Technology Agency, CREST, Kawaguchi, Saitama 330-0012, Japan³Institute of Materials Science, University of Tsukuba, Ibaraki 305-8573, Japan

Abstract: Metallic (M) and semiconducting (S) single-walled carbon nanotubes (SWCNTs) are usually grown together in a complex mixture of many different structure types. These structural variations result in striking difference in their electronic behaviors, therefore often lead to low on-off ratios, low effective field-effect mobility and low-yield high-performance electronic devices. One of the technologically critical tasks to realize applications based on SWCNT films is to obtain SWCNTs with well-defined structures and electronic properties. To date, various strategies, such as enrichment by selective chemistry, electrical breakdown, electrophoretic separation, chromatography, and ultracentrifugation, have been developed to obtain mono-structure SWCNTs [1].

Recently, our research group developed novel and simple methods to large-scale separate MS SWCNTs by agarose gel [2-4]. Especially, continuous MS separation of SWCNTs has been realized by agarose gel chromatography. Here we further investigate the continuous MS separation of SWCNTs by agarose chromatography. We found that, during the collection of metallic and semiconducting nanotubes, the structures of SWCNTs are sensitive to the concentration of surfactant eluant. By the successive addition of the different concentration surfactant solutions and fractional collection at every concentration, we achieved the structure separation of metallic and semiconducting SWCNTs, respectively. These results also demonstrated that the surfactants have selectivity in the adsorption not only on the electronic states but also on the structural difference.

References:

- [1] M. C. Hersam, *Nat. Nanotechnol.* 2008, **3**, 387.
- [2] T. Tanaka, et al., *Appl. Phys. Express* 2008, **1**, 114001
- [3] T. Tanaka, et al., *Nano Lett.* 2009, **9**, 1497.
- [4] T. Tanaka, et al., *Appl. Phys. Express* 2009, **2**, 125002.

* Corresponding author: e-mail h-kataura@aist.go.jp

Graph-Theoretical Study of Finite Length Zigzag Carbon Nanotubes

○Noriyuki Mizoguchi

Meiji Pharmaceutical University, Kiyose, Tokyo 2-522-1, Japan

An interesting aspect of finite-length single-walled carbon nanotubes (SWCNTs) is the quantum finite-size effects of the energy gap between the highest occupied molecular orbital (HOMO) and the lowest unoccupied molecular orbital (LUMO). It has been revealed that the HOMO-LUMO gaps of zigzag SWNTs oscillate with an odd or even number of hexagons in the circular plane of the nanotube [1]. The aim of this paper is to clarify a close relationship between HOMO-LUMO gap and peripheral circuit in the zigzag SWNTs. For this purpose we use graph-theoretical method employing Hückel molecular orbital method.

The constant term $a_N(G)$ in the characteristic polynomial for a graph G is zero if at least one of x_k 's is zero. Here x_k ($k=1,2, \dots, N$) are the roots of $P_G(x)=0$, and N denotes the number in the graph G . Let G be a graph representing the π -network of a $(n,0)_m$ zigzag carbon nanotube with m strips. The number of Kekule structures in G is $K=2^{m+1}$. Note that K does not depend on n . Sachs theorem enables us to generate $a_j(G)$ from the structure of the graph G . By applying Sachs theorem to $a_N(G)$ we showed that

$$\begin{aligned} \text{absolute value of } a_N(G) &= 0 && \text{if } n = \text{even} \\ &= K^2 && \text{if } n = \text{odd} \end{aligned}$$

because the size of the peripheral circuits in G is $4k$ if $n = \text{even}$, and $4k+2$ if $n = \text{odd}$. Thus we proved that the HOMO-LUMO gap of a $(n,0)_m$ zigzag SWNT is zero if the number of hexagons n in a strip is even, and non-zero if n is odd. This result means that peripheral circuits destabilize the system if they are $4n$ -membered circuit, and stabilize if they are $4n+2$ -membered circuit. This statement is in accord with the Hückel $4n+2$ rule for planar conjugated hydrocarbons.

[1] M. M. Mestechkin, *J. Chem.Phys.*, **122**, 074305 (2005).

Corresponding Author: Noriyuki Mizoguchi
TEL: +81-42-495-8611, E-mail: nori@my-pharm.ac.jp

Physical properties of boron-doped Carbon nanotube grown by Microwave Plasma CVD method

○Tohru Watanabe^{1,2}, Shunsuke Tsuda^{1,3}, Takahide Yamaguchi¹, Yoshihiko Takano^{1,2}

¹*National Institute for Materials Science, 1-2-1, Sengen, Tsukuba, Ibaraki, 305-0047*

²*Tsukuba University, 1-1-1, Tennodai, Tsukuba, Ibaraki, 305-8577*

³*WPI-MANA, 1-1, Namiki, Tsukuba, Ibaraki, 305-0044*

Carbon nanotube (CNT), which has low resistivity, is expected to be applied to various devices, for example, transparent electrodes, nanowiring for future LSIs, probes for scanning probe microscopes and so on. However, CNT shows semiconducting and metallic behavior depending on the chiral vector. In general semiconductors, carrier doping reduce resistivity. In diamond case, heavily boron doping makes resistivity lower and finally, it shows superconductivity at low temperature ⁽¹⁾. CNT and diamond are composed of only carbon atom. Therefore, referring boron-doped diamond, growth of boron-doped CNTs was attempted.

We synthesized boron-doped CNT with microwave plasma chemical vapor deposition (MWCVD) method. Methane and tri-methyl-borate gases were used to CNT synthesis as source materials. CNTs were grown on the SiO₂ substrate. We synthesized various boron concentration CNT, and we succeeded to obtain very long and vertically aligned CNT. Obtained CNT were characterized by Raman spectroscopy. And electrical property of individual CNT was measured by four terminals method. Four terminals on a individual CNT were established using electron beam lithography technique. We compared CNTs with various boron concentration with commercial pure CNT. Our boron-doped CNTs have lower resistivity than commercial CNTs.

References: (1) Y.Takano et al. Appl. Phys. Lett., Vol. 85, No. 14, 4

Corresponding Author: WATANABE TOHRU

E-mail: WATANABE.Tohru@nims.go.jp

Tel : 029-859-3354

Fax: 029-859-2601

Energetics and Electronic Structures of Twisted Carbon Nanotubes

○Koichiro Kato and Susumu Saito

*Department of Physics, Tokyo Institute of Technology
2-12-1 Oh-okayama, Meguro-ku, Tokyo 152-8551, Japan*

Carbon nanotube (CNT) has been considered to be one of the most important materials in nanoscience and nanotechnology. The reason of this attention mainly comes from their unique electronic properties. The electronic structures of CNT sensitively depend on the diameter and chirality. Therefore, it is very important to know the accurate electronic properties of CNTs for any possible electronic application. It is often thought CNT is a perfect cylinder made by rolling up a graphene sheet. In reality, however, there are undeniable possibilities that they have structural deformations such as bent, twisted or collapsed. As for the chiral nanotubes, they may be more stable via natural torsion because of their inherent helical structures. According to a density functional study [1], the electronic structures of CNTs sensitively depend on their geometry such as bond-lengths and bond-angles. Hence, the electronic properties of deformed nanotubes are very interesting. Recently, it has been reported that CNTs with torsional strain can be used in a rotational actuator [2] and an electrochemical quantum oscillator [3]. For theoretical studies, some tight-binding based studies have been also reported [4, 5]. However, it has been pointed out from density functional studies that tight-binding studies may not be sufficient especially in thin nanotubes [1, 6].

In the present work, we study the energetics and electronic structures of twisted small-diameter single-walled CNTs in the framework of the density functional theory (DFT). In order to utilize the periodic boundary condition implemented in the DFT computational code, we study chiral CNTs under several discretized twisting levels, and perform geometrical optimizations at each twisting level. Interestingly, it is predicted that the most stable nanotubes should possess slightly twisted geometries. We also study twisting-level dependence of the electronic structures. Importantly, it is found that the fundamental gaps of some CNTs decrease with increasing twisting level. It is confirmed that the DFT study can reveal the detailed electronic structures of twisted CNTs.

- [1] K. Kanamitsu and S. Saito, *J. Phys. Soc. Jpn.* **71**, 483 (2002)
- [2] A. M. Fennimore, T. D. Yuzvinsky, W. -Q. Han, M. S. Fuhrer, J. Cumings and A. Zettl ; *Nature* **424** 408 (2003)
- [3] T. Cohen-Karini, L. Segev, O. Srur-Lavi, S. R. Cohen and E. Joselevich ; *Nature. Nano.* **1** 36 (2006)
- [4] A. Rochefort, P. Avouris, F. Lesage and D. R. Salahub; *Phys. Rev. B* **60** 13824 (1999)
- [5] L. Yang and J. Han ; *Phys. Rev. Lett.* **85** 154 (2000)
- [6] X. Blasé, L. X. Benedict, E. L. Shirey and S. G. Louie, *Phys. Rev. Lett.* **72**, 1878 (1994)

E-mail: kato@stat.phys.titech.ac.jp (K. Kato)

Effects of laser irradiation and heating on HiPco nanotubes probed by Raman spectroscopy

○Mari Hakamatsuka, Dongchul Kang, Kenichi Kojima, Masaru Tachibana
*International Graduate School of Arts and Sciences, Yokohama City University,
22-2 Seto Kanazawa-ku, Yokohama 236-0027, Japan*

In real single-wall carbon nanotubes (SWCNTs), various types of defects such as vacancies, Stone-Wales defects, ad-atoms, or H-C complex are contained. Understanding the properties of defects is important for improving nanotube growth methods, tailoring their physical properties, and controlling the irradiation-induced damages. Resonant Raman spectroscopy is one of the most powerful methods for characterizing defects in SWCNTs [1]. In the Raman spectra, defect induced phonon mode so-called D band is observed around at 1350 cm^{-1} . The D band has the fine structure, or some components.

In previous study [2], we found that D band in CoMoCAT SWCNTs with 0.8 nm mean diameter was significantly influenced by heating and laser irradiation, and is composed of three components (D_{C1} , D_{C2} , and D_{C3}) at ~ 1313 , 1340 , and 1355 cm^{-1} , respectively. It was shown that D_{C1} and D_{C2} intensities were predominantly affected by laser irradiation in air and vacuum, respectively. The D_{C3} intensity largely increased with heating in air. From there results, it was suggested that D_{C1} , D_{C2} , and D_{C3} can be related to C-H complexes, edges of SWCNTs, and amorphous carbon and oxides such as C=O, C-O, and C-OH, respectively.

In this paper, we report similar experiments on heating and laser irradiation for HiPco ones with larger mean diameter of 1.1 nm. Three D components at 1013 , 1334 , and 1374 cm^{-1} are also observed for HiPco ones. It should be noticed that the shape of D band, mainly D_{H2} , is changed by only laser irradiation in air. The D_{H2} for HiPco ones might be related to C-H complexes induced by laser irradiation in air, as D_{C1} in CoMoCAT ones as mentioned above. On the other hand, heating and laser irradiation in air and vacuum lead to no significant change for D_{H1} and D_{H3} . These results are discussed compared with those for CoMoCAT ones.

[1] D.Kang *et al.*, *Appl. Phys. Lett.* **93**, 133102 (2008)

[2] D. Kang *et al.*, *Diamond Relat. Mater.* (2010)

Corresponding Author: Masaru Tachibana

TEL/FAX: 045-787-2307, E-mail: tachiban@yokohama-cu.ac.jp

Evaluation of Electron Transfer Reaction Rate of Redox Species at Carbon Nanotube Interface

Masato Tominaga* and Hiroyuki Yamaguchi

Graduate School of Science and Technology, Kumamoto University,
Kumamoto 860-8555, Japan

Carbon nanotubes (CNTs) are expected for a platform electrode as fuel cell and sensor. To develop such devices, it is important to understand the CNT/liquid interfacial behaviors during electrode reactions. Theoretical studies on optical and electrical characterizations of CNTs have been reported. However, CNT surface would have various functional groups derived from defects of the graphene sheet, when we use the CNTs as an electrode. It is well known that the electrode reaction is sensitive to the interface structure of an electrode surface. In the present study, the effect of oxidation treatment of CNTs on the electron transfer reaction of redox species was investigated in comparison with HOPG surface.

CNTs were synthesized onto a gold (CNTs/Au) electrode surface by CVD method. The average size in diameter was evaluated to be *ca.* 1 nm. Ferrocenecarboxylic acid (Fc) was used as the redox specie. Cyclic voltammetric measurements and its simulation were mainly used for evaluation of the electron transfer rate constant. An Ag/AgCl (saturated KCl) electrode and a platinum electrode were used as the reference and counter electrodes, respectively. The oxidation treatment of CNT was performed by using the potential cycling at 0 – 1.5 V in a neutral solution.

Fig. 1 shows the typical cyclic voltammograms of Fc at various electrodes and its simulated voltammograms. The oxidation treated-CNTs gave the fastest electron transfer rate coefficient (k°) of Fc in comparison with untreated-CNTs/Au and HOPG electrodes. The k° value obtained at the treated-CNTs/Au was evaluated to be *ca.* 30 times higher than that obtained at the untreated one.

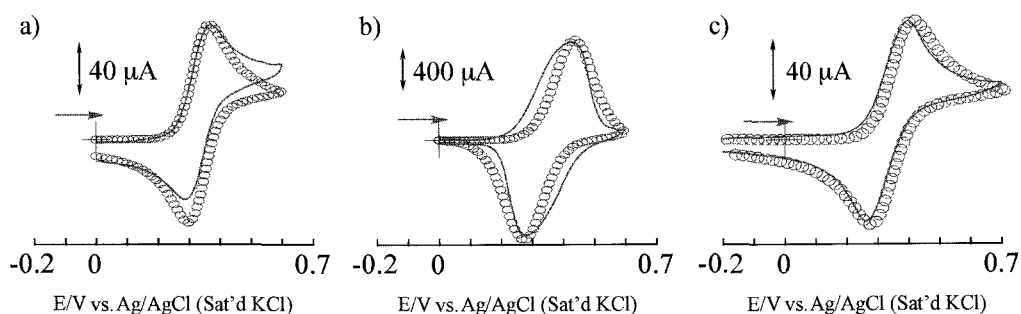


Fig. 1. Cyclic voltammograms of 1mM ferrocenecarboxylic acid at a) oxidation treated-CNTs/Au (0.25 cm^2), b) untreated-CNTs/Au (0.25 cm^2), and c) HOPG (0.34 cm^2) electrodes in a phosphate buffer (pH 7) at potential sweep rate of 160 mV/s, and its simulated voltammograms (circles) using diffusion coefficient (D) = $5.8 \times 10^{-6} \text{ cm}^2/\text{s}$, electron transfer rate coefficient (k°) = 2.9×10^{-2} , 0.1×10^{-2} and $0.3 \times 10^{-2} \text{ cm/s}$ for a), b) and c), respectively.

Corresponding Author: Masato Tominaga

E-mail: masato@gpo.kumamoto-u.a.jp

TEL&FAX: 096-342-3656

Self-consistent calculation of single atom adsorption on a carbon nanotube

○Naoki Hosoya and Koichi Kusakabe

Graduate School of Engineering Science, Osaka University, Toyonaka 560-8531, Japan

Much previous theoretical work has focused on the adsorption properties of one or a small set of metal atoms on carbon nanotube (CNT). Some examples showed the most stable site of various metal atoms [1]. There are some examples that showed carbon-carbon bond breaking in Fe-filled SWNT on metal surfaces [2]. In this study, we explored the possibility of bond breaking by single atom adsorption.

Using first-principle density functional theory (DFT), the adsorption of 9 different metal adatoms (Ca, Sc, Ti, Fe, Cu, Mo, W, Pt, and Au) on single-walled carbon nanotube (SWNT) is studied. The chiralities of SWNT are (5, 0), (4, 2) and (6, 0). The exchange-correlation functional is treated in the Perdew-Wang (PW91) generalized-gradient approximation (GGA). The QUANTUM ESPRESSO 3.2.3[3] is used to perform all calculations.

Among 9 elements, we found significant movement of carbon atoms only for a spin-unpolarized tungsten (W) atom, which is adsorbed on (5, 0) or (4, 2) SWNT (Fig. 1). This movement does not occur in the case of a spin polarized W atom (Fig. 2).

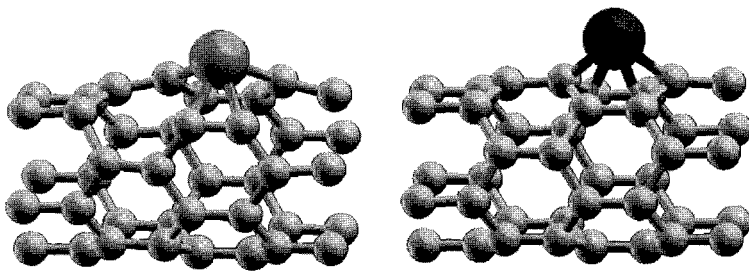


Fig. 1: Spin-unpolarized W (left) and Fe (right) at (5, 0) CNT

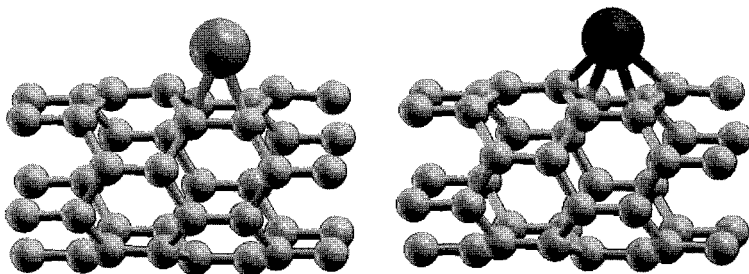


Fig. 2: Spin-polarized W (left) and Fe (right) at (5, 0) CNT

[1] E. Durgun, *et al.*, Phys.Rev. B **67** (2003) 201401

[2] Melanie David, *et al.*, Surface Science **601** (2007) 4366-4369

[3] Giannozzi P, *et al.*, J.Phys.: Condens. Matter **39** (2009) 395502

Corresponding Author: Naoki Hosoya

TEL: +81-6-6850-6407, FAX: +81-6-6850-6407, Email: hosoya@aquarius.mp.es.osaka-u.ac.jp

Stimuli responsive adsorption and desorption of small molecules on SWNTs surfaces in SWNT/polymer gel composite.

○Tatsuro Morimoto¹, Tsuyohiko Fujigaya¹, Naotoshi Nakashima^{1,2}

¹ Department of Applied Chemistry, Kyushu University, Fukuoka, 819-0395, Japan

² JST-CREST, Tokyo, 102-0075, Japan

Adsorption of molecules on SWNTs surfaces are known to play an important role for SWNTs dispersion. [1] In the course of studies for physical adsorptions conducted so far, recently, stimuli responsive adsorption and desorption of small molecules on SWNTs surfaces are paid attention aiming at novel sensors, drug delivery systems, and so on. However, that was rarely reported, and in addition, all of the few reports were conducted in solution, which end up with the aggregation of SWNTs by desorption of small molecules and disturbs the development for applications. In this research, therefore, we prepared the composite gel of SWNTs and poly(*N*-isopropylacrylamide) (PNIPAM) [2] and carried out the adsorption and desorption of small molecule, doxorubicine (DOX), on SWNTs surfaces in the gel (**Fig. 1**). SWNTs surfaces were effectively utilized because the three-dimensional polymer mesh interrupted SWNTs aggregation and allowed SWNTs to be isolated without any dispersants (**Fig. 2**). We employed temperature and pH changes as stimuli, and succeeded in effective release of DOX molecules from SWNTs surfaces in polymer gel for the first time, judging from the UV-vis-NIR absorption and Raman spectra. Light irradiation which is considered to be the advantageous stimulus for many applications was also carried out. The DOX molecules were expected to detach from SWNTs surfaces because of their activated molecular vibration through the photo-thermal effect of SWNTs.

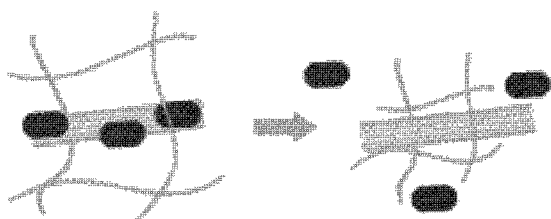


Fig. 1 Schematic image of adsorption and desorption of DOX on SWNTs surfaces.

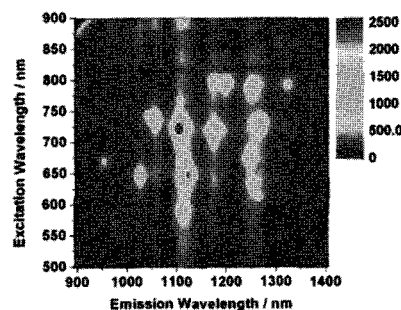


Fig. 2 PL mapping of SWNTs/PNIPAM gel.

[1] N. Nakashima, T. Fujigaya, *Polymer J.* **2008**, *40*, 577.

[2] T. Fujigaya, T. Morimoto, Y. Niidome, N. Nakashima, *Adv. Mater.* **2008**, *20*, 3610.

Corresponding Author: Naotoshi Nakashima

TEL & FAX: +81-92-802-2840, E-mail: nakashima-tcm@mail.cstm.kyushu-u.ac.jp

Performance Enhancement of Organic Solar Cells with Polymer-SWCNT Composite Hole Transport Layer by Inserting Thin Cap Layer

○Naoki Kishi¹, Shinya Kato¹, Takeshi Saito^{2,3}, Daiki Ito¹, Yasuhiko Hayashi¹, Tetsuo Soga¹ and Takashi Jimbo¹

¹*Department of Frontier Materials, Nagoya Institute of Technology,
Nagoya 466-8555, Japan*

²*Nanotube Research Center, National Institute of Advanced Industrial Science and
Technology (AIST), Tsukuba 305-8565, Japan*

³*PRESTO, Japan Science and Technology Agency,
Kawaguchi 332-0012, Japan*

Organic solar cells have attracted much attention in recent years for their potential application as a low cost approach to solar energy conversion. Hole transport layer, which is formed between hole correcting anode and organic active layer, plays an important roll on the controlling the hole injection conditions to the anode. We reported that the performance of organic solar cells can be enhanced by introducing single wall carbon nanotubes (SWCNTs) into the polymer hole transport layer [1]. However, excess incorporating of SWCNTs decreases the photo conversion efficiency of the solar cells because of increment of leakage current. This leakage current results from electron current to the anode via nanotubes exposed on the surface of the hole transport layer.

In the present study, we report performance enhancement of organic solar cells with polymer-SWCNT composite hole transport layer by reducing the leakage current. Thin organic cap layer has been inserted on top of the composite hole transport layer to decrease leakage current. The thin organic cap layer was fabricated by spin casting of organic solution on the hole transport layer, which is composed of PEDOT:PSS and SWCNTs synthesized by e-DIPS method [2]. The performance of the solar cells will be discussed in detailed.

References:

- [1] N. Kishi et. al., The 37th Fullerene Nanotubes General Symposium 1P-24 (2009).
- [2] T. Saito *et. al.*, J. Nanosci. Nanotech., 8, 6153 (2008).

Corresponding Author : Naoki Kishi

E-mail : kishi.naoki@nitech.ac.jp

Tel&Fax : 052-735-5147

Mechanical Strength Improvement of PVA/CNT Composites by Sidewall Functionalization of CNT

○Masaru Sekido¹, Kouki Utsumi¹, Hiroyuki Ohmiya¹, Taihei Yamazaki¹, Susumu Kumagai¹, Hiroshi Kitamura², Hisato Takeuchi³, Masatomi Ohno²

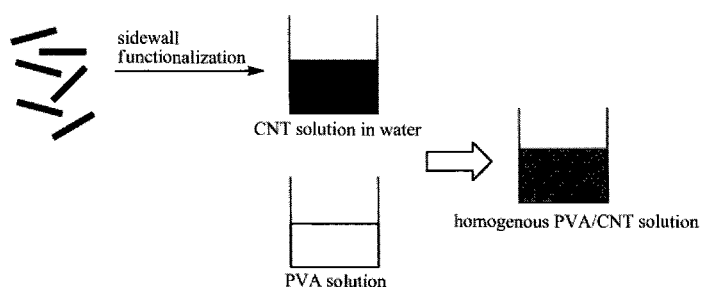
¹*Department of Materials Science and Engineering, Sendai National College of Technology, Natori 981-1239, Japan*

²*Department of Advanced Science and Technology, Toyota Technological Institute, Nagoya 468-8511, Japan*

³*Materials Fundamental Research Department, Toyota Central R & D Labs. Inc, Nagakute, Aichi 480-1192*

The CNT-based nanocomposites have been considered as one of the most promising applications of CNT. In the fabrication of high quality polymer-CNT nanocomposites homogeneous dispersion of CNT in polymer matrix is required. For this purpose we have developed simple methods to produce side-wall functionalized CNT, which shows excellent solubility in water¹.

Since the solubility of functionalized CNT is around 25 mg/ml PVA/functionalized CNT composites were prepared by mixing functionalized aqueous CNT solution with PVA solutions. The obtained PVA/CNT solutions were poured on the smooth surface of Teflon disks and dried in a fan oven at 60°C for 3 h. The resulting film was peeled off from Teflon disks and cut into strips (200 x 30 x 0.05mm). These strips were stored in ambient conditions for 3 days before tensile testing. Mechanical property measurements indicate that the Young's modulus of PVA/functionalized CNT composites film is improved compared with PVA/pristine CNT composites film and PVA film. The improvement of mechanical strength of PVA/ functionalized CNT composites may be explained by well-dispersion of functionalized CNT and interfacial bonding between the functional groups on the surface of CNT and PVA matrix.



[1] H. Kitamura, M. Sekido, H. Takeuchi, M. Ohno The 36th symposium abstract p. 85.

Corresponding Author: Masaru Sekido,

Tel:022-381-0329, Fax:022-381-0318, E-mail: sekido@sendai-nct.ac.jp

Development of microreactors consisting of vertically aligned carbon nanotube films

Hiroshi Kinoshita*, Akira Yamakawa, Nobuo Ohmae

Department of Mechanical Engineering, Faculty of Engineering, Kobe University,
ZIP code: 657-8501 Rokkodai 1-1, Nada-Ku, Kobe, JAPAN
E-mail address: kinohiro@people.kobe-u.ac.jp (H. Kinoshita)

Small chemical reaction devices such as microreactors have advantages over conventional scale reactors for decreasing amount of waste fluid, rapid switching of temperature. Carbon nanotubes (CNTs) have higher chemical stability, thermal and electrical conductivities, and heat resistance than materials used conventionally in microreactors. These CNTs properties are suitable for microreactors' materials. In this study, microreactors consisting of multiwalled carbon nanotube (CNT) microchannels have been developed¹.

The CNT microreactors are fabricated by three steps as schematically shown in Fig. 1. (a) Step 1: Metal masks with a microchannel shape made of a 0.1 mm thick stainless steel are used. Fe layers are deposited on the silicon oxide films with the masks using a vacuum evaporation at room temperature. Fe nanoparticles with the negative pattern of the microchannel shape are formed by an annealing treatment of the films at 700°C with 30 Pa H₂ flow for 30 min. (b) Step 2: CNTs are grown by a thermal CVD with a mixture of C₂H₂ and H₂ gases at the substrate temperature of 700 °C for 30 min. Thus a CNT microchannel is synthesized. (c) Step 3: In order to prevent fluids from flowing over the CNT microchannels, to attach inlet and outlet plugs of fluids, and to obtain clear photoimages, acrylic plates with 1mm thick are attached on the CNT channels by heating the substrates at approximately 100°C. After cooling, the acrylic plate and the CNT microchannel stick together tightly. Finally the CNT microreactor is fabricated.

Fig. 2 shows a photograph of the Fermat's spiral type CNT microreactor with water flowing from the inlet. Water was reflected by luminous color and the end of introduced water is indicated by the circle. Water successfully flowed in the CNT microchannel without water leakage. CNTs are hydrophobic and the silicon oxide film is hydrophilic, fluids can flow in the silicon oxide regions in the CNT microreactors.

¹H. Kinoshita, A. Yamakawa, N. Ohmae, "Development of microreactors made of vertically aligned carbon nanotube films", *Carbon*, Vol. 47, Issue 14, pp. 3374-3377 (2009).

*Corresponding author.

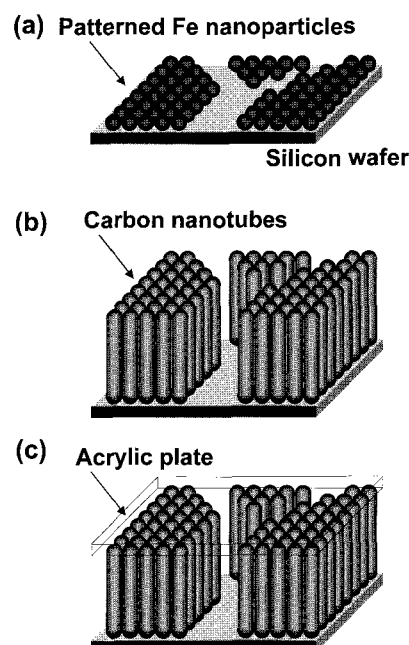


Fig. 1 Schematics of the three step fabrication of CNT microreactor.

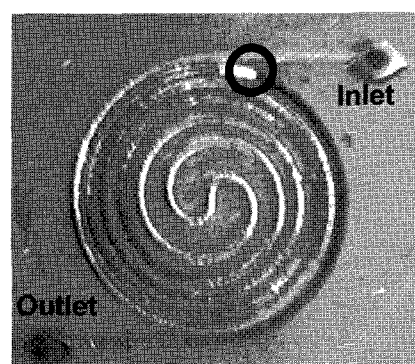


Fig. 2 Photographs of the Fermat's spiral type CNT microreactor. The diameter of the spiral is 5 mm.

Production of hydrogen and fixation of carbon by thermal decomposition of ethanol

○Yosuke Kakimi, Hitoshi Nakahara, Koji Asaka, Yahachi Saito

Department of Quantum Engineering, Nagoya University, Nagoya 464-8603

In this study, a new method of hydrogen generation, which is free from carbon dioxide formation, is proposed based on chemical vapor deposition (CVD). In this method, ethanol is used as a source gas, and carbon nanotubes (CNTs) are formed on a catalyst-deposited substrate. Hydrogen is generated as a by-product of CNTs. Quadrupole mass spectroscopy (QMS) is used to analyze the composition of gaseous species formed by the catalytic CVD.

On Si substrates, SiO₂ (100nm in thickness), Al (2nm) and Co (0.3nm) were deposited. Here, Co works as a catalyst for thermal decomposition of ethanol.

When CNTs grow on the substrate, as shown in Fig. 1, the generation of hydrogen is confirmed. Fig. 2 shows fractions of hydrogen in QMS signals as a function of growth time for the following three conditions.

- (1) normal CVD condition with the catalyst-deposited substrate.
- (2) heating of the CVD furnace without the substrate, corresponding to thermal decomposition of ethanol without catalyst.
- (3) no heating and no substrate, corresponding to simple mass spectroscopy of ethanol vapor.

Differences between curves (1) and (2), and (2) and (3) reflect the amount of hydrogen generated by Co catalyst, and thermal decomposition inside the furnace respectively.

As shown above, hydrogen generation during CNTs growth by ethanol is confirmed.

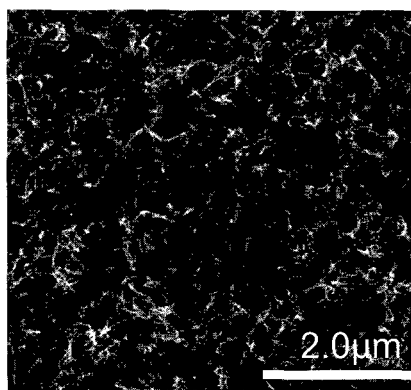


Fig.1 SEM image of CNTs grown on the substrate.

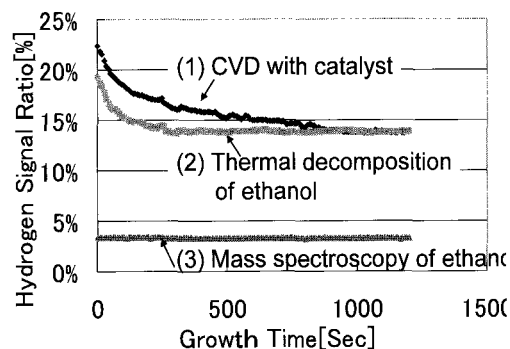


Fig.2 Growth time dependence of QMS signal ratio of hydrogen (m/e=2).

Corresponding Author: Yosuke Kakimi
E-mail: kakimi@surf.nuqe.nagoya-u.ac.jp, Tel: +81-52-789-3714

Growth and Characterization of Co-, Ni-, and Pd-Nanoparticle-Containing CNTs on SPM Probe Apices

Ian Thomas Clark, Chien-Chao Chiu, Masamichi Yoshimura

Research Center for Local Structural Control
Toyota Technological Institute, Nagoya 468-8511

Carbon nanotubes (CNTs) are expected to make excellent probes for scanning probe microscopies (SPM) for a number of reasons, such as their small diameter, large aspect ratio, excellent mechanical properties. CNTs grown using the common vapor-liquid-solid (VLS) catalytic method have an additional advantage, in that one end of the CNT typically contains a nanoparticle of the VLS catalyst. Since many common VLS catalysts for CNT growth (e.g. iron, nickel and cobalt) are magnetic, these nanotubes can be used for magnetic force microscopy (MFM) as well as the more common atomic force microscopy (AFM) and scanning tunneling microscopy (STM).[1] Over the past 13 years, several fabrication methods for CNT-SPM probes have been published, [1–5] but for various reasons, there has been significant difficulty in commercializing any of these methods. In this presentation, we will describe recent results in an ongoing research program aimed at developing low-cost, scalable CNT-SPM probe fabrication methods. Recent results related to the fabrication and testing of cobalt-, nickel-, and palladium-nanoparticle-containing CNT-SPM probes via a solution-phase catalyst deposition/plasma-enhanced chemical vapor deposition (PECVD) method will be described. Cobalt and nickel are desirable tip-materials for MFM applications; Co is a strong ferromagnet and an excellent catalyst for VLS CNT growth, and Ni is suitable for the study of soft magnetic materials due to its low coercivity relative to cobalt and iron. Palladium is non-magnetic, but is known to fill the interior of CNTs, an effect that is expected to provide CNT probes with a larger density of states around the Fermi level, making them more suitable for STM and other electronic applications.

References

- 1) K. Tanaka, M. Yoshimura and K. Ueda: *Journal of Nanomaterials* **2009** (2009) 147204.
- 2) H. Dai, J. H. Hafner, A. G. Rinzler, D. T. Colbert and R. E. Smalley: *Nature* **384** (1996) 147.
- 3) J. H. Hafner, C. L. Cheung and C. M. Lieber: *Journal of the American Chemical Society* **121** (1999) 9750.
- 4) J. Tang, G. Yang, Q. Zhang, A. Parhat, B. Maynor, J. Liu, L.-C. Qin and O. Zhou: *Nano Letters* **5** (2005) 11.
- 5) A. Winkler, T. Mühl, S. Menzel, R. Kozhuharova-Koseva, S. Hampel, A. Leonhardt and B. Büchner: *J. Appl. Phys.* **99** (2006) 104905.

Carbonization of polybenzimidazole-wrapped carbon nanotubes and their oxygen reduction activity

○Takeshi Uchinoumi¹, Tsuyohiko Fujigaya¹, and Naotoshi Nakashima^{1,2}

1 Department of Applied Chemistry, Graduate School of Engineering.

Kyushu University, 744, Motooka Nishi-ku Fukuoka, Japan

2 JST-CREST, 5 Sanbancho, Chiyoda-ku, Tokyo 102-0075, Japan

Abstract : Polymer electrolyte fuel cell systems using non-precious metal as a catalyst are the strong request from industry side. One of the promising approaches for the non-precious metal cathode catalyst is the nitrogen-containing graphite structure proposed by Ozaki et al., which were prepared from the metal complex of the nitrogen-containing polymers¹⁾.

We recently reported the pyridine-containing polybenzimidazole (PyPBI: **Fig. 1**) adsorbed to MWNTs through π - π interaction and act as the solubilizer²⁾. Based on the finding, we fabricated the cobalt(II) complex of the MWNT/PyPBI and the composite was subjected to carbonization at 600 °C for 1 h. The sample was washed with concentrated HCl in order to remove the cobalt species. Fig. 2 shows the linear sweep voltammogram of the composite, which was measured by rotating electrode voltammetry under the following electrolyte condition: rotating speed was 1600 rpm, the electrolyte was 0.5 M H₂SO₄. It is obvious from the comparison between the voltammogram under nitrogen flow (Fig. 2; thin line) and oxygen flow (Fig. 2; bold line), the composite sample exhibited oxygen reduction activity.

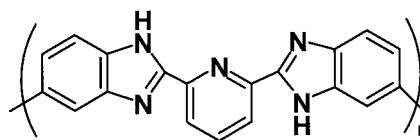


Fig. 1 Chemical structure of PyPBI

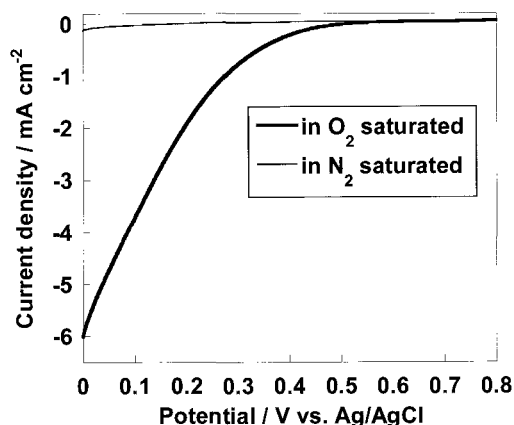


Fig. 2 Oxygen reduction voltammograms for the carbonized composite.

References:

- 1) Jun-ichi Ozaki, Shin-ichi Tanifuji, Naofumi Kimura, Atsuya Furuichi, Asao Oya, *Carbon* **2006**, *44*, 1324.
- 2) Tsuyohiko Fujigaya, Minoru Okamoto, Naotoshi Nakashima, *Carbon* **2009**, *47*, 3227.

Corresponding Author: Naotoshi Nakashima

E-mail: nakashima-tcm@mail.cstm.kyushu-u.ac.jp

Tel&Fax: +81-92-802-2840

Electrical Properties of Carbon Nanotubes / Rubber Composites Prepared with Rotation / Revolution Mixing Technique

○Ayumu Sakai, Koji Tsuchiya, Takeo Furukawa and Hirofumi Yajima

*Department of Applied Chemistry, Faculty of Science, Tokyo University of Science
1-3 Kagurazaka, Shinjuku-ku, Tokyo 162-8601, Japan*

Polymer composite materials of inorganic filler particles dispersed in a polymer matrix are widely used for various industrial fields as the structural and functional material. If the filler ratio is exceeded at a certain threshold value, various phase transitions occur, for example, from the viscosity to the elasticity or from the insulating to the conductivity. Various carbon materials have been used as fillers in a polymer for their functionalization and improvement, such as the electric conduction, mechanical strength and electromagnetic shield. Recently, a high functionalization and a lower percolation threshold are required from viewpoints of the physical property, processing and cost. In particular, carbon nanotubes (CNTs) have attracted a great deal of attention as high performance and multifunctional nanomaterials for extended nanotechnology applications because of their structures; the high-specific surface area and high aspect ratio. If CNTs are used as a filler, a high functionalization and a lower percolation threshold could be expected.

However, when CNTs / polymer composite materials are prepared, conventional methods such as a twin-screw mixer or extruder can not bring out uniform dispersion of CNTs in the insulating matrix and induces to collapse of CNTs due to mechanical shear, resulting in a high percolation threshold to obtain a low conductivity. In this study, in order to develop a practical conductive material, the composites of styrene-butadiene rubber (SBR) with the various species of CNTs were prepared with a rotation / revolution mixing technique without mechanical shear technique. Then, the relationships between the electrical properties of their composite films and the structural characteristics of the CNTs (aspect ratio, disordered graphite degree, etc) were investigated as a parameter of the contents of the CNTs.

Firstly, CNTs were dispersed in tetrahydrofuran by ultrasonication pretreatment to untangle their bundles. Then, the mixing of the composites was carried out with a rotation / revolution type mixer (ARE-310, THINKY Co.) for 10 min. Finally, after vacuum drying, CNTs / SBR composite films were moulded and vulcanized with a hot-press machine at 160 °C for 20 min, and then gold electrodes were deposited on the films with a sputter. For the electric properties of the composite films, the permittivity and conductivity were measured.

As a result, CNTs / SBR composite films were exhibited a higher conductivity and a lower percolation threshold by the present method, compared to carbon black as filler and the films prepared by a conventional kneading method with banbury mixer. The rotation / revolution mixing technique is expected to be a promising procedure for the preparation of the composites of various industrial / practical polymers with the CNTs bring in high functionalities. Detail results will be presented and discussed at the *FNT Symposium*.

Corresponding Author: Hirofumi Yajima

TEL: +81-3-3260-4272(ext.5760), FAX: +81-3-5261-4631, E-mail: yajima@rs.kagu.tus.ac.jp

One-step Fabrication of Single-Walled Carbon Nanotube Thin Film Transistor by Patterned Growth Technique

○Shinya Aikawa^{1,2}, Rong Xiang¹, Erik Einarsson¹, Shohei Chiashi¹, Junichiro Shiomi¹, Eiichi Nishikawa² and Shigeo Maruyama¹

¹*Department of Mechanical Engineering, The University of Tokyo, 7-3-1 Hongo, Bunkyo-ku, Tokyo 113-8656, Japan*

²*Department of Electrical Engineering, Tokyo University of Science, 1-3 Kagurazaka, Shinjuku, Tokyo 162-8601, Japan*

A carbon nanotube field effect transistor (CNT-FET) having an SWNT as its gate channel has been investigated because of its potential applications in next-generation nanoscale organic electronic devices. However the fabrication process using conventional MEMS techniques is quite challenging, and may induce significant damage of the SWNTs, degrading the high-quality characteristics of as-grown SWNTs.

In this study, we fabricated a thin film transistor consisting only of as-grown SWNTs and evaluated its FET properties. An octadecyltrichlorosilane self-assembled monolayer (OTS-SAM) was used to make hydrophilic and hydrophobic regions on a Si substrate (oxide layer thickness, $t_{\text{ox}} = 50\text{nm}$) as follows: OTS-SAM was formed on an OH-terminated Si surface and was selectively removed by vacuum ultraviolet (VUV) irradiation through a photomask to pattern the substrate. After SAM removal, the substrate was dipped into a Co solution to deposit catalyst [1], and SWNTs were grown by alcohol CVD (ACCVD) [2] only in the regions that had been irradiated by VUV [3]. The I - V characteristics were measured using the Si substrate as a back-gate. In this method, no post-processing such as drop-casting of dispersed SWNTs or deposition of electrodes are required. This process has at least two advantages; one is that electric properties of SWNT can be easily measured and the other is that damage induced to the as-grown sample is reduced by minimal post-growth treatment. Here the device process using a scalable liquid-based dip-coating method for catalyst deposition and the I - V characteristics of the fabricated device will be discussed.

[1] Y. Murakami et al., *Chem. Phys. Lett.* **377**, 49 (2003).

[2] S. Maruyama et al., *Chem. Phys. Lett.* **360**, 229 (2002).

[3] R. Xiang et al., *J. Am. Chem. Soc.* **131**, 10344 (2009).

Corresponding Author: Shigeo Maruyama

TEL: +81-3-5841-6421, FAX: +81-3-5800-6983, E-mail: maruyama@photon.t.u-tokyo.ac.jp

Microcontact Printing of Organic Molecules and Carbon Nanotubes

Jan Mehlich,¹ Bart Jan Ravoo,¹ Hisanori Shinohara,²

¹«Synthesis of Nanoscale Systems», Organic Chemistry Institute, Westfälische Wilhelms Universität Münster, Corrensstraße 40, 48149 Münster, Germany, ²Department of Chemistry & Institute for Advanced Research, Nagoya University, Nagoya, 464-8602, Japan

Email: jan.mehlich@uni-muenster.de

Homepage: <http://www.uni-muenster.de/Chemie.oc/research/ravoo/welcome.html>

Microcontact printing (μ CP) developed into a powerful tool to obtain functionalized surfaces which are used in a wide variety of applications. In our group at the WWU Münster, μ CP is used to develop functional surfaces. Using microcontact chemistry, a chemical reaction is induced in the nanoscale confinement between a reactive substrate and an elastomer stamp covered with ink. Whereas reactions in solution require catalysts, long reaction time and/or heat, reactions induced by μ CP often proceed rapidly under ambient conditions and without catalyst.

Here, the kinetic properties of the Huisgen 1,3-dipolar cycloaddition („click reaction“) and the Diels-Alder reaction are investigated. Different fluorescent ink molecules with different reactivity are synthesized and then printed under identical conditions for different times with PDMS stamps onto substrates carrying the corresponding reaction partner in the form of a SAM. Fluorescence images are taken and evaluated by graphical software. Kinetic behaviour as expected from theory is observed, which can only be explained by a chemical reaction taking place.

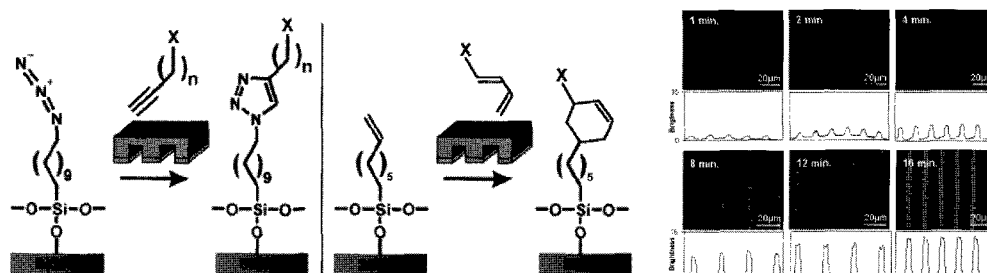


Fig.1: Click reaction (left) and Diels-Alder reaction (middle) induced by μ CP, time-dependent printing reveals information about kinetic behaviour (right)

Currently, we use μ CP to prepare arrays of carbohydrate on a substrate surface. These carbohydrate arrays are useful to investigate protein-carbohydrate interactions.

A second project is carried out in the framework of the International Research Training Group (IRTG) Münster-Nagoya. We try to immobilise carbon nanotubes in a striped pattern on appropriate substrates by μ CP. The linkage between the nanotubes and the substrate is not covalent but based on Coulomb interactions. In preliminary experiments, we use SWCNTs, separated to purely metallic or purely semiconductive, to find the best conditions for printing, and later we intend to print nanopeapods. Final goal is the alignment of the tubes to obtain well-defined patterned films of CNTs or nanopeapods with useful electronic properties in a simple printing process.

Formation of Copper Nanowire-filled Carbon Nanotubes and Polyhedral Graphite Particles by Alcohol Arc Discharge

○Akira Koshio, Makoto Yamamoto, Kazuki Gion, and Fumio Kokai

Division of Chemistry for Materials, Graduate School of Engineering, Mie University, 1577 Kurimamachiya-cho, Tsu, Mie 514-8507, Japan

Metal nanowires have been extensively studied as one-dimensional nanomaterials with nanocable structures suitable for nanoelectronic and sensor applications. However, some problems related to quality, such as stability, crystallinity, and long one-dimensional growth, still remain. The hybridization of metal nanowires and carbon nanotubes has been tried as one of the ideas for improving the quality of metal nanowires. On the other hand, polyhedral graphite (PG) particles having a structure composed of many polyhedra with 100 nm - 1 μ m diameters can be used as a lubricant because of their unique structures and properties, such as chemical and mechanical stability during high-pressure compression. We have reported that copper nanowire-filled carbon nanotubes (CuNW@CNTs) and PG particles were formed by modified arc discharge method using hydrogen and cellulose, respectively. Recently we found more effective formation route of both two materials. In this study, we investigated effective formation condition of CuNW@CNTs and PG particles via high-density carbon arc discharge method using alcohol vapor (alcohol arc discharge method).

CuNW@CNTs and PG particles were produced by conventional carbon arc discharge with ethanol vapor introduced into the arc plasma. Graphite rods were used for electrodes. In the case of CuNW@CNT formation, a hole was drilled in the center of a graphite anode and filled with copper powder. The ethanol vapor was introduced into the chamber by bubbling argon through ethanol heated at 50 °C. The high-density carbon arc discharge was maintained by pyrolysis of ethanol during sublimation of the anode.

Figure 1 shows a TEM image of CuNW@CNTs produced by alcohol arc discharge with copper-containing graphite anode. Copper nanowire-filling rate was extremely high and few hollow CNTs were in the as-grown sample. Figure 2 shows TEM images of PG particles formed by alcohol arc discharge with pure graphite electrodes. The PG particles have facets and highly graphitized concentric structures (Fig. 2(b)). The diameters of the PG particles depended on arc current, and ranged from 100 to 800 nm. These results are better than those for the previous methods. We assume that the additional carbon and hydrogen sources from the ethanol vapor lead to suitable density of carbon and hydrogen species in the arc plasma compared to that of the previous methods.

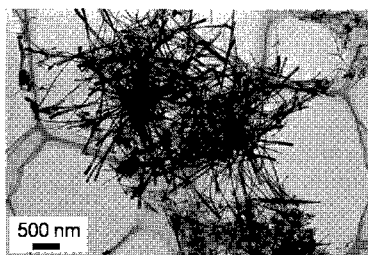


Fig. 1 CuNW@CNTs produced by alcohol arc discharge with Cu-containing graphite anode.

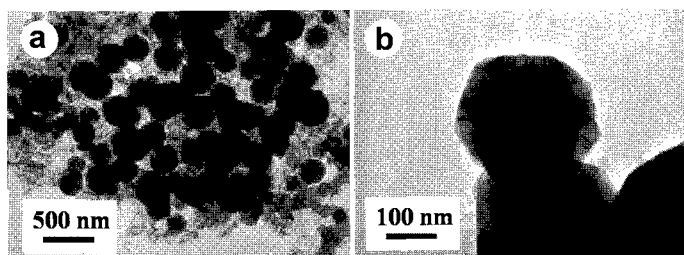


Fig. 2 (a) A TEM image of PG particles produced by arc discharge with pure graphite electrodes. (b) A PG particle having facets.

References: [1] A. Koshio *et al.*, *The 36th Fullerene-Nanotubes General Symposium*, 2-12.

[2] Y. Katagiri *et al.*, *The 36th Fullerene-Nanotubes General Symposium*, 1P-33.

Corresponding Author: Akira Koshio, **E-mail:** koshio@chem.mie-u.ac.jp, **Tel & Fax:** +81-59-231-5370

Effect of high temperature annealing on the ferromagnetism of carbon nanofoam

○ Hirohito Asano, Sumio Iijima, Shunji Bandow

*Department of Materials Science and Engineering, Meijo University,
1-501 Shiogamaguchi, Tenpaku, Nagoya 468-8502, Japan*

All carbon nanomagnet can be produced by the pulsed laser vaporization (LV) of pure carbon (pC) target at around 1,000 °C in the environment of hydrogen containing balance gas [1]. Large magnetic moment reaching ca. 10,000 μ_B is needed to explain the magnetization curve at room temperature and the concentration of magnetic moment is the order of 10^{16} 1/g. Magnitude of the saturation magnetization M_s is the order 10^{-1} - 10^0 emu-G/g that depends on the preparation conditions (mainly H_2 concentration of buffer gas). We carefully checked the existence of extrinsic ferromagnetic impurity and excluded such possibility so far.

From the experimental conditions, possible elements constructing the nanofoam are only carbon and hydrogen. However, the concentration of hydrogen is expected to be very small: hydrogen atoms may act just like termination of the radical edge formed in the carbon network. In the present study, heat treatments of the samples were carried out in order to see how to change ferromagnetism. Because we consider that the origin of the present ferromagnetism is based on the non-bonding states located along the zig-zag edge of sp^2 bonded carbon network and such edge states would be realized in the graphene sheet as defects. Hence the high temperature annealing possibly repairs such defects and decreases the magnetism.

Sample annealing was conducted in a H_2 flux of 50 sccm at various temperatures for 1 h. As-produced sample (generated in 3 % of H_2 containing condition) indicated Curie-Weiss type temperature dependence as shown in Fig. 1. While the annealing at 600 - 800 °C diminishes the Curie component and surprisingly the M_s was increased with increasing annealing temperature from 800 °C as shown in the inset of Fig. 2, and then decreased at 1200 °C at where the change in χ -ray profile was observed (not shown). This may suggest that the thermal assisted reconstruction of ferromagnetic domains would occur below the annealing of ~ 1000 °C in H_2 flux.

[1] H. Asano *et al.*, The 37th Fullerene Nanotubes General Symposium, Sep. 1-3 (2009), Tsukuba, **1P-45**

Corresponding Author: Shunji Bandow, **E-mail:** bandow@ccmfs.meijo-u.ac.jp, **Tel&Fax:** +81-52-834-4001

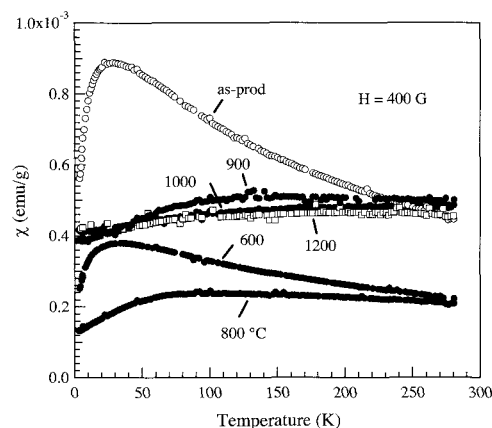


Fig. 1. Temperature dependences of magnetic susceptibility. Original sample (as-prod) was prepared in 3 % of H_2 at 1000 °C by LV-pC. Annealing temperatures were indicated in the figure. One can find that sample annealing diminishes the Curie component.

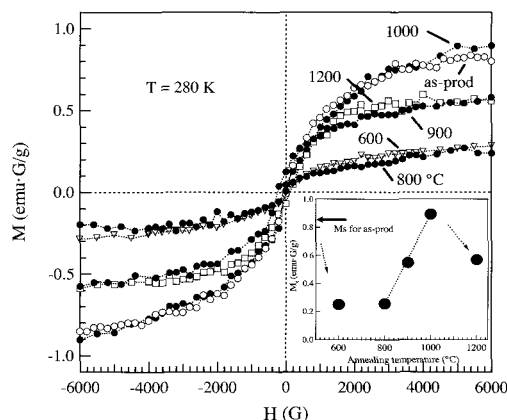


Fig. 2. Magnetization curves taken at 280 K. Inset is annealing temperature dependence of the saturation magnetization M_s .

Electric Properties of Carbon Materials/Polymer Composites Prepared with Rotation/Revolution Kneading Technique

○Ryo Shiotani, Koji Tsuchiya, Takeo Furukawa, and Hirofumi Yajima

*Department of Applied Chemistry, Faculty of Science, Tokyo University of Science
1-3 Kagurazaka, Shinjuku-ku, Tokyo 162-8601, Japan*

Carbon materials/artificial polymer composites have attracted considerable attention because they can be applied to various fields, such as tempered plastic fibers, temperature sensors, and electromagnetic wave absorbents. The conductivity of the composites is abruptly increased at a certain concentration (percolation threshold) because of the formation of an electric conduction path in which carbon fillers penetrate into a polymer matrix. For practical application, a decrease in percolation threshold is demanded from the viewpoints of a weight saving, a reduction in cost, and easy processing. However, conventional mixers such as Banbury mixers and twin screw extruders have disadvantages that large amounts of fillers must be consumed to obtain high conductivity and the structures of fillers would be collapsed by mechanical shear. In order to develop a practical and promising material, we have investigated the electric properties of carbon materials/polymer composites prepared with a rotation/revolution mixer, which allows fillers to be mixed with matrix without mechanical shear.

Low density polyethylene (LDPE) was used as matrix, and carbon black (CB) and vapor grown carbon fiber (VGCF) were used as filler. At first, LDPE was dissolved in toluene at 80 °C and then CB or VGCF was mixed with LDPE/toluene solution using a rotation/revolution mixer (ARE-310, THINKY Co). After drying to remove toluene, composite films were prepared with a hot-press at 120 °C. For the electric properties of the composite films, the permittivity and conductivity were measured.

The percolation threshold of both CB/LDPE and VGCF/LDPE composites was considerably decreased using a rotation/revolution mixer, compared to the composites prepared with a conventional Banbury mixer. This would be ascribed to the features that the fillers kept with the original aspect ratio were efficiently mixed with the polymer without collapse. Detail results will be presented and discussed at the *FNT Symposium*.

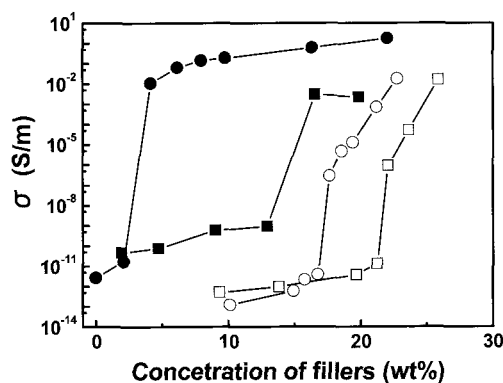


Fig. 1 Conductivity of CB/LDPE and VGCF/LDPE composites prepared with a rotation-revolution mixer and a Banbury mixer as a function of filler concentration. ● VGCF/LDPE(ARE-310), ■ CB/LDPE(ARE-310), ○ VGCF/LDPE(Banbury), □ CB/LDPE(Banbury)

Corresponding Author: Hirofumi Yajima

TEL: +81-3-5228-8705, FAX: +81-3-3235-2214, E-mail: yajima@rs.kagu.tus.ac.jp

Formation of LaC₂ containing multi-shell carbon nanocapsules by rapid heat treatment of La fullerene soot synthesized at 20 Torr He

○Kazunori Yamamoto^a, Takeshi Akasaka^b

^a*Nanomaterials Research Group, Quantum Beam Science Directorate,*

Japan Atomic Energy Agency, Tokai-mura, Naka-gun, Ibaraki 319-1195, Japan

^b*Center for Tsukuba Advanced Research Alliance, University of Tsukuba, Ibaraki 305-8577, Japan*

Abstract:

There has been great interest in the incorporation of metal elements into fullerenes, nanotubes, and fullerene-like multi-shell cage structures such as polyhedral multi-shell nanocapsules.

Fullerenes encapsulating one La atom (called endofullerenes) were discovered in the fullerene soot formed by laser vaporization and following deposition of La with carbon under Ar flow [1]. Soon after the endofullerene soot was produced macroscopically by arc-discharge method [2].

On the other hand, polyhedral multi-shell nanocapsules containing La element were not found in the fullerene soot, which were found in carbonaceous cathode deposits formed on the cathode surface [3, 4]. Electron diffraction (ED) revealed that the capsules were filled with LaC₂ single crystals, not La metals [4]. Transmission electron microscopy (TEM) characterization showed that the endohedral multi-shell nanocapsules were observed in the cathode deposit, not in the fullerene soot.

We previously reported that the endohedral multi-shell nanocapsules were obtained easily by vacuum heat treatment (1000 – 2200 °C) of La fullerene soot, which was prepared at restricted He pressure of 30-50 Torr. The pressure is much lower than preferential pressure of metallofullerene formation (100 – 200 Torr) and carbon nanotube formation (500 Torr)[5]. TEM observation revealed that multi-shell single-digit nanoparticles filled with La were found in La fullerene soot synthesized at 30-50 Torr He, not in that synthesized at 15, 20, 25 Torr He. Recently we have found that the endohedral multi-shell nanocapsules were obtained by rapid heat treatment of La fullerene soot synthesized at 20 and 25 Torr He. Details of rapid heat treatment and results of characterization will be presented in the presentation.

References:

1. Y. Chai, et al., *J Phys Chem.*, **95**, 7564(1991).
2. H. Shinohara, et al., *J Phys Chem.*, **96**, 3571(1992).
3. R. S. Ruoff, et al., *Science*, **259**, 336(1993).
4. M. Tomita, et al., *Jpn. J. Appl. Phys.*, **32**, L280(1993).
5. K. Yamamoto, et. al., The 34th Fullerene Nanotube General Symposium Abstract 2-14.

Corresponding Author: Kazunori Yamamoto

E-mail: yamamoto.kazunori@jaea.go.jp

Tel&Fax: +81-29-282-6474&+81-29-284-3813.

Characterization of lengthsorted DNA-wrapped carbon nanotube thin film transistors

○Yuki Asada¹, Yasumitsu Miyata¹, Kazunari Shiozawa¹, Yutaka Ohno², Ryo Kitaura¹,
Toshiki Sugai¹, Takashi Mizutani² and Hisanori Shinohara¹

¹*Department of Chemistry & Institute for Advanced Research,
Nagoya University, Nagoya 464-8602, Japan*

²*Department of Quantum Engineering, Nagoya University, Nagoya 464-8603 Japan*

The preparation of large scale and uniform networks of SWNTs is very important for high performance electronics such as thin film transistors (TFTs), aimed at potentially replacing silicon devices in the future. To maximize the performance of SWNT-TFTs, it is desirable to obtain SWNTs of similar diameter and chirality for obtaining sufficient on-currents and reproducible device characteristics. The length of SWNTs should also be controllable to meet the requirement of desired channel length.

In the previous symposium, we reported high performance SWNT-TFTs using DNA-wrapped single-wall carbon nanotubes (DNA-SWNTs) which can provide an effective way to fabricate the uniform networks of highly isolated, structure-sorted nanotubes for TFTs[1]. Here, we report the fabrication of SWNT-TFTs and the comparison of the transistor performance among devices of various SWNT density and length. We prepared two different DNA-SWNT lengths of 200 and 400 nm using size exclusion chromatography[2]. DNA-SWNT networks were formed on an amino-coated SiO₂ substrate, and the nanotube density was also controlled by changing deposition times.

Figure 1 shows a typical transfer characteristics of SWNT-TFTs with a SWNT length of 400 nm. Solid and dash lines show I - V curves for low and high density films, respectively. The detail results of the density and length dependence will be discussed.

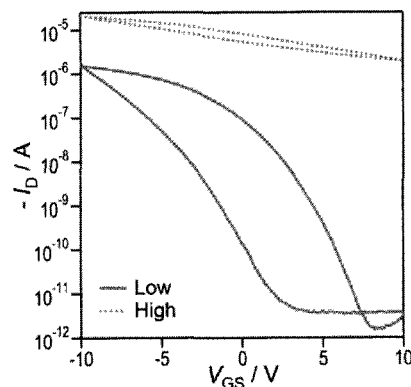


Figure 1 Transfer characteristics of SWNT-TFTs. V_{DS} , channel length and width are - 1 V, 40 μm and 500 μm , respectively.

[1] Y. Asada et al., *The 38th F-NT General Symposium 2009*, 3-11.

[2] Y. Asada et al., *J. Nanomater.* **2009**, 2009, ID 257892

Corresponding Author: Hisanori Shinohara

E-mail: noris@nagoya-u.jp, **TEL:** +81-52-789-2482, **FAX:** +81-52-747-6442

Diameter Tuning of Single-Walled Carbon Nanotubes through H₂ Reaction in Au-Catalyzed Plasma CVD

◦ Z. Ghorannevis, T. Kato, T. Kaneko, and R. Hatakeyama

Department of Electronic Engineering, Tohoku University, Sendai 980-8579, Japan

The ability to obtain narrow diameter distributions at different mean diameters is important for applications that require particular (n, m) carbon nanotubes. In this paper, we show that methane-hydrogen plasma chemical vapor deposition (PCVD) allows diameter tuning of single-walled carbon nanotubes (SWNTs) produced using an Au catalyst [1, 2]. Photoluminescence excitation (PLE) maps of SWNTs produced at different H₂ flow rates were obtained as shown in Fig. 1. The measurements were performed with excitation wavelengths from 500 to 700 nm, and the emission was collected in the range from 900 to 1350 nm. Each peak in the PLE map represents an individual semiconducting (n, m) SWNT. Roughly, the SWNTs become larger in diameter as the peak moves from the lower excitation and emission corner toward the higher excitation and emission corner. The PLE map shows a very narrow chirality distribution of SWNTs at higher H₂ flow rate of 7 sccm, where the small tube (6, 5) is dominant. It was found that the diameter distribution and main diameter become broad and large with an increase in the H₂ flow rate, respectively. This should be because of a strong etching effect of H₂ on the Au catalyst.

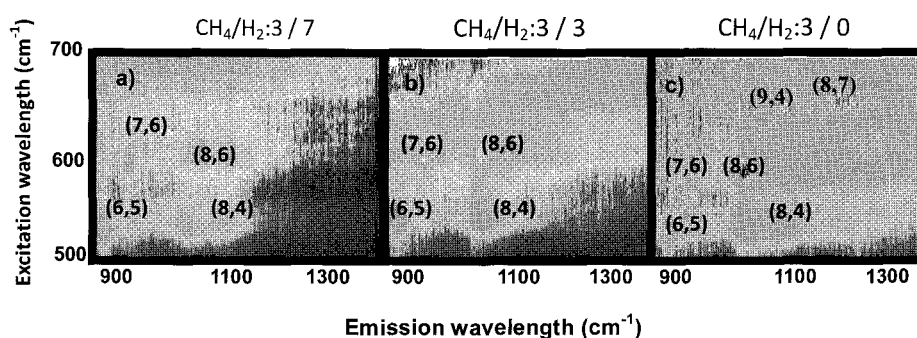


Fig. 1: PLE intensity maps of SWNTs synthesized at different H₂ flow rates from 0 to 7 sccm.

[1] T. Kato and R. Hatakeyama, *Appl. Phys. Lett.* **92**, 031502 (2008).

[2] T. Homma, H. Suzuki, and Y. Kobayashi, *Nano Lett.* **6**, 2642 (2006).

Corresponding Author: Zohreh Ghorannevis

TEL: 022-795-7046, FAX: 022-263-9225, E-mail: zohreh@plasma.ecei.tohoku.ac.jp

Solvent Dependency for Solubilization of Single-Walled Carbon Nanotubes Using Soluble Polybenzoxazoles Precursor

○Takahiro Fukumaru¹, Tsuyohiko Fujigaya¹ and Naotoshi Nakashima^{1,2}

¹Department of Applied Chemistry, Graduate School of Engineering, Kyushu University, 744 Motoooka, Fukuoka 819-0395, Japan

²Japan Science and Technology Agency, CREST, 5 Sanbancho, Chiyoda-ku, Tokyo, 102-0075, Japan

Carbon nanotubes (CNTs) possess remarkable electrical, mechanical, and thermal properties. The superior properties make CNTs excellent candidate to substitute for the conventional fillers in the fabrication of polymer nanocomposites [1]. CNTs usually form bundled structure but homogeneous dispersion of CNTs in polymer matrix is essential to maximize the CNTs' properties of the polymer composites. On the other hand, polybenzoxazoles (PBO) are known to have excellent mechanical strength and thermal stability to organic solvents. CNT/PBO nanocomposites expect to have excellent properties that enable field of application such as super high mechanical strength nanofibers and high thermal conductive films. However, the poor solubility of PBO hinders the fabrication of CNT/PBO nanocomposites.

Recently, we successfully synthesized soluble PBO precursor (**t-Boc prePBO**; **Figure 1**) which acts as solubilizer of single-walled carbon nanotubes (SWNTs) in dimethyl sulfoxide (DMSO). However, the solubility and the stability of the SWNT/**t-Boc prePBO** nanocomposites in DMSO are very low.

Here, we report dimethylacetamide (DMAc) is better solvent for solubilization of SWNTs using **t-Boc prePBO** as dispersant. The UV vis-NIR absorption spectrum of the SWNT/**t-Boc-prePBO** supernatant in DMAc (**Figure 2**: Solid bold line) shows the stronger absorption of the SWNTs in the 600-1500 nm-region than that of DMSO (**Figure 2**: Solid thin line), indicating the better dispersion of SWNTs in DMAc than DMSO. Furthermore SWNT/**t-Boc prePBO** nanocomposites in DMAc are highly stable for more than three months and gave the almost identical absorption spectrum (**Figure 2**: Bold dotted line) compared to the initial solution.

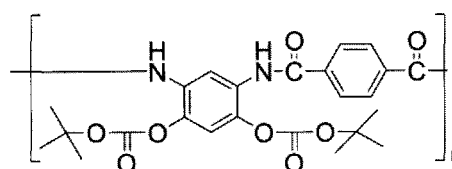


Figure 1. Chemical structure of **t-Boc prePBO**.

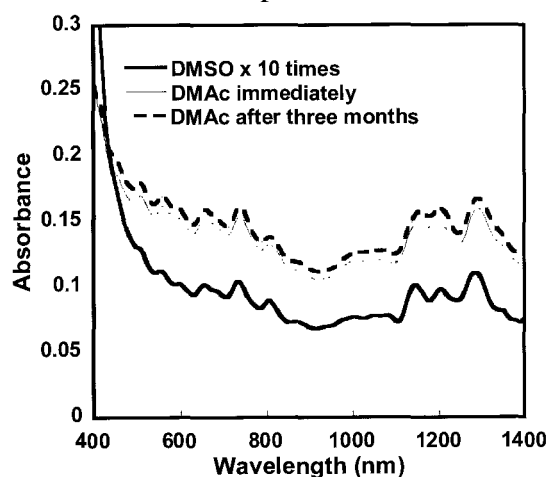


Figure 2. UV vis-NIR absorption spectra of SWNT/**t-Boc prePBO** supernatant.

[1] (a) T. Fujigaya, S. Haraguchi, T. Fukumaru, N. Nakashima, *Adv. Mater.* 20, 2151 (2008). (b) T. Fujigaya, T. Fukumaru, N. Nakashima, *Synthetic Metals* 159, 827 (2009).

Corresponding Author: Naotoshi Nakashima

E-mail: nakashima-tcm@mail.cstm.kyushu-u.ac.jp

Tel&Fax: +81-92-802-284

Structural Characterization of La@C₈₂Cp* Dimer

○Satoru Sato¹, Yutaka Maeda², Hidefumi Nikawa¹, Naomi Mizorogi¹, Takahiro Tsuchiya¹, Takeshi Akasaka¹, Zdenek Slanina¹, and Shigeru Nagase³

¹Center for Tsukuba Advanced Research Alliance, University of Tsukuba, Tsukuba, Ibaraki 305-8577, Japan,

²Department of Chemistry, Tokyo Gakugei University, Koganei, Tokyo 184-8501, Japan,

³Department of Theoretical and Computational Molecular Science, Institute for Molecular Science, Okazaki, Aichi 444-8585, Japan

Endohedral metallofullerenes have attracted much attention because of their novel properties due to the intramolecular electron transfer between the metal atom and the fullerene cage.¹ New electronic properties, such as the low oxidation and reduction potentials, induced by the interaction would allow new application of fullerenes. It has been particularly focus of interest to determine the fullerene cage structure and metal positions, because these are the essential for the properties and reactivities of endohedral metallofullerenes. In this context, a number of endohedral structures of pristine and functionalized endohedral metallofullerenes have been clarified by using XRD analysis so far.²

We have reported the reversible and regiospecific addition reaction of La@C₈₂ with 1,2,3,4,5-pentamethylcyclopentadiene (Cp*), in which the structure and the regioselectivity of La@C₈₂Cp* were clarified.³ From the results of single crystal X-ray crystallographic analysis at 120K, La@C₈₂Cp* takes two orientations in the crystal structure. Actually, 60% of the mono-adduct forms a dimer in the solid state (Figure). The length of C-C bond connecting two C₈₂ cages in La@C₈₂Cp* is 1.606 Å and it is about 0.1 Å longer than the typical C-C single bond length.

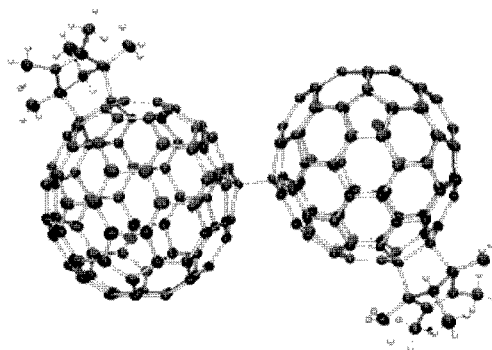


Figure. La@C₈₂Cp* dimer

In this presentation, we report the X-ray single crystal analysis of La@C₈₂Cp* at various temperatures. Furthermore, the factors for dimerization in solid state and bond energy connecting two fullerene cages are also discussed on the basis of theoretical calculation.

References:

- [1] *Endofullerenes: A New Family of Carbon Clusters*; Akasaka, T., Nagase, S., Eds.; Kluwer Academic Publishers: Dordrecht, The Netherlands, 2002.
- [2] For recent reviews, see: (a) M. Yamada; T. Akasaka; S. Nagase, *Acc. Chem. Res.* in press. (b) M. Takata, *Acta Crystallogr.* **2008**, A64, 232.
- [3] Y. Maeda; S. Sato; K. Inada; H. Nikawa; M. Yamada; N. Mizorogi; T. Hasegawa; T. Tsuchiya; T. Akasaka; T. Kato; Z. Slanina; S. Nagase, *Chem. Eur. J.* in press.

Corresponding Author: Takeshi Akasaka

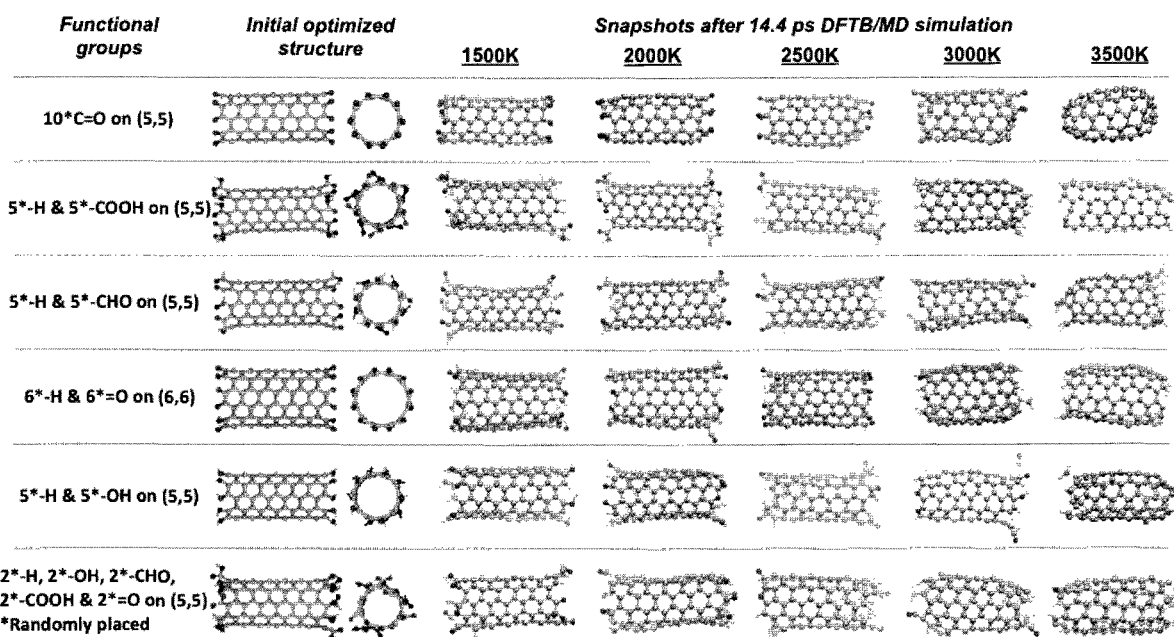
E-mail: akasaka@tara.tsukuba.ac.jp **TEL & FAX:** +81-29-853-6409

DFTB/MD simulations of functionalized open-ended SWCNTs annealing under high-T

○Hironori Hara, Stephan Irle

*Institute for Advanced Research and Department of Chemistry, Nagoya University,
Nagoya 464-8602, Japan*

Using canonical (constant temperature, NVT) molecular dynamics (MD) simulations based on the density-functional tight-binding (DFTB) quantum chemical method, we studied the annealing processes of 15 Å-long, open-ended armchair (5,5) or (6,6) single-walled carbon nanotubes (SWCNTs) at temperatures of 1500 K, 2000 K, 2500 K, 3000 K and 3500 K, using three trajectories for each functional groups set and temperature. The open ends have oxygen containing functional groups as shown in the Figure below. We find that the open ends tend to lose various O and H containing species from their tip, with the rate of fragment loss closely related to temperature. As leaving species we observed H, H₂, OH, H₂O, CO, CO₂, COOH, CHO, HCOOH, H₂CCO, and C₂H₂. As the tubes lose their functional group, the SWCNT self-capping process starts to form a cap at the rim of the open-ended tubes. In case of the 10*C=O (5,5) model tube, complete self-capping of both sides of the SWCNT has been observed after loss of all oxygen functionalities.



Corresponding Author: Stephan Irle

Tel & Fax: +81-52-747-6397/+81-52-788-6151, E-mail: sirle@iar.nagoya-u.ac.jp

Electrical Conductivity Improvement of Carbon Nanotube Wire

○Tomohiro Shimazu, Milan Siry, Kenji Okeyui, Hisayoshi Oshima

*Research Laboratories, DENSO CORPORATION
500-1 Minamiyama, Komenoki, Nisshin-shi, Aichi 470-0111, Japan*

Recently, automotive industry is strongly requested to make deep consideration for the environment, therefore, the weight reduction of automotive parts, including wire harnesses, as well as the efficiency improvement in electric systems are required. One of possible solutions to satisfy these requirements is to apply carbon nanotube (CNT) as electric wire material instead of copper, as CNT is well known as a lightweight material with much higher electric conductivity than copper.

CNT wires are made from a vertically aligned CNTs film grown on a substrate by pulling out and spinning a bunch of CNTs from the sidewall of the film without any binder [1]. In the present study, multi-walled carbon nanotubes (MWNTs) films were grown using a CVD method in a mixture gas of ethylene and argon at an atmosphere pressure. Iron catalysts were coated on a Si substrate using a sputtering method. The thickness of the grown MWNTs film was approximately 300 μm . We built up and utilized our in-house CNT wire pulling and spinning apparatus to make CNT wires. The electrical conductivity of the wires were measured by a four-probe method and was estimated to 100-300 S/cm, which is three orders of magnitude lower than that of copper at present. The conductivity of an individual MWNT was also measured by a two-probe method inside a SEM chamber and estimated to 1×10^4 S/cm. From the obtained conductivity values mentioned above, we have concluded that the reduction of the contact resistance between each MWNT and the improvement of the electrical conductivity of each MWNT are critical to realize CNT wires with high conductivity,

which is comparable with Cu wires. Fig. 1(a) shows a cross sectional TEM image of our as-made CNT wire. There are many vacant areas between each MWNT, and the contact areas of each MWNT are not sufficient, thus the contact resistance is considered not to be negligible. Then, we carried out the amorphous carbon filling treatment to increase the total CNT contact

area. Fig. 1(b) shows a cross sectional TEM image of the CNT wire after the amorphous carbon filling treatment and it can be seen that the vacant areas are filled with the amorphous carbon. The electrical conductivity of the carbon-filled wire has been increased to 600-1,000 S/cm. It is believed that the improvement of the contact resistance is the cause of the CNT wire conductivity improvement.

Reference: [1] Jiang, K et al., *Nature*, **419**, 801(2002)

Corresponding Author: Hisayoshi Oshima, **E-mail:** hoosima@rlab.denso.co.jp

Tel: +81-561-75-1098 **Fax:** +81-561-75-1193

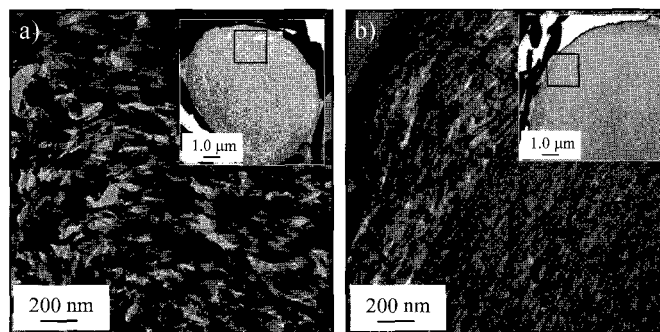


Figure 1. Cross sectional TEM images of the CNT wire a) before b) after the amorphous carbon filling.

***In-situ* transmission electron microscopy of structural change of the contact between gold and a carbon nanotube**

○Motoyuki Karita, Koji Asaka and Yahachi Saito

Department of Quantum Engineering, Nagoya University, Furo-cho, Nagoya 464-8603

Contact resistance between a carbon nanotube (CNT) and a metal electrode is related to the structure of a contact. In order to investigate an effect of the contact structure between a carbon nanotube and a metal electrode on electric properties, we studied the contact structure during the passage of a current by *in-situ* transmission electron microscopy (TEM) with the simultaneous current and bias voltage measurements.

Multi-walled CNTs, synthesized by an arc discharge method, were attached to an edge of a gold plate of 50 μm thickness by electrophoresis. A free end of a CNT was brought into contact with a tip of a gold-coated tungsten needle inside a transmission electron microscope. The bias voltage was applied and the electric current was passed through the contact region. The structural change of the contact was observed by TEM with a television camera.

Figure 1 shows a time-sequence series of high-resolution images of a structural change of the contact between a gold surface and a CNT tip. In Fig. 1, the dark region at the top is the gold surface. The CNT tip is come into contact with the gold surface without applying the bias voltage (Fig. 1(a)). When the bias voltage is increased to 1.42 V, the current increases to 52.3 μA and the shape of the gold surface in contact with the CNT tip is changed and at the same time the CNT tip is inserted into gold by 1.8 nm in depth (Fig. 1(b)). After a further increase of the voltage to 1.86 V, the CNT tip is inserted toward the gold surface more deeply and the contact area between the gold and the CNT increases (Fig. 1(c)). We measured the current-voltage characteristics before and after the insertion of the CNT into the gold (Fig. 1(a) and (c)). The current at 1.2 V after burying the CNT tip in the electrode increased 1.7 times larger than that at the just touching.

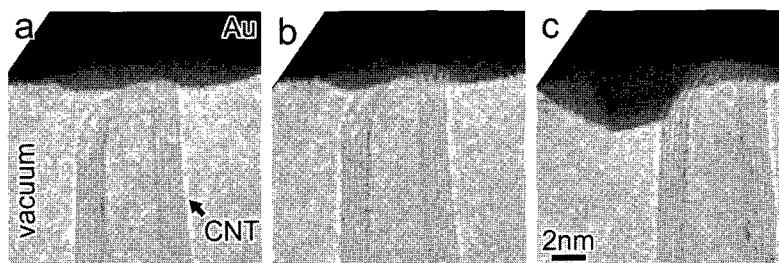


Fig. 1 Time-sequence series of high-resolution images of the structural change of the contact between a gold surface and a CNT tip.

Corresponding Author: Motoyuki Karita

E-mail: karita@surf.nuqe.nagoya-u.ac.jp, **Tel&Fax:** +81-52-789-3714,+81-52-789-3703

Isomerization of a Carbene Derivative of Metal Carbide Endofullerene $\text{Sc}_2\text{C}_2@C_{80}$

○ Hiroki Kurihara¹, Yuko Yamazaki¹, Hidefumi Nikawa¹, Naomi Mizorogi¹, Takahiro Tsuchiya¹, Shigeru Nagase² and Takeshi Akasaka¹

¹*Center for Tsukuba Advanced Research Alliance, University of Tsukuba,
Tsukuba, Ibaraki 305-8577, Japan*

²*Department of Theoretical and Computational Molecular Science,
Institute for Molecular Science, Okazaki, Aichi 444-8585, Japan*

Endohedral metallofullerenes (EMFs) have attracted wide interest in recent years because of the promising material, catalytic, and biomedical applications [1]. Scandium metallofullerenes are of special interest because of the high variety of fullerene sizes and of encapsulated structures inside a hollow fullerene cage. Especially, it is the unique structure that encapsulation of not only the metal but also the carbide inside a hollow fullerenes ($\text{Sc}_2\text{C}_2@C_{84}$ [2], $\text{Sc}_2\text{C}_2@C_{82}$ [3], $\text{Sc}_3\text{C}_2@C_{80}$ [4] etc).

Functionalization of EMFs is crucial to incorporate them in devices and to open new avenues of research and potential applications. As of today, there have been a few reports of functionalization of EMFs, and only a handful of these reports described the isolation of well-characterized adducts. Among of these, isomerization of some regioisomeric derivatives on fullerene cages has been detected only the monoadducts of [6,6]-pyrrolidinofullerenes of $\text{M}_3\text{N}@C_{80}$ (M=Y, Er) to the [5,6]-regioisomers [5].

Here, we were carried out chemical functionalization of metal carbide Endofullerene $\text{Sc}_2\text{C}_2@C_{80}$ by adamantylidene carbene (Ad) to obtain the cycloadducts, $\text{Sc}_2\text{C}_2@C_{80}\text{Ad}$ (I, II). Therefore, we report an isomerization of the $\text{Sc}_2\text{C}_2@C_{80}\text{Ad}$ (I) to give rise exclusively to the $\text{Sc}_2\text{C}_2@C_{80}\text{Ad}$ (II) and these characterization by means of spectroscopic analysis, and redox property, theoretical calculation and X-ray single-crystal structure analysis.

References

- [1] Endofullerenes: A New Family of Carbon Clusters; Akasaka, T., Nagase, S.; Eds.; Kluwer: Dordrecht, 2002.
- [2] Wang, C. R. et al. *Angew. Chem. Int. Ed.* **2001**, *40*, 397.
- [3] Iiduka, Y. et al. *Chem. Commun.* **2006**, 2057.
- [4] Iiduka, Y. et al. *J. Am. Chem. Soc.* **2005**, *127*, 12500.
- [5] Echegoyen, L. et al. *J. Am. Chem. Soc.* **2006**, *128*, 6480.

Corresponding Author: Takeshi Akasaka

Tel & Fax : +81-298-53-6409, E-mail : akasaka@tara.tsukuba.ac.jp

Linewidth of Raman G⁺-Band Features of Individual Single-Walled Carbon Nanotubes from Isotopic Carbon Sources

○Pei Zhao, Rong Xiang, Kentaro Sato, Erik Einarsson, Shigeo Maruyama

Department of Mechanical Engineering, The University of Tokyo

We analyze the room-temperature linewidth of the G⁺-band features occurring in resonance Raman spectra observed for individual, isolated single-walled carbon nanotubes (SWNTs) grown from different isotopic carbon gas sources (i.e., from ¹²C₂H₅OH, ¹³C₂H₅OH, and their mixture) by a no-flow alcohol catalytic chemical vapor deposition (ACCVD) method.^[1] Measurement of the G-band spectra of 30 isolated, suspended SWNTs allow us to investigate intrinsic properties related to phonon and electron dispersions through a linewidth fitting and analysis, especially the corresponding in-plane longitudinal optical (LO) phonon mode and phonon lifetime.^[2] Results show that all the Raman G⁺-band features of isolated SWNTs exhibit narrower linewidth compared with SWNT films grown from the same carbon sources. Moreover, SWNTs grown from isotopic mixture show a significant broadening (10~20%) in this Raman feature compared to those synthesized from single carbon species source. This indicates a shorter LO phonon lifetime, which may involve a more complicated coupling between carbon atoms of different mass.

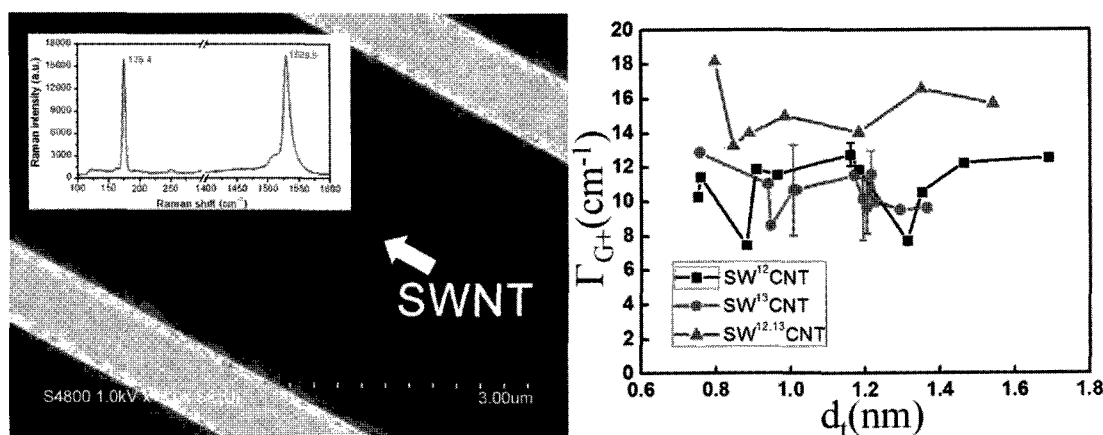


Figure 1: Left: Scanning electron microscopy (SEM) image of isolated, suspended SWNTs, indicated by the arrow. Inset: Resonance Raman spectra from an isolated SWNT grown from ¹³C₂H₅OH, whose RBM-band is centered at 175 cm⁻¹; Right: Linewidth distribution of G⁺-band features of isolated SWNTs grown from ¹²C₂H₅OH, ¹³C₂H₅OH and ^{12,13}C₂H₅OH, denoted by square, dot, and triangle symbols, respectively.

[1] S. Maruyama, R. Kojima, Y. Miyauchi, S. Chiashi, M. Kohno, *Chem. Phys. Lett.* **360**, 229 (2002).

[2] M. S. Dresselhaus, G. Dresselhaus, R. Saito, A. Jorio, *Physics Report* **409**, 47 (2005).

Corresponding Author: Shigeo Maruyama

TEL: +81-3-5841-6421, FAX: +81-3-5841-6983, E-mail: maruyama@photon.t.u-tokyo.ac.jp

Nickel-Atom Endohedral Fullerenes Synthesized by Irradiation of Nickel Ions Generated by Plasma Sputtering

○T. Umakoshi, H. Ishida, T. Kaneko, and R. Hatakeyama

Department of Electronic Engineering, Tohoku University, Sendai 980-8579, Japan

Fullerenes such as C_{60} can produce compounds by trapping other atoms inside their cage, which are called endohedral fullerenes. Since the endohedral fullerenes have attracted considerable interest as candidates for organic devices, they have been synthesized using ion implantation, arc discharge plasma, and glow discharge plasma methods [1]. However, magnetic-atom endohedral fullerenes have not been synthesized by the methods using the conventional arc discharge or laser ablation. Therefore, in order to synthesize the nickel-atom endohedral fullerene ($Ni@C_{60}$), we adopt a plasma irradiation method by which we have efficiently generated a nitrogen-atom endohedral fullerene [2].

An experimental apparatus is schematically shown in Fig. 1. In this experiment, a nickel plate and a grid, to which arbitrary voltages can be applied, are placed in directions parallel and perpendicular to magnetic-field lines, respectively. Argon ions generated from an ECR discharge plasma sputter the negatively biased nickel plate and grid expected to high energy impact. Therefore nickel ions are effectively generated by the hybrid sputtering. C_{60} molecules are sublimated to a substrate terminating the plasma, and the nickel ions are irradiated to the C_{60} molecules. Figure 2(a) shows mass spectra of samples deposited on the substrate. Both the peaks corresponding to $Ni-C_{60}$ (mass number 778) and $Ni-C_{59}$ which is generated by replacing C with Ni (mass number 766) are observed by optimizing the plasma parameters. A calculated isotope distribution of $Ni-C_{60}$ is presented in Fig. 2(b), and coincides with the distribution of mass spectrum of the sample on the substrate. Therefore, we can conclude that the sample indicates the existence of $Ni-C_{60}$.

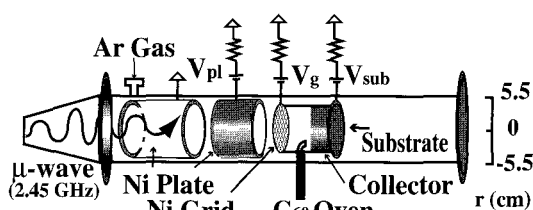


Fig. 1. Experimental apparatus.

[1] T. Almeida Murphy *et al.*, *Phys. Rev. Lett.*, **77**, 1075 (1996).

[2] T. Kaneko *et al.*, *Phys. Plasmas*, **14**, 110705 (2007).

Corresponding Author: Tatsuya Umakoshi

TEL: +81-22-795-7046, FAX: +81-22-263-9225, E-mail: umakoshi@plasma.ecei.tohoku.ac.jp

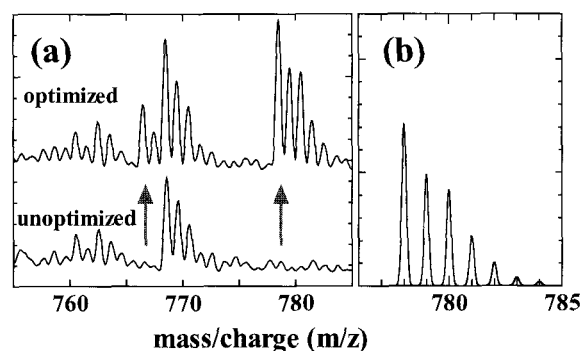


Fig. 2. (a) Mass spectra of samples deposited on the substrate, (b) a calculated isotope distribution of $Ni-C_{60}$.

Nature of chemical bonding in endohedral di-metallofullerenes and their carbides: $M_2(C_2)@C_{2n}$ ($M=Y, La, Er, Lu$; $2n=82$ and 80)

○Jian Wang and Stephan Irle

*Institute for Advanced Research and Department of Chemistry, Nagoya University, Nagoya
464-8602, Japan*

A systematic investigation on the chemical bonding in di-metallofullerenes and corresponding carbides has been performed using density functional theory. Cages C_{82} with $C_s(6)$ (I), $C_{2v}(9)$ (II) and $C_{3v}(8)$ (III), and C_{80-I_h} were considered. Transition metal atoms M, such as Y (experimental ground state configuration: $4d^15s^2$), La ($5d^16s^2$), Er ($4f^{12}6s^2$), and Lu ($4f^{14}5d^16s^2$) were selected to study molecular structures and electronic properties. We have employed B3LYP using Ahlrich's SVP basis sets for carbon, and the Stuttgart-Dresden SRSC97 effective core potential and basis sets for metal atoms.

Our calculations show for $M_2@C_{2n}$ metallofullerenes that two electrons from the metal's outer s-shell are transferred to the cage, while valence d or f electrons may transfer to the cage or engage in M-M bonding depending on the electropositivity of the metal and the electronegativity of the cage. Based on orbital occupancy of $M_2@C_{82}$ electronic ground states, with the single exception of La, the fullerene cage is found to be formally 4-fold negatively charged and metal atoms maintain formal dicationic configuration while promotion of open-shell d or f electrons occurs. This promotion may allow for M photoemission from 3+-like f-f transitions such as in the case of $Er_2@C_{82}$ [1]. On the other hand, in the case of dimetallofullerenes of the more electronegative C_{80} cage ($M_2@C_{80}$), the fullerene cage is either 5-fold ($M=Lu, Er, Y$) or 6-fold ($M=La$) negatively charged.

When a C_2 unit is encapsulated inside the cage, the metal d or f electrons are instead formally transferred into the energetically low-lying C_2 bonding $2p \sigma_g$ orbital (-7.091eV), creating formally a C_2^{2-} dianion. Due to large orbital overlap, electron donation from C_2^{2-} to the highly charged metal core ensues, reducing unfavorable charge accumulation on the C_2 unit. No neutral C_2 was ever found in our calculations in contrast to experimental results. Generally, we always find in metallocarbides of type $M_2C_2@C_{2n}$ that the cage is 4-fold negatively charged and C_2 has a formal charge of 2-, while metal atoms are formally triply positively charged.

Consistent with this observation, we show that for hypothetical $M_2C_2@C_{80}$ compounds the cage can only attain 4 negative charges although C_{80} has a strong affinity for a 6- charge. The resulting $M_2C_2@C_{80}$ has small HOMO-LUMO gap, therefore the absence of such species in fullerenic soot is explained by the electronic configuration of the encapsulated M_2C_2 .

Overall, we show that a) metal atoms inside dimetallofullerenes have the tendency to form M-M bonds with open-shell d or f electrons depending on their electropositivity, b) encapsulated M_2C_2 have a positive charge of 4+, never higher, and c) C_2 is always formally a dianion.

[1] Y. Ito, T. Okazaki, S. Okubo, M. Akachi, Y. Ohno, T. Mizutani, T. Nakamura, R. Kitaura, T. Sugai, and H. Shinohara, *ACS NANO*, 1(5), 456 (2007).

Corresponding Author: Stephan Irle

TEL: +81 (052) 747-6397, FAX: +81 (052) 788-6151, E-mail: sirle@iar.nagoya-u.ac.jp

Purification and Characterization of $[\text{Li}@\text{C}_{60}]^+$ salts

○Takeshi Sakai¹, Hiroshi Okada¹, Yoshihiro Ono¹, Kazuhiko Kawachi¹, Kenji Omote¹,
Yasuhiko Kasama¹, Kuniyoshi Yokoo¹, Shoichi Ono¹,
Takashi Komuro², and Hiromi Tobita²

¹*ideal star Inc., ICR Bldg, 6-6-3 Minamiyoshinari, Aoba-ku, Sendai 989-3204, Japan*

²*Department of Chemistry, Graduate School of Science, Tohoku University,
Sendai 980-8578, Japan*

In 1996, Campbell et al. reported for the first time the synthesis of a lithium endohedral fullerene $\text{Li}@\text{C}_{60}$ using Li ion implantation to a C_{60} layer [1] and described its extraction and purification [2]. They have extensively investigated the properties of alkali endohedral fullerenes (thermal stability, electric conductivity, IR, Raman, ESR, etc.) [3]. However, the structural characterization of them has not been achieved yet due to their low production efficiency and insufficient purity.

Recently, we succeeded in the synthesis of a sufficient amount of $\text{Li}@\text{C}_{60}$ and complete isolation of a salt $[\text{Li}@\text{C}_{60}](\text{SbCl}_6)$, which led to the achievement of its structural determination [4]. In this paper, we report an effective purification process of $[\text{Li}@\text{C}_{60}]^+$ ion by HPLC (Figure 1) and characterization of the resultant salt $[\text{Li}@\text{C}_{60}](\text{PF}_6)$ by NMR, IR, and UV-vis spectroscopy. In particular, its ^7Li NMR spectrum in a solution shows a large high-field shift due to the shielding effect of the C_{60} cage, which is consistent with its Li^+ -encapsulated structure.

We will discuss the electronic structure of the new metallofullerene $[\text{Li}@\text{C}_{60}]^+$ based on the spectroscopic data.

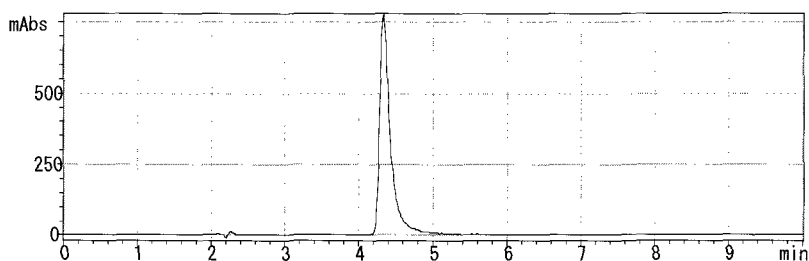


Figure 1. HPLC of isolated $[\text{Li}@\text{C}_{60}](\text{PF}_6)$

[1] Campbell et al., *Nature*, **382**, 407 (1996).

[2] Campbell et al., *Appl. Phys.*, **A66**, 293 (1998).

[3] (a) Campbell et al., *Eur. Phys. J. D*, **9**, 345 (1999). (b) Campbell et al., *J. Phys. Chem. B*, **107**, 11290 (2003). (c) Campbell et al., *Solid State Communications*, **133**, 499 (2005).

[4] H. Okada et al., *The 38th Fullerene-Nanotubes General Symposium*, (2010).

Corresponding Author: Yasuhiko Kasama

TEL: +81-22-303-7336, FAX: +81-22-303-7339, E-mail: idealstar@idealstar-net.com

Synthetic and Structural Studies on an Iridium Complex of the Li@C₆₀ Cation

○Takahito Watanabe¹, Takashi Komuro¹, Hiroshi Okada², Takeshi Sakai², Yoshihiro Ono², Yasuhiko Kasama², and Hiromi Tobita¹

¹Department of Chemistry, Graduate School of Science, Tohoku University, Sendai 980-8578, Japan

²ideal star Inc., ICR Bldg, 6-6-3 Minamiyoshinari, Aoba-ku, Sendai 989-3204, Japan

Endohedral metallofullerenes have attracted much attention for their unique structural and electronic properties [1]. C₆₀-based endohedral metallofullerene Li@C₆₀ has been synthesized by Campbell and coworkers for the first time in 1996 [2]. However, the structural characterization was not achieved. We have recently succeeded in the bulk synthesis of Li@C₆₀, its oxidation, and structural determination of a salt [Li@C₆₀](SbCl₆) by single-crystal X-ray crystallography.

The empty C₆₀ with significant π -acceptor capacity is known to form stable adducts with electron-rich metal fragments such as Pt(PPh₃)₂ [3] and IrCl(CO)(PPh₃)₂ [4]. However, to our knowledge, there is no transition-metal complex bound to endohedral metallofullerenes. Consequently, we started the research on the synthesis of transition-metal complexes of the Li@C₆₀ cation. In this paper, we report the synthesis of mononuclear iridium complex [(Li@C₆₀){IrCl(CO)(PPh₃)₂]}(PF₆) (**1**)(PF₆). The solid-state structure was determined by X-ray crystal structure analysis. As shown in Figure, the encapsulated lithium atom is located at a single site adjacent to the iridium fragment.

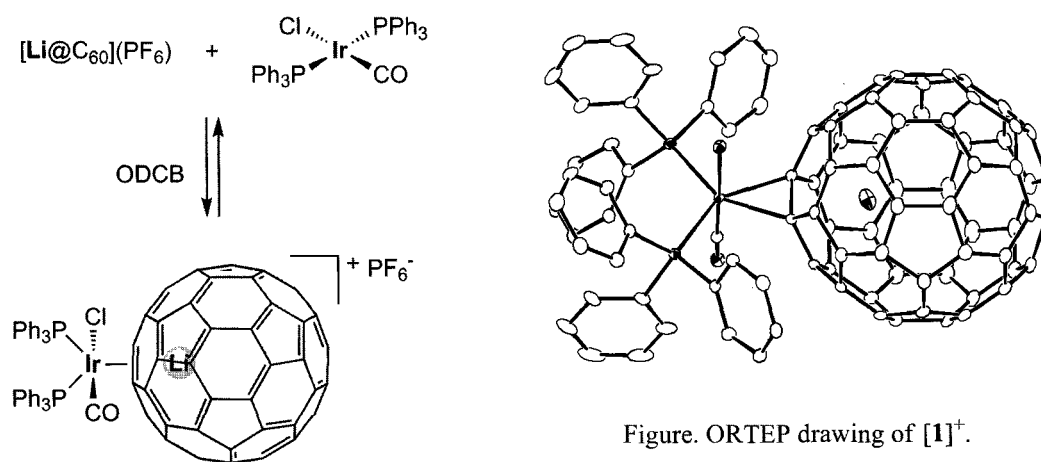


Figure. ORTEP drawing of **1**⁺.

- [1] M. Yamada, T. Akasaka, and Shigeru Nagase, *Acc. Chem. Res.*, ASAP.
 [2] R. Tellgmann, N. Krawez, S.-H. Lin, I. V. Hertel, and E. E. B. Campbell, *Nature*, **382**, 407 (1996).
 [3] P. J. Fagan, J. C. Calabrese, and B. Malone, *Acc. Chem. Res.*, **25**, 134 (1992).
 [4] A. L. Balch, V. J. Catalano, and J. W. Lee, *Inorg. Chem.*, **30**, 3980 (1991).

Corresponding Author: Hiromi Tobita

TEL: +81-22-795-6539, FAX: +81-22-795-6543, E-mail: tobita@m.tains.tohoku.ac.jp

Gd@C₈₂ derivatives based MRI contrast agents

○Jinying Zhang, Yasumitsu Miyata, and Hisanori Shinohara*

Department of Chemistry, Nagoya University, Nagoya, 464-8602, Japan

As promising MRI contrast agents, Gadolinium metallofullerenols (Gd@C₈₂(OH)₄₀) were reported to have paramagnetic properties much higher (20 times) than a commercial available Gd-DTPA.¹ However, gadolinium metallofullerenols were reported to be unstable when the adduct groups are more than 36.² Amino groups, were introduced into Gd@C₈₂ in this report. Water soluble Gd@C₈₂ derivatives, fulleropyrrolidine amino chlorides, were produced to a solubility of 10⁻⁴M. The proton relaxations of the product mixture were measured with a 4.7T magnetic field. R₁ was observed to be comparable to a commercial available Gd-DTPA, while R₂ was 20 times as large as that of DTPA. Both R₁ and R₂ were demonstrated to be non-linear according to gadolinium concentration. Gadolinium concentrations were measured by ICP at a series of different wavelength. The pre-products of fulleropyrrolidine amino chlorides, protected by *tert*-butyloxycarbonyl (BOC) group, were separated using HPLC (Column: Buckyprep-M, 4.6×250mm, eluent solvent: toluene: methanol=7:3, flow rate: 0.5ml/min). The fraction with retention time centered at around 7min was characterized to be mono-functionalized products. The pure product was characterized by MALDI mass spectrometry, H-NMR and UV-vis spectroscopies.

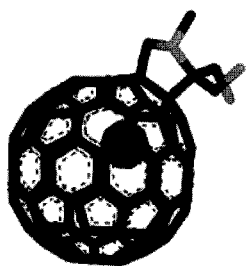


Fig 1 Schematic molecular structure of Gd@C₈₂ fulleropyrrolidine amino chloride

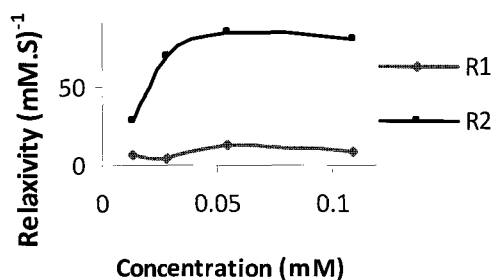


Fig. 2 Proton relaxation results of Gd@C₈₂ fulleropyrrolidine amino chloride

References:

1. M. Mikawa, H. Kato, M. Okumura, *et. al. Bioconjugate chem.*, 2001, 12(4), 510.
2. G. Xing, J. Zhang, Y. Zhao, *et. al. J. Phys. Chem. B*, 2004, 108(31), 11473.

*Corresponding Author: Hisanori Shinohara

E-mail : noris@nagoya-u.ac.jp

Tel & Fax : 052-789-2482

Spectroscopic Characterization of Singly Reduced $\text{Li}^+\text{@C}_{60}$

○Kimio AKIYAMA¹, Hiroshi Okada², Takeshi Sakai², Yoshihiro Ono²,
Yasuhiko Kasama², and Hiromi Tobita³

¹*Institute of Multidisciplinary Research for Advanced Materials, Tohoku University, Sendai 980-8577, Japan*

²*Ideal star Inc., ICR Bldg, 6-6-3 Minamiyoshinari, Aoba-ku, Sendai 989-3204, Japan*

³*Department of Chemistry, Graduate School of Science, Tohoku University, Sendai 980-8578, Japan*

Fullerenes have a unique type of carbon-based nanocage structures. A wide variety of metals have been encapsulated into this space with little perturbation to the cage structure. Recently we have successfully developed the method to synthesize a Li^+ ion endohedral C_{60} complex ($\text{Li}^+\text{@C}_{60}$) using the reaction of empty C_{60} with Li plasma, subsequent oxidation, and HPLC purification. Here, we present the first study on the properties of singly reduced $\text{Li}^+\text{@C}_{60}$ with reductive voltammetry, near-infrared (NIR) and electron paramagnetic resonance (EPR) spectroscopy.

Electrochemical studies of $\text{Li}^+\text{@C}_{60}$ were performed in *o*-dichlorobenzene (ODCB) at room temperature. Up to four one-electron reductions were appeared in cathodic cyclic and differential pulse voltammograms and the reversibility of the first two stages was confirmed. The large positive shifts in half-wave potentials of $\text{Li}^+\text{@C}_{60}$ redox couples were observed as compared to those of C_{60} reduction.

By the bulk electrolysis (with Bu_4BF_4 as the supporting electrolyte) at first reduction potential of $\text{Li}^+\text{@C}_{60}$ the NIR and broad visible absorption bands grow without changing their shapes under oxygen- and water-free condition. NIR absorptions of the $\text{Li}^+\text{@C}_{60}$ anion radical ($\text{Li}^+\text{@C}_{60}^-$) are slightly shifted to higher wavenumber ($\sim 400 \text{ cm}^{-1}$) with respect to C_{60} anion (C_{60}^-), indicating the Li^+ ion inside of the C_{60} cage slightly perturbs the electronic states in energy.

NIR band and a broad EPR signal increase in parallel during electrochemical reduction. Referring EPR and NIR studies on the C_{60} anion, we assigned the observed broad EPR spectrum to $\text{Li}^+\text{@C}_{60}^-$, on the basis of following results:

1. Line width both in solution and rigid matrix.
2. Small g-value.
3. Saturation behavior of EPR signal intensities at low temperature.

Although Li^+ ion was captured inside the carbon cage a resolved hyperfine (HF) pattern of Li atom could not be observed. The lack of the HF structure is attributed to extremely broad features in solution and the large (and rapidly changing, as the molecule and/or Li^+ in a cage vibrate) differences in spin densities on each carbon atom. The Jahn-Teller distortions are thought to be responsible for the observed broad EPR spectrum of C_{60}^- . The distortion dynamics should be affected by the Li^+ ion in the cage and reflected in the electron spin relaxation dynamics. The solvent and counter cation effects will be discussed in detail.

Corresponding Author: Kimio AKIYAMA

E-mail: akiyama@tagen.tohoku.ac.jp, TEL: 022-217-5613

Encapsulation of metals by arc plasma reactor with twelve-phase alternating current discharge

○Tsugio Matsuura and Norio Maki

Industrial Technology Center of Fukui Prefecture, Fukui 910-0102, Japan

Carbon nano-capsules encapsulated some kinds of metals have attracted special interests due to their unique electronic behaviors and chemical properties, which had not seen in empty carbon nano-capsules. Several methods for producing the carbon nano-capsules such as DC arc-discharge [1], laser vaporization and following depositions [2], chemical reaction chamber sealed in Pyrex glass [3] have been presented. However, its yields are very much lower. In order to avoid the disadvantage of the DC arc-discharge method, the twelve-phase AC arc-discharge method has been developed [4]. In general, multiple-phase AC discharge plasma has unique features as follow; (a) no discharge break in spite of using very low frequency (in this case 60Hz) discharge, (b) rotation of discharge area depend on the frequency of the power source, (c) very low velocity and enriched uniform plasma production in wide space, almost 180mm in diameter, surrounded by multiple electrodes, (d) no deposits remain on the tip of electrodes. The carbon nano-capsules are synthesized by using this new type of arc plasma reactor in high purity and high yields. Fig.1 shows the twelve-phase AC arc-discharge at 100Pa in helium (He) gas. The metal was fed from the carbon electrodes containing 10%wt Nickel (Ni). The typical TEM image of the soot shown in Fig.2 has the inner diameter of about 30nm. Encapsulated metal of Ni was characterized by an energy dispersive X-ray analysis (EDX) too. The modifications from the heat processing have been followed by a thermo gravimetric (TG) measurement. The effects of gas pressure, kind of gas and total wattage of the reactor were investigated.

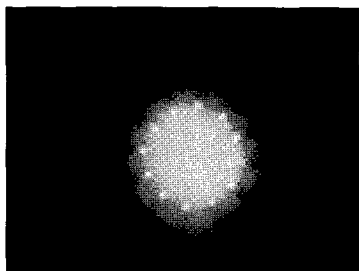


Fig.1 twelve-phase AC arc-discharge

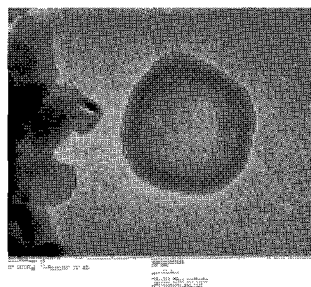


Fig.2 SEM image of carbon nano-capsule

References

- [1] H. Shinohara, et al, J. Phys. Chem., 96, 3571 (1992)
- [2] Y. Chai, et al, J. Phys. Chem., 95, 7564 (1991)
- [3] R. Nakanishi et al, 35th Commemorative Fullerene-Nanotubes General Symposium, 3p-47 (2008)
- [4] T. Matsuura, et al, 17th Int. Sym. on Plasma Che. (2005)

Corresponding Author: Tsugio Matsuura

E-mail: Tsugio_Matsuura@fklab.fukui.fukui.jp

Tel: 0776-55-0664 Fax: 0776-55-0665

**Electronic Properties of Di-Scandium and Di-Scandium Carbide Endohedral Fullerenes
Sc₂(C₂)@C₈₂ : Comparison Between DFT and DFTB**

○Yoshio Nishimoto, Stephan Irle

*Institute for Advanced Research and Department of Chemistry, Nagoya University,
Nagoya 464-8602, Japan*

The electronic structure of di-scandium and di-scandium carbide endohedral metallofullerenes (EMFs), Sc₂(C₂)@C₈₂, was studied using the self-consistent-charge density functional tight-binding (DFTB) quantum chemical method. This method is computationally considerably more economical than first principles density functional theory (DFT) yet shows comparable accuracy. Here, as a first step in a greater DFTB-based study of formation and dynamics of scandium-containing EMFs at high temperatures, we compared DFT and DFTB results for geometries, energies, and orbital occupations of selected model compounds. For di-scandium carbide compounds we used the DFT calculations performed with the Becke and Perdew exchange-correlation functional along with triple- ζ -polarized basis sets of Valencia *et al.* [1] as benchmark reference. According to their report, the ionic model, (Sc₂C₂)⁴⁺@(C₈₂)⁴⁻, is a valid description of the charge transfer in these compounds, and the transfer of four electrons from the Sc₂C₂ cluster onto the C₈₂ cage and that of two electrons from Sc to the C₂ unit is confirmed in the Kohn-Sham orbital picture. It was also found in calculations of hundreds of empty carbon cages that only the C_{3v}-C₈₂:**8** isomer displays a favorable electronic structure to display a very large (LUMO+2) – (LUMO+1) gap, which makes this cage an outstanding candidate for photoluminescence from encapsulated metal atoms in the visible light range when it is fourfold negatively charged. We performed DFTB geometry optimizations for the six isomers of the Sc₂C₂@C₈₂ compounds reported by Valencia *et al.* and found that DFTB calculations could reproduce trends in relative isomer energies. Most importantly, the Kohn-Sham orbital occupation patterns agree, which indicates that in both DFTB and DFT methods, only four electrons are transferred to the cage, while C₂ is clearly formally a dianion. The DFTB calculation for the C₈₂ empty cage also confirmed that the (LUMO+2) – (LUMO+1) gap is large with a value close to that of DFT. In case of the Sc₂@C₈₂ compounds with same cage isomers we found in agreement for relative isomer energies with own DFT (B3LYP) calculations. In conclusion, we find that DFTB calculations are useful for evaluating electronic properties of di-scandium and di-scandium carbide EMFs.

References[1] R. Valencia, A. Rodriguez-Fortea, J. M. Poblet, *J. Phys. Chem. A* **2008**, *112*, 4550-4555.**Corresponding Author:** Stephan Irle**TEL/FAX:** +81-52-747-6397/+81-52-788-6151, **E-mail:** sirle@iar.nagoya-u.ac.jp

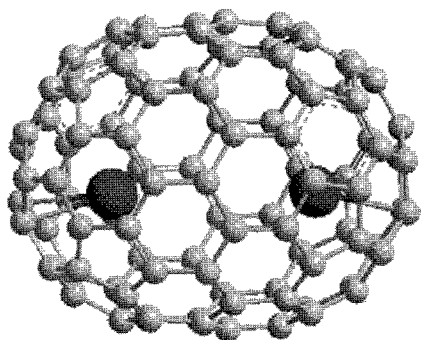
Computed Structures and Relative Stabilities of Dy₂@C₁₀₀

T. Yang and X. Zhao*

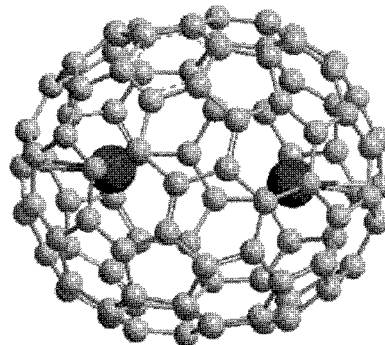
*Institute for Chemical Physics and Department of Chemistry,
Xi'an Jiaotong University, Xi'an 710049, P. R. China*

We herein report our systematical theoretical study of metallofullerenes Dy₂@C₁₀₀. All C₁₀₀ isomers beyond IPR and non-IPR species (PA=0~2) are screened on the hexa-anion state by AM1 level semiempirical calculations. Some best structures of C₁₀₀⁶⁻ and their corresponding metallofullerenes Dy₂@C₁₀₀ were fully optimized at the B3LYP level, where 6-31G(d) basis set was used for carbon and a *quasi*-relativistic pseudopotential with a corresponding valence basis set^[2] was applied for dysprosium. Upon the optimized geometries, the harmonic vibrational analyses were carried out at the same quantum-chemical level of theory.

The optimizations of C₁₀₀⁶⁻ cages at B3LYP/6-31G(d) level generally support the AM1 conclusions, revealing a structure labeled 285913:D₅ as the lowest energy isomer with a large HOMO-LUMO gap (2.50 eV) and following with 285864:C₂ species as the second stable one. In contrast to hexaanion energies, the order of Dy₂@C₁₀₀ relative energy changes when two dysprosium atoms are encapsulated in C₁₀₀ cages, predicting the Dy₂@285864:C₂ to be the lowest energy isomer (with an energy difference of 1.85 kcal/mol compared to the Dy₂@285913:D₅) holding a rather large HOMO-LUMO gap (1.16 eV) vs a small one (0.70 eV) of the latter.



#285913:D₅



#285864:C₂

To obtain further insight into the thermodynamic stability of Dy₂@C₁₀₀, we have investigated the entropy effects and evaluated the relative concentrations through the Gibbs free energy terms. It turns out that even though the 285864:C₂ structure must of course prevail at very low temperatures, its relative stability decreases rapidly as the temperature increases and the stability interchange occurred after 400 K. Then 285913:D₅ structure increases sharply to a temperature of 1400 K with its maximum yield of 71%. Clearly, it is shown that the 285913:D₅ isomer should be the most thermodynamically stable one over a wide temperature region with respect to the metallofullerene formation. The computed small HOMO-LUMO gap (0.70 eV) is in good agreement with the experimental observation^[2]. The general feature of overall stability on the Dy₂@C₁₀₀ will be discussed in details^[3].

Reference:

- [1] a) M. Dolg, *et al. Theor. Chem. Acc.* **1989**, 75, 173. b) M. Dolg, *et al. ibid.* **1993**, 85, 441.
[2] S. Yang, L. Dunsch, *Angew. Chem. Int. Ed.* **2006**, 45, 1299-1302.
[3] Manuscript in preparation.

* Corresponding Author: X. Zhao, xzhao@mail.xjtu.edu.cn, or x86zhao@yahoo.co.jp

Direct observation of a Li cation inside C₆₀ by the charge density analysis

○Shinobu Aoyagi¹, Eiji Nishibori¹, Ryo Kitaura², Hiroshi Okada³, Takeshi Sakai³, Yoshihiro Ono³, Yasuhiko Kasama³, Hiromi Tobita⁴, Hisanori Shinohara² and Hiroshi Sawa¹

¹*Department of Applied Physics, Nagoya University, Nagoya 464-8603, Japan*

²*Department of Chemistry and Institute for Advanced Research, Nagoya University, Nagoya 464-8602, Japan*

³*idealstar Inc., ICR Bldg, 6-6-3 Minamiyoshinari, Aoba-ku, Sendai 989-3204, Japan*

⁴*Department of Chemistry, Graduate School of Science, Tohoku University, Sendai 980-8578, Japan*

C₆₀-based metallofullerenes have a potential to accelerate the practical use of the fullerene materials in the field of electronics because C₆₀ is the most abundant fullerene and the encapsulation of metal atoms is a promising way to control the physical properties. However, the isolation of the C₆₀-based metallofullerenes has been quite difficult due to their insolubility. Recently, we have succeeded in bulk synthesis and complete isolation of Li@C₆₀ and crystallization of [Li@C₆₀](SbCl₆). Here, we report the result of x-ray structure determination of [Li@C₆₀](SbCl₆) single crystal using synchrotron radiation (SR).

The endohedral structure of Li@C₆₀ was revealed by the single crystal SR x-ray diffraction. The experiment was carried out at SPring-8 BL02B1. It has been difficult to specifically locate a Li cation with such a small scattering cross section by the conventional least-square refinement. The charge density distribution of a Li cation inside C₆₀ was clearly visualized by the maximum entropy method (MEM).

A Li cation occupies two off-centered disordered sites which are close to the center of the six-membered rings of the C₆₀ cage. The distance from the center of the C₆₀ cage to the Li cation is 1.34 Å which is close to the theoretically predicted values of 1.2 ~ 1.4 Å [1,2]. The Li sites are close to Cl atoms of SbCl₆ anions outside the C₆₀ cage. This fact suggests the existence of electrostatic attractive interaction between a Li cation and SbCl₆ anions through the C₆₀ cage and the position of the Li cation may be controlled by an external electric field outside the cage.

[1] M. Pavanello, A. F. Jalbout, B. Trzaskowski and L. Adamowicz, *Chem. Phys. Lett.*, **442**, 339-343 (2007).

[2] Z. Slanina, F. Uhlik, S.-L. Lee, L. Adamowicz and S. Nagase, *Chem. Phys. Lett.*, **463**, 121-123 (2008).

Corresponding Author: Hiroshi Sawa

TEL: +81-789-4453, FAX: +81-789-3724, E-mail: hiroshi.sawa@cc.nagoya-u.ac.jp

ReaxFF Simulation of Fullerene Formation in Benzene Combustions

Hu-Jun Qian,¹ Adri van Duin², Biswajit Saha³, Keiji Morokuma³ and Stephan Irle¹

¹*Institute for Advanced Research and Department of Chemistry, Nagoya University, Nagoya 464-8602, Japan*

²*Department of Mechanical and Nuclear Engineering, Pennsylvania State University, University Park, PA 16802, USA*

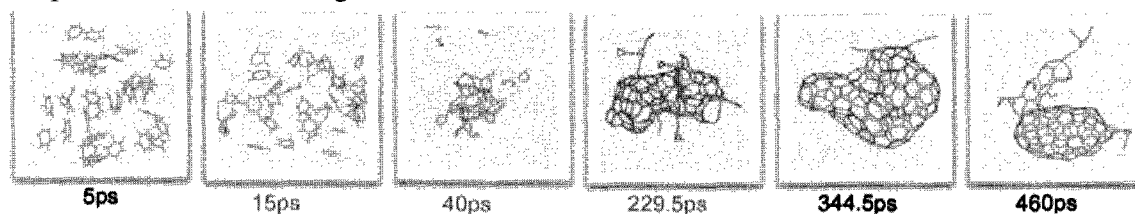
³*Fukui Institute for Fundamental Chemistry, Kyoto University, Kyoto, 606-8103, Japan*

Fullerenes are leading contenders for the design of organic field effect transistors, and have fantastic electronic properties. Extensive quantum chemical molecular dynamics (QM/MD) simulations (B. Saha, *et.al. ACS NANO*, 3, 2241, 2009) based on density-functional tight-binding (DFTB) potential have predicted a straightforward mechanisms for dynamic fullerene self-assembly both in pure-carbon plasma/vapors and combustion flames. Despite this fact, the actual mechanisms of fullerene formation under different experimental conditions are still subject to investigation. The empirical Reactive Force Field (ReaxFF) approach (A. C. T. van Duin, *et.al. J. Phys. Chem. A*, 105, 9396, 2001), a less expensive and much faster approach which can be used to study chemical reactions at classical mechanical level, is employed in this study to elucidate the fullerene formation mechanism in benzene combustion flames.

In this study, NVT simulations with time step of $\Delta t = 0.1$ at $T_0 = 2500\text{K}$ and 3000K with the temperature controlled constant by Berendsen thermostat. The following simulation strategy is adopted in this study to mimic the combustion process in benzene flame:



The ReaxFF trajectories suggest a common mechanism for giant fullerene formation that differs somewhat from DFTB/MD simulations. It follows 4 steps: (i) radical creation and ring-opening/fragmentation; (ii) nucleation of amorphous network with decrease of cyclic rings; (iii) ring condensation to fullerene precursors; and (iv) eventually, cage formed with the number of 6C-member rings reaching a maximum. Compared to DFTB/MD simulation, there are no bowl-like open cages found, instead, we found abundance of 3-member carbon rings and encapsulated structures in ReaxFF simulation. However, the formed caged are mostly distributed in the range from 150 to 210 carbon atoms, with the distribution shift toward larger cages at lower temperature, which is in agreement with the DFTB/MD simulations.



Corresponding Author: Stephan Irle

TEL/FAX: +81-52-747-6397/+81-52-788-6151, E-mail: sirle@iar.nagoya-u.ac.jp

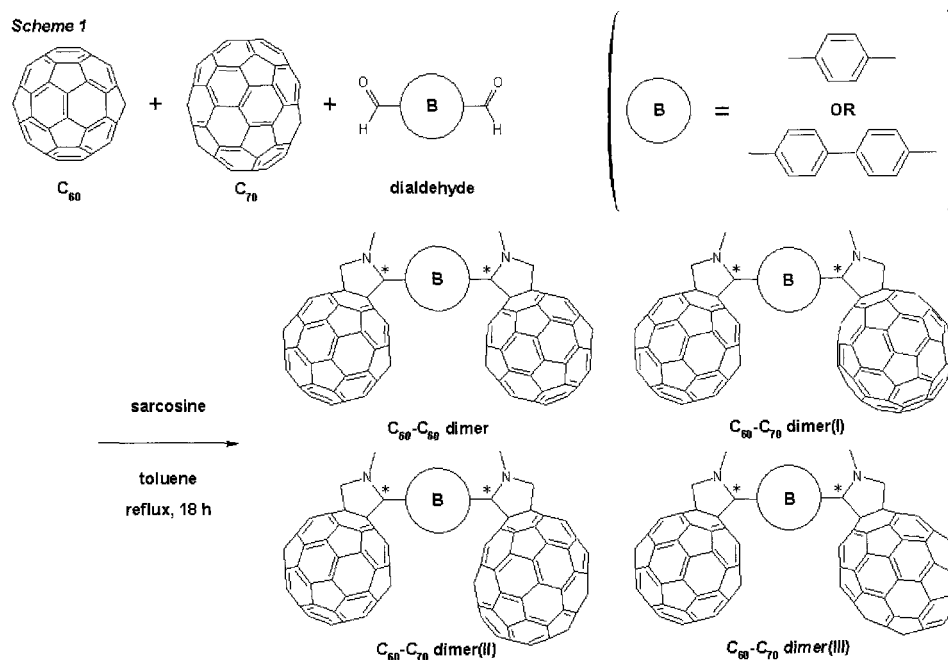
Synthesis and Characterization of Benzene-bridged Fullerene Dimers

○ Yasuhiro Ito¹, Jamie H. Warner¹, Maria del Carmen Gimenez-Lopez²,
Kyriakos Porfyrakis¹, Andrei N. Khlobystov² and G. Andrew D. Briggs¹

¹ *Department of Materials, Quantum Information Processing Interdisciplinary Research Collaboration (QIP IRC), University of Oxford, Parks Rd, Oxford, OX1 3PH, UK.*

² *School of Chemistry, University of Nottingham, NG7 2RD, UK.*

In order to build the architecture of QIP systems using fullerenes and endofullerenes, it is necessary to arrange fullerenes in solid state or carbon nanotube (peapod). Fullerene dimers which are the minimum unit in one-, two- or three-dimensional arrays, can be synthesized by a high-speed vibration milling (HSVM) technique¹⁾ or Prato reaction.²⁻⁴⁾ Meanwhile, empty fullerenes such as C₆₀ and C₇₀ are well known as excellent electron-acceptors and these anions show ESR spectra. In this study, we report the synthesis of benzene-bridged fullerene dimers. Benzene-bridged C₆₀-C₇₀ dimers can be obtained using terephthalaldehyde or 4,4'-Biphenyldicarboxaldehyde (Scheme 1). We will discuss the optical and magnetic properties of these dimers. Furthermore, we report the synthesis of isomer-free benzene-bridged dimers using 1,4-di(1,3-oxazolidin-5-one-3-yl)benzene, which form linear structures.



References

- 1) K. Komatsu *et al.*, *Chem. Commun.* 1583 (2000).
- 2) M. Maggini *et al.*, *J. Am. Chem. Soc.* **115**, 9798 (1993).
- 3) Y. Sun *et al.*, *J. Org. Chem.* **62**, 3642 (1997).
- 4) J. L. Delgado *et al.*, *Chem. Eur. J.* **15**, 13474 (2009).

Corresponding Author: Yasuhiro Ito

TEL: +44-1865-273790, **FAX:** +44-1865-273789, **E-mail:** yasuhito.ito@materials.ox.ac.uk

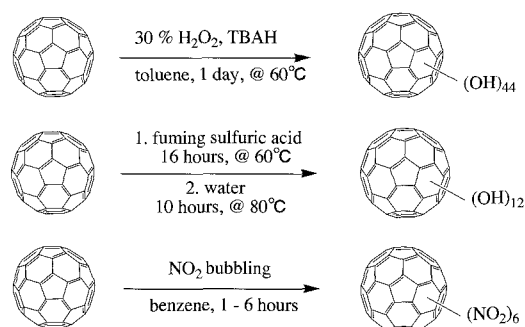
Polyhydroxylated Fullerene Salts

○Hiroshi Ueno, Toshiki Sugai, and Hiroshi Moriyama

Department of Chemistry, Toho University, Funabashi, 274-8510 Japan

There have been reported many kinds of chemically modified fullerenes. Above all, polyhydroxylated fullerene (fullerenol) has drawn attention because it has high water solubility and has been recognized to perform further chemical modification for the potential application to biological system. However, it is still an open question how many and where hydroxyl groups add to fullerene surface. To determine these issues and analyze its intrinsic properties, we are trying to synthesize fullerenol by selective addition of hydroxyl group to fullerene controllably and obtain its single crystals or salts.

We synthesized fullerenols which probably have 12 and 44 of hydroxyl groups and hexanitrofullerene which is fullerenol precursor using reported methods (Scheme 1.) [1 – 3]. IR spectra of them are shown in Fig 1. According to HPLC profiles, these fullerenols had several isomers, and hexanitrofullerene which probably had few isomers could be obtained. Thus, we tried to synthesize single crystal salts of hexanitrofullerene or its derivatives by recrystallization, diffusion method with the aid of coordination ability of substituent moieties, and electrocrystallization on the basis of electron acceptability of fullerene in the presence of appropriate cations. To circumvent the production of the mixture of modified fullerene, we are trying to develop site-selective unique method by modification of fullerene through hexanitrofullerene.



Scheme 1.

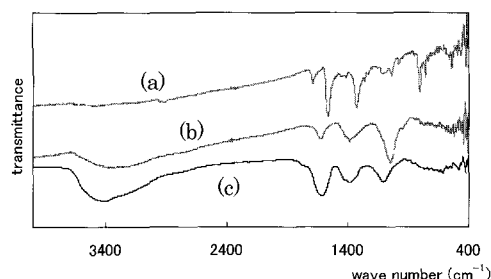


Fig 1. IR spectra of $C_{60}(NO_2)_6$ (a), $C_{60}(OH)_{12}$ (b) and $C_{60}(OH)_{44}$ (c).

Reference

- [1] Kokubo, K.; Matsubayashi, K.; Tategaki, H.; Takada, H.; Oshima, T. *ACS Nano*. **2008**, *2*, 327-333.
- [2] Chiang, L. Y.; Wang, L. Y.; Swirczewski, J. W.; Soled, S.; Cameron, S. *J. Org. Chem.* **1994**, *59*, 3960-3968.
- [3] Anantharaj, V.; Bhonsle, J.; Canteenwala, Taizoon.; Chiang, L. Y. *J. Chem. Soc., Perkin Trans.* **1999**, *1*, 31-36.

Corresponding Author : Hiroshi Moriyama

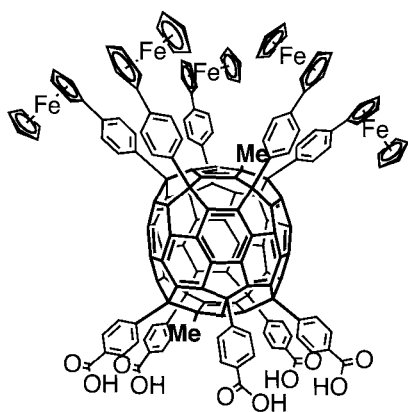
TEL: +81-47-472-1211, FAX: +81-47-476-9449, E-mail: moriyama@chem.sci.toho-u.ac.jp

Loading Pentapod Deca(organo)[60]fullerenes with Electron Donors: From Photophysics to Photoelectrochemical Bilayers

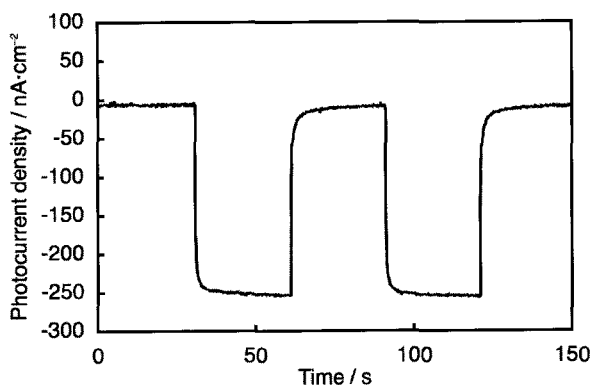
○Takahiko Ichiki, Yutaka Matsuo, and Eiichi Nakamura

Department of Chemistry and The University of Tokyo, 7-3-1 Hongo, Bunkyo-ku, Tokyo 113-0033, Japan, and Nakamura Functional Carbon Cluster Project, ERATO, JST, 7-3-1 Hongo, Bunkyo-ku, Tokyo 113-0033, Japan

A pentapod deca(aryl)[60]fullerene, $C_{60}(C_6H_4CO_2H)_5(C_6H_4Fc)_5Me_2$ (**1**, Fc = ferrocenyl), bearing five carboxylic acid and five ferrocenyl groups was synthesized through top and bottom functionalization of [60]fullerene by means of copper-mediated penta-addition reactions. **1** was probed by performing femtosecond flash photolysis experiments in a variety of organic solvents. And penta(carboxylic acid)-penta(ferrocenyl) compound **1** was deposited on indium tin oxide (ITO) electrodes¹ with a surface coverage (i.e., 0.14 nmol/cm²) that corresponded to a unique bilayer structure. The novel **1**/ITO photoelectrode gave rise to a cathodic photocurrent with a high quantum yield in the presence of methyl viologen. The unique molecular architecture of **1**, in combination with its remarkable donor/acceptor properties, validates the use of the pentapod deca(aryl)[60]fullerene in photoelectrochemically active molecular devices.



$C_{60}(C_6H_4CO_2H)_5(C_6H_4Fc)_5Me_2$, **1**



Referenece: (1) Matsuo, Y. Nakamura, E *et al.* *J. Am. Chem. Soc.* **2008**, *130*, 5016–5017.

Corresponding Author: Yutaka Matsuo and Eiichi Nakamura

E-mail: matsuo@chem.s.u-tokyo.ac.jp; nakamura@chem.s.u-tokyo.ac.jp

Tel&Fax: +81-(0)3- 5841-1476

Structure of Thin Polymerized C₆₀ Coatings Formed by Electron-Beam Dispersion with Additional Electric Field Assistance

Ihar Razanau^{1,2} ○, Tetsu Mieno¹, Viktor Kazachenko^{2,3}

1 – Department of Physics, Faculty of Science, Shizuoka University, Shizuoka 422-8529, Japan

2 – Francisk Skorina Gomel State University, Gomel 246019, Belarus

3 – Belarusian State University of Transport, Gomel 246653, Belarus

There are different methods for fullerite polymerization such as UV laser irradiation, high temperature high pressure treatment, alkali metal doping, mechanical milling, chemical techniques, electron-beam irradiation. Structure of polymerized material differs significantly for different methods changing from dimers to linear chains, 2D polymer networks or even 3D polymers, from single bond between C₆₀ molecules to [2+2] cycloaddition or even so called “peanut-shaped” polymers [1, 2].

We have previously showed that thin polymerised C₆₀ coatings can be deposited in vacuum by electron-beam dispersion (EBD) of the initial fullerite powder and structure of the coating depends strongly on the deposition parameters changing from almost nonpolymerised to highly polymerised fullerite [3]. The main peculiarity and at the same time advantage of EBD method is that coating is being deposited onto the substrate from the active gas phase containing neutral and excited molecules, ions and electrons. Thus different reactions and processes determine the final structure of the deposited coating.

In this work Raman and ATR FT-IR spectroscopy, MALDI and LDI mass-spectrometry techniques were used to analyse structure of thin coatings formed by EBD with additional electric field assistance.

A stable deposition regime of fullerite EBD was found which allowed depositing coatings with thickness about 200-300 nm and reproducible structure. Additional electric field applied to the substrates was used as an independent parameter to change and control charge composition of the depositing molecular flow and thus to change the coating structure.

Study of the coatings deposited at different electric potentials (from -10 to +300 V) applied to the substrate showed that fullerite powder EBD products contain positive fullerene ions and electrons. The quantity of ions in the molecular flow is estimated to be not more than 3-5%. When accelerated by substrate potential positive ions produce significant structural modification of the deposited layer leading not just to decrease of monomer phase content but to formation of the new carbon phase probably disordered and highly inter-connected. Similar to ion energy increase of ion content in the depositing molecular flow by their electro-static focusing onto the substrate leads to formation of even more of the new carbon phase with monomer content below detectable limit. Molecular structure of the deposited material and the role of oxygen in polymerization processes are also being discussed.

1. V.A. Karachevtsev, P.V. Mateichenko, N.Yu. Nedbailo, A.V. Peschanskii, A.M. Plokhotnichenko, O.M. Vovk, E.N. Zubarev, A.M. Rao, Carbon 42 (2004) 2091.

2. J. Onoe, T. Nakayama, M. Aono, T. Hara, Appl. Phys. Lett. 82 (2003) 595.

3. V.P. Kazachenko, I.V. Ryazanov, Physics of the Solid State 51 (2009) 870.

Corresponding author: Ihar Razanau

e-mail: ir23.by@gmail.com

tel.: 080-6927-1152

2P-16

C₆₀ Crystal Growth Directly between Electrodes on the Surface Treated Substrate

○S. Kato, K. Kurihara, Y. Iio, N. Iwata and H. Yamamoto

*College of Science and Technology, Nihon University,
7-24-1 Narashinodai, Funaba-shi Chiba, Japan 274-8501*

C₆₀ is a promising candidate as a high performance n-channel organic material demonstrated by a high electron mobility of 6 cm²/Vs in ref[1]. The purpose of our study is to grow a C₆₀ channel between source and drain electrodes directly by a simple dipping technique in a nano-scale. As well known nano-whisker, -crystal, -rod and -tube of C₆₀ crystal was grown by just evaporating solvent from C₆₀ solution and/or liquid-liquid-interfacial precipitation (LLIP) method. Crystal growth from organic solvent is much paid attention from the view of mass-production, because expensive equipment is not required.

In our previous report, the C₆₀ crystal growth was influenced by surface treatment, electrodes shapes, where on a hydrophilic surface, needle-like C₆₀ grew, and on a hydrophobic surface, C₆₀ particles grew with toluene solvent[2]. The solvent can be another parameter to control the crystal growth.

The Au electrodes sputtered substrate was treated by butyltrichlorosilane to be hydrophobic, and by 6-Mercapto-1-hexanol to be hydrophilic for only Au surface. Electrodes had a gap of 30 ~100 μm. The substrates were dipped into the C₆₀ saturation o-xylene solution with 1 μm/sec after soaking for 10 min.

Optical microscope after dipping is shown in figure 1. Rather larger C₆₀ crystal with the size of 5 μm in diameter was grown at the edge of the electrodes. Since there is a big difference in wettability between on the substrate surface, on Au surface and o-xylene solvent, C₆₀ molecules were expected to be precipitated at the interface and grew larger. We expect such the crystal bridge the electrode gaps and crystallinity can be controlled by surface treatment, dipping speed, solution temperature, shape of electrodes and so on.

[1] T.D.Anthopoulos et al., *Appl. Phys. Lett.* 89 (2006) 213504.

[2] N. Iwata, Y. Iio, K. Kurihara, H. Yamamoto, The 37th Commemorative Fullerene-Nanotubes General Symposium, 3P-10 (2009)

iwata@ecs.cst.nihon-u.ac.jp

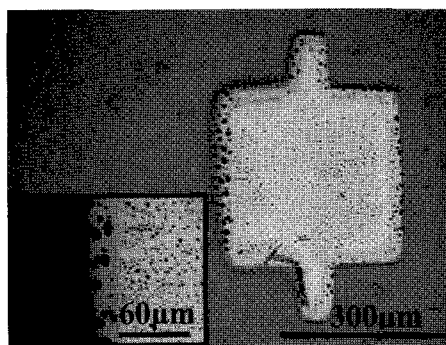


Figure 1 : C₆₀ particles between Au electrodes with the solvent : O-xylene

Structure and electronic properties of Na-H-C₆₀ compounds

○ Hideyuki Ohnami¹ and Hironori Ogata²

¹Research Center for Micro-Nano Technology, Hosei University,
3-11-15 Midori-cho, Koganei, Tokyo 184-0003, Japan

²Department of Chemical Science and Technology,
Faculty of Bioscience and Applied Chemistry, Hosei University,
3-7-2 Kajino-cho, Koganei, Tokyo, 184-8584, Japan

It has been reported that Na-H-C₆₀ ternary compounds have a superconducting phase [1][2]. However, detailed structure of Na-H-C₆₀ superconductor has not been clarified. In this study, the structural and electronic properties of Na-H-C₆₀ compounds were investigated. The Rietveld refinement [3] was carried out from its powder X-ray diffraction (PXD) pattern to determine the structure and composition of Na-H-C₆₀ compounds.

We prepared Na-H-C₆₀ compounds by solid reaction method of sodium hydride (NaH) to C₆₀. Stoichiometric amount of NaH and C₆₀ ($x = 3$ or 4 for (NaH)_xC₆₀) were mixed in a mortar and transferred to ESR quartz tubes in a glove box filled with argon gas. The quartz tubes sealed in a vacuum were heated under various conditions by an electric furnace. It was confirmed that prepared samples were single phase by solid state ¹³C-NMR measurement. The PXD patterns were measured with both synchrotron radiation of $\lambda = 1.000 \text{ \AA}$ at BL-8B of KEK-PF. The Rietveld refinement was carried out by the RIETAN2000 program [4].

Figure 1 shows the Rietveld fit pattern for the observed PXD pattern of $x = 4$. The minimum R -factor value is $R_{wp} = 9.51 \%$ at this time. The detailed results of Rietveld refinement of superconducting and non-superconducting phases and their electronic properties will be presented in the conference.

[1] K. Imaeda *et al.*, *Solid State Commun.*, **87**, 375(1993).

[2] K. Imaeda *et al.*, *Solid State Commun.*, **99**, 479(1996).

[3] C. Nakano *et al.*, *Chem. Lett.*, 343(1997).

[4] F. Izumi and T. Ikeda, *Mater. Sci Forum*, **321-324**, 198(2000).

Corresponding Author: Hideyuki Ohnami

Tel: +81-24-387-5108, Fax: +81-24-387-5121,

E-mail: hideyuki.ohnami.14@k.hosei.ac.jp

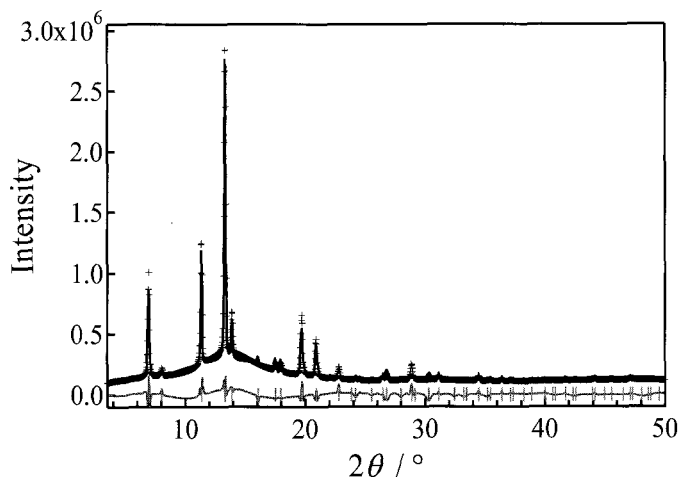


Figure 1. Rietveld fit pattern and observed PXD pattern.

Structural change of Mg-doped C₆₀ films along with growth temperature increasing

Seiji Nishi, Masato Natori, Nobuaki Kojima, and Masafumi Yamaguchi
 Toyota Technological Institute, 2-12-1 Hisakata Tenpaku, Nagoya 468-8511, Japan

Mg-doped C₆₀ is expected as solar cells and FETs application because of the improving in electric conductivity and mobility. However, its electrical conduction mechanism and the crystal structure are not clear. We have researched Mg concentration dependence and crystallinity dependence of the electric conductivity. We confirmed a remarkable increase in the electric conductivity by crystal quality improvement in epitaxial grown Mg-doped C₆₀ thin film on a mica(001) substrate. In addition, we observed that the crystal grains become smaller with increasing Mg concentration. It is necessary to understand the deposition process to make further improvement of the crystal quality. In this paper, we report the changes of surface morphology and the intermolecular bonding state in Mg-doped C₆₀ films prepared at various growth temperatures.

Mg-doped C₆₀ films were grown on mica(001) substrates by molecular beam epitaxy (MBE). In our previous work, we fixed the growth temperature at 165°C, which is the optimum growth temperature for the epitaxial growth of undoped C₆₀ film. The growth temperature was varied from 165°C to 220°C for Mg-doped C₆₀ in this study. The Mg/C₆₀ molar ratio of the sample was adjusted to around 0.3, in which we had obtained relatively good crystallinity at the growth temperature of 165°C. The structural characterization was done by X-ray diffraction (XRD), atomic force microscopy (AFM), and Raman spectroscopy.

Fig. 1 shows the Raman spectra of the Mg-doped C₆₀ films grown at various temperatures. The peak correspond to A_g(2) mode can be seen at around 1469[cm⁻¹] in all the films. New peak appears on lower wavenumber in the films grown with higher temperatures (180°C and up). With increasing growth temperature, this new peak shifts to lower wavenumber, and the peak area ratio of the new peak to the A_g(2) mode peak becomes larger. The wavenumber of the new peak consist with the position of peak for C₆₀ polymeric that has been reported in the literature. Therefore, there is a possibility that Mg-doped C₆₀ films are polymerized at the higher growth temperature. Changes in the crystal structure was suggested by XRD measurement and the surface morphology observed with AFM was greatly changed by the growth temperatures. It was shown that the growth temperature influences not only the crystal grain size but also the bonding state of the molecules in Mg-dope C₆₀ films.

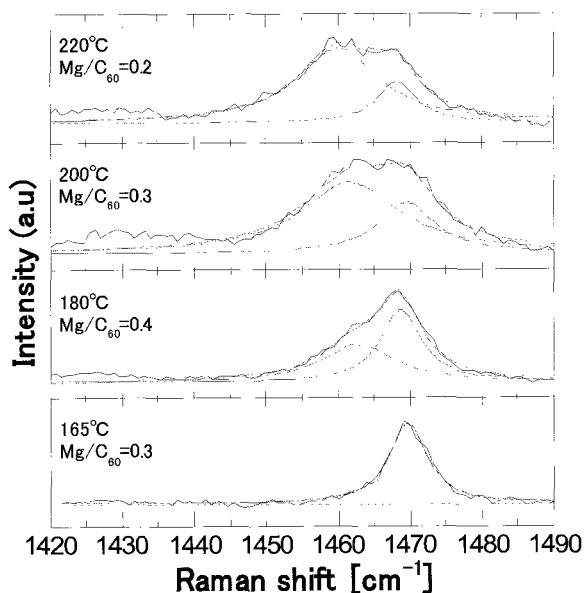


Fig.1 Raman spectra of Mg-doped C₆₀ grown at various temperatures

Corresponding Author: Seiji Nishi
E-mail: sd09426@toyota-ti.ac.jp
Tel: +81-52-809-1877
Fax: +81-52-809-1879

Electronic Structure of Metal-Doped C₆₀ Polymers

Tasuku Chiba and Susumu Okada

*Graduate School of Pure and Applied Sciences, Center for Computational Sciences,
University of Tsukuba, Tennodai, Tsukuba 305-8577, Japan*

Polymerized fullerenes are the class of carbon allotropes with one/two-dimensional covalent network comprising sp² and sp³ C atoms, and are derived from solid C₆₀ by applying pressure at elevated temperature [1]. The rhombohedral phase is found to be the majority phase possessing the layered structure of polymerized C₆₀ forming triangular lattice. Thus, there is two distinct interstitial sites, two tetrahedral sites (T-site) and an octahedral site (O-site) per unit cell, originated from those in the fcc C₆₀. Such spaces can accommodate the foreign atoms/molecules as in the case of solid C₆₀. Indeed, Na-doped rhombohedral C₆₀ polymer has been synthesized experimentally [2]. However, it has been still unclear its geometric and electronic structures. Thus, we elucidate the energetics and electronic structure of metal-doped rhombohedral C₆₀ polymers. To study the energetics and electronic structure, we perform total-energy electronic-structure calculation in the framework of the density functional theory (DFT).

Figure 1(a) and 1(b) show the electronic structures of Na-doped C₆₀ polymers in which the Na atoms are intercalated into T-site and O-site, respectively. In both cases, Na-doped C₆₀ polymers are found to be a metal with half filled energy band indicating the charge transfer from Na atoms to C₆₀. Furthermore, the electronic structure around the Fermi level does not depend on the position of Na atoms intercalated. Total energy calculations clarify that the T-site is energetically favorable for intercalation compared with the O-site. The stability of the T-site is ascribed to smaller size of interstitial leading to the larger Coulomb interaction.

[1]Y.Iwasa et al., *Science*, **264**, 1570 (1995).

[2]M.Yasukawa, S.Yamanaka, *Fullerenes, Nanotubes and Carbon Nanostructure*, **7**, 795(1999).

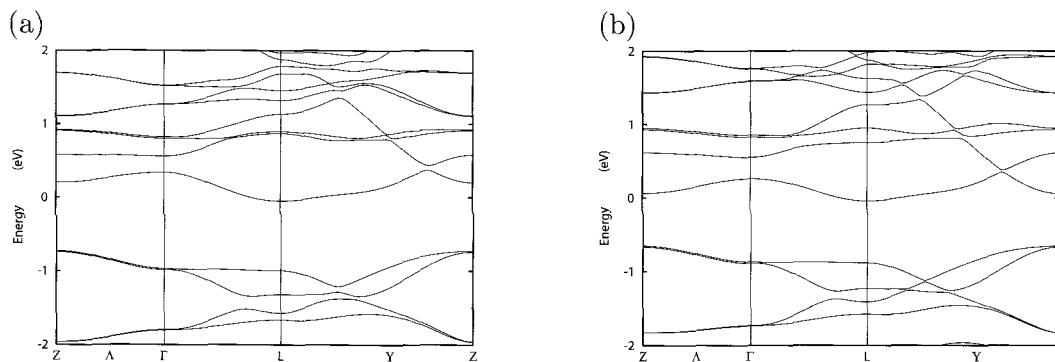


Fig1. Electronic structure of NaC₆₀ polymer (a)T-site doping and (b)O-site doping

Corresponding Author: Tasuku Chiba (Susumu Okada), sokada@comas.frsc.tsukuba.ac.jp

Hydrogen Etching Effect of Carbon Nanowalls Grown by Microwave Plasma Enhanced Chemical Vapor Deposition

○Seiya Suzuki and Masamichi Yoshimura

*Graduate School of Engineering, Toyota Technological Institute,
2-12-1 Hisakata, Tempaku, Nagoya 468-8511, Japan*

Carbon nanowall (CNW) is a nanostructure consisting of graphene sheets which stand from the substrate like a wall. Because of its high surface area, it can be applied to batteries, catalyst carriers, etc. From this viewpoint, the growth mechanism should be understood to control the structure of CNWs, mainly, their size and quality. It is well known that hydrogen plays an important role in etching amorphous carbon and in promoting graphitization. Shimabukuro et al. examined this hydrogen effect using hot-wire chemical vapor deposition (HWCVD) and suggested the existence of optimum hydrogen amount [1].

In this study, CNW films have been prepared on Si or SiO₂ substrate by microwave plasma enhanced chemical vapor deposition (MPECVD) with different gas mixture ratio of CH₄ and H₂: (referred to as H₂/CH₄ ratio hereafter)[2]. The total gas pressure was kept at 1.5 Torr. The growth temperature was about 870 K. The surface morphology of CNW films grown has been investigated by scanning electron microscope (SEM) and Raman spectroscopy. The growth mechanism of the CNWs and role of hydrogen have been discussed.

Figure 1 shows the dependence of the wall height on the H₂/CH₄ ratio. Mountain-like curves are observed for both substrates. Figure 2(a) shows the H₂/CH₄ dependence of the I_G/I_D. Taking both results into account, there are two different areas observed: from 0 to 2, and from 2 to 4 in H₂/CH₄ ratio. In the former region, the wall height increased but the I_G/I_D ratio was almost constant. In this region nucleation density was reduced because of less carbon source, while the growth rate increased through the effective incorporation of carbon due to large space between CNWs. In the latter region, however, the I_G/I_D ratio increased while the wall height

decreased with H₂/CH₄ ratio. Although the hydrogen promoted graphitization, less carbon source would be responsible to the reduction in the wall height. These behaviors are different from those reported for HWCVD[1]. The detailed growth mechanism will be discussed.

- [1] S. Shimabukuro, Y. Hatakeyama, M. Takeuchi, T. Itoh, and S. Nonomura, *Thin Solid Films*, 516 (2008) 710.
[2] K. Tanaka, M. Yoshimura, A. Okamoto, and K. Ueda, *Jpn. J. Appl. Phys. Part 1*, 44 (2005) 2074.

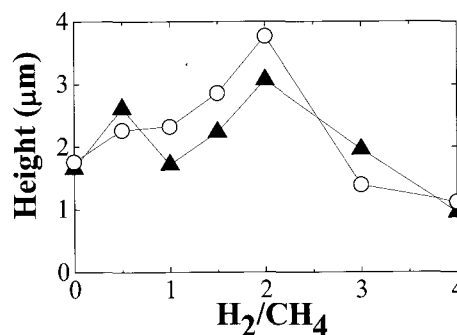


Figure 1. The H₂/CH₄ ratio dependence of the wall height of CNWs prepared on Si (▲) and SiO₂(○).

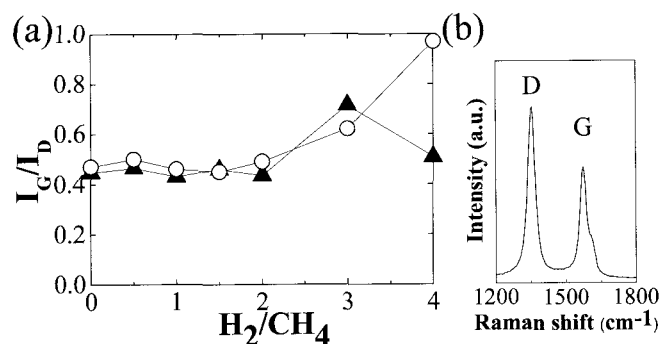


Figure 2. (a) The H₂/CH₄ ratio dependence of the I_G/I_D intensity ratio of CNWs prepared on Si (▲) and SiO₂(○). (b) A typical Raman spectrum of CNW.

Notices for single molecular imaging by HR-TEM.

○Yoshiko Niimi¹, Masanori Koshino^{1,2}, Eiichi Nakamura^{1,3}, Kazutomo Suenaga²

¹*Nakamura Functional Carbon Cluster Project, ERATO, JST, 4-1-8 Honcho Kawaguchi, Saitama, 332-0012 Japan*

²*Nanotube Research Center, National Institute of Advanced Industrial Science and Technology (AIST), Tsukuba, 305-8565, JAPAN*

³*Department of Chemistry, The University of Tokyo, Hongo, Bunkyo-ku, Tokyo 113-0033, Japan*

The observation of "a small molecule" has been spread recently with the development of high-resolution transmission electron microscopy (HR-TEM). The specimen supporting materials for single molecular imaging must be thin and inert enough so carbon nanotubes (CNTs) and carbon nanohorns (CNHs) are good candidates. The CNTs and CNHs intrinsically contain unwanted materials such as small carbon-based molecules, fullerenes, carbon onions, metal catalysts, leading to the misinterpretations of HR-TEM imaging. We hereby show several important notices in the sample preparations in order to achieve reliable characterizations.

First of all, it is important to utilize carbon materials (CNTs and CNHs) with high purity and high cleanliness as a primary product. Washing treatment is efficient only when the primary products are clean enough. Secondly, washing treatment can remove small particles to some degrees. Carbon-based contaminants with small molecular weights can be removed by washing with a certain solvent. We need not put too much attention to the metal particles when focusing on the observations of small organic molecules. Selections of the solvent as well as heating treatment are very important when a carbon-coated TEM grid is used. Thirdly, identification by a molecular "tag" works quite well. It is possible to distinguish the target molecule from the impurities by putting, for instances, a fullerene tag [1-5] or a carborane tag [6] and by analyzing elemental component or characteristic contrast. Finally, the experimental conditions such as temperature, pressure, and selection of gases or solvents require a certain skill when introducing a target organic molecule to supporting carbon materials of CNTs or CNHs.

It is thus indispensable to notice that there are several intrinsic problems when using nano-carbon materials for HR-TEM imaging.

[1] Liu, et al., Phys Rev. Lett., 2006

[2] Liu, et al., Nature Nanotech, 2007

[3] N. Solin, et al., Chem. Lett 2007

[4] E. Nakamura, et al., J. Amer. Chem. Soc. 2008

[5] M. Koshino, et al., Nature Nanotech 2008

[6] M. Koshino, et al., Science, 2007

Corresponding Author: Yoshiko Niimi

TEL: +81-29-861-6850 FAX: +81-29-861-4806, E-mail:runa.brown-niimi@aist.go.jp

Magnetic Properties of Rare Earth Metal Graphite Intercalation Compounds

○Satoshi Heguri, Mototada Kobayashi

*Department of Material Science, Graduate School of Material Science
University of Hyogo, Ako, Hyogo 678-1297, Japan*

Graphite is known to show anisotropic physical properties due to its two dimensional structure. Graphite intercalation compounds (GICs) may also show anisotropic electronic and magnetic properties reflecting their stage structures. Magnetic metal GICs can be good model for low dimensional magnets.

There have been many reports on transition metal chloride GICs [1, 2]. In those chloride-GICs, however, the magnetic properties are not so simple because the magnetic ions are surrounded by chlorine ions. The first stage Eu-GIC EuC_6 accommodates only magnetic elements, while it showed the peculiar magnetic behavior [3]. The magnetic properties of the higher stage Eu-GIC have not been reported.

In this study, we report magnetic properties of Sm- and Tm-GICs. We expect that those GICs show a variety of interesting magnetic characteristics reflecting the number of f-electrons of intercalants and their stage structures.

Sm- and Tm-GICs were synthesized from highly oriented pyrolytic graphite (grade ZYA), and excess Sm metal (99.9%) or Tm metal (99.9%). They were sealed into a quartz tube after evacuation. Thermal treatment was carried out in a furnace at 893~1023K for several weeks. After the reaction, the surface color of those compounds changed from that of graphite, and the sample thickness was found to be increased. Sm- and Tm-GICs show ferromagnetic characteristics at low temperature. Figure 1 shows the magnetic field dependence of magnetization of Sm-GIC at several temperatures. A large cohesive force of 27 kOe was detected at 45 K under applied field perpendicular to the *ab* plane. This value is equivalent to that of a permanent magnet SmCo_5 .

Details will be discussed together with the results of the magnetic field dependence of magnetization of Tm-GIC at the meeting.

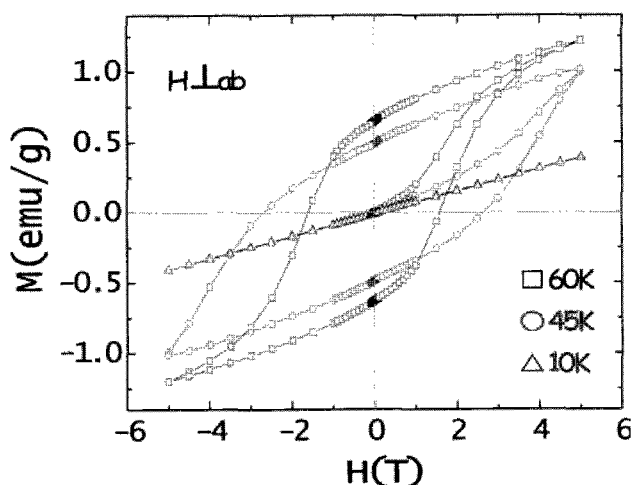


Fig.1. Magnetic field dependence of magnetization of Sm-GIC at several temperatures.

- References:** [1] K. Ohhashi and I. Tsujikawa, *J. Phys. Soc. Jpn.* 37 (1974) 63.
[2] H. Suematsu et al., *J. Phys. Soc. Jpn.* 52 (1983) 3874.
[3] H. Suematsu et al., *Synthetic Metals* 8 (1983) 23.

Corresponding Author: Satoshi Heguri

E-mail: rk07d004@stkt.u-hyogo.ac.jp

Tel&Fax: +81-791-58-0156/+81-791-58-0131

Comparison of combustion between catalyst-supported carbon nanocoil and graphitized carbon nanocoil

○T. Kawabata¹, K. Takimoto¹, M. Yokota¹, T. Ikeda¹, Y. Suda¹, H. Takikawa¹,
S. Oke², H. Ue³, Y. Umeda⁴, K. Shimizu⁵

¹ *Department of Electrical and Electronic Engineering, Toyohashi University of Technology*

² *Electronics and Control Engineering, Tsuyama National College of Technology*

³ *Fuji Research Laboratory, Tokai Carbon Co., Ltd.*

⁴ *Fundamental Research Department, Toho Gas Co., Ltd.*

⁵ *Development Department, Shonan Plastic Mfg. Co., Ltd.*

In direct methanol fuel cell (DMFC), there is a problem that flow of fuel and air is disturbed and the catalyst efficiency may be decreased when catalyst-support materials are closely packed. When carbon nanocoil (CNC) is used as a catalyst-support material, the flow is expected to be smooth because CNC has a helical and hollow structure. We could support PtRu and Pt catalysts as nanosized particles on CNC in the last report [1]. In this study, we tried to use graphitized CNC (GCNC) as a catalyst support material. We made a comparison between catalyst-supported GCNC and CNC by thermogravimetric analysis (TGA). GCNC was formed as follows. CNC was treated in a 30 wt.% H₂O₂ solution and heated in an argon atmosphere at 2,400°C. PtRu or Pt catalyst was supported on these two kinds of CNCs [1]. Fig. 1 shows the result of TGA. The weight decrease of catalyst-supported GCNC occurs at higher temperature than that of catalyst-supported CNC. It is thought that GCNC includes a lot of graphite structure so that the resistance for the oxidation reaction is high.

This work has been partly supported by the Outstanding Research Project of the Research Center for Future Technology, Toyohashi University of Technology (TUT); the Research Project of the Venture Business Laboratory (TUT); Global COE Program "Frontiers of Intelligent Sensing" from the Ministry of Education, Culture, Sports, Science and Technology (MEXT); CASIO Science Promotion Foundation.

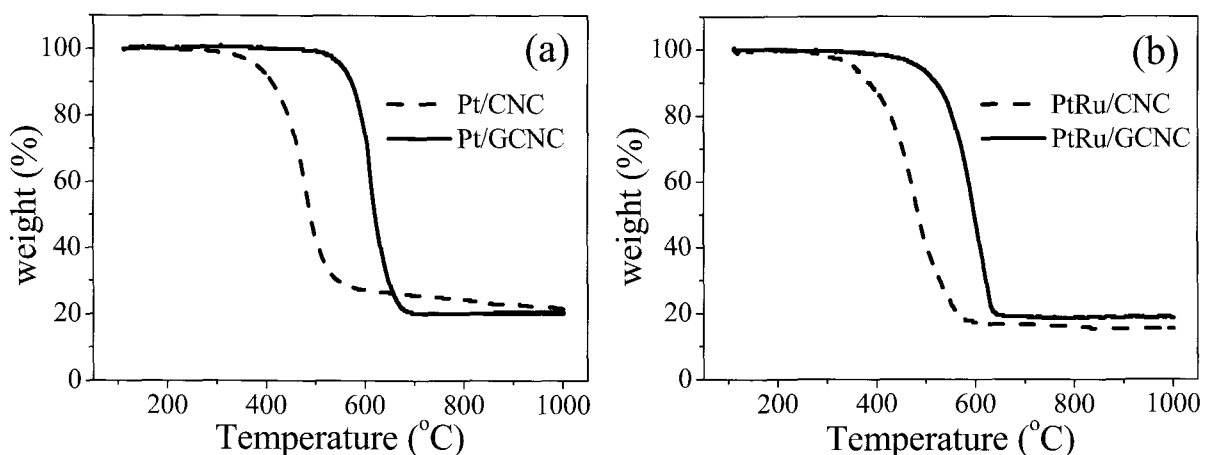


Fig. 1. TGA of catalyst-supported CNC and GCNC. (a) Pt supported and (b) PtRu supported

[1] T. Kawabata, et al., The 37th Fullerene-Nanotubes general Symposium, 2009

Corresponding Author: Yoshiyuki Suda

E-mail: suda@eee.tut.ac.jp, Tel: +81-532-44-6726

Development of optical responsive carbon nanotubes cell cultured substrate

○Takao Sada¹, Tsuyohiko Fujigaya¹, Naotoshi Nakashima^{1,2}

¹*Department of Applied Chemistry, Graduate School of Engineering, Kyushu University,
744 Motoooka, Fukuoka 819-0395, Japan*

²*JST-CREST, 5 Sanbancho, Chiyoda-ku, Tokyo, 102-0075, Japan*

Single-walled carbon nanotubes (SWNTs) are nanomaterials that possess remarkable electrical, mechanical, and thermal properties and have been explored for biological applications [1]. One of the applications of SWNTs in biology is the cell culture substrate, where the unique one-dimensional high aspect structure and hydrophobic nature of SWNTs gave better substrate to culture the cells [2]. In this report, we describe the novel concept of photo active SWNTs dish for selective cell collection.

SWNT-coated cell culture substrate was fabricated using the spray coating method. Fig. 1 shows atomic force microscope (AFM) image of the coated substrate and SWNTs network structure was clearly observed. Fig. 2 displayed the optical microscope image of the HeLa cells cultured for 3 days on the SWNTs-coated dish. Compared to the HeLa cells cultured on the non-coated dish, SWNT-coated dish lead the similar cellular proliferation rate for HeLa cell culturing. We observed selective removal of HeLa cells by the near-infrared (NIR) irradiation of the substrate. Cell viability after NIR irradiation was estimated by the MTT assay. It suggested that the HeLa cells removed after NIR irradiation are still viable and this selective removal method have no influence on the proliferation rate of the cells.

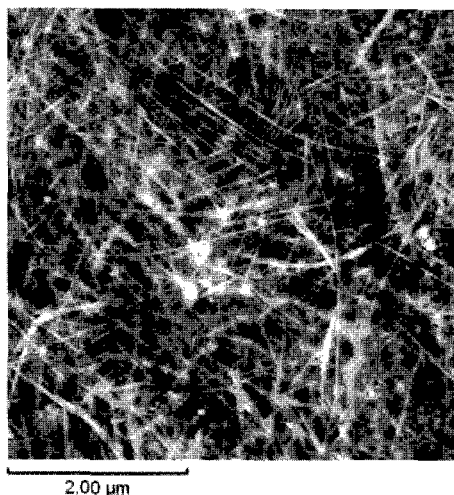


Fig. 1 AFM image of SWNT-coated cell culture substrate.

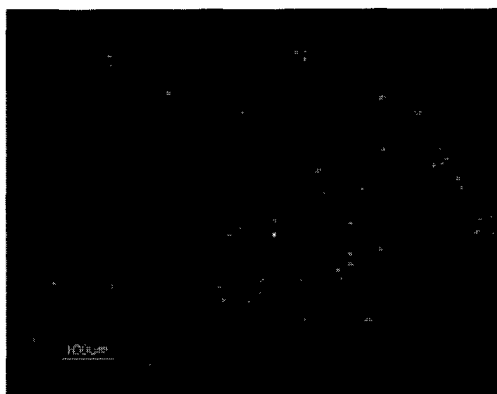


Fig. 2 Light microscopic image of HeLa cells on SWNT-coated cell culture substrate after NIR irradiation.

[1] Z. Liu, S. Tabakman, K. Welsher, and H. Dai, *Nano Res.* **2009**, 2, 85.

[2] N. Aoki, T. Akasaka, F. Watari and A. Yokoyama, *Dent. Mater. J.* **2007**, 26, 178.

Corresponding Author: Naotoshi Nakashima

E-mail: nakashima-tcm@mail.cstm.kyushu-u.ac.jp

Tel&Fax: +81-92-802-2840

Synthesis of Polyynes Molecules from n-Hexane and n-Decane by Irradiation of Intense Femtosecond Laser Pulses

Yuki Sato¹, Takeshi Kodama¹, Haruo Shiromaru¹, Joseph H. Sanderson², Tatsuya Fujino¹, Yoriko Wada³, Tomonari Wakabayashi³, Yohji Achiba¹

¹Department of Chemistry, Tokyo Metropolitan University, Hachioji, 192-0397, Japan

²Department of Physics and Astronomy, University of Waterloo, Waterloo, N2L 3G1, Canada

³Department of Chemistry, Kinki University, Higashi-Osaka, 577-8502, Japan

Polyynes are linear carbon chains with an even number of carbon atoms alternating triple and single sp-hybridized C-C bonds and typically terminated by hydrogen atoms. Nanosecond laser interaction with suspended carbon particles (from graphite to fullerenes and nano-diamond) in organic solvents has become a widely employed method for synthesis of polyynes[1]. Although the formation mechanism is still not well understood, it is assumed that the evaporation of the particulate carbon plays a key role.

Recently, a new method of producing polyynes molecules has been demonstrated in which femtosecond laser radiation directly initiates synthesis from a liquid containing organic molecules without the need for the introduction of any carbon particles [2]. The formation of C_6H_2 was confirmed by surface enhanced Raman spectroscopy, but the signals of longer chains are hidden by the signals of various species. In the present study, n-hexane and n-decane were irradiated by an intense femtosecond laser and analyzed in detail to confirm that polyynes with various chain lengths are formed.

The laser used for the experiment was a Ti:Sapphire ($\lambda = 800$ nm) with a regenerative amplifier, which provided at maximum about 0.9 mJ/pulse with a duration of about 100 fs and 1 kHz repetition rate. Pure n-hexane liquid was mainly employed as the irradiation target, and to examine the effect of carbon chain length, n-decane was also used.

In order to detect minor components of the irradiated samples, we employed high performance liquid chromatography (HPLC) to distinguish the signal from the different fractions. The chromatogram is shown in the inset in fig. 1, in which small peaks appear at the known retention times of polyynes. The absorption spectra of fractions, F1-F5, are shown in the main panel in fig. 1. Fractions F2, F3 and F5 clearly show a signal of polyynes C_6H_2 to $C_{12}H_2$. [3]

[1] Tsuji M, et al. *Chem. Phys. Lett.* **355**, 101 (2002).

[2] Hu A, et al. *Carbon* **46**, 1823 (2008).

[3] Sato Y, et al. *Carbon* in press.

Corresponding Author: Haruo Shiromaru

E-mail: shiromaru-haruo@tmu.ac.jp

Tel:+81-42-677-2533, Fax:+81-42-677-2525

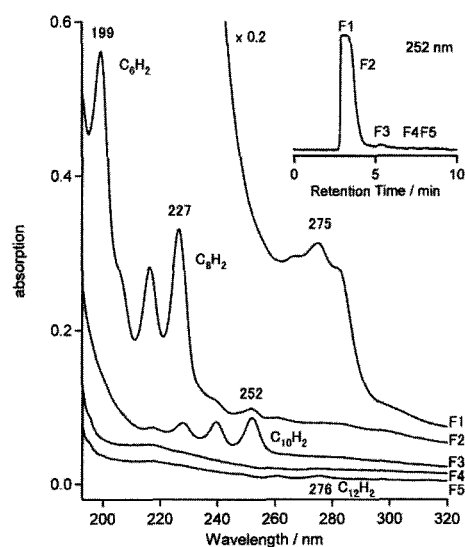


Fig 1. Absorption spectrum of each the fraction, F1-F5, indicated in the inserted preparative HPLC chart of the sample irradiated 3 hours with the power 0.90 mJ/ pulse.

Optical Detection of N@C₆₀ upon Recycling HPLC

○Airi Yoshikawa and Tomonari Wakabayashi*

Department of Chemistry, Kinki University, Higashi-Osaka 577-8502, Japan

Atomic nitrogen can be accommodated into a fullerene cage forming N@C₆₀ [1]. The endohedral nitrogen is detected by its electron spin, $S=3/2$, by electron spin resonance (ESR) or electron-nuclear double resonance (ENDOR) spectroscopy. Due to the narrowness of the spectral lines, N@C₆₀ is detectable in high sensitivity. This is an advantage for the study of the molecule but is also a limit for pursuing diverse properties other than magnetism. Optical detection of N@C₆₀ [2] will open a way for laser spectroscopy and accelerate related experiments concerning, e.g., manipulation of the molecular spins [3].

So far, we have developed experimental procedures for production and concentration of N@C₆₀ by ion bombardment and by recycling operation in high performance liquid chromatography (HPLC). The number of molecules available now in our laboratory is on the order of 10^{14} . Successful removal of C₆₀ from the mixture of N@C₆₀/C₆₀ enabled us to detect the target molecule, N@C₆₀, by its UV absorption upon recycling HPLC. Figure 1 shows the chromatogram for the first step. Using a three-fold tandem column on HPLC, the solution of N@C₆₀/C₆₀ mixture was subjected for separation by 12-times recycling, then collected into fractions. Figure 1 (right) compares chromatograms for the last cycle by UV absorption (solid line) and by ESR (squares). For further purification of N@C₆₀, the same procedure was repeated four times collecting only the fractions containing N@C₆₀. Figure 2 shows chromatogram showing the detection of N@C₆₀ by UV absorption. The number of N@C₆₀ molecules estimated is consistent with that from the ESR measurement.

[1] T. Almeida-Murphy *et al.* PRL 77, 1075 (1996). [2] P. Jakes *et al.* PCCP 5, 4080 (2003). [3] T. Wakabayashi, "Fullerene C₆₀: A Possible Molecular Quantum Computer", in *Molecular Realizations of Quantum Computing 2007*, p.p. 163-192 (2009).

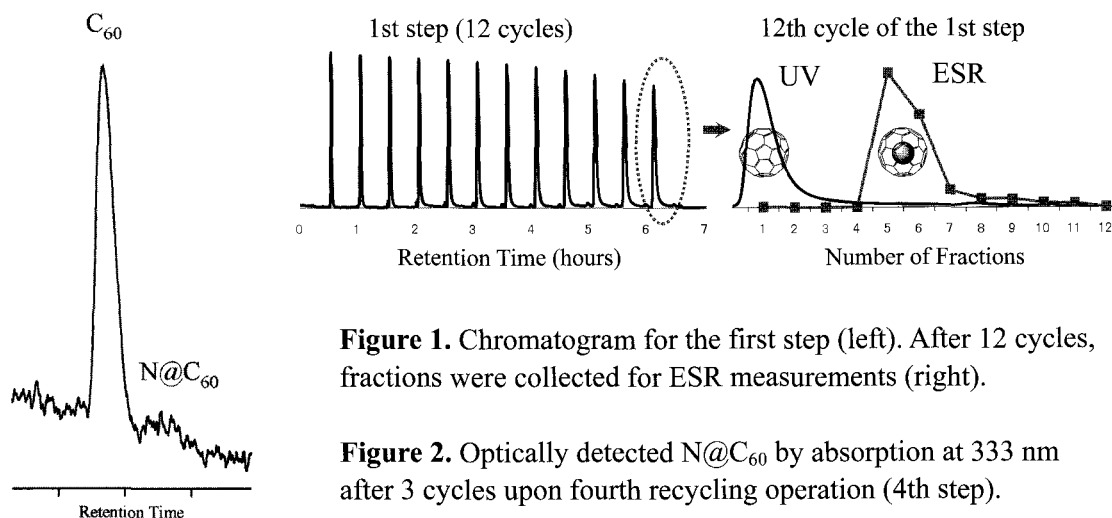


Figure 1. Chromatogram for the first step (left). After 12 cycles, fractions were collected for ESR measurements (right).

Figure 2. Optically detected N@C₆₀ by absorption at 333 nm after 3 cycles upon fourth recycling operation (4th step).

Corresponding Author: Tomonari Wakabayashi

E-mail: wakaba@chem.kindai.ac.jp

Tel. 06-6730-5880 (ex. 4101) / FAX 06-6723-2721

Isotope Scrambling in the Formation of Cyanopolyynes

○Mao Saikawa and Tomonari Wakabayashi*

Department of Chemistry, Kinki University, Higashi-Osaka 577-8502, Japan

Cyanopolyynes are linear molecules consisting of a sp-hybridized carbon chain that is bonded with a hydrogen atom at one end and a cyano group at the other, $\text{H}(\text{C}\equiv\text{C})_n\text{C}\equiv\text{N}$. We have prepared the series of molecules, $n=3-6$, by laser ablation of carbon particles in acetonitrile and separated them according to the size n . The NMR spectra for HC_7N clearly showed a single peak for ^1H and seven peaks for ^{13}C nuclei. The spin-spin coupling constants, J_{CH} and J_{CC} , were measured for the studies on connectivity of the isotopes within a molecule.

In this work, we took the advantage of ^{13}C -enriched powders not only for increasing the intensity of the NMR signals but also for detailed analysis on the abundance ratio for *isotopomers* present in the solution of HC_7N . Figure 1 shows ^1H -NMR spectra for HC_7N . When the molecule is produced from highly enriched ^{13}C powder (e.g. $\sim 96\%$) and acetonitrile of natural abundance, the proton signal splits into a few to several lines according to the isotopic sequence for adjacent three to four carbon nuclei. From the spectral analysis, the abundance ratio for possible *isotopomers* can be deduced. We discuss on the mixing of isotopes within a carbon chain of cyanopolyynes upon laser ablation.

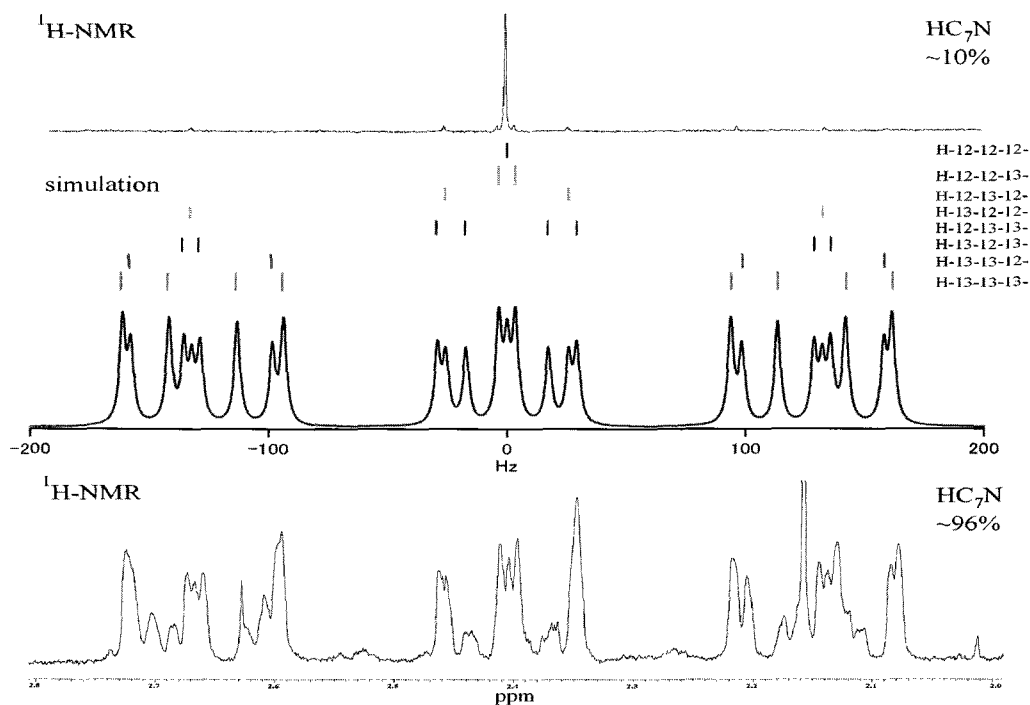


Figure 1. ^1H -NMR spectra for HC_7N produced from ^{13}C -enriched carbon powder, $\sim 10\%$ (top) and $\sim 96\%$ (bottom). The rich structure in the bottom spectrum is due to superposition of spectra for many *isotopomers*. A simulated spectrum for eight *isotopomers* at $^{13}\text{C} \sim 70\%$ is also shown (middle).

Corresponding Author: Tomonari Wakabayashi

E-mail: wakaba@chem.kindai.ac.jp

Tel. 06-6730-5880 (ex. 4101) / FAX 06-6723-2721

A Model Structure for the Polyene-Iodine Complex $C_{10}H_2-I_6$

○Yoriko Wada¹, Yasunori Kai², Tatsuhisa Kato², Tomonari Wakabayashi¹

¹Department of Chemistry, Kinki University, Higashi-Osaka 577-8502, Japan

²Department of Chemistry, Josai University, Sakado, Saitama 350-0295, Japan

Polyynes, $H(C\equiv C)_nH$ ($n\geq 2$), are sp -hybridized carbon chain molecules with two hydrogen atoms at both ends. These molecules exhibit absorption bands for an allowed transition in the UV and those for a forbidden transition in the near UV. So far, we have reported that the former disappear and the latter increase in intensity upon addition of iodine molecules into solutions of polyene molecules. Further investigations clarified that the spectral change was induced by irradiation of visible light. These results indicated that polyene and iodine molecules formed a relatively stable, stoichiometric complex in solutions.

In this work, we performed 1H - and ^{13}C -NMR spectroscopy for $C_{10}H_2/I_2$ and $C_{12}H_2/I_2$ systems, in order to get insight into molecular structures for the polyene-iodine complex. For this purpose, polyynes are prepared in size-selective manner and contacted with I_2 molecules in 1,1,2,2-tetrachloroethane- d_2 . Figure 1 shows ^{13}C -NMR spectrum for $C_{10}H_2/I_2$. Representing the molecular symmetry, five peaks are clearly seen. Table 1 compares the ^{13}C -chemical shifts for $C_{10}H_2/I_2$ and $C_{10}H_2$. All the 5 peaks for $C_{10}H_2/I_2$ appear in lower fields compared to the corresponding peaks for $C_{10}H_2$. This indicates that the complex has a unique structure retaining C_2 symmetry. We propose a model structure for the polyene-iodine complex, taking all the experimental facts into considerations.

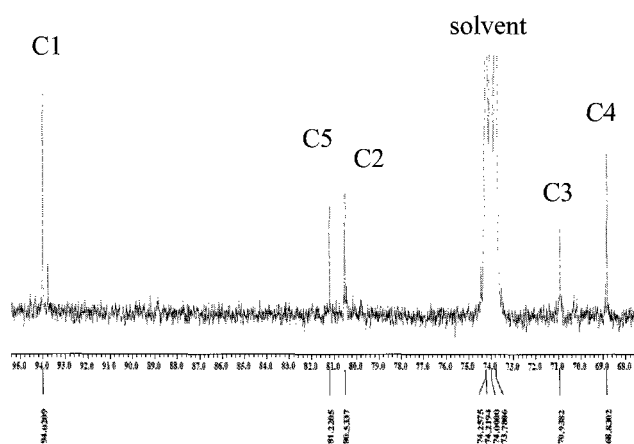


Figure 1. ^{13}C -NMR spectrum for $C_{10}H_2/I_2$.

Table 1. Comparison in ^{13}C chemical shifts for $C_{10}H_2/I_2$ and $C_{10}H_2$ systems.

	$C_{10}H_2/I_2$ δ (ppm)	$C_{10}H_2$ δ (ppm)	Difference $\Delta\delta$ (ppm)
C1	94.02	68.06	+25.96
C2	80.53	68.22	+12.31
C3	70.94	61.71	+9.22
C4	68.83	61.57	+7.26
C5	81.22	60.84	+20.38

Corresponding Author: Tomonari Wakabayashi

E-mail: wakaba@chem.kindai.ac.jp

Tel. 06-6730-5880 (ex. 4101) / FAX 06-6723-2721

Assembling Molecular Polyynes in Single-Wall Carbon Nanotubes

○Masashi Teshiba, Arisa Yoshimoto, Tomonari Wakabayashi*

Department of Chemistry, Kinki University, Higashi-Osaka 577-8502, Japan

Closely packed, well-aligned assemblies of polyyne molecules inside SWNTs can be promising precursory nanostructures for controlled growth of single atomic chains composed of sp-hybridized carbon atoms. In these systems, uniformity in packing density is crucial for the chain reaction to elongate carbon chains inside SWNTs. So far, we have improved the trapping efficiency for polyynes into SWNTs by taking advantage of laser ablated SWNT samples with controlled diameter distributions [1]. In this work, we employed oxidation of SWNTs prior to encapsulation of polyyne C₁₀H₂. In addition, other polyynes than C₁₀H₂ are examined to be accommodated into SWNTs.

Figure 1 shows Raman spectra for C₁₀H₂@SWNT. The signal at 2064 cm⁻¹, namely P band, is associated with the excitation of polyyne CC stretching vibration for C₁₀H₂ inside SWNT. The relative intensity for this signal was increased by several times compared to that in the previous work. We consider that major factors for the improvement in packing density are 1) high purity in amorphous free condition, 2) less-bundled morphology, and 3) opened edge for the nanotubes. These factors are related to accessibility for polyyne molecules toward the surface of SWNTs. Oxidation by H₂O₂ worked well for realizing such a condition.
[1] T. Wakabayashi et al. Eur. Phys. J. D 52, 79-82 (2009).

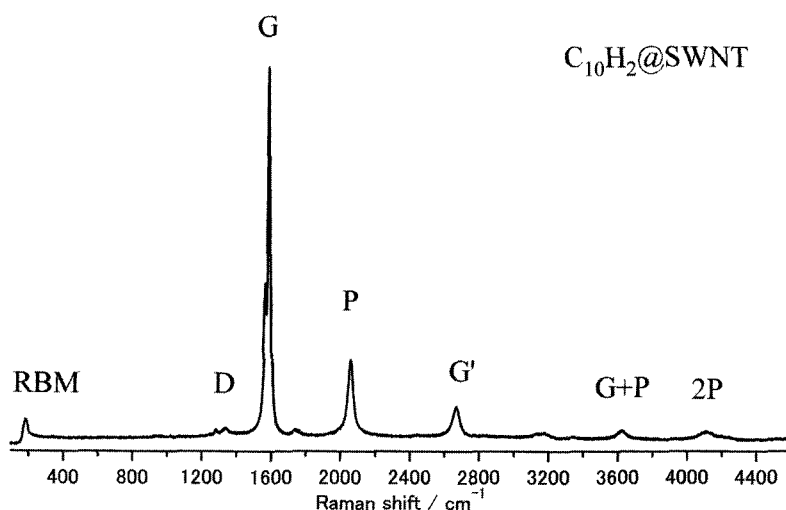


Figure 1. Raman spectra of C₁₀H₂@SWNT (excitation at 532 nm).

Corresponding Author: Tomonari Wakabayashi

E-mail: wakaba@chem.kindai.ac.jp

Tel. 06-6730-5880 (ex. 4101) / FAX 06-6723-2721

Detection and lifetime measurements of C_4H^- and C_6H^- metastables

Jun Matsumoto¹, Motoshi Goto¹, Yu Zama¹, Takuya Majima², Hajime Tanuma²,
Toshiyuki Azuma^{2,3}, ○Haruo Shiromaru¹, Yohji Achiba¹

¹Department of Chemistry, Tokyo Metropolitan University, Hachioji, 192-0397, Japan

²Department of Physics, Tokyo Metropolitan University, Hachioji, 192-0397, Japan

³AMO Physics Laboratory, RIKEN, Wako, Saitama 351-0198, Japan.

Identification of chain hydrocarbon anions C_nH^- ($n = 4, 6, 8$) in space has stimulated discussion about the mechanism of the anion formation in the circumstellar cloud, where only two-body collisions may occur [1]. For the reaction $C_nH + e^- \rightarrow C_nH^-$, survival probability of transient anions C_nH^* would be important. If the lifetime is in the order of milliseconds, reverse reaction (autodetachment) would be suppressed by radiative cooling and stable C_nH^- would be eventually formed. In the present study, we measured lifetime of metastables of the chain hydrocarbon anions, C_4H^- and C_6H^- , in the time range of milliseconds ~ seconds by using an electrostatic ion storage ring at Tokyo Metropolitan University (TMU E-ring) [2].

The anions extracted from a cesium sputter ion source at energy of 20 keV were stored in the ring. Then, neutral particles due to electron detachment during the anion storage were detected by micro-channel plates located at an extension of a straight section of the ring. The vacuum in the ring was kept at $2 \sim 5 \times 10^{-9}$ Pa under operation.

Figures 1 (a) and (b) show decay plots of the C_4H^- and C_6H^- anions, respectively. Rapid decays for the anions were observed in the time range below 50 ms due to electron detachment from metastable anions. Each decay curve can be fitted neither single exponential nor $1/t$ functions, but a multiple exponential function. The longer decays observed in the range of seconds, due to collision-induced electron detachment with residual gas in the ring, were not perceptible in the figures. The decay rate sharply depends on the carbon chain length; C_6H^- is faster.

From the lifetime measurements with different ring temperature, the decay signals are attributed to auto-detachment processes.

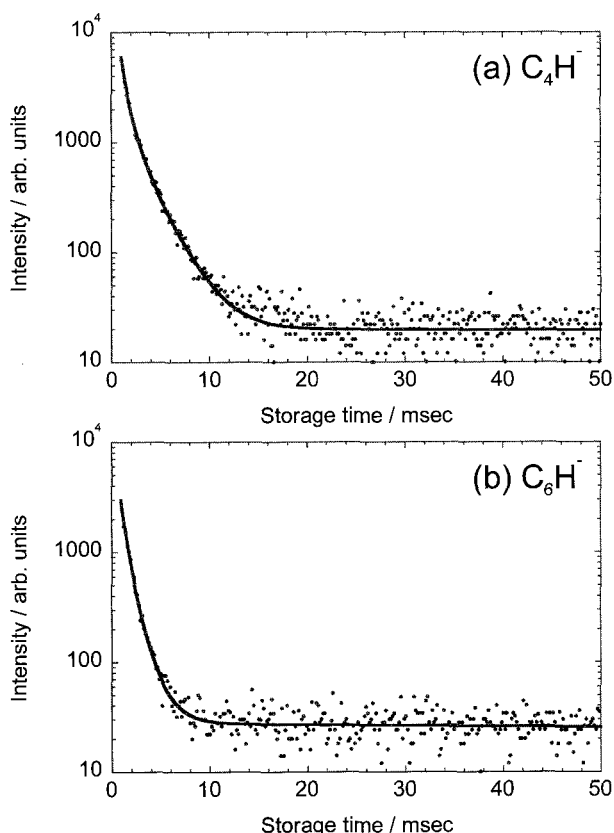


Fig 1. Decay plots of (a) C_4H^- and (b) C_6H^- anions stored in the ring. Each plot shows the data acquired at the first 50 ms. Solid line: the curve in each plot was fitted with multiple exponential components.

[1] McCarthy M C et al. *ApJ* **652**, L141 (2006).

[2] Jinno S et al. *NIM. A* **572** 568 (2007).

Corresponding Author: Haruo Shiromaru

E-mail: shiromaru-haruo@tmu.ac.jp

Tel:+81-42-677-2533, Fax:+81-42-677-2525

Magnetite-Loaded Carbon Nanohorns

Michiko Irie¹, Jin Miyawaki^{2,†}, Sumio Iijima^{1,2,3}, and ○Masako Yudasaka¹

¹ *Nanotube Research Center, National Institute of Advanced Science and Technology (AIST), Central 5, 1-1-1 Higashi, Tsukuba, 305-8565, Japan*

² *SORST, Japan Science and Technology Agency, Yaesu-Dori Building 6F, 3-4-15 Nihonbashi, Chuo-ku, Tokyo 103-0027, Japan Nano*

³ *Meijo University, 1-501 Shiogamaguchi, Tenpaku-ku, Nagoya, 468-8502, Japan*

[†] *Current address: Institute for Materials Chemistry and Engineering, Kyushu University*

We previously reported that magnetite-loaded single-walled carbon nanohorns (SWNHs) were useful for the biodistribution study with magnetic resonance imaging [1]. Other than the magnetic resonance imaging, the magnetite-loaded SWNHs are useful for leading the SWNHs to the desired sites in a living body with a magnetic field or for the hyperthermia therapy with high-frequency magnetic fields. For these various applications, in this report, we changed conditions to load the magnetite nanoparticles on SWNHs.

Magnetite nanoparticles were loaded on as-grown SWNHs (asSWNHs) and hole-opened SWNHs (oxSWNHs) by the procedure described in reference 1. In short, iron acetate was first deposited on the spherical aggregates of asSWNHs and oxSWNHs in ethanol and dried, then they were heat treated in Ar gas at 300-500°C for 1-5 hours. The magnetite quantities deposited on oxSWNHs were ~50% larger than those on asSWNHs, therefore we mainly used oxSWNHs in this study. The optimum HT temperature was 400°C. At the lower HT temperatures, the iron acetate did not fully change to the magnetite, and at the higher HT temperature, the oxSWNH structures were damaged and deformed. The optimum HT period was 2-3 hours. When the HT period was shorter, the yield of magnetite was low, and when the longer-period HT was applied, the oxSWNH aggregate structure was more or less destructed. To increase the amount of magnetite on the oxSWNHs, the increase of the starting quantity of iron acetate was not so effective, therefore we repeated the iron acetate deposition and heating processes which was found to be very effective. The magnetite-loaded oxSWNHs prepared by two times repetition of deposition/HT with the HT condition of 400°C and 2 hours kept the oxSWNH aggregate forms, and the obtained magnetite-loaded oxSWNH particles were dispersed well in water (DLS size distribution: about 120 nm). The magnetite content was about 27%. We also show an easy method to compare the magnetization of the magnetite-loaded oxSWNHs in the talk.

Reference: [1] J. Miyawaki, *et al*, *Adv. Mater.*, **18**, 1010-1014 (2006).

Corresponding Author: M. Yudasaka, TEL: 029-861-4818, E-mail: m-yudasaka@aist.go.jp

In Vivo Study of SWNHs with Different Sizes on Biodistribution

○M. Zhang¹, T. Yamaguchi², S. Iijima^{1,2}, M. Yudasaka¹
¹AIST, Tsukuba, ²Nagoya University

Our studies have shown that single-wall carbon nanohorns (SWNHs) are potentially useful in biomedicine, especially in drug delivery system (DDS), due to their unique structures and physicochemical properties. However, the study about biodistribution of SWNHs in vivo showed that SWNHs were easily trapped by the reticuloendothelial system, which made it difficult for the SWNH-DDS to reach the tumors through intravenous injections. Recently, we have successfully separated small-sized SWNHs from as-grown SWNHs aggregate ^[1] and found an appropriate dispersant of SWNHs: polyethylene glycol ceramide (PEG-c) ^[2]. Herein, we studied the effects of these small-sized SWNHs with PEG-c modification on biodistribution including blood circulation using mice.

SWNHs with two different sizes were used in this study. One is 70-100 nm SWNHs aggregates (y-SWNHs) and another is 30-50 nm SWNHs aggregates (s-SWNHs) that were obtained from CO₂ laser ablation and oxidation followed by sucrose gradient centrifugation ^[1]. For the study of biodistribution, the SWNHs were labeled with Gd-oxide ^[3]. SWNHs-Gd were dispersed in PEG-c solution with a concentration of about 1 mg/ml and intravenously administrated into mice (single dose: ~ 10 mg/kg). We estimated the quantities of SWNHs in each organ by measuring the quantity of Gd with inductively coupled plasma atomic emission spectroscopy (ICP-AES). The difference of biodistribution between two types of SWNHs aggregates was small. The blood circulation time of both s-SWNHs and y-SWNHs were 1-6 h. This is much longer than the previous report that used SWNHs with sizes of 100-120 nm and no PEG-c modification ^[3]. After 24 h since the administration, s-SWNHs and y-SWNHs were mainly localized in liver and spleen. Significantly, we found that there were about 4-7% s-SWNHs and 0.7-4% y-SWNHs existed in intestines of mice after 24 h since administration and trace amount of SWNHs in feces from one mouse. These results suggested that the SWNHs could be excreted from mouse.

References:

- [1] M. Zhang, T. Yamaguchi, S. Iijima, M. Yudasaka, *J. Phys. Chem. C* 113 (2009) 11184
- [2] J. Xu, S. Iijima, M. Yudasaka. The 37 th Fullerene-Nanotube General symposium (2009).
- [3] J. Miyawaki et al. *ACS Nano* 3 (2009) 1399.

Corresponding Author: M. Zhang, M. Yudasaka

E-mail: m-zhang@aist.go.jp; m-yudasaka@aist.go.jp

Tel&FAX: 029-861-6290

Biodistribution of Hole-Opened Carbon Nanohorns

Jin Miyawaki^{1,†}, Minfang Zhang², Sumio Iijima^{1,2,3}, and Masako Yudasaka²

¹ *SORST, Japan Science and Technology Agency, Yaesu-Dori Building 6F, 3-4-15 Nihonbashi, Chuo-ku, Tokyo 103-0027, Japan Nano*

² *Nanotube Research Center, National Institute of Advanced Science and Technology (AIST), Central 5, 1-1-1 Higashi, Tsukuba, 305-8565, Japan*

³ *Meijo University, 1-501 Shiogamaguchi, Tenpaku-ku, Nagoya, 468-8502, Japan*

[†] *Current address: Institute for Materials Chemistry and Engineering, Kyushu University*

To realize drug delivery applications of single-walled carbon nanohorns (SWNHs), the clarification of biodistribution of SWNHs is an essential issue. We have reported that the biodistribution hole-closed SWNHs were measurable by using Gd₂O₃ nanoparticles as labels embedded in the hole-closed SWNH aggregates [1]. In this report, we show the biodistribution of hole-opened SWNHs (oxSWNHs) and their functionalized species, which was clarified by careful histological observations.

The oxSWNHs were prepared by the “slow combustion”: Temperature was increased at a rate of 1°C/min in dry air flow to a target temperature of 550°C followed by natural cooling in dry air flow. We prepared the LAOx-SWNHs by light-assisted oxidation in hydrogen peroxide solution at about 70-80°C for 2 h. BSA-LAOx-SWNH was obtained by attaching bovine serum albumin (BSA) to LAOx-SWNH via the amide bonds. These specimens were intravenously injected to mice from tail veins (dosage: 6 mg/kg body weight).

Highly hydrophobic oxSWNHs mostly formed large agglomerate also in lungs of mice, refusing the uptake by the macrophages, and they were partly found to be removed from lungs at 26 weeks after the injection (26w). The removed portion could be excreted through trachea, because the increase of oxSWNH amount was not found in other organs. Contrary to the case of oxSWNHs, due to the hydrophilic properties, LAOx-SWNHs evenly distributed in lungs, liver, and spleen, where they were caught by macrophages. BSA-LAOx-SWNHs were highly hydrophilic, however, many of them were trapped by the macrophages in the lungs, which amount increased from 2w to 26 w. Intra-organ movements were clearly observed in the spleen for all three specimens: at 2w, they were largely found in the marginal zones, and 26w, they moved to the white pulps and red pulps most likely to be mediated by the macrophages.

In summary, we showed that the biodistribution and its temporal changes of hole-opened SWNHs were well clarified by the optical-microscope observation of the histological sections. And it became apparent that the biodistribution of hole-opened SWNHs greatly depended on the inherent functional groups as well as acquired chemical functionalizations.

Reference: [1] J. Miyawaki, *et al.*, *ACS Nano*, **3**, 1399-1406 (2009).

Corresponding Author: M. Yudasaka, TEL: 029-861-4818, E-mail: m-yudasaka@aist.go.jp

Water-free, rapid growth of millimeter-tall single-walled carbon nanotube

Kei Hasegawa and Suguru Noda

Dept. of Chemical System Engineering, The University of Tokyo, Tokyo 113-8656, Japan

Hata, Futaba, et al. realized rapid growth of millimeter-tall single-walled carbon nanotube (SWCNT) forests in 10 min by adding small amount of water to $C_2H_4/H_2/He$ during chemical vapor deposition (CVD) [1]. The effect of water is significantly large to keep the catalytic activity, however, how to feed water at a low level uniformly should become a key issue when this method is applied to large-scale reactors. By using our combinatorial method for catalyst optimization [2], we previously clarified the growth window of millimeter-tall SWCNT forests [3]. This time, we found a window for millimeter-tall SWCNT forests growing in several minutes by CVD using only C_2H_2/Ar without any water addition.

A gradient thickness profile of Fe was prepared on Al-Si-O layer on a substrate and CVD was carried out on it. The sample was set in a tubular CVD reactor, heated to and kept for 5 min at 1073 K in 5vol% H_2/Ar , and then CVD was carried out by switching the gas to 0.30vol% C_2H_2/Ar under ambient pressure. Samples were monitored in real-time by a digital camera [4].

Figure 1 shows a photograph of a SWCNT forest grown on combinatorial catalyst library. SWCNTs grew to 1.3 mm in 720 s by the 0.5-nm-thick Fe catalyst. The height of the SWCNT forest largely depended on the Fe thickness. We also studied the effect of water for SWCNT and found that water has a small effect on the CNT growth rate, but has a large effect on the growth lifetime for high C_2H_2 pressure (Fig. 2). SWCNT forests grew to millimeter in height without water addition only when the C_2H_2 partial pressure was sufficiently small.

The simple gas condition of this growth method makes the clear discussion on the growth mechanism possible. Effects of Fe catalyst thickness, C_2H_2 pressure and water addition on growth termination and structural change of SWCNTs during growth will be discussed in detail.

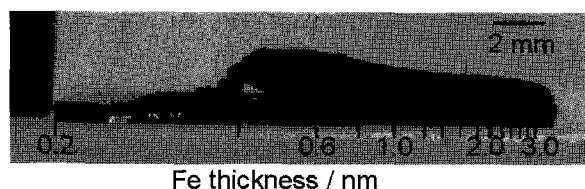


Fig. 1 Side-view photograph of a SWCNT forest grown on a combinatorial catalyst library.

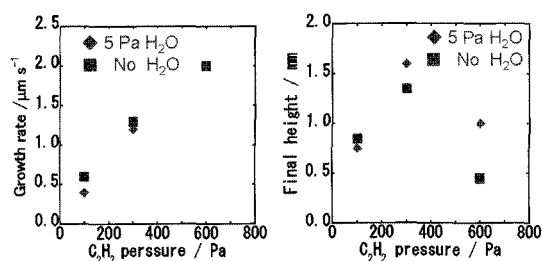


Fig. 2 Effects of C_2H_2 and water on growth rate (left) and final height of forest (right).

[1] K. Hata, et al., *Science* **306**, 1362 (2004). [2] S. Noda, et al., *Appl. Phys. Lett.* **86**, 173106 (2005). [3] K. Hasegawa, et al., *J. Nanosci. Nanotechnol.* **8** (2008), 6123. [4] K. Hasegawa, et al., *Nanotube2008*, contributed talks 23.

Corresponding Author: Suguru Noda

TEL: +81-3-5841-7330, FAX: +81-3-5841-7332, E-mail: noda@chemsys.t.u-tokyo.ac.jp

Crossover from weak localization to exponential localization in conduction of metallic and semiconducting single-wall carbon nanotube buckypaper

○H.Udoguchi¹, K.Yanagi¹, S.Sagitani¹, Y.Oshima², T.Takenobu³, H.Kataura^{4,5},
K.Matsuda¹, Y.Maniwa^{1,5}

1. Department of Physics, Tokyo Metropolitan University

2. RIKEN

3. Institute for Material Research, Tohoku University

4. Nanotechnology Research Institute, National Institute of Advanced Industrial Science and Technology (AIST)

5. JST-CREST

Understanding of electric conduction mechanisms in networks of single-wall carbon nanotubes (SWCNTs) is very important for their FET applications. A lot of studies for this subject have been performed,¹ however, most of the experiments so far were done using mixture of metallic and semiconducting types. In this research, to understand the mechanism more precisely, we tried to clarify how the content ratio of the metallic to the semiconducting types (MS content ratio) affects the electronic conduction properties. We prepared five sheets of SWCNT buckypaper with a series of different MS content ratio, and measured temperature dependence of resistance in a four-probe method and magnetoresistance (MR). In a high purity semiconducting SWCNT sample, as the temperature lowered, the resistance rapidly increased and became more than 10 M Ω . In contrast, the resistance of a high purity metallic sample did not vary so much. There was more than 10⁶ times difference between above two samples at 4K (see the fig.1 below). We analyzed each sample's temperature dependence of resistance by using variable range hopping (VRH) model and found the dimension of VRH varies with the MS content ratio (fig.2). But in the high-purity metallic sample negative MR and the $\ln T$ dependence were observed, suggesting that weak localization (WL) was a main cause for the resistance of the metallic sample. Crossover from weak localization to exponential localization (hopping conduction) was clearly observed by adjusting the MS content ratio in the sheets of SWCNTs. This study was partially supported by Industrial Technology Research Grant Program in 2007 from NEDO, and a Grant-in-Aid for Scientific Research on Innovative Areas (π -Space) from MEXT, Japan.

Reference: [1] as an example, Yoshida & Oguro J. Appl. Phys. 86 999 (1999),

Corresponding Author: K. Yanagi

E-mail: yanagi@phys.metro-u.ac.jp,

Tel & Fax: 042-677-2494 (& 2483)

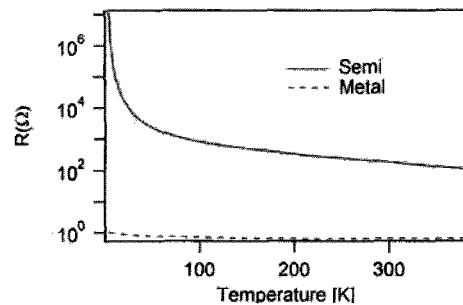


FIG 1: Resistance of the metallic and semiconducting SWCNT networks as a function of temperature

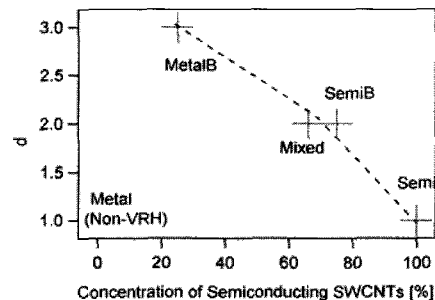


FIG 2: Relationship between the MS content ratio and the dimension of VRH

Uniform single-layer graphene synthesis using flash-cooling CVD

○ Keiichi Kamon, Yasumitsu Miyata, Ryo Kitaura and Hisanori Shinohara

Department of Chemistry, Nagoya University, Nagoya 464-8602, Japan

Graphenes have attracted much attention as important components of future electronic devices because of their high carrier mobility. To realize these potential applications, it is essential to synthesize the high-quality and large-area graphenes. Recently, it has been reported that the synthesis of large-area graphenes has been performed on a metal substrate by chemical vapor deposition (CVD). In a previous study, uniform single-layer graphenes have been produced only on copper (Cu) substrates [1]. On the other hand, such uniform graphenes have never been obtained on the other metal substrates such as nickel (Ni) due to the segregation of excess carbon from these metals during the cooling process.

Here, we report the synthesis of uniform single-layer graphenes on a Ni substrate by using, what we call, “flash cooling” after CVD growth. The CVD was carried out using ethanol as a carbon source under argon atmosphere at 900 °C. After the CVD, the Ni substrate was immediately removed from an electric furnace for the flash cooling of the substrate. The synthesized graphenes were found to be mainly single-layer and high-quality as revealed by Raman spectrum (Figure 1). These single-layer graphenes covered about 60% of the substrate. Interestingly, the graphenes have never been observed for the naturally-cooled substrates in the present CVD condition. This means that the synthesized graphenes were decomposed during the natural cooling and that the flash cooling does not lead to this decomposition. We, therefore, conclude that carbon absorption on the Ni surface consist mainly of the following two different processes: the carbon dissolution into the Ni and the direct formation of graphenes on the surface.

The present results show a promising uniform graphene synthesis on various metal substrates and could provide a more facile synthesis method.

References: [1] X. Li et al., *Science* **324**, 1312 (2009)

Corresponding Author: Hisanori Shinohara

E-mail: noris@.nagoya-u.jp, **Tel:** +81-52-789-2482

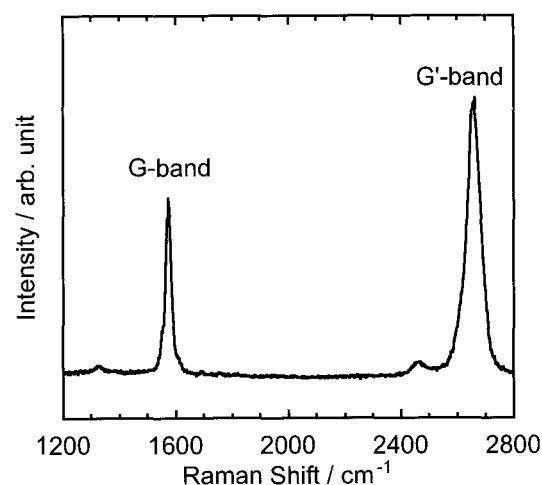


Figure 1: Raman spectrum of graphene synthesized on a nickel substrate by the flash-cooling CVD.

Thin film transistors using unbundled pure semiconducting single-wall carbon nanotubes

○Kazunari Shiozawa¹, Yuki Aasada¹, Yasumitsu Miyata¹,
Ryo Kitaura¹ Yutaka Ohno², Takashi Mizutani² and Hisanori Shinohara¹

¹ Department of Chemistry & Institute for Advanced Research,
Nagoya University, Nagoya 464-8602, Japan

²Department of Quantum Engineering, Nagoya University, Nagoya 464-8603, Japan

Single-wall carbon nanotubes (SWCNTs) are expected as a promising material for thin film transistors (TFTs) because of their high carrier mobility, flexibility, and solution processability. Although there have been many studies on the SWCNT TFTs, they have suffered from problems of the aggregation of individual nanotubes and/or the unavoidable co-existence of metallic and semiconducting SWCNTs in as-synthesized materials. To maximize the potentiality for such TFTs, it is still essential to develop sophisticated fabrication processes of the TFTs. Recently, Asada et al. have reported a fabrication method of the networks of purely isolated SWCNTs and that these networks show a high transistor performance even without the removal of metallic SWCNTs [1]. For further improvements, the use of highly-pure semiconducting SWCNTs is desirable.

In this study, we have fabricated the TFTs using the networks of pure semiconducting SWCNTs. The SWCNTs were purchased from Meijo Inc. (Meijo Arc SO type) and used as a starting material. Semiconducting SWCNTs were separated using gel chromatography [2,3]. The sample was finally dispersed in water with salmon DNA or surfactants. To fabricate TFTs, the sample solution was displayed on an amino-coated Si/SiO₂ substrate, followed by the deposition of Ti/Au electrodes. Figure 1 shows a typical I_D - V_{DS} characteristic of the TFT fabricated. The device has an on/off ratio of $\sim 10^6$ and a mobility of $\sim 1 \text{ cm}^2\text{V}^{-1}\text{s}^{-1}$. In this presentation, a detailed comparison of TFT characteristics between the pristine and the separated samples will be discussed.

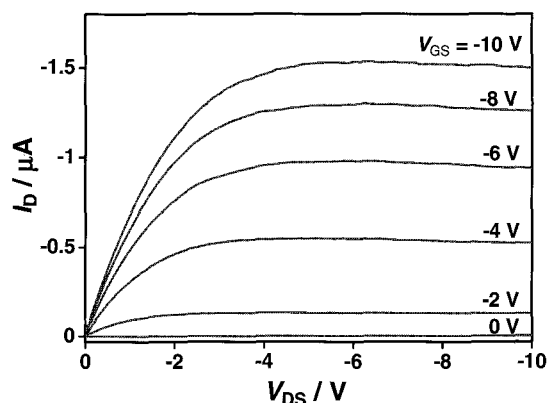


Figure 1. I_D - V_{DS} characteristics of semiconducting SWCNTs TFT at $V_{GS} = 0$ to -10 V. Channel length $L = 40 \mu\text{m}$ and width $W = 500 \mu\text{m}$.

[1] Y. Asada et al., 37th Fullerene-Nanotubes General Symposium abstract P.53, [2] K. Moshhammer et al., *Nano Res.*, **2**, 599 (2009) [3] T. Tanaka et al., *Appl. Phys. Express*, **2**, 125002 (2009)

Corresponding Author: Hisanori Shinohara

TEL: +81-52-789-2482, **FAX:** +81-52-747-6442, **E-mail:** noris@nagoya-u.jp

Exciton and free carrier electroluminescence from a SWNT observed through simultaneous measurements of electrical conductivity and emission spectra

○ Hiroyuki Wakahara^{1,2}, Hideyuki Maki¹, Tetsuya Sato¹ and Satoru Suzuki²

¹*Department of Applied Physics and Physico-Informatics, Faculty of Science and Technology
Keio University, Hiyoshi, Yokohama 223-8522, Japan*

²*NTT Basic Research Laboratories, Nippon Telegraph and Telephone Corporation,
Morinosato-Wakamiya, Atsugi 243-0198, Japan*

Single-walled carbon nanotubes (SWNTs) are expected to be applied to the materials for the small size light emitting devices because of its small diameter and optoelectronic properties. As the origin of electroluminescence (EL) from a SWNT, three different excitation mechanisms: an electron and hole injection[1], impact excitation[2], and thermal excitation[3] are reported. However, relationship between electrical conductivity and luminescence has not been clarified. In this study, we investigate the EL mechanism of a SWNT by simultaneous measurements of electrical conductivity and emission spectra.

We measured EL spectra from a single SWNT by applying bias and gate voltage. The EL spectra observed from the device is shown in Fig. 1. In this experiment, two peaks with the energy of 840meV and 1130meV are observed from a single SWNT, although only one luminescence peak is usually observed from a single SWNT. The results of the simultaneous measurements of the drain current and integrated luminescence intensity as a function of the back gate voltage indicate that the lower energy peak is due to the luminescence by impact excitation and the higher energy peak is due to the luminescence by electron and hole injection. The energy difference of the two peaks is ~ 290 meV, which is consistent with the exciton binding energy estimated by the theoretical calculation[4]. These indicate that the lower energy emission is due to the recombination of excitons excited by impact excitation and the higher one is due to the interband recombination excited by electron and hole injection (Fig. 2).

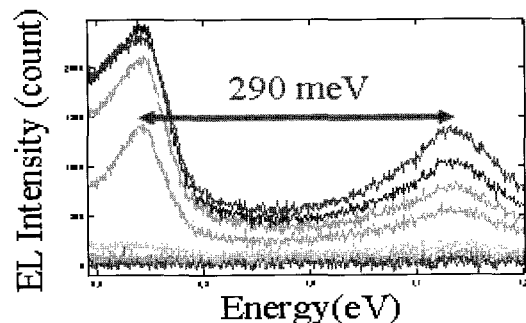


Fig.1 Emission spectra of the device at drain voltages of 4V-12 V.

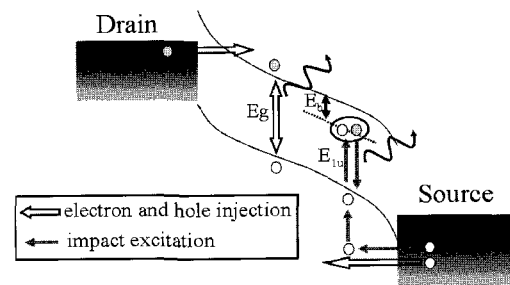


Fig. 2 model of the two emission

- [1]J.A.Misewich et al., Science, **300**, 785(2003), [2]J.Chen et al, Science,**310**,1171(2005),
[3]D.Mann et al, Naturetechnology, **2**, 33(2007), [4]G.Dukovic et al, Nano Lett, **5**, 2314(2005)
E-mail:maki@appi.keio.ac.jp TEL:045-566-1643

Instant Implementation of CNT field emitter arrays by pulse current heating

○Kotaro Sekiguchi¹, Koji Furuichi², Yosuke Shiratori¹, Hisashi Sugime¹, and Suguru Noda¹

¹Dept. of Chemical System Engineering, The University of Tokyo, Tokyo 113-8656, Japan

²DAINIPPON SCREEN MFG. CO., LTD., Kyoto 602-8585, Japan

Field electron emitter is one of the most promising applications of carbon nanotubes (CNTs). In order to implement emitters in micro-devices such as electron guns in field emission displays (FEDs), direct and selective growth of CNTs through chemical vapor deposition (CVD) routes is desired. However a main drawback is a high reaction temperature over a glass strain point (around 500 °C). According to Arrhenius' law, growth time exponentially increases with decreasing reaction temperature. Here one can note that the approach combining a high temperature and a short reaction time is also reasonable and worth investigating as a practical route. We have been studying growth mechanisms of millimeter tall vertically aligned single-walled CNTs (SWCNTs) [1]. Here the rate of CNT growth is several $\mu\text{m/s}$, indicating CNT emitters can be formed at a high temperature but only in 1 second or possibly in subsecond tolerable for conventional glass substrates.

We implanted CNTs on the line-patterned cathodes, which were heated by a well controlled pulsed current. The underlayer of the cathodes (Mo) patterned with 0.1-0.3 μm thickness, 1-3 μm width and 3-200 μm pitch, respectively, was formed on glass substrates through conventional photolithography and sputtering processes. An Al_2O_3 buffer layer (20 nm) and a Fe catalytic layer (0.1-3.0 nm thickness) were subsequently sputtered on the cathode lines. The substrates were set in a tubular quartz glass reactor, and a pulsed voltage was applied to the lines under a gas atmosphere of 0.5-1.0 % C_2H_2 / 0-26 % H_2 / Ar at ambient pressure. A variety of emitter morphologies prepared through the combinatorial masked deposition of a catalytic layer [2] and subsequent pulse current CVD revealed a variety of FE properties as shown in Fig. 1. A high current density of 5 mA/cm^2 was recorded at an applied electric field of 3 $\text{V}/\mu\text{m}$ for the sparsely grown SWCNTs.

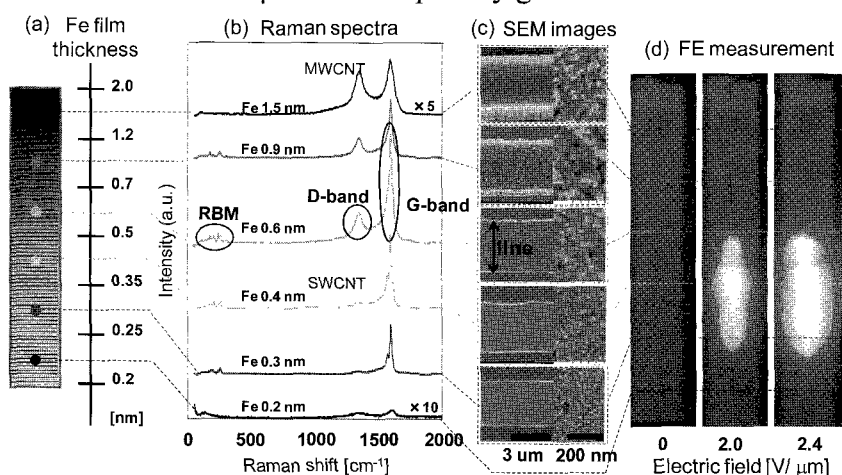


Fig. 1. (a) A distribution of the nominal Fe thickness on a line-patterned cathode, (b) Raman spectra and (c) SEM micrographs recorded at specific positions, and (d) photographs of cathode luminescence at applied electric fields of 0, 2.0, 2.4 $\text{V}/\mu\text{m}$.

[1] K. Hasegawa et al., *J Nanosci. Nanotechnol.* **8** (2008) 6123 [2] S. Noda et al., *Carbon* **44** (2006) 1414

Corresponding Author: Suguru Noda TEL/FAX: +81-3-5841-7330/7332, E-mail: noda@chemsys.t.u-tokyo.ac.jp

Biodegradation Assessment of Fullerene Nanowhiskers using Macrophage-like Cells

○Shin-ichi Nudejima¹, Kun'ichi Miyazawa¹,
Junko Okuda-Shimazaki² and Akiyoshi Taniguchi²

¹*Fullerene Engineering Group, Exploratory Nanotechnology Research Laboratory,
National Institute for Materials Science (NIMS), Tsukuba 305-0044, Japan*

²*Advanced Medical Material Group, Biomaterials Center, NIMS, Tsukuba 305-0044, Japan*

Fullerene nanowhiskers (FNWs) are composed of fullerene molecules that are usually bonded via van der Waals forces and are synthesized by the liquid-liquid interfacial precipitation method [1]. The FNWs are promising nanomaterials for various applications. But the biological impact of FNWs should be studied before the practical use of them because the nanosized needle-like structure resembling asbestos has been suspected to induce the asbestosis via inhalation [2].

Macrophages may be able to decompose FNWs into individual fullerene molecules as the primary immune response owing to their weak van der Waals bonding forces, and the fullerene molecules may exert the effect which is not similar to that of the needle-like structure but is similar to that of fullerene molecules on organisms. In our previous pilot study, we observed the macrophage-like cells exposed to the C₆₀ fullerene nanowhiskers (C₆₀NWs) with the average length of 6.0 μm and the average diameter of 660 nm by an inverted optical microscope for 48 h [3]. The macrophage-like cells were observed to internalize the C₆₀NWs gradually, but the exposed C₆₀NWs didn't affect the morphology of the cells.

In this study, to assess the biodegradability of C₆₀NWs, we observed the macrophage-like cells and the exposed C₆₀NWs by an inverted optical microscope for 28 days after the exposure of C₆₀NWs. And after the long-term co-culture of macrophage-like cells and C₆₀NWs, we observed the change of exposed C₆₀NWs by an optical microscope and a scanning electron microscope and got a result suggesting the decomposition of C₆₀NWs by the cells.

[1] K. Miyazawa, et al., *J. Mater. Res.*, **17**, 83 (2002).

[2] C. A. Poland, et al., *Nature Nanotechnol.*, **3**, 423 (2008).

[3] S. Nudejima, et al., *J. Physics: Conf. Series*, **159**, 012008 (2009).

Corresponding Author: Shin-ichi Nudejima

E-mail: NUDEJIMA.Shinichi@nims.go.jp

Tel: 029-851-3354 (EXT: 8463), Fax: 029-860-4667

Preparation of Metallophthalocyanine loaded Multi-walled Carbon Nanotubes for Fuel Cell Cathode

○Tsutomu Yao, Takeshi Hashishin, Jun Tamaki

Department of Applied Chemistry, Ritsumeikan University, Shiga 525-8577, Japan

One of the possibilities is the application of carbon nanotubes (CNTs) as a support of fuel cell catalysts because CNTs has high electrical conductor, high gas diffuseness, and high surface area. In addition, the structure of CNTs directly grown on the surface of carbon paper (CP) is improved an connection between CNTs and CP, and reduces ohmic losses at the interface of CNTs and CP. Metallophthalocyanine (MePc) with macrocyclic structure tends to spread widely on basal plate and to be an efficient catalyst [1].

In this study, multi-walled carbon nanotubes (MWNTs) were directly grown on CP by ethanol CVD using nickel as a catalyst. The MWNTs grown on CP (MWNTs/CP) treated by 0.5 M HNO₃ were immersed in MePc solution and vacuumed to 10 Torr. The loading states and cathode properties of MePc on MWNTs/CP were estimated by FE-SEM and cyclic voltammogram (CV), respectively.

Cobalt-phthalocyanine (CoPc) loaded on MWNTs/CP was shown in Fig.1 (a). However, It was difficult from the SEM image of Fig. 1 (a) to confirm the existence of CoPc on MWNTs. Cobalt oxide nanoparticles were deposited on discrete MWNTs by heating CoPc-MWNTs at 600 °C in argon, as shown in Fig. 1 (b), indicating the existence of CoPc on MWNTs in Fig. 1 (a). On the other hand, the existence of CoPc was also confirmed from CV of Fig. 2. The cathodic curve of MWNTs/CP was shifted to positive potential compared with that of CoPc-MWNTs/CP, suggesting electron transfer catalyzed by CoPc.

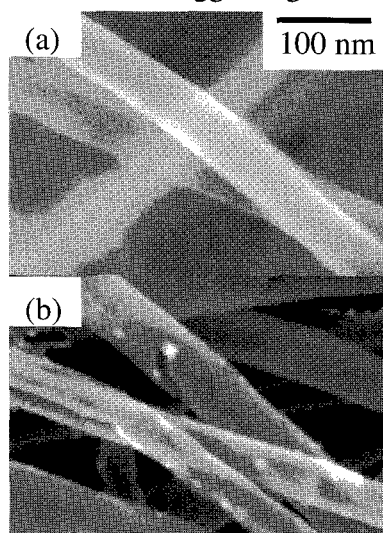


Fig. 1 SEM image of CoPc-MWNTs/CP.
(a) as-deposited CoPc-MWNTs,
(b) heat-treated CoPc-MWNTs.

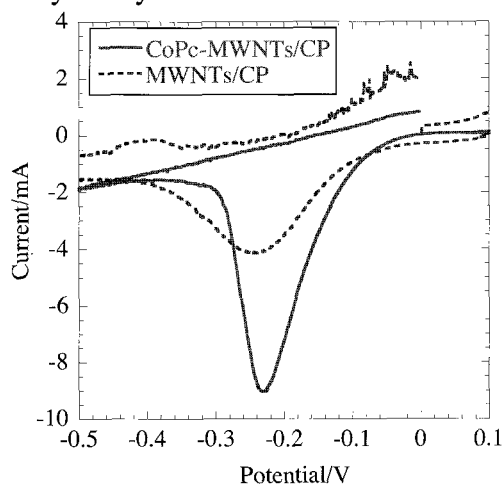


Fig. 2 Cyclic voltammogram of oxygen saturated alkaline solution.
(Solid line) CoPc-MWNTs/CP,
(dash line) MWNTs/CP.
Electrolyte: 4.7 M KOH, Scan rate: 10 mV/s.

[1] Z. Yang, H. Pu, J. Yuan, D. Wana, and Y. Liu, *Chem. Phys. Lett.*, **463** 73 (2008)

Corresponding Author: Jun Tamaki, Takeshi Hashishin

TEL: +81-77-566-1111, FAX: +81-77-566-2659, E-mail: juntrc@sk.ritsumeai.ac.jp, hasisin@sk.ritsumeai.ac.jp

Experimentally Determined Electronic States of Isolated (n,m) HiPco & CoMoCAT Single-Walled Carbon Nanotubes

○Yasuhiko Hirana¹, Yasuhiko Tanaka¹, Yasuro Niidome¹ and Naotoshi Nakashima^{1,2}

¹Department of Applied Chemistry, Graduate School of Engineering,
Kyushu University, Fukuoka 819-0395, Japan.

²CREST, Japan Science and Technology Agency, 5 Sanbancho, Chiyoda-ku,
Tokyo 102-0075, Japan

The redox properties (i.e. electronic densities, the Fermi levels, redox potentials) of single-walled carbon nanotubes (SWNTs) are related to the structures of SWNTs that have a specified diameter and chirality angle uniquely related to a pair of integers (n,m); the so-called chiral indices. Electronic structure, one of the most fundamental features of SWNTs, strongly depend on their diameter and chirality. For many practical applications of nanotubes, redox behavior of nanotubes plays a central role. Here we report the in situ near-IR photoluminescence (PL) spectroelectrochemical method to determine the redox potentials of isolated SWNTs having their own chirality indices [1]. It was found that PL signals from the isolated SWNTs showed strong applied-potential dependence and that the potential dependence of PL intensity was exactly Nernst response. Using the Nernst equation analysis of the PL data, the precise redox potentials of HiPco and CoMoCAT SWNTs have been determined (Figure 1).

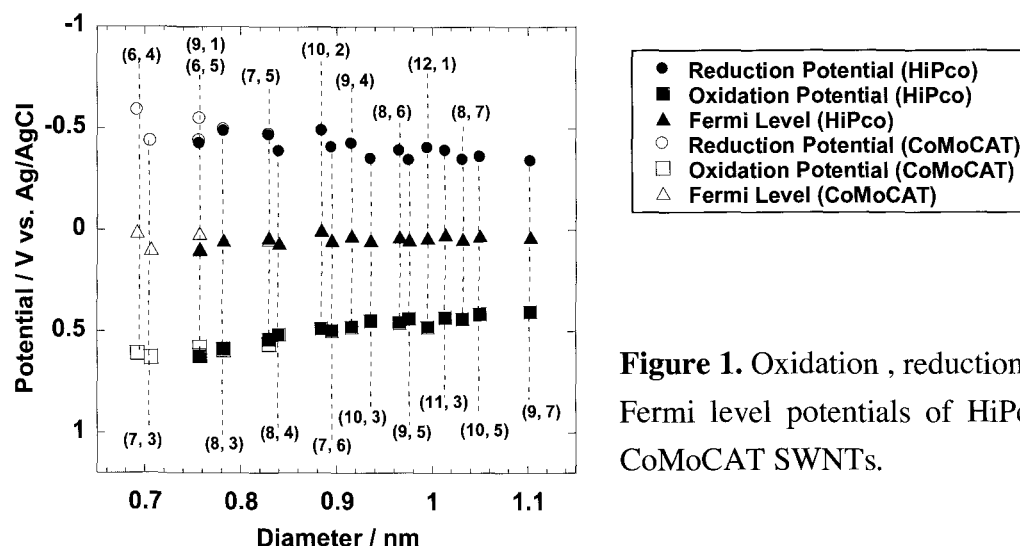


Figure 1. Oxidation, reduction, and Fermi level potentials of HiPco & CoMoCAT SWNTs.

References:

[1] Y. Tanaka, Y. Hirana, Y. Niidome, K. Kato, S. Saito, N. Nakashima, *Angew. Chem. Int. Ed.* **2009**, *48*, 7655.

Corresponding Author: Naotoshi Nakashima

E-mail: nakashima-tcm@mail.cstm.kyushu-u.ac.jp

Tel & Fax 092-802-2840

Synthesis and Electrical Transport Properties of C₆₉N Azafullerenes Encapsulated Single-Walled Carbon Nanotubes

○Y. F. Li, T. Kaneko, and R. Hatakeyama

Department of Electronic Engineering, Tohoku University, Sendai 980-8579, Japan

In this work, the synthesis of azafullerenes C₆₉N is realized by a nitrogen-plasma irradiation method, which is confirmed by a laser-deposition time-of-flight mass spectrometer as shown in Fig. 1(a). It is found that C₆₉N has a purity much higher than that of C₅₉N synthesized under the same experimental conditions, which is possibly ascribed to high reactivity of N atom with C₇₀, rather than with C₆₀. The work functions of C₆₉N and C₅₉N are investigated by measuring ultraviolet photoemission spectroscopy (UPS), and our results suggest that the work function of C₆₉N is about 0.2 eV smaller than that of C₅₉N.

The encapsulation of C₆₉N azafullerenes into single-walled carbon nanotubes (SWNTs) has been prepared by either a vapor reaction method or a plasma irradiation method, which is confirmed in detail by a transmission electron microscope (TEM, Hitachi HF-2000) operated at 200 kV and Raman spectroscopy (Seiki Technotoron) with laser excited at both 488 nm and 633 nm. Compared with *p*-type characteristics of C₇₀ fullerene encapsulated SWNTs our results indicate that air stable *n*-type semiconducting SWNTs can be formed by the C₆₉N fullerene encapsulation as seen in Fig. 1(b), where the source-drain current (I_{DS}) is measured as a function of gate voltage (V_G), demonstrating strong electron donor behavior of C₆₉N, similar to the case of C₅₉N [1].

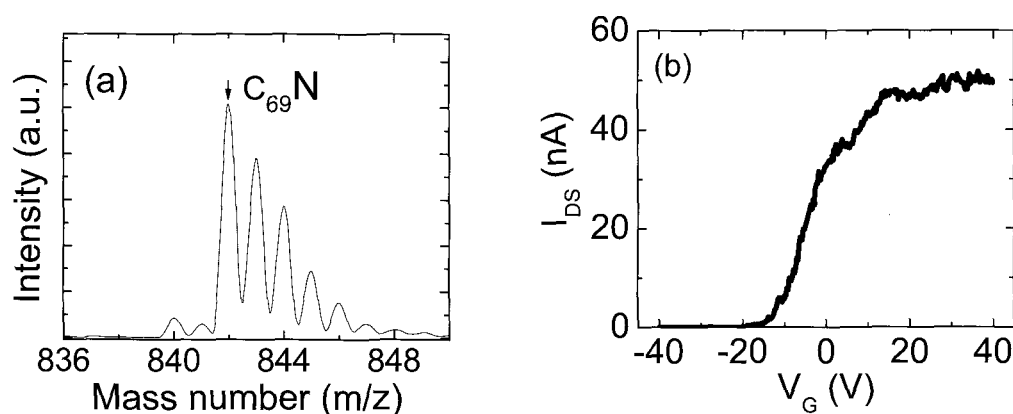


Fig.1: (a) Mass spectrum of C₆₉N azafullerenes. (b) *n*-type transport behavior of C₆₉N encapsulated SWNT

[1] T. Kaneko, Y.F. Li, S. Nishigaki, and R. Hatakeyama, *J. Am. Chem. Soc.* **130**, 2714 (2008).

Corresponding Author: Yongfeng Li

TEL: +81-22-795-7046, FAX: +81-22-263-9225, E-mail: yfli@plasma.ecei.tohoku.ac.jp

3P-2

HR-TEM of KCl nano-crystals in single-walled carbon nanotubes

○Kaori Takai Hirose, Zheng Liu, Takeshi Saito and Kazu Suenaga

Nanotube Research Center, National Institute of Advanced Industrial Science and Technology (AIST), Tsukuba, 305-8565, JAPAN

Filling carbon nanotubes with other materials has been a central topic for many researchers because it can be used to modify the physical and chemical properties of the host nanotubes as well as the guest materials. Three major methods to encapsulate the materials inside nanotubes have been so far reported, namely, the sublimation process, the molten phase encapsulation and the solution phase chemistry [1]. Using solvents is indeed a simple and efficient way to encapsulate various salts into nanotubes. We have chosen the KCl for the inner materials and attempted to optimize the filling yield.

The filling of KCl was evidenced by HR-TEM (fig. 1). The encapsulated KCl is not as long as the host nanotube and a lot of empty space, voids, are found. The diameter of KCl nano-crystals range from 1.7 – 2.3 nm corresponding to the host nanotube diameters (Fig. 2). The yield or the length of KCl nano-crystals inside nanotubes seems to be very much affected by the original solution concentration and the recrystallization rate. Local structure and chemical analysis by means of STEM is now being made.

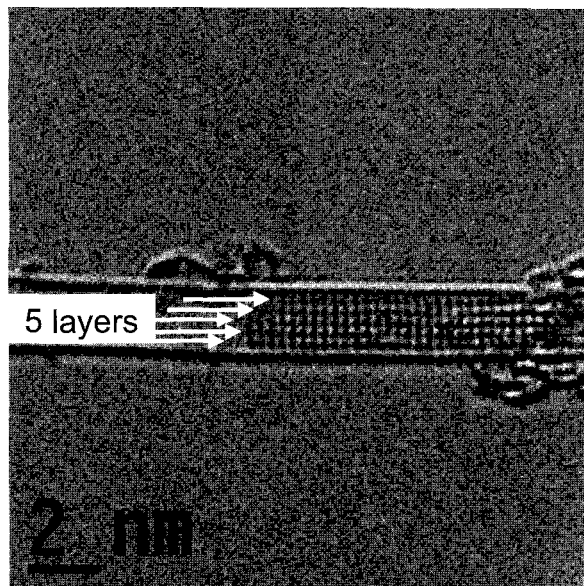


Fig. 1 HR-TEM image of KCl@SWNT (Here we denominate 5 layers of KCl are encapsulated in the SWNT shown in this figure).

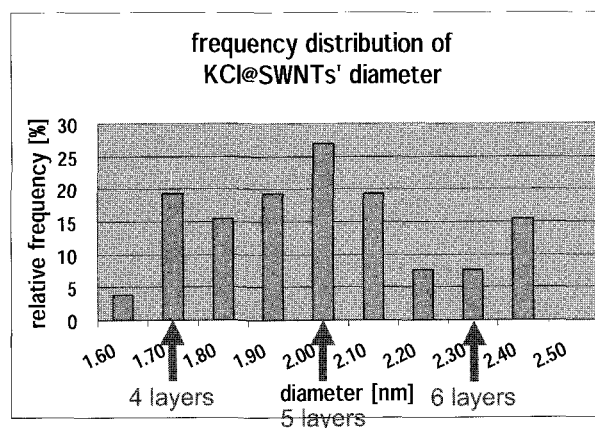


Fig. 2 The frequency distribution of KCl@SWNTs' diameter. And the corresponding diameters of SWNT encapsulated 4 to 6 layers of KCl were shown by arrows.

References: [1] M. Monthieux, *Carbon*, **40**, 1809-1823 (2002)

Corresponding Author: Kazu Suenaga

TEL: +81-29-861-6850, FAX: +81-29-861-4806, E-mail: suenaga-kazu@aist.go.jp

Magnetic properties of carbon nanotubes filled with ferromagnetic metal

○Yusuke Matsui, Daijiro Hisada, Tetsuya Kaneko, Yuki Ichikawa, Hideki Sato,
Yuji Fujiwara, Koichi Hata

*Graduate School of Engineering, Mie University,
1577 Kurima-machiya-cho, Tsu, Mie, 514-8507, Japan*

Carbon nanotubes (CNTs) filled with ferromagnetic metal show shape anisotropy owing to the high-aspect ratio of magnetic particles [1], and are promising candidates for magnetic recording media, radio-frequency devices, and biomedical applications. In this study, we have investigated magnetic properties of Fe(Co) filled CNTs synthesized by the microwave plasma enhanced CVD (MPECVD) and the thermal CVD (TCVD) method. The MPECVD process was carried out under the atmosphere of H_2 and CH_4 mixture gas. FeCo-filled CNTs were synthesized on Si substrates covered with 70 nm FeCo alloy. In the TCVD process using ferrocene as a source gas, Fe-filled CNTs were synthesized on SiO_x/Si substrates covered with 2 nm Fe layer under the conditions of $785^\circ C$, 1 atm. In the MPECVD, cone-shaped FeCo nanoparticles are found at the tip of CNTs [Fig. 1(a)]. The easy axis of magnetization was perpendicular to the substrate. The coercivity in perpendicular to the substrate was 1.2 kOe [Fig.2(a)]. The dependence of coercivity on Fe/Co ratio was confirmed, indicating that control of magnetic property is possible. On the other hand, the TCVD gives vertically oriented CNTs almost entirely filled with Fe [Fig. 1(b)]. The coercivity in perpendicular to the substrate was 1.1 kOe [Fig.2(b)], which is almost twice larger than that in parallel to the substrate. It is also expected in TCVD that the magnetic properties of metal filled CNTs can be controlled by the composition of magnetic alloy encapsulated in CNTs.

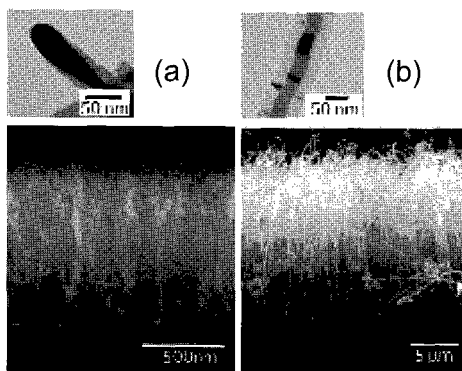


Fig.1 TEM and SEM images of CNTs grown by (a) MPECVD and (b) TCVD.

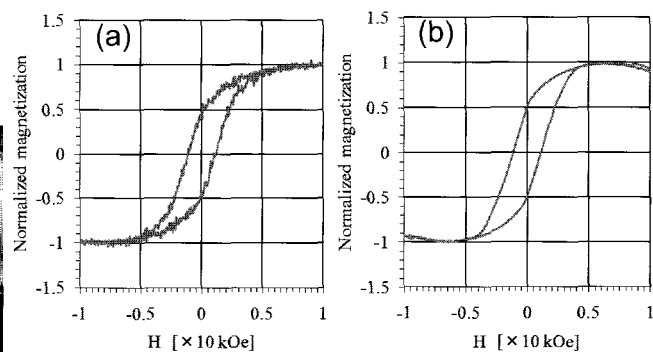


Fig.2 Magnetic hysteresis loop of metal-filled CNTs grown by (a) MPECVD and (b) TCVD.

Acknowledgment: This study has been partly supported by Mie University VBL.

References: [1] Y. Fujiwara et al., J. Appl. Phys. 95, 7118(2004).

Corresponding Author: Yusuke Matsui

E-mail: yuusuke.matsui@eds.elec.mie-u.ac.jp, **Tel&Fax:** 059-231-9404

A zigzag carbon nanotube: Growth and optical properties

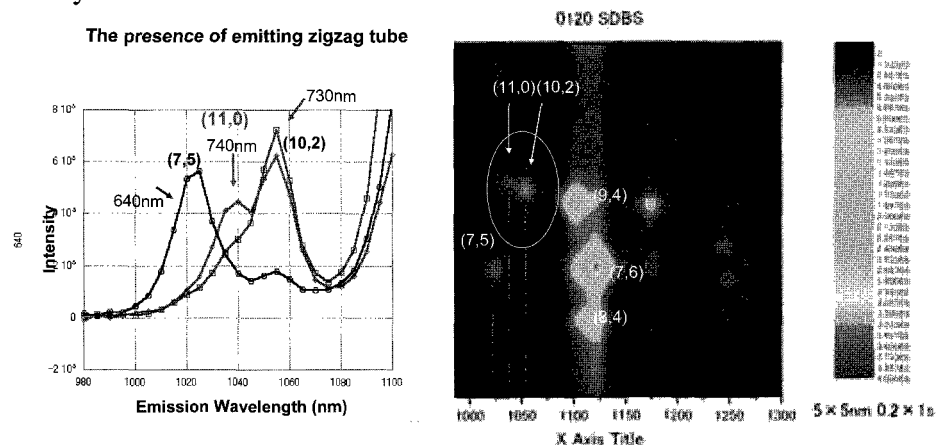
○Yohji Achiba¹⁾, Yuuki Onishi¹⁾, Takeshi Kodama and Toshiya Okazaki²⁾

1) *Department of Chemistry, Tokyo Metropolitan University, Hachioji, Tokyo 192-0397, Japan*

2) *Advanced Industrial Science and Technology (AIST), Tsukuba 305-8565, Japan*

Electronic structures of single-walled carbon nanotubes (SWNTs) depend strongly on their diameters and chiralities. Thus the chirality controlling is very important for future application of SWNTs to the field of nano-electronics, nano-optoelectronics as well as bio-electronics. Since 2002, the isolation and dispersion technique of bundled SWNTs has been well established and a lot of optical spectroscopic works on the SWNTs in solution have been appeared during last 8 years. Resonance Raman scattering and photoluminescence measurements are of particular importance to understand the optical properties of SWNTs. In the earlier studies of SWNTs by optical measurement methods, there have been significant difference in the estimation of abundance of SWNTs with different chirality. Resonance Raman scattering measurement generally suggests rather flat chirality distribution from armchair to zigzag structures. On the other hand, the photoluminescence measurement strongly suggests the more abundance of near armchair structures which is sharply contrast to the results from the resonance Raman data. Actually, so far, no fluorescence measurement on the zigzag structure has been appeared. In the present work, we demonstrate some clear evidences of the presence of (11,0) zigzag tube by fluorescence and absorption methods and we also show the formation process of the zigzag tube in detail by

comparing the process of the tubes with near armchair.



Corresponding Author Yohji Achiba

E-mail achiba-yohji@tmu.ac.jp **Tel & Fax** 042-677-2534

Mass-Production of Carbon Nanotubes by Semi-Continuous Fluidized-Bed

○Dong Young Kim, Hisashi Sugime, Kei Hasegawa, Toshio Osawa, Suguru Noda*

*Department of Chemical System Engineering, School of Engineering,
The University of Tokyo, 7-3-1 Hongo, Bunkyo-ku, Tokyo 113-8656, Japan*

Mass-production of high-quality single-walled carbon nanotubes (SWCNTs) accelerates SWCNT-based nanotechnology industries such as nanoscale electronic devices, flexible displays, solar cells/batteries, and nanocomposites. However, we have not fully applied the basics of CNT growth to mass-production yet, irrespective of abundant researches and challenges. In the preceding study, we have realized large-scale synthesis of sub-millimeter-long SWCNTs on catalyst-supported ceramic beads in a batch operation by applying the rapid growth method on substrates [1] to fluidized-bed.

In this study, we report an efficient semi-continuous fluidized-bed process with a novel catalyst-(re)supporting method by CVD for high-yield production of sub-millimeter-long CNTs. Fe/Al₂O₃ catalyst was prepared on commercially available Al₂O₃ beads of 0.5 mm in average diameter by feeding metallorganic vapors of aluminium-isopropoxide and ferrocene. The catalyst-supported beads were treated under H₂/Ar and fluidized-bed CVD was carried out for 10 min with an C₂H₂ feedstock. Then, the synthesized sub-millimeter long CNTs on Al₂O₃ beads were rapidly separated by only gas flow for 1 min. By reusing beads by re-supporting catalysts, the semi-continuous operation repeated production of CNTs for realized 30 cycles only by switching the gases with a temperature fixed at 1093 K, as shown in Fig. 1. And over 0.5-mm-long, about 90wt%-pure CNTs were synthesized at an yield over 70% (about 260 mg/batch) in semi-continuous operation by using a fluidized bed reactor of about 30 cm³ volume (Fig. 2). This productivity corresponds to 0.1~0.2kg-CNT/L-reactor/day, if the semi-continuous operation is fully developed. Morphology and structural properties of the synthesized CNTs will be also discussed in detail in this presentation.

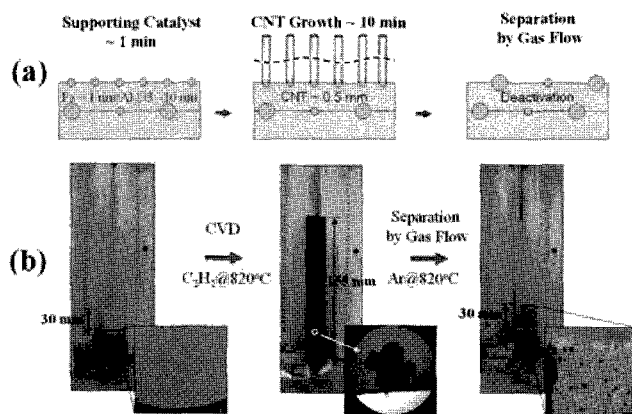


Fig. 1. Semi-continuous operation by flow modulation at fixed temperature

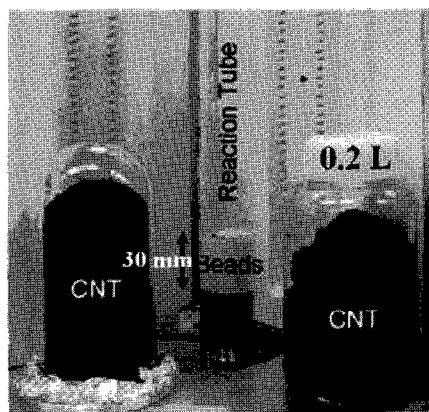


Fig. 2. Fluidized-bed reactor and synthesized high-yield CNTs

[1] D. Y. Kim, H. Fukai, H. Sugime, K. Hasegawa, T. Osawa, S. Noda, *CT-05 in NT09, Beijing, China*, June 22, 2009.

*Corresponding Author: Suguru Noda, Tel&Fax: +81-3-5841-7332, E-mail: noda@chemsys.t.u-tokyo.ac.jp

Diameter Control of SWNTs by Nano-diamond Catalyst

Shohei Chiashi¹, Norihiro Hiramatsu¹, Daisuke Takagi², Yoshikazu Homma³ and Shigeo Maruyama¹

¹*Department of Mechanical Engineering, The University of Tokyo, Bunkyo, Tokyo 113-8656, Japan*

²*NTT Basic Research Laboratories, NTT Corporation, Atsugi, Kanagawa 243-0198, Japan*

³*Department of Physics, Tokyo University of Science, Shinjuku, Tokyo 162-8601, Japan*

Chirality control is one of the most challenging topics in SWNT growth research. Tube diameter control techniques using solid phase catalysts are one of the approaches being used to realize this goal. In this study, we used nano-diamond as catalyst from which we synthesized SWNTs [1]. A colloidal nano-diamond solution was dispersed on a silicon substrate and then pre-heated (500-800 °C) in air in a thermogravimetric analyzer (TGA). In the TGA device, the sample temperature was precisely controlled. The heating rate was 1°C/min and the sample was kept at the target temperature for 150 min. During SWNT synthesis the CVD temperature was 800 °C and the pressure of ethanol gas was 1.2 kPa.

Figure 1 shows (A) SEM image and (B) Raman scattering spectra of SWNTs synthesized from nano-diamond particles (the pre-heating temperature was 600 °C). SWNTs uniformly grew on the silicon substrate. The G/D ratio was high and the RBM peaks clearly appeared. Figure 1(C) shows the pre-heating temperature dependence of RBM peaks. The RBM peaks gradually up-shifted with increasing of the pre-heating temperature. This indicates that the pre-heating process decreases the diameter of nano-diamond, which results in smaller diameter SWNTs. Since the nano-diamond is quite stable during the CVD process, the pre-CVD size control of nano-diamond should directly affect the SWNT structure.

[1] D. Takagi, *et al.*, *J. Am. Chem. Soc.*, **131** (2009) 6922.

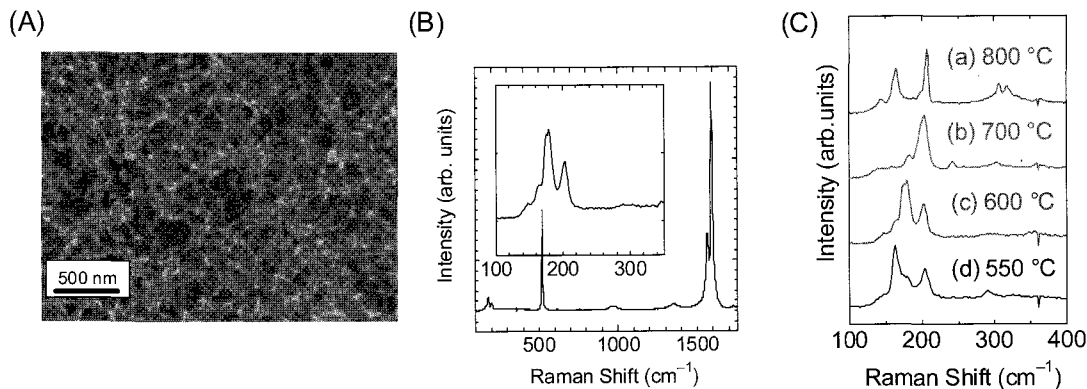


Fig. 1 (A) SEM image and (B) Raman scattering spectra from SWNTs synthesized using nano-diamond particles. (C) Pre-heating temperature dependence of the RBM peaks.

Corresponding Author: Shigeo Maruyama

E-mail: maruyama@photon.t.u-tokyo.ac.jp, Tel: +81-3-5841-6421, Fax: +81-3-5841-6983

SWNT Growth on $\text{Al}_2\text{O}_x/\text{Co}/\text{Al}_2\text{O}_x$ Multilayer Catalyst using Alcohol Gas Source Method in High Vacuum

○Yoshihiro Mizutani, Kuninori Sato,
*Takahiro Maruyama and Shigeeya Naritsuka

*Department of Materials Science and Engineering, Meijo University,
1-501 Shiogamaguchi, Tempaku, Nagoya 468-8502, Japan*

Carbon nanotubes (CNTs) have been anticipated for application in a lot of future nanodevices. However, to fabricate devices compatible with conventional LSI, the current growth temperature is too high. Recently, we reported SWNT growth by alcohol gas source method in an ultra-high vacuum (UHV) chamber [1]. This growth technique enables SWNT growth at low temperature [2]. However, the yield of grown SWNTs has not been sufficient. In this study, we attempted to increase the SWNT yield by using $\text{Al}_2\text{O}_x/\text{Co}/\text{Al}_2\text{O}_x$ multilayer catalysts.

$\text{Al}_2\text{O}_x/\text{Co}/\text{Al}_2\text{O}_x/\text{SiO}_2/\text{Si}$ and $\text{Co}/\text{Al}_2\text{O}_x/\text{SiO}_2/\text{Si}$ were used as substrates. Firstly, Al_2O_x layers were formed by Al deposition (thickness: 30 nm) using a pulsed arc plasma gun in a UHV chamber, followed by exposure to the air. Co (thickness: 0.1 nm) was deposited by an e-beam evaporator on the substrates. Furthermore, Al_2O_x layers (thickness: 1 nm) were deposited on some of the substrates to form the $\text{Al}_2\text{O}_x/\text{Co}/\text{Al}_2\text{O}_x$ multilayers. Then, they were heated to the growth temperature (typically 700°C), and ethanol gas (ambient pressure: 1.0×10^{-1} Pa) was supplied to grow SWNTs. The samples were characterized by scanning electron microscopy (SEM) and Raman spectroscopy.

Fig. 1 shows Raman spectra of the grown SWNTs measured with a Nd-YAG laser (532 nm). Compared to the SWNTs on $\text{Co}/\text{Al}_2\text{O}_x/\text{SiO}_2/\text{Si}$ substrate, G band intensity of the SWNTs on $\text{Al}_2\text{O}_x/\text{Co}/\text{Al}_2\text{O}_x/\text{SiO}_2/\text{Si}$ substrate was 6.4 times larger and the G/D ratio increased to 17.7. In the RBM region, relative peak intensities from SWNTs of about 1 nm in diameter became larger. These results show that the support of $\text{Al}_2\text{O}_x/\text{Co}/\text{Al}_2\text{O}_x$ multilayer catalyst is effective to increase the SWNT yield in the alcohol gas source method.

This work was partially supported by the Japan Society for the Promotion of Science (JSPS), Grant-in-aid for Scientific Research (C) 21510119. We are indebted to Prof. Yakushi and Dr. Uruichi from the Institute for Molecular Science (IMS) for the Raman measurements.

References

- [1] K. Tanioku et al., *Diam. Relat. Mater.*
Diamond Relat. Mater. 17 (2008) 589.
[2] T. Maruyama et al. *J. Nanosci.*
Nanotechnol. in press.

Corresponding Author: Takahiro Maruyama
E-mail: takamaru@ccmfs.meijo-u.ac.jp
Tel: +81-52-838-2386, **Fax:** +81-52-832-1172

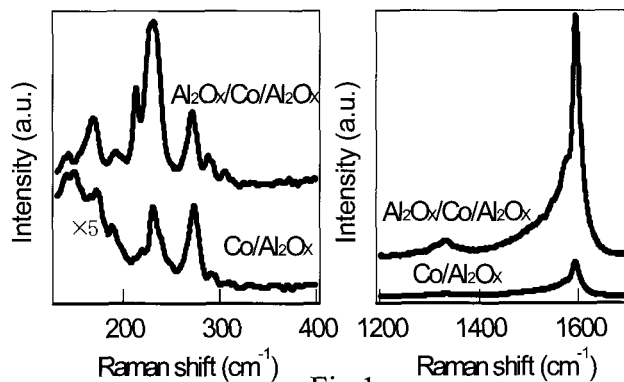


Fig.1

Change in Chirality Distribution of CoMoCAT[®] Nanotubes Using Excimer Laser

○Masaki Hashimoto, Norio Maki, Masaaki Ashihara, Tsugio Matsuura

Industrial Technology Center of Fukui Prefecture, Fukui 910-0102, Japan

We have investigated the change in chirality distribution after the Excimer laser was irradiated at prepared CoMoCAT[®] samples. The laser pulse energy was adopted three conditions. In evaluating the changes, we used the Near-infrared photoluminescence spectroscopy (PL) and the Resonance Raman spectroscopy (RRS); the PL for the chirality distribution and the RRS for the G/D ratio were measured with the samples irradiated the Excimer laser for 10 minutes. This process was repeated six times, resulting in a total of 60 minutes of the laser irradiation at the samples.

The chirality distribution of the samples, which was obtained by no laser irradiation (Fig. 1a) and a total of 20 minutes of laser irradiation (Fig. 1b) are shown. It was so considerably changed after laser irradiation that many fluorescent peaks near 1100 nm were detected.

In addition, we investigated the effect of the laser irradiation duration about the fluorescent intensities of (6,5) and (8,4), which had indicated major differences from the others. These intensities were increased and decreased while irradiating. And, this tendency was corresponded to that of the G/D ratio partially. Thus, the samples have different characteristics for each chirality (n,m) after laser irradiation. The reason will result from the different chiralities having different laser absorption characteristics.

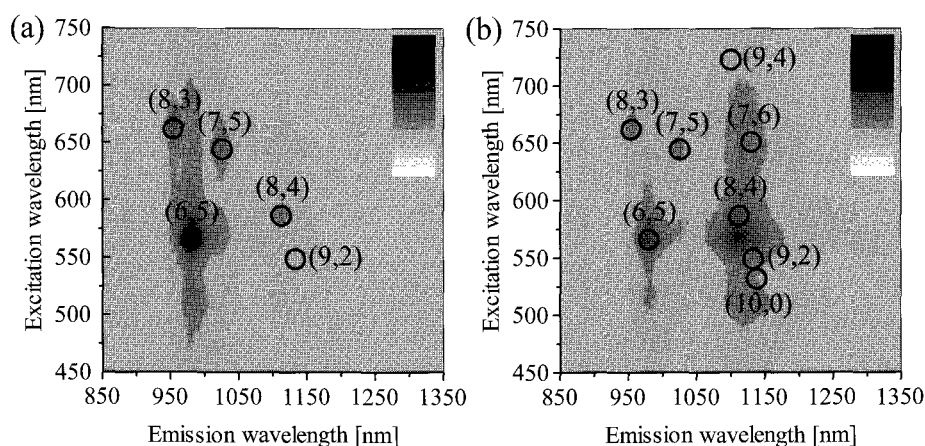


Fig. 1. The chirality distribution of the CoMoCAT[®] samples (a) with no laser irradiation (b) with a total of 20 min. laser irradiation. The scale in the figure shows the intensity whose maximum is 2600 [a.u.].

Corresponding Author: Masaki Hashimoto

E-mail: hashimoto@fklab.fukui.fukui.jp

TEL +81-776-55-0664 FAX +81-776-55-0665

Controllable yield of metallic single-walled carbon nanotubes by aerosol-assisted chemical vapor deposition

○ Shinya Koike, Shunji Bandow, Yoshinori Ando

*Department of Materials Science and Engineering, Meijo University,
1-501 Shiogamaguchi, Tenpaku, Nagoya 468-8502, Japan*

Ferrocene is widely used as the catalyst source for the production of single-walled carbon nanotubes by the chemical vapor deposition (CVD). Normally the sublimation temperature of ferrocene is controlled when changing the concentration of catalyst is required.¹⁾ In this study, we applied the sonication driven mist generation technique for supplying simultaneously both sources of catalyst and carbon to the CVD furnace. Merit of this mist technique is that we can widely and precisely vary the catalyst contents by changing the concentration in the solution. At the present, the concentrations of ferrocene in ethanol were changed in the range between 0.1 and 1.0 % by weight. Then the mist generated by sonication was carried by the Ar flux of 1,500 sccm to a 30 mm diameter tube furnace set at 825 °C.

Products were examined by the Raman scattering using the excitation sources of 532 and 785 nm. By using a 532 nm, metallic tubes around 1 nm diameters (RBM of $\sim 250 \text{ cm}^{-1}$) and semiconducting tubes around 1.6 nm ($\sim 160 \text{ cm}^{-1}$) can be resonantly picked up. For a 785 nm, we can alternatively pick up the metallic tubes around 1.6 nm and the semiconducting ones around 1 nm. From RBM, it was found that the thick tubes with 1.6 nm class of diameters cannot be included in the samples. G-band spectral feature taken for a 785 nm excitation can be well fit by using Lorentzian components (not shown), and no remarkable change on the spectral shape can be found. Hence we conclude that the yield of semiconducting tubes cannot be affected by the ferrocene concentration. While the intensity for the metallic tube component detected by a 532 nm excitation closely depended on the ferrocene concentration as shown in Fig. 1. In Fig. 2, we summarized the Fano-line intensity against ferrocene concentration. Detail of the analyses will be discussed in the meeting.

1) R. Kozuharova-Koseva *et al.*, *Fullerenes, Nanotubes and Carbon Nanostructures* **15** (2), 135-143 (2007).

Corresponding Author: Shunji Bandow, **E-mail:** bandow@ccmfs.meijo-u.ac.jp, **Tel&Fax:** +81-52-834-4001

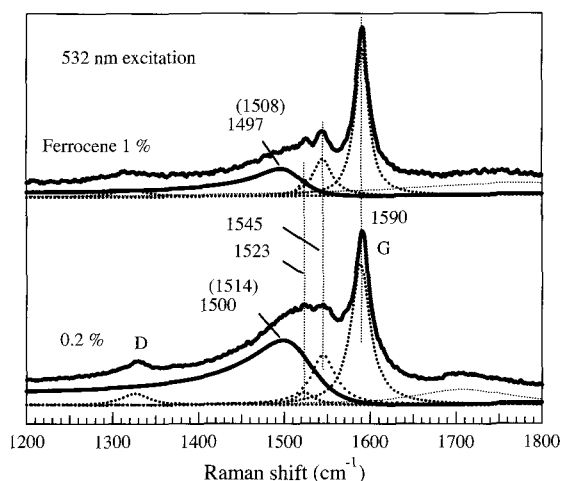


Fig. 1. G-band analyses of the products. Top spectrum is for the sample prepared by using ethanol mist containing 1 % of ferrocene, and the bottom is from 0.2 %. Thick solid lines are the Fano-component associated with the metallic nanotubes.

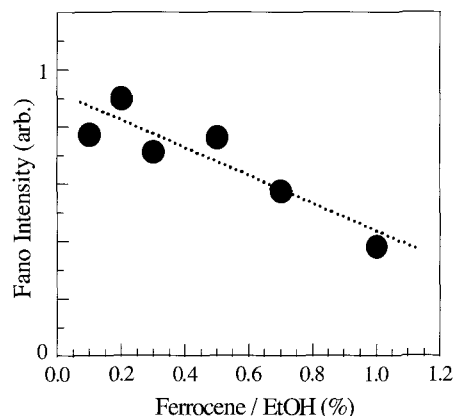


Fig. 2. Dependence of the Fano-line intensity on the ferrocene concentration.

Progress in the electrochemical cutting method of single-wall carbon nanotubes

○Shigekazu Ohmori^a, Takeshi Saito^{a,b}, Bikau Shukla^a, Motoo Yumura^a and Sumio Iijima^a

^a*Nanotube Research Center, National Institute of Advanced Industrial Science and Technology (AIST), Japan*

^b*PRESTO, Japan Science and Technology Agency, Japan*

Production of length controlled single-wall carbon nanotubes (SWCNTs) are anticipated from the various applications such as electronic and nano-medical devices, because of the length of SWCNTs is one of the most important structural parameters that affect on their dispersibility and processability. Although various cutting processes of SWCNTs have been reported [1,2], it is extremely difficult to cut of SWCNTs, because of its chemically stable structure formed by one-dimensionally rolling up a sheet of graphene. In this sense, cutting SWCNTs needs extreme conditions. We have previously reported the electrochemical behavior of SWCNTs in water with applying direct current (DC) voltage. In this electrochemical procedure in water with the DC voltage around 4–10 V, considerable amount of short SWCNTs were produced with their oxidative degradation. However the detailed degradation potential threshold has not been clarified yet.

In this work, we have investigated oxidative degradation potential threshold of SWCNTs by applying DC voltage between SWCNTs and counter Pt electrodes in 9 M conc. H₂SO₄ aqueous solution as electrolyte. Even after applying 1.5 V for 4 hours, although continuous production of oxygen gas by normal electrolysis of water was observed, transmission electron microscopic (TEM) observation suggested that no obvious degradation in SWCNTs' structure was occurred. On the other hand, when the applying voltage was increased to 2 V, considerable amount of SWCNTs were degraded by oxidation. This result leads that the most probable mediates in the oxidative degradation of SWCNTs was considered as hydrogen peroxide (+1.78 V vs SHE) and its derivatives. This work has been supported by New Energy and Industrial Technology Development Organization (NEDO) project.

References:

[1] Z. Gu, et. al., Nano Letters, 2002, 2, 1009.

[2] S. Ohmori, et. al., The 34th symposium abstract 1-17.

Corresponding Author: Shigekazu Ohmori

E-mail ohmori-sh@aist.go.jp

Tel: +81-29-861-6276, Fax: +81-29-861-4413

Effect of Buffer Layers on the Synthesis of Carbon Nanotubes by Alcohol Catalytic Chemical Vapor Deposition

○Yuki Matsuoka and Masamichi Yoshimura

*Graduate School of Engineering, Toyota Technological Institute,
2-12-2 Hisakata, Tenpaku, Nagoya 468-8511, Japan.*

Abstract:

Single-walled carbon nanotube (SWCNT) is a promising candidate for a probe of scanning probe microscope due to thin diameter (~1 nm), high aspect ratio, high elasticity and physical and chemical stability. It is necessary for SWCNTs synthesis to enhance the catalytic activities of catalysts. Therefore, some buffer layers are often inserted between catalyst and substrate[1]. Growth temperature also influences the catalytic activity. In this study, the effect of the buffer layers and growth temperature upon crystallinity of CNT synthesized in alcohol catalytic chemical vapor deposition (ACCVD) has been investigated.

Aluminum oxide (AlO_x , 20 nm) and silicon oxide (SiO_2 , 50 nm) layers were used as buffer layer. Pressure of ethanol vapor was kept at 85 torr and CNTs were synthesized at various growth temperatures (600~800 °C). The crystallinities of grown CNTs were estimated by the ratio of G, D peak intensity (I_G/I_D) in Raman spectra. Fig.1 shows the relationship between I_G/I_D and growth temperature. It is found that aluminum oxide layer was not effective to grow SWCNTs because the I_G/I_D ratios were kept low through all the temperatures examined. Fig.2 shows Raman spectra of CNTs synthesized at 800 °C and 750 °C on Co/ AlO_x /Si. The number of peaks at 800 °C was less than that at 750 °C, suggesting the synthesis of SWCNTs was suppressed except the tubes of a specific diameter, 1.10 nm.

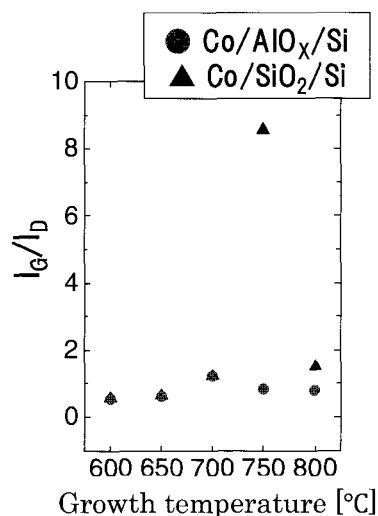


Fig.1 I_G/I_D ratio at various growth temperatures

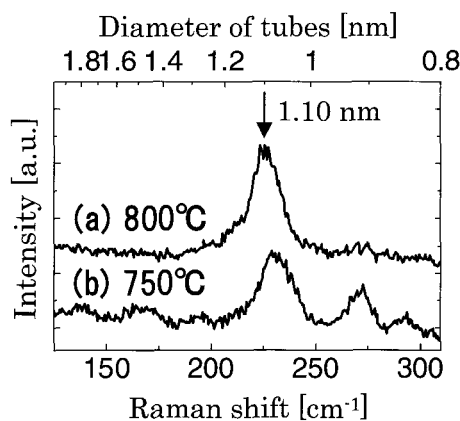


Fig.2 Raman spectra of synthesized at (a) 800 °C, (b)750 °C (Co(0.5 nm)/ SiO_2 (20 nm)/Si, 85 torr)

Reference:

[1] C. Mattevi et al. *J. Phys. Chem. C*, **112** (2008) 12207.

Purification of mono-dispersed single-walled carbon nanotubes made with arc-burning technique in nitrogen atmosphere

○Takashi Mizusawa¹, Shinzo Suzuki¹, Toshiya Okazaki², and Yohji Achiba³

¹*Department of Physics, Kyoto Sangyo University, Kyoto 603-8555, Japan*

²*Nanotube Research Center., AIST, Tsukuba 305-8565, Japan*

³*Department of Chemistry, Tokyo Metropolitan University, Tokyo 192-0397, Japan*

Abstract:

Recently, several different kinds of purification and separation technique, including density-gradient ultra-centrifugation, agarose gel electrophoresis, gel-based separation technique, and ion-exchange chromatography procedure have been proposed and extensively used for mono-dispersed single-walled carbon nanotubes (SWNTs). When using ion-exchange chromatography technique, it was found that one can now separate SWNTs of different chiral index [1], though different kind of special home-made DNA-oligomer is necessary for each SWNT of different chiral index, and the yield seems to be still low after purification procedure.

In this presentation, a simpler column chromatography technique is tested for purification of mono-dispersed SWNTs made with arc-burning technique in nitrogen atmosphere [2], aimed for further application of HPLC technique to SWNT purification. Figs. 1 and 2 show typical examples of absorption spectra for different fractions after chromatographic separation by using different column/eluent combination. These results demonstrate that, different combination of column/eluent influences much on the purification behavior of mono-dispersed SWNTs.

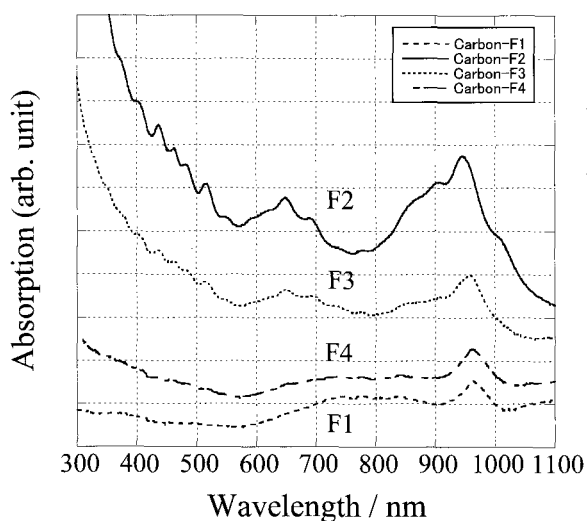


Fig.1

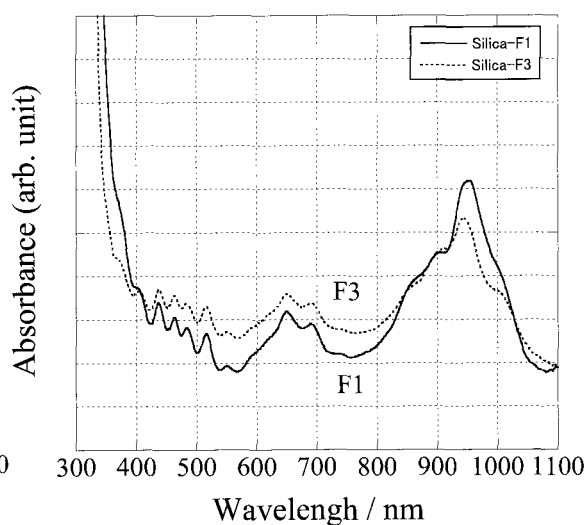


Fig.2

References:

- [1] X. Tu, S. Manohar, a. Jagota, and M. Zheng, *Nature*, **460**, 250-253(2009).
 [2] S. Suzuki, T. Mizusawa, T. Okazaki, and Y. Achiba, *Eur. Phys. J. D*, **52**, 83-86 (2009).

Corresponding Author: Shinzo Suzuki

TEL: +81-75-705-1631, FAX: +81-75-705-1640, E-mail: suzukish@cc.kyoto-su.ac.jp

Adsorption of a Water Molecule on Graphene: Accuracy of Density Functional Methods with Localized Orbitals

Mari Ohfuchi

*Nanoelectronics Research Center, Fujitsu Laboratories Ltd.,
10-1 Morinosato-Wakamiya, Atsugi 243-0197, Japan*

We have studied the non-covalent adsorption between single-wall carbon nanotubes (SWCNTs) and molecules, such as sodium dodecyl sulfate (SDS)¹ or agarose,² to understand the separation of metallic and semiconducting SWCNTs. The density functional (DF) methods with localized atomic orbitals³ have been adopted, because they would make large scale calculations possible to treat SWCNTs in solution in the future. However we always need to pay attention to the accuracy of the calculations. In this study, we examine the adsorption energy of a water molecule on graphene and the results are verified by comparing with several previous studies.^{4,5}

As shown in figures, the two orientations and three sites of the water molecule with regard to graphene are examined. We have already reported¹ that fine meshes in the real and reciprocal spaces can give the enough accuracy of 0.01 eV to examine non-covalent adsorption energy, which is approximately 0.1 eV. On the other hand, basis set superposition error (BSSE)⁶ is a well-known problem originated from the localized orbitals applied to non-covalent adsorption. The BSSE correction reduces the adsorption energies and the geometry where a hydrogen atom is on the top (T) site gives the strongest.

Our results have been found to be in good agreement with the DF study with plane waves.⁴ They are also compared with the results based on the coupled-cluster methods⁵ that can describe van der Waals (vdW) interactions unlike the DF theory. It has been found that the absolute values of the adsorption energies are different because of the vdW interactions but the differences among those of the different geometries agree. Thus our methods seem to be sufficient to discuss the differences among the adsorption energies of different geometries.

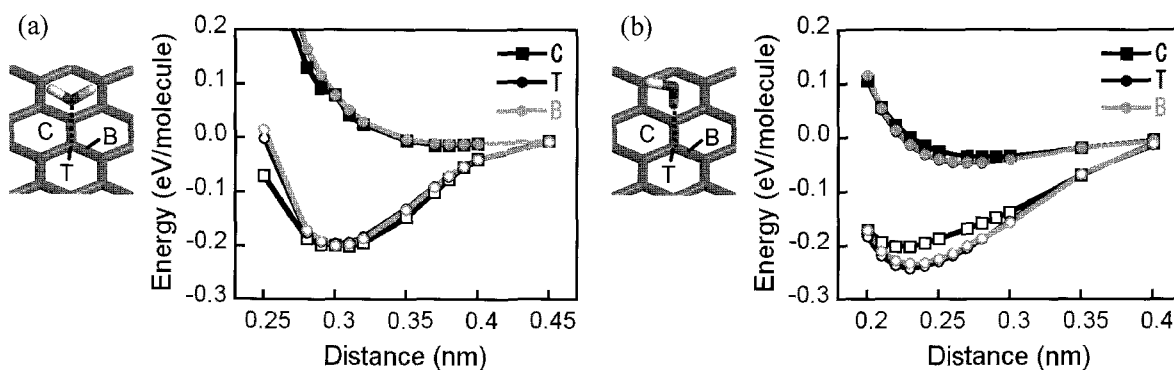


FIG. Adsorption energies of a water molecule on graphene. The open and close symbols represent the results without and with BSSE correction, respectively.

1. M. Ohfuchi, The 36th Fullerene-Nanotubes General Symposium 3-9 (2009).
2. M. Ohfuchi, The 37th Fullerene-Nanotubes General Symposium 1P-36 (2009).
3. T. Ozaki, Phys. Rev. B **67**, 155108 (2003).
4. O. Leenaerts, B. Partoens, and F. M. Peeters, Phys. Rev. B **77**, 125416 (2008).
5. M. Rubeš, P. Nachtigall, J. Vondrášek, and O. Bludský, J. Phys. Chem. C **113**, 8412 (2009).
6. S. F. Boys and F. Bernardi, Mol. Phys. **19**, 553 (1970).

Corresponding Author: Mari Ohfuchi

Tel: +81-46-250-8843, Fax: +81-46-250-8844, E-mail: mari.ohfuti@jp.fujitsu.com

SWNT Nucleation, Growth and Healing: Insights from Density-Functional Tight-Binding Molecular Dynamics Simulations

Alister J. Page^{1,○}, Stephan Irle² and Keiji Morokuma^{1,3}

¹*Fukui Institute for Fundamental Chemistry, Kyoto University, Kyoto 606-8103, Japan*

²*Institute for Advanced Research and Department of Chemistry, Nagoya University, Nagoya 464-8602, Japan*

³*Cherry L. Emerson Center for Scientific Computation and Department of Chemistry, Emory University, Atlanta, GA 30322, USA*

We summarize our recent QM/MD investigations [1-6] concerning the nucleation, growth and defect-healing of single-walled carbon nanotubes (SWNTs) (Figure 1). Our theoretical approach is based on the self-consistent-charge density functional tight-binding (SCC-DFTB/MD) method, and so is a compromise between QM accuracy and classical force-field efficiency. Consequently, we are able to simulate these SWNT growth phenomena over timescales of *ca.* 100 ps - 1 ns.

Despite the fact that CVD synthesis using transition-metal catalysts is now a commercially viable process, the mechanisms underpinning most facets of SWNT nucleation, growth and healing are yet to be understood. With respect to transition-metal nanoparticle catalysts, we observe that these SWNT growth phenomena exhibit distinct dependences on both the size and composition of the catalyst. In addition, the efficiency of SWNT growth is inversely related to the rate at which feedstock carbon is incorporated into the SWNT itself. The abundance of defective structural elements in a growing SWNT is also inversely proportional to this rate. These relationships, in conjunction with defect-healing mechanisms observed during our simulations (such as the removal of 5-7 defects *via* ring-isomerization processes akin to the Stone-Wales transformation), provide a route towards chirality-controlled SWNT growth.

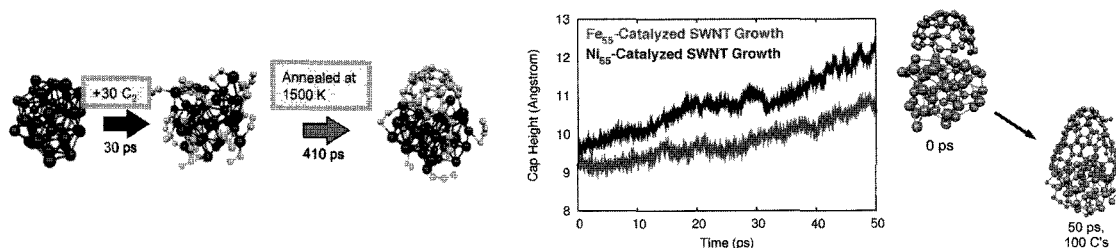


Figure 1. Summary of QM/MD investigations SWNT nucleation & growth from Fe & Ni nanoparticles described in references [1-6].

References

- [1] Y. Ohta, Y. Okamoto, A. J. Page, S. Irle, K. Morokuma. *ACS Nano* 2009, **3**, 3413.
- [2] A. J. Page, Y. Ohta, Y. Okamoto, S. Irle, K. Morokuma. *J. Phys. Chem. C*, 2009, **113**, 20198.
- [3] Ohta, Y.; Okamoto, Y.; Irle, S.; Morokuma, K. *ACS Nano* 2008, **2**, 1437.
- [4] Ohta, Y.; Okamoto, Y.; Irle, S.; Morokuma, K. *Carbon* 2009, **47**, 1270.
- [5] A. J. Page, S. Minami, Y. Ohta, S. Irle, K. Morokuma. *Carbon*, Submitted.
- [6] A. J. Page, S. Irle, K. Morokuma. *Nano Lett.*, Submitted.

Email: alisterpage@fukui.kyoto-u.ac.jp

Tel: +81-75-711-7831; Fax: +81-75-781-4757

CVD Fabrication of Thin Carbon Nanocoil with Sn/Fe Catalyst on Mesoporous Particles

○K. Takimoto¹, M. Yokota¹, Lim Siew Ling¹, Y. Suda¹, H. Takikawa¹,
H. Ue², K. Shimizu³, Y. Umeda⁴

¹ Department of Electrical and Electronic Engineering, Toyohashi University of Technology

² Fuji Research Laboratory, Tokai Carbon Co., Ltd.

³ Shonan Plastic Mfg. Co., Ltd.

⁴ Fundamental Research Department, Toho Gas Co., Ltd.

Carbon nanocoil (CNC) is a material of carbon nanofiber with helical shape. CNCs are synthesized by chemical vapor deposition on a substrate using a composite catalyst of Fe and Sn. Thin CNCs are expected to be used as electromagnetic ray absorbent and nanospring. In the previous study, thin CNCs were synthesized by using Y-type zeolite, on which Fe and Sn were supported [1]. In this study, we supported Fe catalyst prior to Sn catalysts to raise thin CNC yield. We used Y-type zeolite and MCM-41-type mesoporous silica as mesoporous particles. Fe catalyst was supported on mesoporous particles in iron acetate-mixed ethanol solution. They were dried by electric furnace at 100°C for 24 hours. Sn catalyst was deposited over Fe catalyst by vacuum-evaporation. The Sn/Fe catalysts were placed in the center of a quartz reactor tube. The reaction temperature, the gas flow rates of nitrogen as a dilution gas and acetylene as a source gas, and the reaction time were 700°C, 1000 sccm, 50 sccm, and 10 min, respectively. Thin CNCs were observed by scanning electron microscopy (SEM) as shown in Fig. 1. The fiber diameters of CNCs from zeolite and mesoporous silica were 15-45 nm and 20-26 nm, respectively. The thinnest CNC was obtained on zeolite and the fiber diameter was about 15 nm. The yields of thin CNCs grown from Sn/Fe catalysts on both the mesoporous particles were higher than the previous result [1].

This work has been partly supported by the Outstanding Research Project of the Research Center for Future Technology, Toyohashi University of Technology (TUT); the Research Project of the Venture Business Laboratory, and Global COE Program "Frontiers of Intelligent Sensing" from the Ministry of Education, Culture, Sports, Science and Technology (MEXT); and The Japan Society for the Promotion of Science (JSPS), Core University Programs (JSPS-KOSEF program in the field of "R&D of Advanced Semiconductor"; JSPS-CAS program in the field of "Plasma and Nuclear Fusion").

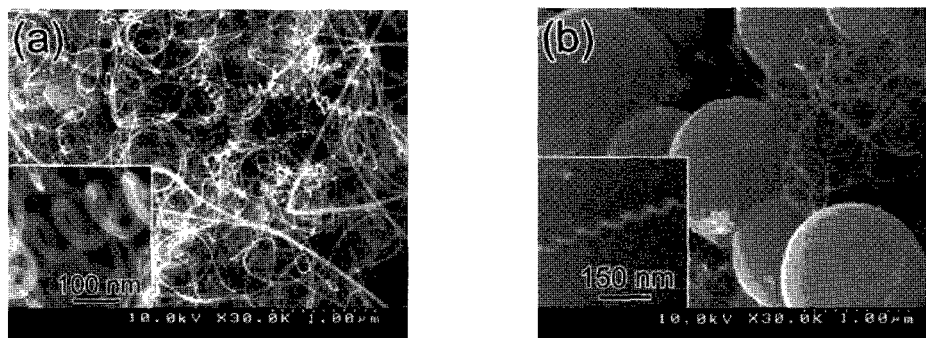


Fig.1 SEM image of thin CNC synthesized from Sn/Fe catalyst supported on (a) zeolite and (b) mesoporous silica

[1] Yokota, et al, The 36th Fullerene-Nanotubes General Symposium (2009) 3P-9

Corresponding Author. Yoshiyuki Suda

E-mail: suda@eee.tut.ac.jp, Tel: +81-532-44-6726

High-purity semiconducting single-wall carbon nanotubes separation by density gradient ultracentrifugation

○Ye Feng^{1,2,3}, Yasumitsu Miyata⁴, Shunjiro Fujii², Kiyoto Matsuishi¹, Hiromichi Kataura^{2,3}

¹Graduate school of Pure and applied Physics, Tsukuba University, 1-1-1 Tenodai, Tsukuba, Ibaraki 305-8573, Japan

²Nanotechnology Research Institute, AIST, 1-1-1 Higashi, Tsukuba 305-8562, Japan

³JST-CREST, Kawaguchi 330-0012, Japan

⁴Department of Chemistry, Nagoya University, Nagoya, Aichi 464-8602, Japan

The mixing of metallic and semiconducting single wall carbon nanotubes is a unique and interesting property, which also hinders their applications in electronic devices. Many methods had been reported to sort the SWCNTs by their electronic states [1,2]. However, higher purity and simple separation processes are needed for the application. This study optimized the separation condition of density gradient ultracentrifugation (DGU) for better separation effects, and used the uniform density separation to simplify the process. And a second separation was applied to get higher-purity. With the repeat of the operation, it is predicted to get 99.99% semiconducting single wall carbon nanotubes.

We used two kinds of surfactants to separate the nanotubes, sodium dodecyl sulphate (SDS) and sodium cholate (SC). The result of separation with uniform density was shown in Figure 1, in which the green layer is metallic and the orange layer is semiconducting SWCNTs. Although we can further purify the semiconducting carbon nanotubes by 2nd separation, the small metallic peak (600nm~800nm in Figure 2) was observed to remain. It decreased with longer sonication time. It can be described by the small bundles of metallic nanotubes. A better dispersion is necessary to get the higher purity semiconducting nanotubes.

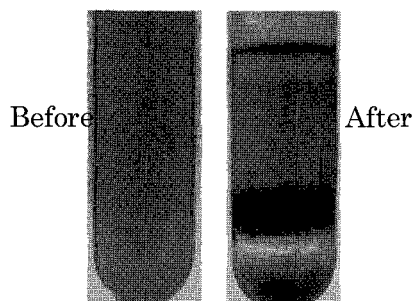


Fig 1. Separation with uniform density

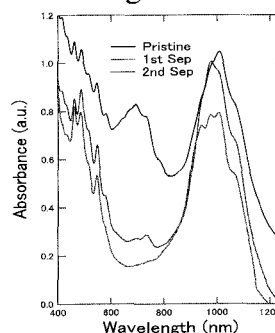


Fig. 2 Absorption spectra of pristine and separated samples after 1st and 2nd processes.

References:

- [1] Arnold et al., Nat. Nanotechnol. 1 (2006) 60
 [2] T. Tanaka et al., Nano lett. 9 (2009) 1497

Corresponding Author: Hiromichi Kataura

E-mail: h-kataura@aist.go.jp, **Tel:** +81-29-861-2551, **Fax:** +81-29-861-2786

Catalysts and supports for rapid growth of vertically-aligned CNTs

○Keisuke Nomura, Kei Hasegawa, and Suguru Noda*

Dept. of Chemical System Engineering, The University of Tokyo, Tokyo, 113-8656, Japan

Rapid, millimeter-scale growth of single-walled carbon nanotubes (SWCNTs) by chemical vapor deposition (CVD) has been realized by several research groups [1-3]. Fe/Al₂O_x is a popular catalyst, however, there is still some debate over the effect of Al₂O_x support [2,3]. In this work, we aim at the better understanding on it.

Fe/Al₂O_x and Al₂O_x/Fe catalysts were sputter deposited on Si wafers with thermal oxide layer. The Al₂O_x layer was formed by depositing Al on the substrates, and then exposing the layer to air. Gradient-thickness profiles were formed for both Al and Fe by using the combinatorial method previously described [4]. The substrates were set in a tubular CVD reactor and heated to and kept for 10 min at a target temperature of 1093 K under a flow of 26vol% H₂/ 50ppmv H₂O/ Ar balance at ambient pressure. After the heat treatment, CVD was carried out by switching the gas to 7.9vol% C₂H₄/ 26vol% H₂/ 50ppmvH₂O/ Ar balance. Figure 1 shows photographs of the nanotubes grown for 10 min. CNTs grew in millimeter-scale on both Fe/Al₂O_x and Al₂O_x/Fe when Al was relatively thick (≥1 nm), and optimum thickness was larger for the former (i.e. Al₂O_x underlayer) than for the latter (i.e. Al₂O_x cap). This result indicates that the coexistence of Al(-oxide) rather than the continuous Al₂O_x underlayer is indispensable for the rapid SWCNT growth. We also examined the reactivity of Al₂O_x and SiO₂ underlayers without any Fe loading. Figure 2 shows Raman spectra of the samples after CVD. G and D-bands were clearly observed only for Al₂O_x. This result confirms that Al₂O_x is catalytically active in forming graphitic carbon, however, further study is needed to clarify if this effect contributes to the millimeter-scale growth of CNTs.

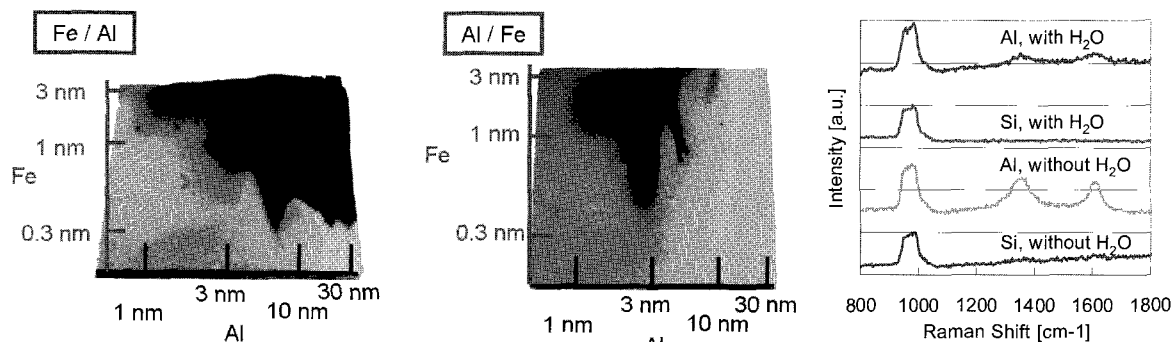


Fig. 1 Photographs of nanotubes grown by using Fe/Al₂O_x and Al₂O_x/Fe combinatorial catalyst libraries.

Fig. 2 Raman spectra for Fe-free substrates after CVD.

[1] K. Hata, et al., *Science* **306**, 1362 (2004). [2] S.Chakrabarti, et al., *J. Phys. Chem. B* **111** (2007) 1929. [3] K. Hasegawa, et al., *J. Nanosci. Nanotechnol.* **8**, 6123 (2008). [4] S. Noda, et al., *Carbon* **44**, 1414 (2006).

Corresponding Author: Suguru Noda TEL/FAX: +81-3-5841-7330/7332, E-mail: noda@chemsys.t.u-tokyo.ac.jp

Gas-phase synthesis of SWCNTs using ferrocene and C₂H₂/CH₄ feedstocks

○Youkou Ishitsuka, Yoshikuni Sato, Toshio Osawa, and Suguru Noda*

Dept. of Chemical System Engineering, The University of Tokyo, Tokyo, 113-8656, Japan

Chemical vapor deposition (CVD) method is now widely used in producing carbon nanotubes (CNTs). CNTs can be synthesized either on substrates by supported catalysts or in the gas-phase by floating catalysts. The latter method is advantageous in continuous operation, which can be easily realized by feeding both sources for CNTs and catalyst simultaneously^[1,2]. However, this simultaneous feeding causes inherent contamination of catalysts in CNTs, and therefore it is important to enhance the catalytic performance and reduce the amount of the floating catalyst particles based on their better understanding.

In this study, we used popular source gases, i.e. ferrocene for catalyst and either C₂H₂ or CH₄ for CNTs. We grew CNTs by using a tubular CVD reactor and collected grown CNTs by using a membrane filter. Figure 1(a) and 1(b) show the typical Raman spectrum and SEM image of CNTs grown from 0.26vol% C₂H₂/ Ar balance at ambient pressure and 900 °C. Although the Raman spectrum indicates high quality SWCNTs, the SEM image shows many catalyst particles attaching on SWCNTs. Such catalyst contamination was also found for CNTs grown at 800 °C whereas soot became the major contaminants at 1000 °C. Because of the similar decomposition rates of ferrocene and C₂H₂, nucleation and growth occur for both catalyst particles and CNTs simultaneously, and therefore the combination of the popular catalyst and carbon sources of ferrocene and C₂H₂ did not work well.

We replaced C₂H₂ with 0.53vol% CH₄ to suppress the soot formation through the gas-phase pyrolysis of the carbon feedstock. Figure 1(c) and 1(d) show the typical Raman spectrum and SEM image of CNTs grown at 800 °C. Catalyst contamination was largely suppressed. We will discuss the possible mechanisms both for the catalyst particle formation and for the CNT growth at the presentation.

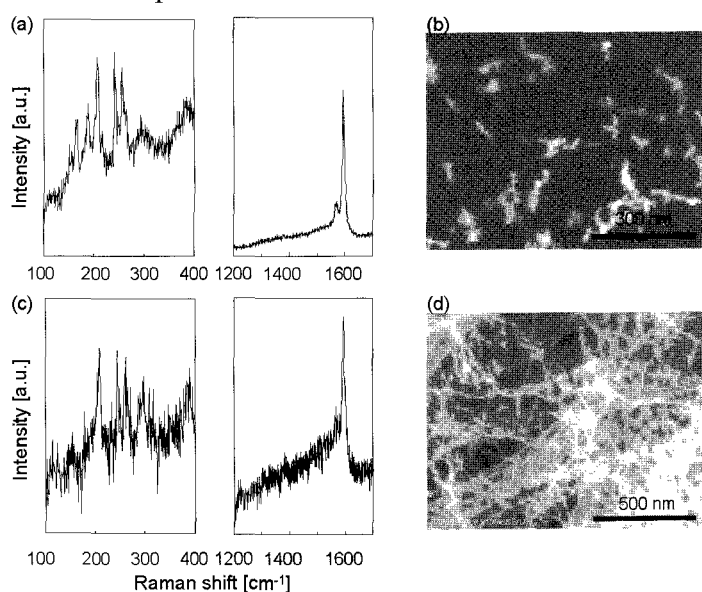


Fig. 1 Raman spectra and SEM images of gas-phase synthesized CNTs from (a,b) C₂H₂ and (c,d) CH₄.

[1] A. Moisala, et al., *Carbon* **43**, 2066 (2005). [2] P. Nikolaev, et al., *Chem. Phys. Lett.* **313**, 91 (1999).

Corresponding Author: Suguru Noda TEL/FAX: +81-3-5841-7330/7332, E-mail: noda@chemsys.t.u-tokyo.ac.jp

Experimental and numerical study on the effect of carbon feedstock decomposition on CVD synthesis of single-walled carbon nanotubes

○Bo Hou¹, Rong Xiang¹, Erik Einarsson¹, Junichiro Shiomi¹, Akira Miyoshi², Shigeo Maruyama¹

¹Department of Mechanical Engineering, The University of Tokyo, Tokyo 113-8656, Japan

²Department of Chemical System Engineering, The University of Tokyo, Tokyo 113-8656, Japan

In previous studies on the growth of single-walled carbon nanotubes (SWNTs) from ethanol at typical CVD temperatures and pressures, it was found that various parameters such as flow rate affect the SWNT growth process. Sudden termination of SWNT growth from ethanol was found to occur in the extreme low-flow (complete-decomposition) case [1, 2], indicating the effect of carbon feedstock decomposition on the growth process is significant.

To understand the effect of carbon feedstock decomposition conditions on CVD synthesis of SWNTs, gas-phase thermal decomposition of ethanol and dimethyl ether (DME) at typical SWNT growth conditions was simulated using the chemical kinetic model. Profiles of reaction species were compared to the predicted thermal decomposition mechanism [3], which confirmed simulation reaction trends and byproducts. FT-IR spectroscopy was used to analyze the concentration of species resulting from ethanol and DME decomposition, and the molar fractions were correlated against residence time in the reactor by adjusting the feedstock flow rate. FT-IR experimental results at various temperatures and pressures were in agreement with corresponding simulations.

In addition, to clarify the SWNT growth mechanism, aligned SWNTs arrays were synthesized from various isotopes of ethanol using both steady-flow and no-flow CVD methods. Characterization by resonance Raman spectroscopy clearly revealed the dependence on the decomposition condition of the feedstock in CVD for synthesis of SWNTs.

[1] R. Xiang, Z. Zhang, K. Ogura, J. Okawa, E. Einarsson, Y. Miyauchi, J. Shiomi, S. Maruyama. *Jpn. J. Appl. Phys.* **47**, (2008), 1971.

[2] R. Xiang, E. Einarsson, J. Okawa, T. Thurakitserree, Y. Murakami, J. Shiomi, Y. Ohno, S. Maruyama. *J. Nanosci. Nanotech.* **10**, (2010), in press.

[3] E. W. Kaiser, T. J. Wallington, M. D. Hurley. *J. Phys. Chem. A* **104**, (2000), 8194.

Corresponding Author: Shigeo Maruyama

E-mail: maruyama@photon.t.u-tokyo.ac.jp

TEL: +81-03-5841-6421 FAX: +81-03-5800-6983

Raman Analysis with Multi Excitation Laser
of Single-Walled Carbon Nanotubes
Grown with Free Electron Laser Irradiation during Growth

○Keijiro Sakai¹, Daisuke Ishiduka¹, Takuya Sonomura¹, Hiroaki Takeshita¹,
Kunihide Kaneki², Hirofumi Yajima², Nobuyuki Iwata¹ and Hiroshi Yamamoto¹

¹*Department of Electronics & Computer Science, College of Science & Technology, Nihon University, 7-24-1 Narashinodai, Funabashi-shi, Chiba, 274-8501 Japan*

²*Department of Applied Chemistry, Faculty of Science, Tokyo University of Science, 1-3 Kagurazaka, Shinjuku-ku, Tokyo, 162-8601 Japan*

Single-walled carbon nanotubes (SWNTs) are classified as metal or semiconductor depending on their diameter and chirality. For applying SWNTs to the nanoscale electronic devices, the preparation volume, the diameter, the alignment and the chirality must be controlled. Chirality control method has not yet been reported in these.

In our previous report, the SWNTs grown by ACCVD were analyzed by Raman spectra with 532 nm and 785 nm excitation laser[1]. However, it was not enough to reveal what kind of chirality was actually present or controllability of chirality by free electron laser (FEL) irradiation during growth. In this report, Raman analysis was carried out with multi excitation laser, 441, 532, 632, and 785 nm.

The Co/Mo catalyst was dipped and annealed. The SWNTs was grown by ACCVD method for 30 min at 1000°C after deoxidization with H₂.

The irradiated wavelength of FEL was 532, 800, 1300, 1350, 1400 nm during growth. Figure 1 and 2 show the Raman spectra with non-FEL and 800 nm FEL irradiation, respectively. Both of figures show the Raman spectra with (a) 441 nm, (b) 532nm, (c) 632 nm, and (d) 785 nm excitation laser. In non-FEL, radial breathing mode (RBM) was confirmed in all excitation wavelength, indicating the mixture growth of metallic and semiconducting SWNTs. The number of possible chiral indices was 31 in the grown SWNTs, investigated using honeycomb graphene lattice. However, when 800 nm FEL was irradiated, the RBM peaks were observed with only 785nm excitation laser. We can address that the possible chiral indices were 5 more accurately. Irradiating FEL during growth enhanced the semiconducting SWNTs growth and much reduced the possibility of chiral index of SWNTs. Other FEL wavelengths will be discussed on the day.

[1] N. Iwata et al., Fullerene-Nanotube General Symposium. 37(2009)91
cske09009@g.nihon-u.ac.jp

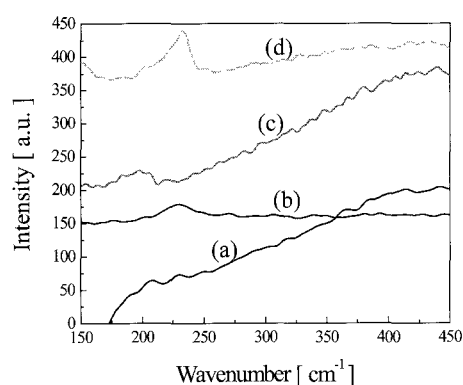


Fig.1 Raman spectra with non-FEL. (a) 441nm, (b) 532nm, (c) 632nm and (d) 785nm excitation wavelength.

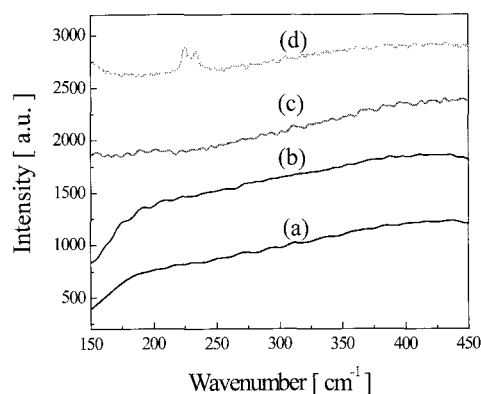


Fig.2 Raman spectra with 800 nm FEL irradiation. (a) 441nm, (b) 532nm, (c) 632nm and (d) 785nm excitation wavelength.

Synthesis of Carbon Nanotubes by a “Submarine”-style Substrate Heating Method

○Hiroyuki Yokoi, Hiroshi Momota, Tomohiro Iwamoto

*Graduate School of Science and Technology, Kumamoto University, Kumamoto 860-8555,
Japan*

A new method for the synthesis of carbon nanotubes (CNTs) is reported. Our method is based on the liquid-phase deposition method [1], in which a catalyst-coated silicon substrate is electrically heated to high temperatures around 1000 K in liquid hydrocarbon. The liquid-phase deposition method has realized a simple and rapid growth of CNTs. However, the catalyst coating on the silicon substrate needs to be controlled as thin as 1 nm in order to obtain single-walled CNTs (SWCNTs) [1], and to be fixed firmly so as not to be peeled off during the synthesis. This disadvantage has prevented one from applying zeolite- or silica-supported catalysts, which are recognized to be excellent catalysts for the synthesis of SWCNTs. We have resolved the disadvantage by setting a cover over the catalyst-coated substrate and providing a vapor space (reaction space) around the substrate (“submarine”-style substrate heating method, Fig. 1). The bottom of the cover is left open in order to supply alcohol gas vaporized due to radiation heat from the substrate, to the catalysts.

In the experiments, iron-cobalt composite catalyst supported on ultra-stable Y-type zeolite was employed [2]. Catalyst-dispersed ethanol was dropped on a silicon substrate and dried to form a catalyst coating. The substrate was inserted into ethanol liquid (99.5% in purity) with the reaction space being filled with nitrogen gas. The substrate was electrically heated to 1173 K for 10 min. Deposit on the substrate was analyzed through scanning electron microscopy, transmission electron microscopy and Raman scattering spectroscopy. SWCNTs with the diameters around 1 nm were observed and corresponding radial breathing mode was detected.

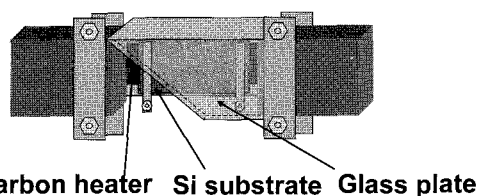


Fig. 1 Reaction part of the “submarine”-style substrate heating method. A part of the glass plate is omitted in order to show that the bottom of the cover around the substrate is left open.

[1] M. Nishitani-Gamo et al., *Jpn. J. Appl. Phys.*, **46**, 6329 (2007).

[2] K. Mukhopadhyay et al., *Chem. Phys. Lett.*, **303**, 117 (1999).

Corresponding Author: Hiroyuki Yokoi

TEL: +81-96-342-3727, FAX: +81-96-342-3710, E-mail: yokoihr@kumamoto-u.ac.jp

Effect of Catalyst Oxidation on Carbon Nanotube Growth by Low Pressure Chemical Vapor Deposition

○Tomoyuki Minami, Daiki Sawaguchi, Hideki Sato, Koichi Hata

*Graduate School of Engineering, Mie University,
1577 Kurima-Matiya-cho.Tsu-shi 514-8507, Japan*

Recently, it has been reported that single-wall carbon nanotubes (SWNTs) can be grown at the low temperature by alcohol catalytic chemical vapor deposition (ACCVD) at lower pressure than conventional ACCVD[1,2]. However, the low growth pressure gives rises to lowering of CNT yield, and improvement of the yield has been required. We have reported that the oxidation of catalyst enhances the growth of CNTs by ACCVD[3]. Here we report the effect of catalyst oxidation on the growth of CNTs at the low pressure range of < 100 Pa.

Co catalyst (1 nm) and Al underlayers (2 nm) were deposited on SiO₂/Si substrate by magnetron sputtering method. For the oxidation of catalyst, the substrate was heated at 400°C for 60 min in the air. The substrate was introduced into a high vacuum chamber (base pressure: 1×10⁻⁴ Pa) and then preannealed at 750°C for 60 min. After that, the ethanol gas was introduced into the chamber as a carbon source, and CNT growth was carried out at 750°C in a pressure of 0.5 Pa for 60 min.

Fig. 1(a) and (b) show cross-sectional SEM images of CNTs grown on the substrates without and with catalyst oxidation treatment, respectively. Randomly oriented CNT growth is observed in Fig. 1(a). On the other hand, vertically aligned CNTs are observed in Fig. 1(b), indicating that the catalyst oxidation enhances the CNT growth. Fig. 2 shows the corresponding Raman spectra. The G/D ratios of the spectra (a) and (b) are almost the same (=17), showing the oxidation treatment does not degrade the quality of CNT. Similar result was obtained for the catalyst without the Al underlayer. Thus it is considered that oxidation of the catalyst is effective to promote the growth of CNTs by the low-pressure CVD method.

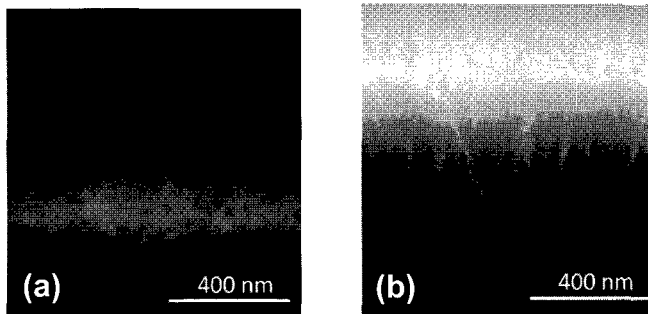


Fig. 1 Cross-sectional SEM images of CNTs grown by low-pressure CVD using catalysts (a) without and (b) with oxidation treatment.

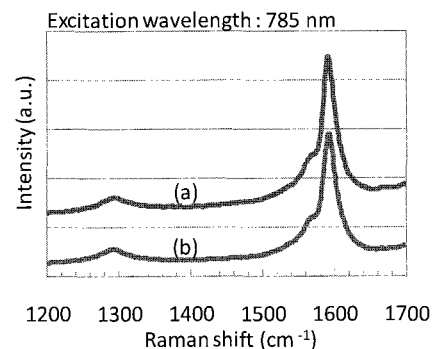


Fig. 2 Raman spectra of CNTs. (a) and (b) in the panel correspond to those in Fig.1.

Acknowledgment: This study has been partly supported by Mie University VBL.

References:

- [1] T. Shiokawa, et al., Jpn.J.Appl.Phys.45(2006)L605. [2] K. Tanioku, et al., Diamond Relat. Mater., 17 (2008)589. [3] H. Sato et al., Proc. of the 48th Annual Symposium of the Vac. Soc. of Japan, (2008)54.

Corresponding Author: Tomoyuki Minami

E-mail: tomoyuki.minami@em.elec.mie-u.ac.jp **Tel&Fax:** 059-231-9404

Influence of catalyst reduction conditions on single-walled carbon nanotube diameter

○ Theerapol Thurakitserree, Erik Einarsson, Rong Xiang, Shohei Chiashi,
Junichiro Shiomi, Shigeo Maruyama

Department of Mechanical Engineering, The University of Tokyo, Tokyo 113-8656, Japan

Here we investigate the catalyst reduction conditions on the mean diameter of single-walled carbon nanotubes (SWNTs) synthesized on substrates by the alcohol catalytic chemical vapor deposition (ACCVD) process [1,2]. A Co/Mo binary catalyst solution containing 0.01%wt of each metal species was dip-coated onto quartz substrates [3]. Prior to the introduction of ethanol, the catalyst was reduced by Ar containing 3% H₂ (Ar/H₂) at different temperatures ranging from 300 to 800°C (Fig. 1a). Following this reduction, SWNTs were synthesized at 800°C for 5 min. The SWNTs were characterized by resonance Raman spectroscopy, UV-vis-NIR spectroscopy and SEM observation. The results from this reduction process were compared with the case of continuous H₂ reduction, in which Ar/H₂ was present throughout the heating process. We found that the SWNT diameter depends on both reduction temperature and time, with lower reduction temperature tending to result in smaller diameter SWNTs (Fig. 1b). The morphology of SWNTs also changed from vertically aligned for reduction temperatures above 500°C to random when reduction occurred at or below 500°C. Furthermore, the diameter of the SWNTs appeared to increase after extended reduction at a given temperature.

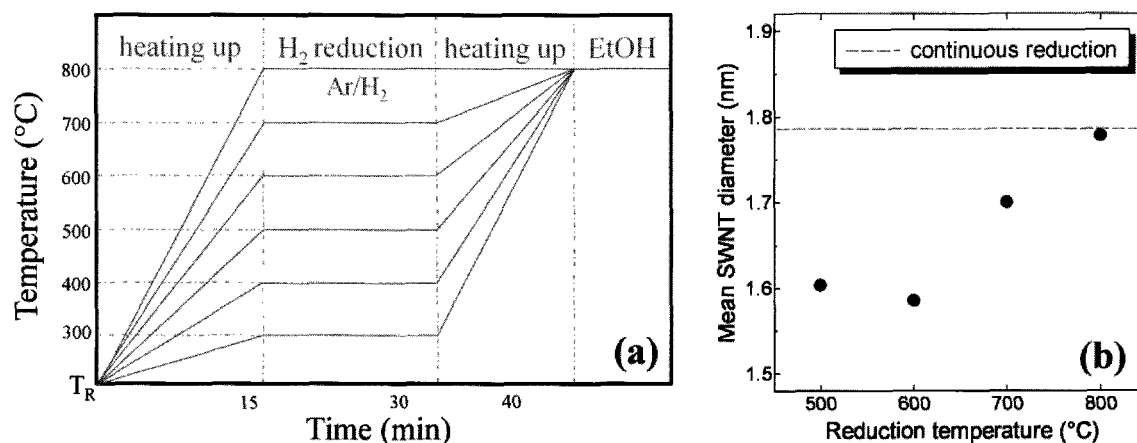


Fig. 1. (a) Temperature profiles of different catalyst reduction processes, and (b) influence of reduction temperature on mean diameter of SWNTs synthesized by the ACCVD method.

- [1] S. Maruyama, R. Kojima, Y. Miyauchi, S. Chiashi, M. Kohno, *Chem. Phys. Lett.* **360** (2002) 229.
 [2] Y. Murakami, S. Chiashi, Y. Miyauchi, M. Hu, M. Ogura, T. Okubo, S. Maruyama, *Chem. Phys. Lett.* **385** (2004) 298.
 [3] Y. Murakami, Y. Miyauchi, S. Chiashi, S. Maruyama, *Chem. Phys. Lett.* **377** (2003) 49.

Corresponding Author: Shigeo Maruyama

TEL: +81-3-5841-6421, FAX: +81-3-5800-6983, E-mail: maruyama@photon.t.u-tokyo.ac.jp

Low-temperature preparation of Carbon Nanotubes by Plasma Enhanced Chemical Vapor Deposition

Masato Miyake^{a)}, Toru Iijima^{b)}, Kenneth Teo^{c)}, Nalin Rupesinghe^{c)}, Kazunori Horikawa^{a)}
Kenjiro Onuma^{a)}, Katsuyoshi Abe^{a)}, Masayuki Satoh^{a)} and Yasuhiko Hayashi^{b)}

^{a)} AIXTRON K.K, 9F Davinci Shinagawa II, 1-8-11, Kita-shinagawa Shinagawa-ku Tokyo
140-0001, Japan

^{b)} Department of Frontier Materials, Nagoya Institute of Technology, Gokiso Showa
Nagoya 466-8555, Japan

^{c)} AIXTRON Ltd, Anderson Road, Buckingway Business Park Swavesey, Cambridge CB24
4FQ, U.K.

Many potential applications have been reported for carbon nanotubes (CNTs) including transistors, interconnects, sensors, displays, thermal interfaces, electron guns, micro fluidics, microwave amplifiers, super capacitors and fuel cells. Many researchers widely study the CNTs and nanofibers (NFs). In the next step, the scaling-up of mass production of CNTs on the large wafer size becomes the challenge. We have already manufactured the extended CVD system based on the "black magic II" by Aixtron Ltd., which enables us to grow very uniform and well reproduced CNTs on the large wafer size up to 12-inches. In addition, it enables us to use both plasma enhanced and thermal chemical vapor depositions (PECVD/thermal CVD modes) by the same system. We have already reported these results of the PECVD and the thermal CVD in the 37th Fullerene-Nano Tubes General Symposium (September, 2009). We are currently working on the PECVD and the thermal CVD. However, we focused on effect of plasma enhanced CVD in this conference. Because we will separately report the thermal CVD results in The Japan Society of Applied Physics(The 57th spring meeting March 2010). In this study, CNTs were grown by catalytic decomposition of acetylene on Ni/SiO₂/Si substrate by PECVD. We have investigated the effect of process pressure by using PECVD. It was found that vertically aligned CNTs were reproducibly synthesized at (b) 6.2mbar. On other hand, there are thick and narrow CNTs at (a) 4.2mbar, and CNTs bent on top area and low growth rate at (c) 7.2mbar in Fig1. The samples were characterized by Raman spectroscopy, scanning electron microscopy (SEM), transmission electron microscopy (TEM) and atomic force microscopy (AFM) respectively.

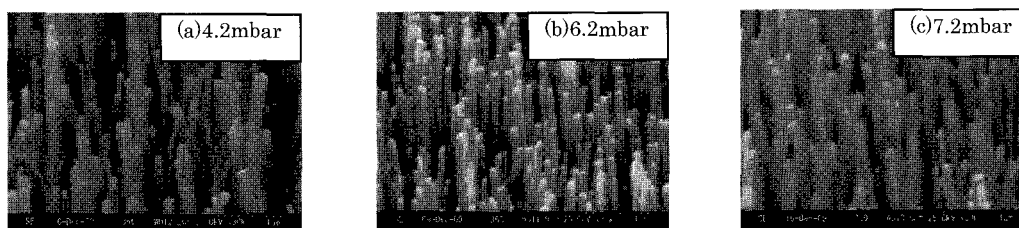


Fig1. SEM images of CNTs at (a)4.2mbar, (b)6.2mbar, (c)7.2mbar .

Masato Miyake : E-mail : m.miyake@aixtron.com, Tel&Fax : +81-3-5781-0931, +81-3-5781-0940

Screening of Surfactants for Metallic/semiconducting Separation of Single-Wall Carbon Nanotubes Using Agarose Gel

○Takeshi Tanaka¹, Yasuko Urabe¹ and Hiromichi Kataura^{1,2}

¹*Nanotechnology Research Institute, National Institute of Advanced Industrial Science and Technology (AIST), Tsukuba, Ibaraki 305-8562, Japan*

²*JST, CREST, Kawaguchi, Saitama, 332-0012, Japan*

Single wall carbon nanotubes (SWCNTs) have attracted a great deal of attention towards versatile applications, especially in the field of electronics, such as flexible transistor and transparent conducting film. However, electrical heterogeneity of as-produced SWCNTs (metal/semiconductor) is one of the most crucial problems preventing useful application of SWCNTs. Previously, we reported novel separation methods of metallic and semiconducting SWCNTs (MS separation) using agarose gel¹⁻³. These studies showed that the combination of gel and surfactant, agarose and sodium dodecyl sulfate (SDS) is very important for the MS separation. In this presentation, we report the result of high throughput screening of surfactants for the separation.

Gel centrifugation method² was applied for the screening because the method was suitable for the separation of multiple samples at a time. About 100 kinds of amphiphiles were used for the first screening, and we found that two kinds of surfactants (sodium dodecanoyl sarcosine and dodecylphosphocholine) had a tendency to show a slight MS separation. From the common feature of these surfactants and SDS, straight alkyl tail and charged head group, several kinds of surfactants were selected and applied for the second screening. Two kinds of surfactants (sodium dodecanoate and sodium dodecanesulfonate) were newly discovered as a result of the second screening. Especially, the metallic/semiconducting purity after the separation using sodium dodecanesulfonate was almost same with the case of SDS. Detailed methods and results will be discussed.

This study was supported by the industrial technology research grant program of the New Energy and Industrial Technology Development Organization (NEDO) of Japan.

References:

[1] T. Tanaka et al., *Appl. Phys. Express* 2008, **1**, 114001.

[2] T. Tanaka et al., *Nano Lett.* 2009, **9**, 1497

[3] T. Tanaka et al., *Appl. Phys. Express* 2009, **2**, 125002.

Corresponding Author: Takeshi Tanaka

Tel: +81-29-861-2903, Fax: +81-29-861-2786, E-mail: tanaka-t@aist.go.jp

CVD Growth of Vertically Aligned SWNT Films Using Dimethyl Ether as the Carbon Source

OTaiki Inoue, Hiroto Okabe, Bo Hou, Shohei Chiashi, Makoto Watanabe,
Junichiro Shiomi and Shigeo Maruyama

Department of Mechanical Engineering, The University of Tokyo, Tokyo 113-8656, Japan

The chemical vapor deposition (CVD) using ethanol as the carbon source [1] has been a popular method to grow high-purity vertically aligned single-walled carbon nanotube (VA-SWNT) films. Ethanol contains oxygen atom, which is thought to thermally decompose and remove amorphous carbon and enhance the SWNT growth. In this study, we have synthesized VA-SWNT films by CVD method using dimethyl ether (DME), which has the same compositional formula as ethanol, as the carbon source. DME has an advantage in handling since it is gas in standard temperatures and pressures while ethanol is liquid. We obtained the growth curves of VA-SWNT films using in-situ optical absorbance measurement [2] and studied the dependence on the reaction temperature, the gas pressure and flow rate. Figure 1 shows the growth curves of VA-SWNT films grown from (a) DME and (b) ethanol, at the optimal temperature and pressure for the flow rate of 450 sccm. On varying the flow rate to 100 sccm for the same temperature and pressure, the two carbon sources clearly exhibit different parameter dependences. The overall results show that DME and ethanol have the different CVD condition suitable for growing VA-SWNT films reflecting the difference in the thermal decomposition characteristics. The results show that DME is also an efficient carbon source for growth of VA-SWNT films.

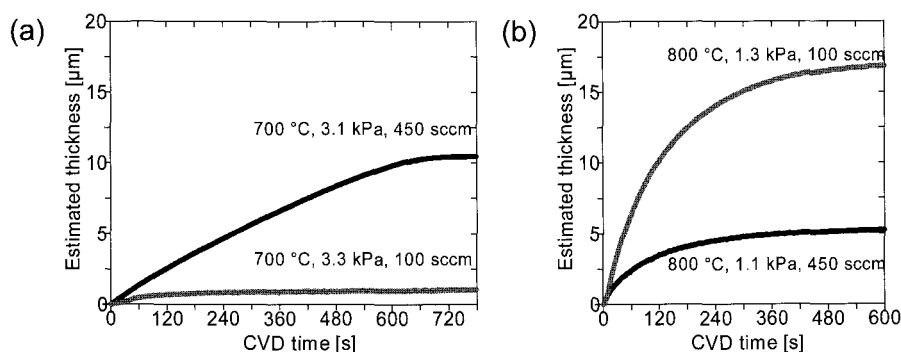


Fig. 1 Growth curves of VA-SWNT films grown from (a) DME and (b) ethanol.

[1] S. Maruyama, R. Kojima, Y. Miyauchi, S. Chiashi and M. Kohno, *Chem. Phys. Lett.*, **360** (2002) 229.

[2] S. Maruyama, E. Einarsson, Y. Murakami and T. Edamura, *Chem. Phys. Lett.*, **403** (2005) 320.

Corresponding Author: Shigeo Maruyama

TEL: +81-3-5841-6421, FAX: +81-3-5800-6983, E-mail: maruyama@photon.t.u-tokyo.ac.jp

Sorting of Single-Wall Carbon Nanotubes combined by Gel-Separation and Density-Gradient Ultracentrifugation

○D. Nishide¹, H. Liu^{1,2}, T. Tanaka¹, H. Kataura^{1,2}

¹*Nanotechnology Research Institute, AIST, Tsukuba, Ibaraki 305-8562, Japan*

²*JST, CREST, Kawaguchi, Saitama, 332-0012, Japan*

To investigate the intrinsic optical and electronic properties of single-wall carbon nanotubes (SWCNTs), sorting a single chirality of SWCNTs is one of the most important tasks, because SWCNTs are usually produced as mixture of various structures. Aiming at the solution, some methods for enrichment of specific SWCNTs were reported to date. For example, density gradient ultracentrifugation (DGU) can enrich (6,5) SWCNT using sodium cholate (SC) as a surfactant. However, it is known that obtained sample still contains small amount of metallic SWCNTs as an impurity. To solve this problem, in this work, we have combined two separation techniques, gel filtration and DGU to sort SWCNTs.

Pristine HiPco SWCNTs were firstly dispersed in SC solution, then isolated and purified by ultracentrifugation [1]. The supernatant was filtered through gel medium to separate metallic and semiconducting SWCNTs [2]. After obtaining semiconductor-enriched SWCNTs, the solution was sorted by DGU [3].

Fig. 1 shows optical absorption spectra of pristine, gel-filtered, and DGU operated SWCNTs solution. Final products showed successful enrichment of (6,5) SWCNT and most of metallic SWCNTs were well removed. Detailed protocols and characterization will be discussed.

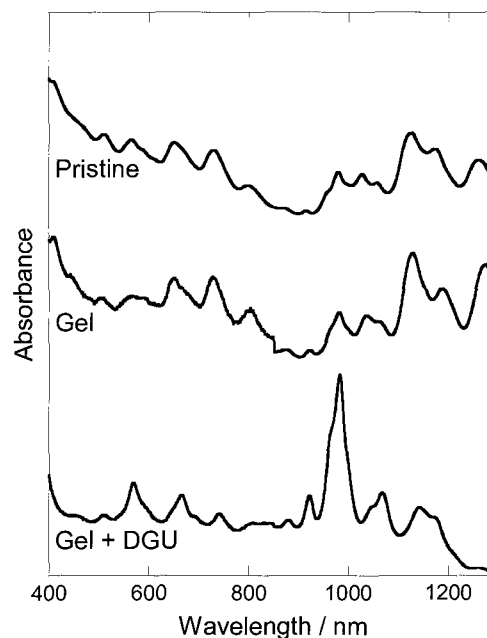


Fig. 1: Absorption spectra of pristine, gel-separated, and DGU operated SWCNTs.

[1] D. Nishide *et al.*, *Jpn. J. App. Phys.* **48** (2009) 015004.

[2] T. Tanaka *et al.*, *App. Phys. Exp.* **2** (2009) 125002.

[3] M. S. Arnold *et al.*, *Nat. Nanotechnol.* **1** (2006) 60.

Corresponding Author: Hiromichi Kataura

E-mail: h-kataura@aist.go.jp / **Tel:** +81-29-861-2551 / **Fax:** +81-29-861-2786

Preparation of single wall carbon nanotubes by CO₂ laser ablation method at room temperature

○Takashi Yamaguchi¹, Ryo Nakanishi¹, Ryo Kitaura¹, Shunji Bandow²,
Masako Yudasaka³, Hisanori Shinohara¹, Sumio Iijima^{1,2,3}

¹ Department of chemistry, Nagoya University, Nagoya 464-8602, Japan

² Department of materials science and engineering, Meijo University,
Nagoya 468-8502, Japan

³ National institute of advanced industrial science and Technology (AIST),
Tsukuba 305-8565, Japan

A preparation method of single wall carbon nanotubes (SWNTs) by using CO₂ laser at room temperature has been investigated. SWNTs prepared by using conventional laser ablation such as an Nd-YAG laser has been known to result in a highly crystalline structure. In the method, however an electric furnace is essential for the SWNT production. Moreover, its yield is too low (several mg/h). If large amount of SWNTs is required, we should choose other preparation methods such as arc discharge or chemical vapor deposition method.

In this presentation, we will report a highly efficient preparation method of SWNTs by CO₂ laser ablation at room temperature. A TEM image and a Raman spectrum of the SWNTs which we developed recently are shown in Fig. 1 and Fig. 2 respectively. The yield of the SWNTs is 10 - 20 mg/min (0.6 - 1.2 g/h) which is 2 orders of magnitude higher than that of conventional laser ablation method of SWNTs.

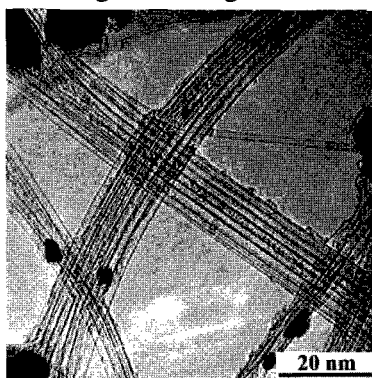


Fig. 1. A TEM image of SWNTs prepared by CO₂ laser ablation method

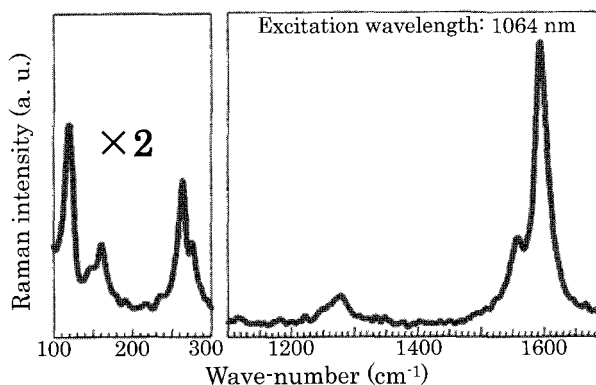


Fig. 2. A Raman spectrum of SWNTs prepared by CO₂ laser ablation method

Corresponding Author: Takashi Yamaguchi

E-mail: yamaguchi.takashi@b.mbox.nagoya-u.ac.jp

TEL: +81-(0)52-747-6503, FAX: +81-(0)52-747-6442

Carbon Spiral Helix, a Novel Nanoarchitecture Derived from Monovacancy Defects in Graphene

○ Lili Liu,¹ Xingfa Gao,² Shigeru Nagase,² Stephan Irle¹

*1. Institute for Advanced Research and Department of Chemistry, Nagoya University,
Furo-cho, Chikusa-ku Nagoya 464-8602, Japan*

*2. Department of Theoretical and Computational Molecular Science, Institute for Molecular
Science, Myodaiji, Okazaki 444-8585, Japan*

Graphene is considered one of the most remarkable materials in the area of nanometer-scale electronics, and imperfections are introduced into graphene unavoidably during graphene growth and the defects are known to significantly affect electronic and chemical properties. Monovacancy is one of the most important defects, which has attracted great attention due to its fundamental nature. Here the molecular and electronic structures of graphene monovacancy defects were studied by B3LYP/6-31G(d), GGA-PBE/DZP, and Self-Consistent-Charge Density-Functional Tight-Binding (SCC-DFTB) with finite electronic temperature (without and with spin-polarization included) methods. We studied the planar 5/9 and non-planar spiro monovacancy isomers whose relative stabilities are determined by their distance from the graphene edge using a structure model (See Figure 1). Different from

previous that describe graphene monovacancies only as a planar 5/9-isomer with lowered symmetry, we found that the non-planar spiro-isomer is the most stable structure for monovacancies when the defect is close to the graphene flake periphery ($d < 7 \text{ \AA}$). We also performed high-temperature thermal annealing using quantum chemical molecular dynamics (QM/MD) simulations based on the SCC-DFTB method, and found that an interior monovacancy defect is subject to migration towards the outermost periphery of a graphene flake, indicating an efficient route for defect healing.

The associated dihedral angles and considerable room-temperature stability make the spiro-isomer an ideal structural building block for the design and synthesis of carbon spiral helixes. Our results predict a family of novel carbon architectures that can be derived from graphene monovacancies (Figure 2).

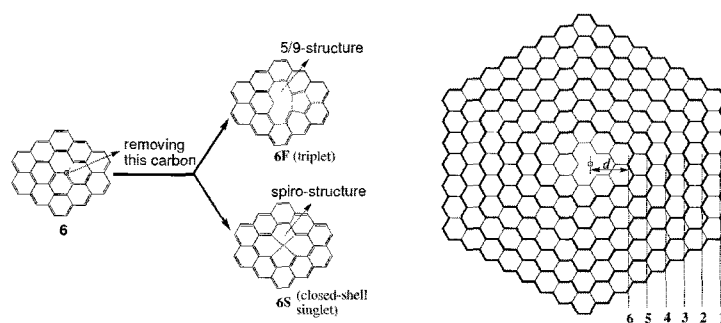


Figure 1: The calculation model and the structures of two kinds of monovacancies

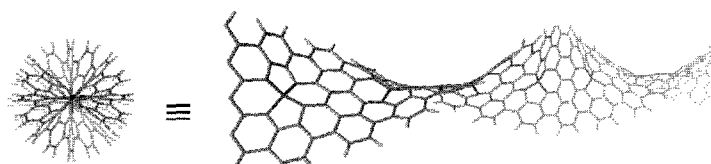


Figure 2: The novel spiral helix designed using graphene monovacancies.

Corresponding Author: Prof. Stephan Irle

TEL: +81-52-747-6397, FAX: +81-52-788-6151, E-mail: sirle@iar.nagoya-u.ac.jp

DFT investigation of stability of adatom adsorption on graphene

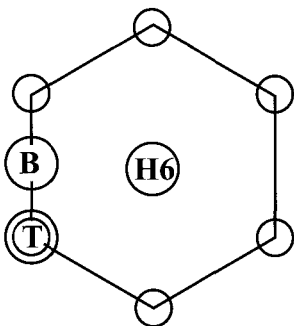
K. Nakada^{1,2}, A. Ishii^{1,2}

¹Department of Applied Mathematics and Physics, Tottori University

²JST-CREST

Email: nakada@damp.tottori-u.ac.jp

DFT calculation of various atomic species on graphene sheet is investigated as prototypes for formation of nano-structures on carbon nanotube(CNT) wall. We investigate computationally adsorption energies and adsorption sites on graphene sheet for a lot of atomic species including transition metals, noble metals, nitrogen and oxygen, from atomic number 1 to 83, using the DFT calculation as a prototype for CNT. The calculations are done for adatom at three site having symmetry, H6, B and T on 3 x 3 super cell. We discuss stability of the adatom in the graphene by analysis from the electronic structure. The calculated results show that adsorption in the H6-site mainly and, in metal and the transition metal element, the nonmetallic element showed the tendency which adsorbed in the B-site. We present analysis and the tendency of each detailed electronic state in conference.



The three adsorption sites of graphene sheet, T, B and H6.

Preparation and Evaluation of Graphene by Cleavage Method

○K.Matsuyama , T.Maeda , N.Iwata , H.Yamamoto
College of Science and Technology, Nihon University,

7-24-1 Narashinodai, Funabashi, Chiba 274-8501, Japan

In recent years, graphite intercalation compounds (GIC) is prepared on various substances^[1-3]. Superconducting transition temperature T_c of GIC with Ca are reported at 11.5K^[1]. According to the BCS theory, the T_c is expected to be higher than room temperature. However, as far as we know, the highest T_c of graphite is 11.5K mentioned above^[1], and the major reason why the room temperature T_c is not realized is expected to be disorder of graphene layers. A double layer graphene with intercalated metal atoms is promising materials showing much higher T_c , because the reduction of the disorder is expected.

As a first step to achieve high temperature superconductivity, a few or less graphene layers were prepared. Graphene was made by the cleavage method with a scotch tape. A SiO₂/Si (the oxide film thickness 300 nm and 90 nm) substrate was used to distinguish the nm-order thickness of transferred graphene on the substrate by only optical microscope.

Graphene was searched with the optical microscope, and measured by Raman spectroscopy. Raman peak of graphene is different from graphite. Afterwards, thickness is measured by Atomic Force Microscope (AFM).

Figure 1 shows (a) graphite Raman spectrum and (b) Raman spectrum of transferred few-layers graphene made by cleavage method. From the result of the Raman spectroscopy, it was confirmed that the 2D peak shifted to the lower wavelength side by approximately 40cm⁻¹. Peak intensity of 2D became higher than that of G peak, indicating the presence of mono-layer graphene. The AFM observation showed that the thickness of the specimen was approximately 1nm, which was consistent with the results of monolayer graphene reported in reference^[4]. Graphene-preparation method, and electric properties will be discussed in detail.

References: 1) Akimitsu, "parity", MARUZEN, **05**(2008)6-12, 2) K.Kadowaki, "Superconductivity", **1**(2007)460-462, 3)M. Ellerby, "Condensed Matter", **378-380**(2006)636-639, 4)T.Inoshita, "Journal of the Physical Society of Japan", **43**(1977)1237

Corresponding Author Keiichirou Matsuyama E-mail : g0905107ux@yahoo.co.jp; 047-469-5457

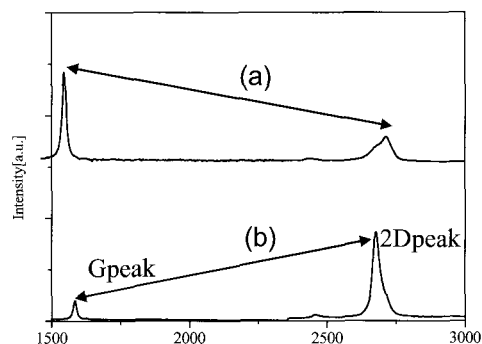


Fig.1 The Raman spectra of the typical graphite and the specimen nominated as a single-layered graphene

Raman spectroscopy of few-layer graphene grown on graphene flakes

°R. Negishi¹, H. Hirano¹, Y. Kobayashi¹, Y. Ohno², K. Maehashi², K. Matsumoto²

¹Department of applied physics, Osaka University, 2-1 Yamadaoka Suita 565-0871, Japan

²ISIR, Osaka University, 8-1 Mihogaoka, Ibaraki 567-0047, Japan

Graphene, a two-dimensional honeycomb lattice of sp^2 bonded carbon atoms, has recently attracted considerable attention because of its novel electrical properties, such as high carrier mobility [1], long range ballistic transport at room temperature [2] and quantum confinement [3]. For the application of nano-devices including graphene as a building block, reliable technique for controlling the number of layers and edge structures in graphene is required. In this work, we report a novel process to control the graphene film thickness through layer-by-layer growth of graphenes on template graphene flakes by using multi-temperature chemical vapor deposition (CVD) system.

We mechanically peeled off graphene flakes from natural graphite and stuck them onto a $\text{SiO}_2(300\text{nm})/\text{Si}$ substrate as the growth template. The graphene was grown using CVD apparatus. Figure 1 shows the typical examples of optical microscope images of graphene flakes (a) before and (b) after CVD growth. A weak contrast region is observed between two thick graphite flakes showing metallic gloss (Fig. 1(a)). As shown in Fig. 2(a), a typical 2D-band Raman spectrum (532-nm excitation) obtained from the weak contrast region can be decomposed into Raman signals of one main Lorentzian peak around 2687 cm^{-1} and three Lorentzian sub-peaks. This result indicates that the bilayer graphene is observed with the weak contrast [4]. After CVD growth, we should note that contrast of this weak contrast region becomes remarkably strong as shown in Fig. 1(b). The Raman signal obtained from the strong contrast region can be decomposed into one main Lorentzian peak around 2698 cm^{-1} and one Lorentzian sub-peak. This result demonstrates the formation of six-layers graphene from bilayer graphene [4]. Figure 3 shows the graphene flakes (a) before and (b) after CVD growth under the higher temperature condition for the thermal decomposition of carbon feedstock and the graphene growth in CVD process. Dramatic changes by CVD growth are recognized in the contrast observed from the graphene flake. Raman spectrum obtained from the graphene flake after CVD growth was quite similar to that of bulk graphite as shown in Fig. 3(c). Since the graphene after CVD growth shows a uniform contrast, we conclude that the layer-by-layer growth of graphenes on graphene flake progresses during the CVD growth.

[1] K. S. Novoselov et al., *Science* **306** (2004) 666. [2] C. Berger et al., *Science* **312** (2006) 1191.

[3] S. Moriyama et al., *Nano Lett.* **9** (2009) 2891. [4] D. Graf et al., *Nano Lett.* **7** (2007) 238.

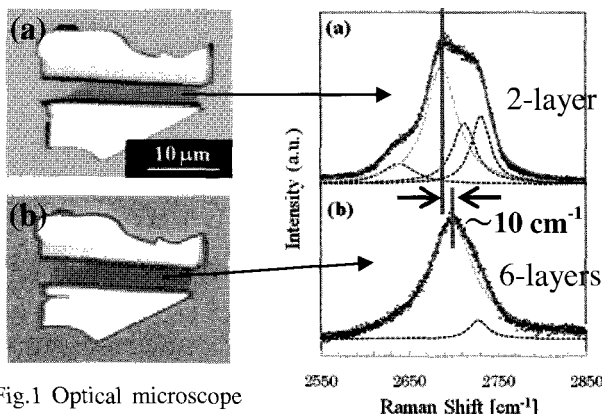


Fig.1 Optical microscope images of graphene (a) before and (b) after CVD growth.

Fig.2 Raman spectra obtained from graphene (a) before and (b) after CVD growth.

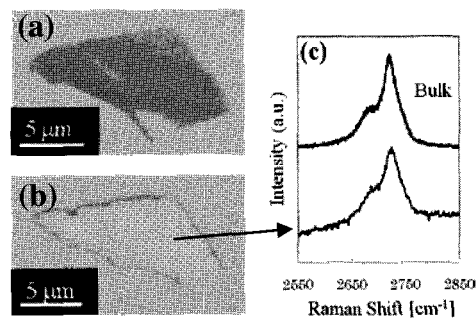


Fig.3 Optical microscope images of graphene (a) before and (b) after CVD growth. (c) Raman spectra obtained from thick graphite and graphene flakes as shown in Fig. 3(b), respectively.

Corresponding Author: R. Negishi, TEL: +81-66879-4684, E-mail: Negishi@ap.eng.osaka-u.ac.jp

Photomodification of Fullerene Bilayer Vesicles and Control of their Membrane Permeability to Water

○Akimitsu Narita¹, Koji Harano¹, Eiichi Nakamura^{1,2}

¹Department of Chemistry, The University of Tokyo, Tokyo 113-0033, Japan

²ERATO, JST, Tokyo 113-0033, Japan

Amphiphilic fullerene $\text{Ph}_5\text{C}_{60}\text{K}$ (**1**) self-assembles in water to form spherical bilayer vesicles with an average diameter of ca. 34 nm (Figure 1). The fullerene vesicles possess unique properties such as high thermal stability and low water permeability, which is considered to be due to the close packing of rigid fullerene cores in the membrane [1]. We envisioned that the fullerene vesicles can be modified by employing photoreactivities of the fullerene to control the membrane properties. In this work, we carried out photomodification of the fullerene vesicles in two ways, namely, post- and pre-modification, which allowed control of the membrane permeability to water (Figure 2).

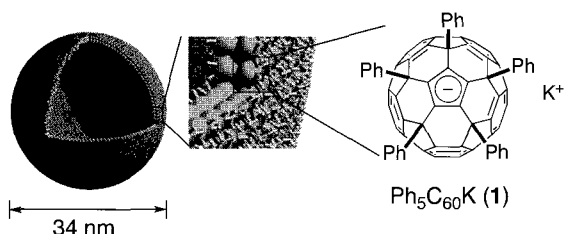


Figure 1. An image of a fullerene bilayer vesicle formed from $\text{Ph}_5\text{C}_{60}\text{K}$ (**1**) in water.

Post-modification was conducted by UV irradiation to preformed vesicles and induced photoaddition reactions between the neighboring fullerene cores in the fullerene membrane. Although concomitant photooxidation was inevitable, the water permeability of the fullerene membrane was reduced due to the tightening of the membrane packing. In contrast, pre-modification by photomodification of $\text{Ph}_5\text{C}_{60}\text{K}$ (**1**) prior to the vesicle formation resulted in the photooxidation of the fullerene cores without photoaddition reactions. The water permeability was enhanced due to looser packing in the fullerene membrane.

Thermodynamic analyses using the Eyring equation revealed that the pre- and the post-modified membrane works as an entropy barrier against the water permeation, retaining the unique nature of the fullerene membrane. The pre-modification resulted in the reduction of the entropy barrier as well as the enhancement of the enthalpy barrier. In contrast, the post-modified vesicles showed enhanced entropy barrier and reduced enthalpy barrier.

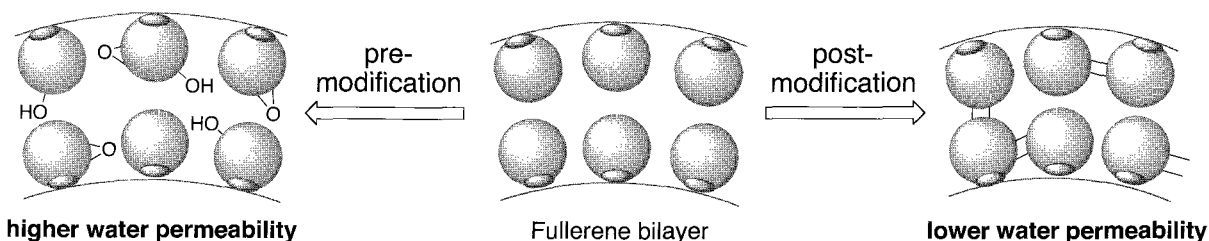


Figure 2. Schematic illustration of pre- and post-modification of the fullerene membrane.

[1] Isobe, H.; Homma, T.; Nakamura, E. *Proc. Natl. Acad. Sci. U.S.A.* **2007**, *104*, 14895–14898.

Corresponding Author: Eiichi Nakamura

TEL: +81-3-5841-4356, FAX: +81-3-5841-4356, E-mail: nakamura@chem.s.u-tokyo.ac.jp

This work is supported by the Global COE Program for Chemistry Innovation.

Fabrication of transparent conductive films using carbon nanotubes encapsulating metal-nanowires

Daeheon Choi¹, Ryo Kitaura¹, Miyata Yasumitsu¹, Hisanori Shinohara*¹,

¹ *Department of Chemistry & Institute for Advanced Research, Nagoya University,
Nagoya 464-8620, Japan*

Transparent conducting films (TCFs) based on carbon nanotubes (CNTs) have attracted significant interests for alternative of indium tin oxide (ITO). There are two important factors for the fabrication of high-performance CNT-TCFs: high electric conductivity and high transparency. In general, electric conductivity of CNT-TCFs is greatly affected by electronic structure of CNTs. If CNT networks are consisted with only metallic tubes, the TCFs are expected to perform high electric conductivity. Furthermore, high electric conductivity also leads to high transparency, because one can reduce thickness of the film with retaining high electric conductivity.

Doping of various atoms and molecules into CNTs inner-hole, generally leads to stable modulation of CNTs electronic structure. Recently developed high-yield doping technique enables us to prepare CNT-TCFs with highly doped CNTs. In particular, metal-nanowire doped CNTs are expected to be metallic CNTs. In this study, we have prepared various TCFs with highly doped CNTs and characterized by electron microscopy, Raman, absorption spectroscopy and 4-probe conductivity measurements.

SWCNTs synthesized by the arc-discharge method (FHP-SO, meijo nano carbon inc.) were used in this study. Eu-nanowires@SWCNTs and fullerene-peapods were synthesized according to the previously reported procedures. [1, 2] The estimated filling ratio of Eu and C₆₀ is ca. 90%. CNT-TCFs were fabricated by vacuum filtration method and transferred to a quartz substrate. As shown in Figure 1, CNTs form uniform network structure without amorphous like impurity. Sheet resistance of CNT-TCFs using pristine SWCNTs is 200-400 ohm/sq with transmittance of 70%. In this poster presentation, we will discuss doping effects of the CNT-TCFs in detail.

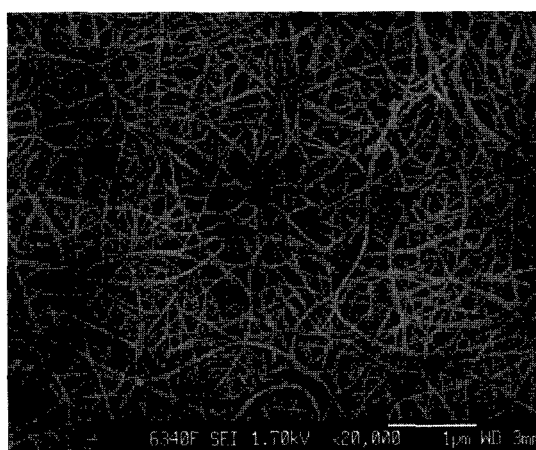


Figure 1. SEM image of CNT networks employed

References:

- [1] R. Kitaura et al., Nano Lett. 8 693 (2008)
- [2] R. Kitaura et al., Angew. Chem. Int. Ed. (2009)

*Email address: noris@nagoya-u.jp

Growth control of Multi-Walled Carbon Nanotubes for fuel cell

○Shinya Kitamura, Rika Yamamoto, Takeshi Hashishin, Jun Tamaki

Department of Applied Chemistry, Ritsumeikan University, Shiga 525-8577, Japan

In this study, the current collector composed of multi-walled carbon nanotubes (MWNTs) directly grown on the surface of carbon paper (CP) was prepared to improve an electrical connection between MWNTs and CP. This structure contributes to reduce ohmic losses at the interface of MWNTs and CP, leading to an efficient electron transfer. Based on this research background, we tried to control the graphitization of MWNTs by the growth conditions of CVD method.

At first, the CP oxidized by 0.1 M HNO₃ aqueous solution was coated with nickel by electroless plating (Ni / CP). After the Ni / CP set in quartz tube equipped with an electric furnace, MWNTs were grown from Ni / CP by ethanol CVD method at 700°C for 60 min (MWNTs / CP). The morphology of the synthesized MWNTs was examined by FE-SEM and Raman spectroscopy.

According to the SEM observation, the as-grown MWNTs on the CP composed of discrete carbon fibers with ca. 5 μm in diameter had the size of 40-90 nm in diameter and 3-10 μm in length (Fig. 1 (a) and (b); the background vacuum of (a) is 10 times than that of (b) within quartz tube during ethanol CVD). The relative intensity ratio of the G-band to the D-band peak of Raman scattering spectra in Figs. 1 (a) and (b) are 8.3 and 0.6, respectively, indicating that the graphitization of MWNTs as shown in Fig. 1 (a) is higher than that in Fig. 1 (b).

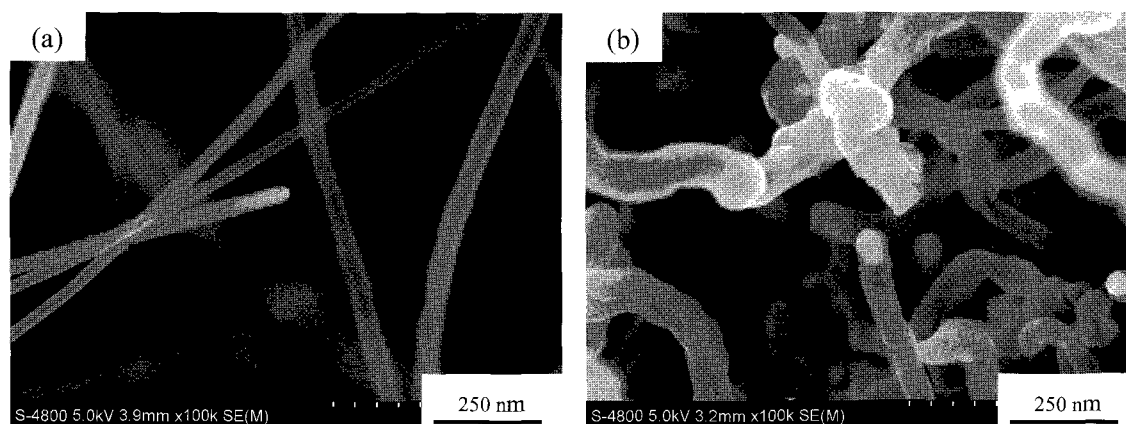


Fig. 1. SEM images of MWNTs

TEL: 077-566-1111 (ext. 8413), FAX: 077-561-2659, E-mail: hasisin@sk.ritsumei.ac.jp

Synthesis of Highly Electron Accepting [60]Fullerene Bisadduct

○Riyah S. Arastoo,^a Ken Kokubo,^{a,b} Hao Geng,^b Hsing-Lin Wang,^c Takumi Oshima,^a
and Long Y. Chiang^b

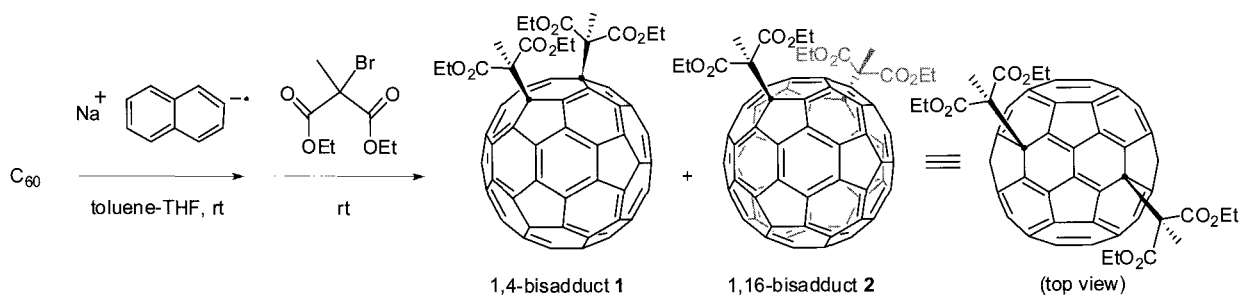
^a*Division of Applied Chemistry, Graduate School of Engineering, Osaka University,
Suita, Osaka 565-0871, Japan*

^b*Department of Chemistry, University of Massachusetts Lowell, Lowell, MA 01854, USA*

^c*Physical Chemistry Group, Chemistry Division, Los Alamos National Laboratory,
Los Alamos, NM 87545, USA*

High electron accepting ability of fullerenes and their derivatives is one of the most attractive and useful properties in view of the application of nanocarbon materials to electronic and optoelectronic devices. Chemical modifications of [60]fullerene are commonly used to bring about the improvement of solubility and many other desirable properties. However, the introduction of two substituents on fullerene 60 carbons (58π system) tends to lower its electron accepting ability as compared to that of pristine 60π system.

In the course of our study of an intriguing emerald green [60]fullerene hexaadduct $C_{60}[CCH_3(COOR)_2]_6$ synthesized by reductive coupling of [60]fullerene with bromomethylmalonate via fullerene anions C_{60}^{n-} [1], we succeeded in isolating the similar bisadducts $C_{60}[CCH_3(COOEt)_2]_2$ [2] and characterized them as 1,4-bisadduct **1** and 1,16-bisadduct **2** by NMR, UV-Vis-NIR, MS, and X-ray structural analysis. The latter minor adduct **2** which has two malonate substituents in rather remote positions (1,6-addition) showed the absorption bands in NIR region ($\lambda_{max} = 706, 806, \text{ and } 906 \text{ nm}$) as well as the higher electron accepting ability (first reduction potential $E_{1red}^0 = -0.73 \text{ V vs Ag/Ag}^+$ in *o*-DCB) than those of pristine [60]fullerene (-0.82 V) and major bisadduct **1** (-0.95 V).



[1] Canteenwala, T.; Padmawar, P. A.; Chiang, L. Y. *J. Am. Chem. Soc.* **2005**, *127*, 26. [2] Kokubo, K.; Thota, S.; Wang, H.-L.; Chiang, L. Y. *J. Macromol. Science, Part A: Pure and Appl. Chem.* **2009**, *46*, 1176.
Corresponding Author: Ken Kokubo

TEL: +81-6-6879-4592, FAX: +81-6-6879-4593, E-mail: kokubo@chem.eng.osaka-u.ac.jp

Electronic transport properties of doped nanotube heterostructure

○Masahiro Sakurai and Susumu Saito

*Department of Physics, Tokyo Institute of Technology
2-12-1 Oh-okayama, Meguro-ku, Tokyo 152-8551, Japan*

Carrier doping into carbon nanotube affects its electronic structure and may induce various interesting phenomena because of the low dimensionality of the system. For example, superconductivity in boron-doped carbon nanotubes has been experimentally and theoretically discussed [1]. For the electronic transport properties, carrier doping also plays an important role. A p - n junction consists of two semiconductor regions with opposite type doping and is one of the fundamental building blocks for modern semiconductor devices. Not only electrostatic doping by gate electrodes [2] but also modulation doping by boron- and nitrogen-substitution can lead to a nanotube p - n junction which has a high potential importance for nanoelectronics devices.

In this work, we study electronic transport properties of nanotube heterostructure (p - n junction) by first-principles method [3] based on the density-functional theory (DFT). Figure 1 shows the junction structure which consists of B-doped and N-doped (10,0) carbon nanotubes. The junction region connects two semi-infinite carbon nanotubes with different impurities and contains the unit cells of both B-doped and N-doped carbon nanotubes. The Hamiltonian for the entire system is constructed from the Hamiltonian matrices for three separated regions and intercell matrices. These matrices are given by the DFT electronic-structure calculation for each region. Matrix size is reduced by basis transformation from plane-wave basis into Gaussian-orbital basis. Transmission probabilities are calculated using Green's function scheme. We will report on the current-voltage (I - V) characteristics of the system from a perspective of potential applications.

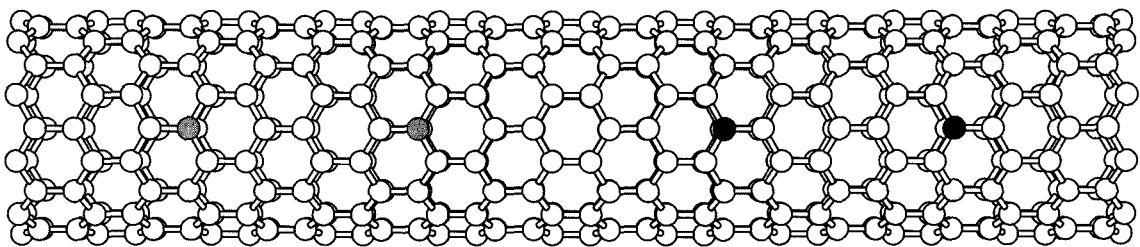


FIG. 1. Schematic picture of nanotube heterostructure consisting of boron- and nitrogen-doped carbon nanotubes. White, shaded, and black circles represent C, B, and N atoms, respectively.

References:

- [1] I. Takesue *et al.*, *Phys. Rev. Lett.* **96**, 57001 (2006); N. Murata *et al.*, *Phys. Rev. Lett.* **101**, 027002 (2008); T. Koretsune and S. Saito, *Phys. Rev. B* **77**, 165417 (2008).
- [2] J. U. Lee, P. P. Gipp, and C. M. Heller, *Appl. Phys. Lett.* **85**, 145 (2004).
- [3] T. Matsumoto and S. Saito, *Physica E* **29**, 560 (2005).

Corresponding Author: Masahiro Sakurai

E-mail: sakurai@stat.phys.titech.ac.jp

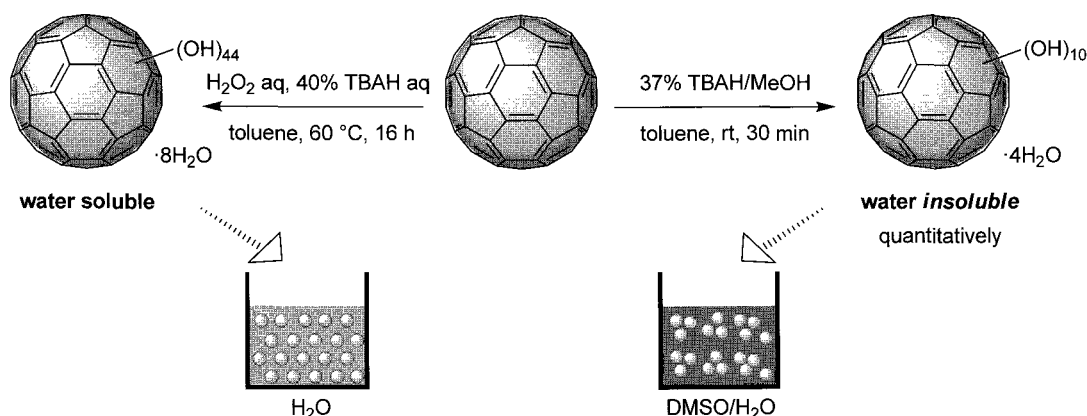
Facile Synthesis of Water-Insoluble Lowly Hydroxylated Fullerenol and its Nanoparticle Property

○Naoki Kobayashi, Ken Kokubo, and Takumi Oshima

*Division of Applied Chemistry, Graduate School of Engineering, Osaka University,
Suita, Osaka 565-0871, Japan*

Polyhydroxylated fullerene, so-called fullerenol, has attracted much attention in the field of life science and materials chemistry in view of its bioactivities including high antioxidant ability and low toxicity as compared with pristine fullerene or other derivatives. To access to this class of compounds, several synthetic methods have already been reported so far, *e.g.*, Oleum method for $C_{60}(OH)_{12}$ [1], NaOH/TBAH for $C_{60}(OH)_{24-26}$ [2], and H_2O_2 for $C_{60}(OH)_{36} \cdot 8H_2O$ [3], and some of them have been commercially available. However, the Oleum method as well as other methods giving water insoluble lowly hydroxylated fullerenols ($C_{60}(OH)_n$; $n < 16$) requires a hazardous reagent and multi steps.

In this study, we succeeded in synthesizing the water-insoluble moderately hydroxylated fullerenol $C_{60}(OH)_{10} \cdot 4H_2O$ quantitatively from C_{60} only using methanolic solution of tetra-*n*-butylammonium hydroxide (TBAH) as a hydroxylation reagent under very mild condition. The analysis of nanoparticle property of this fullerenol in DMSO/ H_2O (1:1 v/v) solution by Induced Grating (IG) method revealed its aggregation nature as compared with the high dispersion nature of $C_{60}(OH)_{44} \cdot 8H_2O$ in aqueous solution which was previously synthesized using the similar H_2O_2 /TBAH method.



[1] Chiang, L. Y.; Wang, L.-Y.; Swirczewski, J. W.; Soled, S.; Cameron, S. *J. Org. Chem.* **1994**, *59*, 3960.

[2] Li, J.; Takeuchi, A.; Ozawa, M.; Li, X.; Saigo, K.; Kitazawa, K. *J. Chem. Soc., Chem. Commun.* **1993**, 1785.

[3] Kokubo, K.; Matsubayashi, K.; Tategaki, H.; Takada, H.; Oshima T. *ACS Nano* **2008**, *2*, 327.

Corresponding Author: Ken Kokubo

TEL: +81-6-6879-4592, FAX: +81-6-6879-4593, E-mail: kokubo@chem.eng.osaka-u.ac.jp

Highly Localized Photoelectrochemical Reaction of an Isolated Single-Walled Carbon Nanotube at Metal Nanogap

○Mai Takase, Hideki Nabika, Satoshi Yasuda, Kei Murakoshi

*Division of Chemistry, Graduate School of Science, Hokkaido University,
Sapporo, 060-0810, Japan*

Controlling and understanding the localized photoelectrochemical response on a single isolated SWNT have important issues for the development of novel photoenergy and optoelectronic information transducers. SWNT may play an important role as unique ultra-small functionalized unit to detect, convert, and modulate localized electromagnetic field induced by localized surface plasmon at vicinity of metal surface. Recently, we have succeeded in fabrication of optimized metal nano-dimer arrays for obtaining intense local surface plasmon [1, 2]. In the present work, we investigate the characteristics of electronic structure and optical property of a single SWNT at highly localized electromagnetic field at metal nano-gap by *in-situ* surface-enhanced Raman scattering (SERS) measurement under electrochemical potential control. The SERS spectra clearly showed that a single isolated SWNT is located at the gap of the nano-dimer structure. It was found that the intensities of vibrational bands in *in-situ* SERS spectrum depended upon the electrochemical potential. Absolute potential of the Fermi level of a single SWNT was determined based on the model of electron doping/undoping at SWNTs as shown Fig. (a) [3]. Highly localized photochemical reaction of a single SWNT was also induced under the same condition. Over the duration under certain power of photo-irradiation, the intensity of RBM decreased, but in contrast, the intensity of D-band increased with time (Fig. (b)), reflecting local photo oxidation of SWNT. These results prove successful control on structure of a single SWNT in localized electromagnetic field.

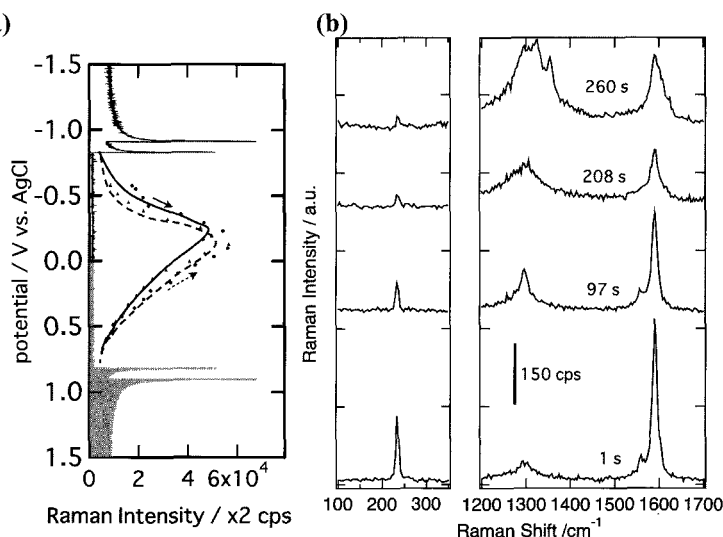


Figure (a) Electrochemical potential dependence of RBM Raman intensity of a single (17, 2) SWNT ($\omega_{\text{RBM}} = 160 \text{ cm}^{-1}$, $d = 1.42 \text{ nm}$) and the band position. (b) SERS spectrum of a single (11, 3) SWNT ($\omega_{\text{RBM}} = 234 \text{ cm}^{-1}$, $d = 1.00 \text{ nm}$) under photo-irradiation.

- [1] Y. Sawai, B. Takimoto, H. Nabika, K. Ajito, K. Murakoshi, *J. Am. Chem. Soc.*, **129**, 1658-1662 (2007)
 [2] M. Takase, S. Yoshitaka, H. Nabika, K. Murakoshi, *Trans. Mater. Res. Soc. Jpn.*, **32**, 409-412 (2007)
 [3] K. Okazaki, Y. Nakato, K. Murakoshi, *Phys. Rev. B* **68**, 035434 (2003)

Corresponding Author: Mai Takase

E-mail: maitakase@mail.sci.hokudai.ac.jp, Tel: +81-(0)11-706-4662, Fax: +81-(0)11-706-4810

Preparation of TiO₂-filled MWNTs

○Hidehiro Ikenoko, Takeshi Hashishin, Jun Tamaki

Department of Applied Chemistry, Ritsumeikan University, Shiga 525-8577, Japan

Recently, CNTs have attracted a lot of attention because of their unique physical and chemical properties. Interestingly, there are also utilizable spaces inside CNTs for filling materials such as metal, metal oxide, their composites and so on. Filling of semiconductive oxides inside MWNTs has one of possibility to discover its new functionalization.

In this study, we tried to prepare SnO₂ inside/outside MWNTs, and NO₂ clarify the adsorption property of NO₂ depended on the precipitation state of SnO₂[1]. Especially, SnO₂ inside MWNTs indicated the excellent adsorption properties of NO₂[1,2]. This phenomenon was considered to be based on increasing the depletion layer caused by p-n junction[3]. In this study, TiO₂-filled MWNTs were prepared to investigate the gas adsorption.

MWNTs (inside diameter 20~50 nm) was immersed in conc. nitric acid and the oxidized-MWNTs were agitated at 120 °C for 6 hr, and continuously dispersed in each TiCl₄ solution (concentration: 0.32×10^{-2} , 0.98×10^{-1} , 1.6×10^{-1} wt %), and agitated for one night after vacuumed at 10 torr. In addition, the precursor inside MWNTs was washed and dried at 80 °C for one night. Moreover, the precursor inside MWNTs was annealed at 600 °C for 6hr in Ar and at 400 °C for 3 hr in Air.

TEM images of TiO₂ inside MWNTs shown in Fig.1 indicated that sample B had a good filling state.

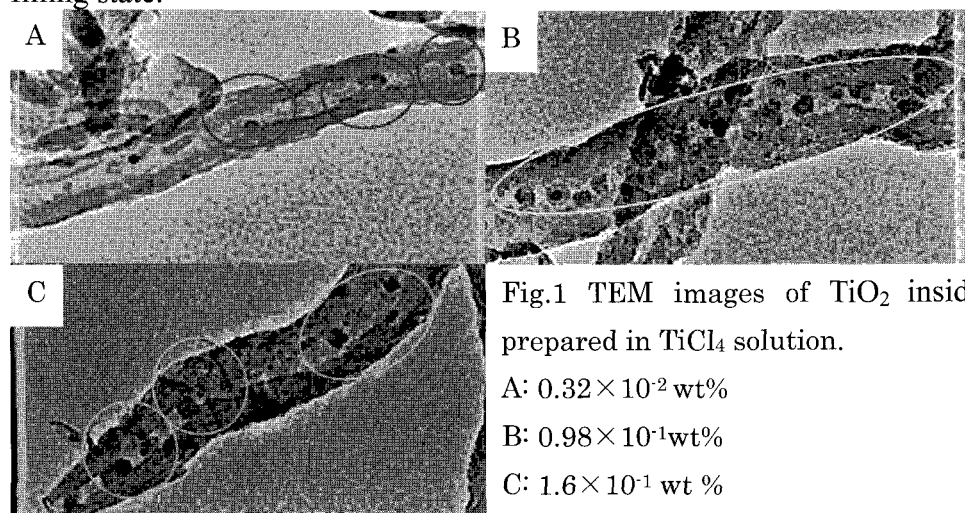


Fig.1 TEM images of TiO₂ inside MWNTs prepared in TiCl₄ solution.

A: 0.32×10^{-2} wt%

B: 0.98×10^{-1} wt%

C: 1.6×10^{-1} wt %

References:

- [1] Takahiro Kishi, Takeshi Hashishin, Jun Tamaki, *Proc. of PRIME 2008*, 2702 (2008).
 [2] Takahiro Kishi, Takeshi Hashishin, Jun Tamaki, *Chemical Sensor Symposium*, **47**, 55 (2009).
 [3] Takeshi Hashishin, Jun Tamaki, *Sensors and Materials*, **21**, 265, (2009).

Corresponding Author: Takeshi Hashishin, Jun Tamaki

E-mail: hasisin@sk.ritsumeikan.ac.jp, juntrc@sk.ritsumeikan.ac.jp

Tel: +81-77-566-1111(Ext. 8413) Fax: +81-77-561-2659

Stark effect of SWNT photoluminescence induced by external electric field

○ Yuji Kawai, Hideyuki Maki, Tetsuya Sato

*Department of Applied Physics and Physico-Informatics, Faculty of Science and Technology
Keio University, Hiyoshi, Yokohama 223-8522, Japan*

Single-walled carbon nanotubes (SWNTs) have attracted great attention for nano-size opto-electronic device applications because of its outstanding physical properties and its sensitivity to external inputs. Stark shifting of the optical transition energy is an effect that could lead to such application. Although external field induced stark effect of SWNT has been measured from the absorption spectrum [1], it has never been observed from the luminescence of SWNTs. In this study we fabricated a suspended SWNT transistor and measured the photoluminescence (PL) spectrum in order to observe the stark effect from the PL of SWNT.

PL measurements were performed at low temperature (~ 10 K) in an optical cryostat. A single SWNT was excited with a focused laser and the PL was measured spectroscopically. A mapping measurement was performed by moving the device and taking the spectra at each 500nm step. The mapping image of the background and the PL peak from a SWNT are shown in Fig. 1(a) and (b) respectively. The color scale represents the spectrally integrated intensity. The relatively black parts in Fig. 1(a) are the electrodes, and a PL peak from a SWNT was observed between the source and drain electrodes. When drain voltage (V_{sd} : parallel to the SWNT axis) was applied to this device, stark shifting of the peak energy was observed. The black crosses in Fig. 2 indicate V_{sd} and the red dots indicate the emission energy from the SWNT. The peak red-shifted when negative voltage was applied and blue-shifted when positive voltage was applied. This asymmetry can be explained by considering the structure of the device. Because Pt (high work function compared to SWNT) is used as the electrode, the energy band of the SWNT is spatially bent making a strong built-in electric field at the SWNT-electrode interface. This local electric field, which contributes strongly to the stark effect, can become stronger or weaker depending on the applied V_{sd} inducing the stark effect in an asymmetric manner.

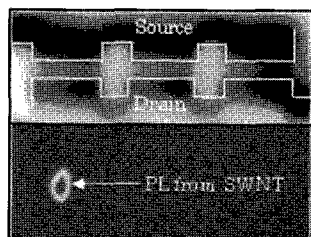


Fig. 1 Mapping image of the integrated spectrum
(a)Background, (b)PL from SWNT

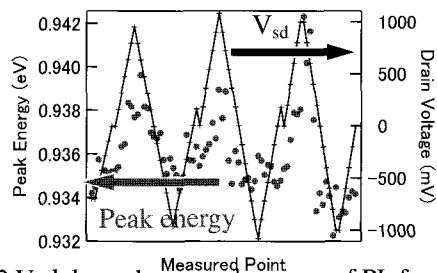


Fig. 2 V_{sd} dependence peak energy of PL from SWNT

[1] D.Aditya, et.al., Nano lett., 8, 1, 142 (2008)

E-mail:maki@appi.keio.ac.jp TEL:045-566-1643

発表索引
Author Index

Author Index

～A～

Abe, Katsuyoshi 3P-24
 Achiba, Yohji 2P-25, 2P-30, 3-4, 3P-12,
 3P-4
 Aikawa, Shinya 1P-27
 Akasaka, Takeshi 1P-32, 1P-36, 1P-40, 2-2
 Akiba, Eiji 3S-5
 Akiyama, Kimio 2P-6
 Ando, Yoshinori 3P-9
 Aoki, Nobuyuki 2-7
 Aoki, Yasushi 2-13
 Aoki, Yusuke 2-3
 Aoyagi, Shinobu 2-4, 2P-10
 Arastoo, Riyah S. 3P-36
 Araujo, Paulo T. 1P-8
 Asada, Yuki 1-2, 2P-37, 1P-33
 Asaka, Koji 1P-23, 1P-39
 Asano, Hirohito 1P-30

Ashihara, Masaaki 3P-8
 Azuma, Toshiyuki 2P-30

～B～

Bandow, Shunji 1P-30, 3P-28, 3P-9
 Briggs, G. Andrew D. 2P-12

～C～

Chen, Shimou 1-14
 Chen, Zhihong 3-7
 Chiang, Long Y. 3P-36
 Chiashi, Shohei 1P-2, 1P-27, 3-5, 3P-23,
 3P-26, 3P-6
 Chiba, Tasuku 2P-19
 Choi, Daeheon 3P-34
 Clark 1P-24

～D～

Doi, Tatsuya 2-7
 Duin, Adri van 2P-11

～E～

Einarsson, Erik 1P-27, 1P-41, 3-2, 3P-19,
 3P-23

Enoki, Toshiaki 3-10
 Est, Art van der 2-5

～F～

Farmer, Damon B. 3-7
 Feng, Ye 1P-12, 3P-16
 Fueno, Hiroyuki 1P-6
 Fujigaya, Tsuyohiko 1-12, 1-15, 1P-19, 1P-25,
 1P-35, 2P-24
 Fujii, Shunjiro 1-9, 3P-16
 Fujimoto, Yoshitaka 1P-1
 Fujino, Masahisa 1-16
 Fujino, Tatsuya 2P-25
 Fujiwara, Yuji 3P-3
 Fukumaru, Takahiro 1P-35
 Furuichi, Koji 2P-39
 Furukawa, Takeo 1P-26, 1P-31

～G～

Gao, Xingfa 3P-29
 Geng, Hao 3P-36
 Ghorannevis, Zohreh 1P-34
 Gimenez-Lopez, Maria del Carmen 2P-12
 Gion, Kazuki 1P-29
 Goto, Motoshi 2P-30
 Gotoh, Hideki 1-3

～H～

Hakamatsuka, Mari 1P-16
 Hannon, James B. 3-7
 Haque, Md. Mahbulul 1P-7
 Hara, Hironori 1P-37
 Harano, Koji 2-6, 3P-33
 Hasegawa, Kei 2P-34, 3P-17, 3P-5
 Hasegawa, Masayuki 1P-3
 Hashimoto, Masaki 3P-8
 Hashishin, Takeshi 2P-41, 3P-35, 3P-40
 Hasobe, Taku 2-5
 Hata, Koichi 3P-22, 3P-3
 Hatakeyama, Rikizo 1-10, 1P-34, 2-9, 3P-1, 2P-1
 Hayashi, Tsugumi 2-1
 Hayashi, Yasuhiko 1P-20, 3P-24

Heguri,Satoshi	2P-22	Ishizuki,Yoshikatsu	1-16
Hibino,Hiroki	1-3	Isobe,Hiroyuki	2-6
Hibino,Norihito	1-4	Ito,Daiki	1P-20
Hino,S.	2-10, 2-3	Ito,Osamu	2-5
Hiramatsu,Norihiro	3P-6	Ito,Yasuhiro	2-3, 2P-12
Hirana,Yasuhiko	2P-42	Iwai,Taisuke	1-16
Hirano,Hiroki	3P-32	Iwamoto,Tomohiro	3P-21
Hirose,Kaori Takai	3P-2	Iwata,Nobuyuki	2P-16, 3P-20, 3P-31
Hisada,Daijiro	3P-3	Izumi,Noriko	2-3
Hiura,Hidefumi	3S-6		
Homma,Tatsuya	2-6	~J~	
Homma,Yoshikazu	3P-6	Jimbo,Takashi	1P-20
Hori,Takuma	1P-2	Jorio,Ado	1P-8
Horikawa,Kazunori	3P-24		
Hosoya,Naoki	1P-18	~K~	
Hou,Bo	3-2, 3P-19, 3P-26	Kai,Yasunori	2P-28
Hu,Hailong	1P-5	Kakimi,Yosuke	1P-23
		Kako,Masahiro	2-2
~I~		Kalita,Golap	1-11
Ichihashi,Toshinari	1-13, 2-13	kamon,Keiichi	2P-36
Ichikawa,Yuki	3P-3	Kaneki,Kunihide	3P-20
Ichiki,Takahiko	2P-14	Kaneko,Tetsuya	3P-3
Iijima,Sumio	1-8, 1P-30, 2-11, 2-13, 2P-31, 2P-32, 2P-33, 3P-10, 3P-28	Kaneko,Toshiro	1-10, 1P-34, 2-9, 2P-1, 3P-1
Iijima,Toru	3P-24	Kanemitsu,Yoshihiko	1-1
Iio,Yasunari	2P-16	Kang,Dongchul	1P-16
Iizumi,Y.	2-10	Karita,Motoyuki	1P-39
Ikeda,Takashi	2P-23	Kasama,Yasuhiko	2-4, 2P-10, 2P-3, 2P-4, 2P-6
Ikenoko,Hidehiro	3P-40	Katakura,Shin	3-6
Imahori,Hiroshi	1P-6	Kataura,Hiromich	1P-12, 1-2, 1-9, 1P-10, 2P-35, 3P-16, 3P-25, 3P-27
Inoue,Akihito	3-4	Kato,Haruhisa	1-5
Inoue,Akihito	3P-4	Kato,Keiko	1-3
Inoue,Taiki	3P-26	Kato,Koichiro	1P-15
Irie,Michiko	2P-31	Kato,Shinya	1P-20
Irle,Stephan	1P-37, 1P-4, 2P-11, 2P-2, 2P-8, 3-1, 3P-14, 3P-29	Kato,Shota	2P-16
Ishida,Hirosasu	2-9, 2P-1	Kato,Tatsuhisa	2P-28
Ishiduka,Daisuke	3P-20	Kato,Toshiaki	1-10, 1P-34
Ishii,Akira	3P-30	Kawabata,Eisuke	1P-6
Ishii,Fumiyuki	3-8	Kawabata,Takahiro	2P-23
Ishikawa,Kei	1P-2	Kawachi,Kazuhiko	2-4, 2P-3
Ishikawa,Shinsuke	2-4	Kawai,Yuji	3P-41
Ishitsuka,Youkou	3P-18	Kazachenko,Viktor	2P-15
Ishizawa,Atsushi	1-3	Khlobystov,Andrei N.	2P-12
		Kim,Dong Young	3P-5
		Kinoshita,Hiroshi	1P-22

Kinugasa, Sinichi	1-5	~M~	
Kishi, Naoki	1P-20	Maeda, Teppei	3P-31
Kitamura, Hiroshi	1P-21	Maeda, Yutaka	1P-36
Kitamura, Shinya	3P-35	Maehashi, Kenzo	3P-32
Kitauara, Ryo	1P-33, 1-14, 2-4, 2P-10, 2P-36, 2P-37, 3P-28, 3P-34	Majima, Takuya	2P-30
Kobayashi, Keita	1-14, 2-11	Maki, Hideyuki	1-4, 2P-38, 3P-41
Kobayashi, Mototada	2P-22	Maki, Norio	2P-7, 3P-8
Kobayashi, Naoki	3P-38	Maniwa, Yutaka	1P-10, 2P-35
Kobayashi, Yoshihiro	1-3, 3P-32, 1-4	Maruyama, Shigeo	1P-11, 1P-2, 1P-27, 1P-41, 3-2, 3-5, 3P-19, 3P-23, 3P-26, 3P-6
Kodama, Takeshi	2P-25, 3-4	Maruyama, Takahiro	3P-7
Kodama, Takeshi	3P-4	Mashino, Tadahiko	1S-2
Koike, Shinya	3P-9	Matsuda, Kazunari	1-1
Kojima, Kenichi	1P-16	Matsuda, Kazuyuki	1P-10, 2P-35
Kojima, Nobuaki	2P-18	Matsui, Yusuke	3P-3
Kokai, Fumio	1P-29	Matsuishi, Kiyoto	3P-16
Kokubo, Ken	3P-36, 3P-38	Matsumoto, Jun	2P-30
Komeda, Keiichiro	1-6	Matsumoto, Kazuhiko	3P-32
Komuro, Takashi	2-4, 2P-3, 2P-4	Matsumoto, Kazuya	1-12
Kondo, Daiyu	1-16	Matsuo, Yutaka	2P-14
Kono, Shouichi	3-5	Matsuoka, Yuki	3P-11
Koretsune, Takashi	2-8	Matsuura, Tsugio	2P-7, 3P-8
Kosaka, Mayumi	1-13	Matsuyama, Keiichirou	3P-31
Koshino, Masanori	2P-21	McFeely, Fenton R.	3-7
Koshino, Mikito	3-9	Mehlich, Jan	1P-28
Koshio, Akira	1P-29	Mieno, Tetsu	2P-15
Koyama, Kyouhei	2-7	Minami, Tomoyuki	3P-22
Koyama, Takeshi	1-2	Minari, Takeo	1-9
Kumagai, Susumu	1P-21	Minowa, Mari	2-2
Kurihara, Hiroki	1P-40	Miyake, Masato	3P-24
Kurihara, Kohei	2P-16	Miyana, Sunao	2-9
Kuroda, Shunsuke	1-10	Miyata, Yasumitsu	1-14, 1-2, 1P-33, 2P-36, 2P-37, 2P-5, 3P-16, 3P-34
Kuroshima, Sadanori	2-13	Miyauchi, Yuhei	1-1
Kusakabe, Koichi	1P-18	Miyawaki, Jin	2-13, 2P-31, 2P-33
Kyotani, Takashi	3-10	Miyazaki, T.	2-10, 2-3
~L~		Miyazawa, Kunichi	2P-40
Lee, Haeseong	2S-4	Miyoshi, Akira	3P-19
Li, Yongfeng	3P-1	Mizoguchi, Noriyuki	1P-13
Ling, Lim Siew	3P-15	Mizorogi, Naomi	1P-36, 1P-40, 2-2
Liu, Huaping	1P-12, 3P-27	Mizukoshi, Masataka	1-16
Liu, Lili	3P-29	Mizuno, Kohei	1-5
Liu, Zheng	3P-2	Mizusawa, Takashi	3P-12
		Mizutani, Takashi	2P-37, 1P-33
		Mizutani, Yoshihiro	3P-7

Momota,Hiroshi	3P-21	~O~	
Morimoto,Tatsuro	1P-19	Ochiai,Yuichi	2-7
Moriya,Rieko	1P-10	Ogata,Hironori	2P-17
Moriyama,Hiroshi	2P-13	Oguri,Katsuya	1-3
Morokuma,Keiji	2P-11, 3-1, 3P-14	Ohfuchi,Mari	3P-13
Murakoshi,kei	1-6, 3P-39	Ohkawa,Tetsuya	2-13
Murata,Yasujirou	2S-3	Ohmae,Nobuo	1P-22
		Ohmiya,Hiroyuki	1P-21
~N~		Ohmori,Shigekazu	1-8, 3P-10
Nabika,Hideki	1-6, 3P-39	Ohnami,Hideyuki	2P-17
Nagase,Shigeru	1P-36, 1P-40, 2-2, 3P-29	Ohno,Masatomi	1P-21
Naitoh,Yasuhisa	1P-10	Ohno,Yasuhide	3P-32
Nakada,Kengo	3P-30	Ohno,Yutaka	1P-33, 2P-37
Nakahara,Hitoshi	1P-23, 1P-5	Ohta,Yasuhito	3-1
Nakamura,Arao	1-2	Oida,Satoshi	3-7
Nakamura,Ayako	1-5	Okabe,Hiroto	3-5, 3P-26
Nakamura,Eiichi	2-6, 2P-14, 2P-21, 3P-33	Okada,Hiroshi	2-4, 2P-10, 2P-3, 2P-4, 2P-6
Nakamura,Fumishige	1-13	Okada,Susumu	1-7, 2-12, 2P-19, 3-9
Nakamura,Shigeo	1S-2	Okazak,Toshiya	3-4, 2-10, 1-8, 3P-12, 3P-4
Nakanishi,Ryo	3P-28	Oke,Shinichiro	2P-23
Nakano,Hidetoshi	1-3	Okeyui,Kenji	1P-38
Nakashima,Naotoshi	1-12, 1-15, 1P-19, 1P-25, 1P-35, 2P-24, 2P-42	Okimoto,Haruya	2-3
		Okuda-Shimazaki,Junko	2P-40
Nara,Masanobu	1-6	Omote,Kenji	2-4, 2P-3
Narita,Akimitsu	3P-33	Onishi,Yuuki	3P-4
Naritsuka,Shigeya	3P-7	Ono,Shoichi	2-4, 2P-3
Natori,Masato	2P-18	Ono,Yoshihiro	2-4, 2P-10, 2P-3, 2P-4, 2P-6
Negishi,Ryota	3P-32	Onuma,Kenjirou	3P-24
Niidome,Yasuro	2P-42	Osawa, Eiji	1P-1
Niimi,Yoshiko	2P-21	Osawa,Toshio	3P-18, 3P-5
Nikawa,Hidefumi	1P-36, 1P-40	Oshima,Hisayoshi	1P-38
Nishi,Seiji	2P-18	Oshima,Takumi	3P-36, 3P-38
Nishibori,Eiji	2-4, 2P-10	Oshima,Yugo	2P-35
Nishidate,Kazume	1P-3	Otani,Minoru	2-12, 3-9
Nishide,Daisuke	3P-27		
Nishihara,Hiroto	3-10	~P~	
Nishikawa,Eiichi	1P-27	Page,Alister J.	3P-14
Nishimoto,Yoshio	2P-8	Park,Jin Sung	1P-9
Nishimura,Yoshifumi	1P-4	Poddutoori,Prashanth K.	2-5
Noda,Suguru	2P-34, 2P-39, 3-3, 3P-17, 3P-18, 3P-5	Porfyarakis,Kyriakos	2P-12
Nomura,Keisuke	3P-17	~Q~	
Nouchi,Ryo	3-11	Qian,HuJun	2P-11, 3-1
Nudejima,Shin-ichi	2P-40		
Nugraha,Ahmad R. T.	1P-8		

~R~		Shinohara,Hisanori	1-14, 1-2, 1P-28, 1P-33, 2-3,
Ravoo,Bart Jan	1P-28		2-4, 2P-10, 2P-36, 2P-37, 2P-5,
Razanau,Ihar	2P-15		3P-28, 3P-34
Ruammaitree,Akkawat	1P-5	Shiomi,Junichiro	1P-2, 1P-27, 3-2, 3-5, 3P-19,
Rupesinghe,Nalin	3P-24		3P-23, 3P-26
		Shiotani,Ryo	1P-31
~S~		Shiozawa,Kazunari	1P-33, 2P-37
Sada,Takao	2P-24	Shiratori,Yosuke	2P-39
Sagitani,Satoshi	2P-35	Shiromaru,Haruo	2P-25, 2P-30
Saha,Biswajit	2P-11	Shukla,Bikau	1-8, 3P-10
Saikawa,Mao	2-14, 2P-27	Siry,Milan	1P-38
Saito,Mineo	3-8	Slanina,Zdenek	1P-36
Saito,Riichiro	1P-11, 1P-7, 1P-8, 1P-9	Soga,Ikuo	1-16
Saito,Susumu	1P-1, 1P-15, 2-8, 3P-37	Soga,Tetsuo	1P-20
Saito,Takeshi	1-8, 1P-20, 2-11, 3P-10, 3P-2	Somonura,Takuya	3P-20
Saito,Tatsuya	3-11	Suda,Yoshiyuki	2P-23, 3P-15
Saito,Yahachi	1P-23, 1P-39, 1P-5	Suenaga,Kazutomo	1-14, 2-11, 2P-21, 3P-2
Sakai,Ayumu	1P-26	Suga,Tadatomo	1-16
Sakai,Keijiro	3P-20	Sugai,Toshiki	1P-33, 2-15, 2P-13
Sakai,Takeshi	2-4, 2P-10, 2P-3, 2P-4, 2P-6	Sugime,Hisashi	2P-39, 3-3, 3P-5
Sakashita,Takero	1-1	Sumii,Ryohei	2-3
Sakurai,Masahiro	3P-37	Sun,Yanning	3-7
Sandanayaka,Atula D. S.	2-5	Suzuki,Satoru	1-4, 2P-38
Sanderson,Joseph H.	2P-25	Suzuki,Seiya	2P-20
Sano,Masahito	3-6	Suzuki,Shinzo	3P-12
Sato,Hideki	3P-22, 3P-3	Suzuki,Takuya	1P-10
Sato,Kentaro	1P-11, 1P-41, 1P-8, 1P-9	Suzuki,Tuyoshi	3-10
Sato,Kuninori	3P-7		
Sato,Satoru	1P-36	~T~	
Sato,Tadashi	3-5	Tachibana,Masaru	1P-16
Sato,Tetsuya	2P-38, 3P-41	Tagmatarchis,N.	2-10
Sato,Yoshikuni	3P-18	Takagi,Daisuke	1-3, 3P-6
Sato,Yuki	2P-25	Takagi,Yoshiteru	1-7, 3-9
Satoh,Masayuki	3P-24	Takahashi,Hideyuki	2-1
Sawa,Hiroshi	2-4, 2P-10	Takahashi,Kayori	1-5
Sawada,Keisuke	3-8	Takai,Kazuyuki	3-10
Sawaguchi,Daiki	3P-22	Takano,Yoshihiko	1P-14
Sawanishi,Yoshihiko	2-15	Takase,Mai	1-6, 3P-39
Sekido,Masaru	1P-21	Takenobu,Taishi	2P-35
Sekiguchi,Kotaro	2P-39	Takeshita,Hiroki	3P-20
Shimada,Manabu	1-5	Takeuchi,Hisato	1P-21
Shimazu,Tomohiro	1P-38	Takikawa,Hirofumi	2P-23, 3P-15
Shimizu,Kazuki	2P-23, 3P-15	Takimoto,Kotaro	2P-23, 3P-15
		Tamaki,Jun	2P-41, 3P-35, 3P-40
		Tanaka,Kazuyoshi	1P-6

Tanaka, Takeshi	1-9, 1P-12, 3P-25, 3P-27	Warner, Jamie H.	2P-12
Tanaka, Yasuhiko	2P-42	Watanabe, Makoto	1P-2, 3P-26
Tange, Masayoshi	1-8	Watanabe, Takahito	2P-4
Tanigaki, Katsumi	3-11	Watanabe, Tohru	1P-14
Taniguchi, Akiyoshi	2P-40		
Teo, Kenneth	3P-24	〜X〜	
Terasawa, Masami	3-5	Xiang, Rong	1P-2, 1P-27, 1P-41, 3-2, 3P-19, 3P-23
Teshiba, Masashi	2P-29		
Thomas, Ian	1P-24	〜Y〜	
Thurakitsee, Theerapol	1P-2, 3P-23	Yagi, H.	2-10
Tobita, Hiromi	2-4, 2P-10, 2P-3, 2P-4, 2P-6	Yajima, Hirofumi	1P-26, 1P-31, 3P-20
Tohji, Kazuyuki	2-1	Yamada, Michio	2-2
Tokumoto, Youji	2-10, 2-3	Yamaguchi, Hiroyuki	1P-17
Tominaga, Masato	1P-17	Yamaguchi, Masafumi	2P-18
Toyama, Kiyohiko	1-13	Yamaguchi, Takahide	1P-14
Tromp, Rudolf M.	3-7	Yamaguchi, Takashi	2P-32
Tsuchiya, Koji	1P-26, 1P-31	Yamaguchi, Takashi	3P-28
Tsuchiya, Takahiro	1P-36, 1P-40, 2-2	Yamakawa, Akira	1P-22
Tsuda, Shunsuke	1P-14	Yamamoto, Hiroshi	2P-16, 3P-20, 3P-31
Tsukagoshi, Kazuhito	1-9	Yamamoto, Kazunori	1P-32
Tsuruoka, Yasuhiro	3-4	Yamamoto, Makoto	1P-29
Tanuma, Hajime	2P-30	Yamamoto, Rika	3P-35
		Yamazaki, Taihei	1P-21
〜U〜		Yamazaki, Yuko	1P-40
Uchinoumi, Takeshi	1P-25	Yanagi, Kazuhiro	1P-10, 2P-35
Udoguchi, Hiroki	2P-35	Yang, T.	2P-9
Ue, Hitoshi	2P-23, 3P-15	Yao, Tsutomu	2P-41
Ueno, Hiroshi	2P-13	Yasuda, Satoshi	1-6, 3P-39
Umakoshi, Tatsuya	2P-1	Yokoi, Hiroyuki	3P-21
Umeda, Yoshito	2P-23, 3P-15	Yokoo, Kuniyoshi	2-4, 2P-3
Umemoto, Hisashi	2-3	Yokota, Masashi	2P-23, 3P-15
Umeno, Masayoshi	1-11	Yoo, JongTae	1-15
Umeyama, Tomokazu	1P-6	Yoshikawa, Airi	2P-26
Urabe, Yasuko	3P-25	Yoshimoto, Arisa	2P-29
Utsumi, Kouki	1P-21	Yoshimura, Masamichi	2P-20
		Yoshitake, Tsutomu	2-13
〜W〜		Yudasaka, Masako	2-13, 2P-31, 2P-32, 2P-33, 3P-28
Wada, Yoriko	2-14, 2P-25, 2P-28		
Wakabayashi, Tomonari	2-14, 2P-25, 2P-26, 2P-27, 2P-28, 2P-29	Yuge, Ryota	1-13, 2-13
Wakahara, Hiroyuki	2P-38	Yumura, Motoo	1-8, 3P-10
Wakita, Koichi	1-11	Yurkas, John J.	3-7
Wang, Hsing-Lin	3P-36		
Wang, Jian	2P-2		
Wang, Ying	3-1		

複写をご希望の方へ

フラーレン・ナノチューブ学会は、本誌掲載著作物の複写に関する権利を一般社団法人学術著作権協会に委託しております。

本誌に掲載された著作物の複写をご希望の方は、(社)学術著作権協会より許諾を受けて下さい。但し、企業等法人による社内利用目的の複写については、当該企業等法人が社団法人日本複写権センター((社)学術著作権協会が社内利用目的複写に関する権利を再委託している団体)と包括複写許諾契約を締結している場合にあっては、その必要はございません(社外頒布目的の複写については、許諾が必要です)。

権利委託先：一般社団法人学術著作権協会

〒107-0052 東京都港区赤坂 9-6-41 乃木坂ビル 3階

電話：03-3475-5618 FAX：03-3475-5619 E-Mail：info@jaacc.jp

注意：複写以外の許諾(著作物の引用、転載・翻訳等)に関しては、(社)学術著作権協会に委託致しておりません。直接、フラーレン・ナノチューブ学会へお問い合わせください。

Reprographic Reproduction outside Japan

Making a copy of this publication

Please obtain permission from the following Reproduction Rights Organizations (RROs) to which the copyright holder has consigned the management of the copyright regarding reprographic reproduction.

Obtaining permission to quote, reproduce; translate, etc.

Please contact the copyright holder directly.

→Users in countries and regions where there is a local RRO under bilateral contract with Japan Academic Association for Copyright Clearance(JAACC)

Users in countries and regions of which RROs are listed on the following website are requested to contact the respective RROs directly to obtain permission.

Japan Academic Association for Copyright Clearance (JAACC)

Address : 9-6-41 Akasaka, Minato-ku, Tokyo 107-0052 Japan

Website : <http://www.jaacc.jp/>

E-mail : info@jaacc.jp TEL : 81-3-3475-5618 FAX : 81-3-3475-5619

2010年3月2日発行

第38回フラーレン・ナノチューブ総合シンポジウム 講演要旨集

<フラーレン・ナノチューブ学会>

〒464-8602 愛知県名古屋市千種区不老町
名古屋大学大学院理学研究科 物質理学専攻
篠原研究室内

Tel : 052-789-5948

Fax : 052-747-6442

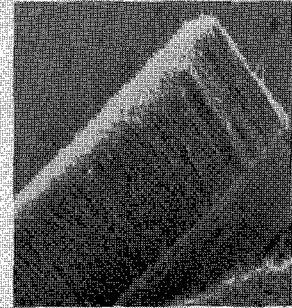
E-mail : fullerene@nano.chem.nagoya-u.ac.jp

URL : <http://fullerene-jp.org>

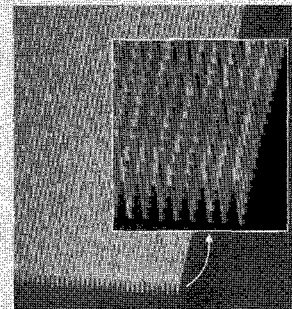
印刷 / 製本 (有) イヅミ印刷所

CVDのリーディングカンパニー

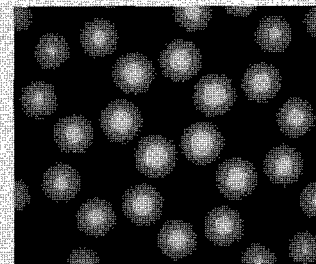
アイクストロン社の**CNT**成膜装置 **Black Magic**



Dense CNT



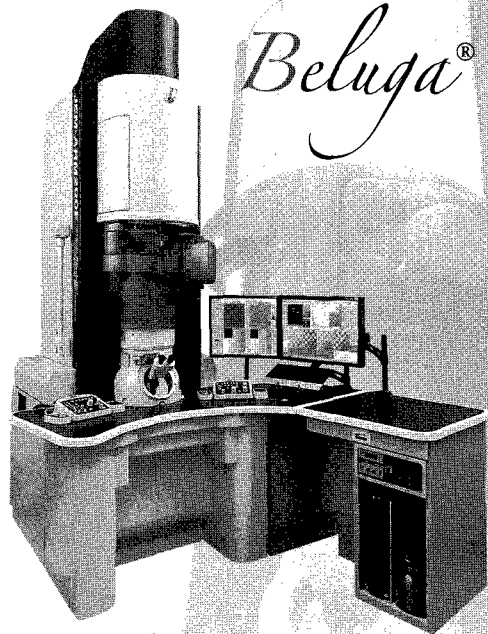
Horizontal SWCNT



Graphene

- ・ 装置導入後、すぐに希望のCNTを成長可能
(装置据付:2日、調整:1日、プロセス確認:2日)
- ・ あらゆる基板サイズに対応
(研究用:1~2インチ、量産用:最大12インチまで)
- ・ オリジナルのレシピ付「Thermal CVD, Plasma CVD 2モードに対応」
(シングルCNT用、ダブルCNT用、マルチCNT用、グラフェン用、横方向CNT用、
低圧プロセス用、高速成長CNT用etc.)
- ・ プラズマによる簡単クリーニングと高メンテナンス性
- ・ 世界中の大学・研究所・企業に導入済み

The Power of STEM Cs corrected Microscope



照射系球面収差補正装置を標準搭載し、機械的・電氣的安定度を極限まで高めることで、商用電子顕微鏡として世界最高の走査透過像 (STEM-HAADF) 分解能0.08nmを実現しました。

新デザイン

空気の流れによる鏡筒の揺れを防ぐため、鏡筒前面を覆うカバーを採用し、装置全体及び操作パネルのデザインを一新

電氣的安定度の向上

変動を従来機種の半分に抑制することで、電氣的安定度が大幅に向上
高圧安定度 $\leq 2\text{ppm/min}$ \rightarrow $\leq 1\text{ppm/min}$
対物レンズ電流安定度 $\leq 1\text{ppm/min}$ \rightarrow $\leq 0.5\text{ppm/min}$

機械的安定度の向上

鏡筒は中間レンズから下の直径を $\phi 250\text{mm}$ から $\phi 300\text{mm}$ にし、コレクタ搭載時の剛性を確保すると共にTEM/STEMの両コレクタ搭載時を想定し、架台の構造を最適化し、装置全体として高剛性化を実現

原子分解能分析電子顕微鏡

JEM-ARM200F

JEOL OPENS NEXT GENERATION SPM

走査形プローブ顕微鏡 (SPM) は、非常に鋭い探針で試料表面を走査し、高分解能で表面形状や表面の物理特性を観察する顕微鏡です。近年のナノテクノロジーの発展の中、様々な分野でSPMが活用されています。

スナップサーチ機能を標準搭載

従来の走査速度の最大10倍まで走査速度が向上

コントローラ・ソフトウェアを刷新

自社開発高圧アンプの採用によりS/Nの良い画像の取得が可能
新アイコンの採用により、ソフトウェアの操作性が向上

環境制御対応SPM

大気中から液中、真空排気、ガス導入、試料加熱・冷却までオプションで対応
オプション付加時にも大気中での操作性が良く、初心者から上級者まで対応

ノンコンタクトモードを標準で搭載

第4世代目となる独自回路によりオートチューニングで簡単に操作可能



走査形プローブ顕微鏡

JSPM-5410

JEOL

Serving Advanced Technology

日本電子株式会社

<http://www.jeol.co.jp/>

本社・昭島製作所 〒196-8558 東京都昭島市武蔵野3-1-2 ☎(042)543-1111
営業統括本部 〒190-0012 東京都立川市曙町2-8-3 (042)528-3381
札幌 (011) 726-9680・仙台 (022) 222-3324・筑波 (029) 856-3220・東京 (042) 528-3211・横浜 (045) 474-2181
名古屋 (052) 581-1406・大阪 (06) 6304-3941・広島 (082) 221-2500・福岡 (092) 411-2381

60
th
Anniversary



COSMOSIL[®] CNT

- 可溶化カーボンナノチューブをサイズで分離！
- 親水性基(中性)コーティングタイプ！
- 3種類の細孔径(300 Å, 1000 Å, 2000 Å)！
- 高い耐久性！

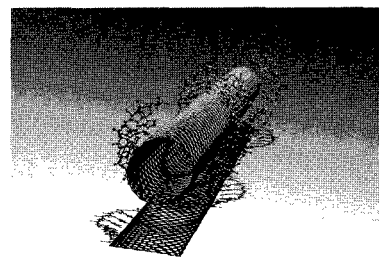
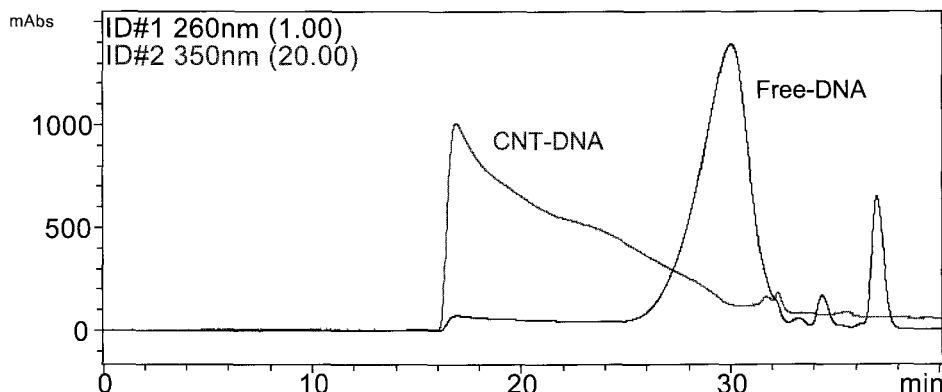


Image courtesy of Dr. Y. Ito, Univ. of Oxford

■分離例

カーボンナノチューブのサイズ分離

細孔径の異なる3種類のカラムを連結し、DNAでラッピングされたカーボンナノチューブを分離しました。



分析条件

カラム	COSMOSIL CNT-300 7.5mm I.D. × 300mm	温度	40 °C
	COSMOSIL CNT-1000 7.5mm I.D. × 300mm	検出	UV260nm (× 1), 350nm (× 20)
	COSMOSIL CNT-2000 7.5mm I.D. × 300mm	サンプル	DNA-wrapped CNT (CNT-DNA)
移動相	0.5mmol/l EDTA, 200mmol/l NaCl, 40mmol/l Tris-Tris HCl (pH7.0)	注入量	500 μl
流速	1.0ml/min	圧力	8.1MPa

【サンプルのご提供 : 名古屋大学大学院理学研究科物質理学専攻 篠原研究室】

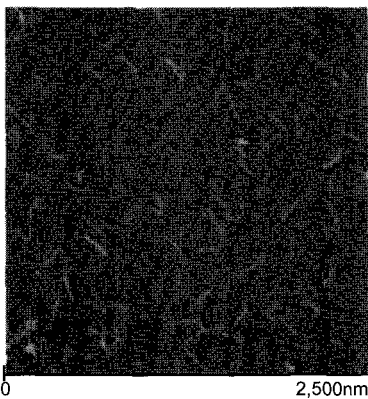
AFM (原子間力顕微鏡) によるサイズ観察

上記分離時に分取した各フラクションをAFMにて観測し、CNTの長さを測定しました。

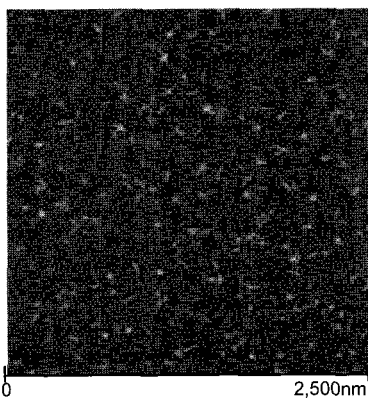
Fr.18 (17~18min)



Fr.20 (19~20min)



Fr.24 (23~24min)



【撮影・データのご提供 : 名古屋大学大学院理学研究科物質理学専攻 篠原 久典教授・浅田 有紀様】

詳しい情報はWeb siteをご覧ください。



Bruker Daltonics

Redefining MALDI-TOF/TOF Performance

... with ultrafleXtreme

smartbeam-II™ レーザー 1 kHz スピード
(MS&MS/MS)

最新のFlashDetector™

4GHz デジタイザー

超高分解能

MALDI Perpetual™ 自動クリーニング
イオン源

1ppm以下の優れた質量精度、40,000以上の超高分解能、そして、MSおよびMS/MSモードにおける真のkHzスピードが達成されています。

MALDIイメージング、LC-MALDI、バイオマーカー定量およびトップ・ダウンシーケンシングといったプロテオミクスアプリケーションにおいて、強化された無敵のパフォーマンスを体験してください。

もっと詳しく知りたい方は、www.bruker.jpをご訪問下さい。

ブルカー・ダルトニクス株式会社
横浜市神奈川区守屋町3-9
TEL:045-440-0471 FAX:045-453-1827
<http://www.bruker-daltonics.jp/>

think forward

MALDI-TOF/TOF MS

波長可変チタンサファイアレーザー 3900S

- 優れた操作性、メンテナンス性と高い変換効率
- 高い安定性を実現し、675~1100nmの超広帯域発振が可能
- フラレン・ナノチューブの分光用およびフォトルミネセンス光源として最適

【主な仕様】

平均入力：5Wおよび10W
 発振波長域：700-1000nm (5W励起)
 発振波長域：675-1100nm (10W励起)
 線幅：40GHz以下 (1GHz以下のオプション有り)
 ノイズ：1%以下
 安定性：3%以下
 空間モード：TEM₀₀

ナノ秒チューナブルOPO Scan Series OPO

- 410nmから2.63 μ mの広帯域波長可変OPO
- ブロードバンド(10-500 cm^{-1})、ミッドバンド(3-7.5 cm^{-1})を選択可能
- UVオプションにより206nm-420nmの紫外波長領域をカバー
- ScanMaster™ソフトウェアによるグラフィックインターフェイスで簡便な操作性
- 独自のキャビティデザイン、特殊なコーティング技術により長い結晶寿命を実現
- Quanta-Ray®のNd:YAGレーザー (INDI、LAB、PROシリーズ)との組み合わせで幅広い励起出力に対応



 Spectra-Physics

A Division of Newport Corporation

スペクトラ・フィジックス株式会社

本社 〒153-0061 東京都目黒区中目黒4-6-1 大和中目黒ビル
 大阪支社 〒550-0005 大阪府大阪市西区西本町3-1-43 西本町ソーラービル

TEL(03)3794-5511 FAX(03)3794-5510
 TEL(06)4390-6770 FAX(06)4390-2760

MAKE LIGHT | MANAGE LIGHT | MEASURE LIGHT

製品情報・お問い合わせは <http://www.spectra-physics.jp>

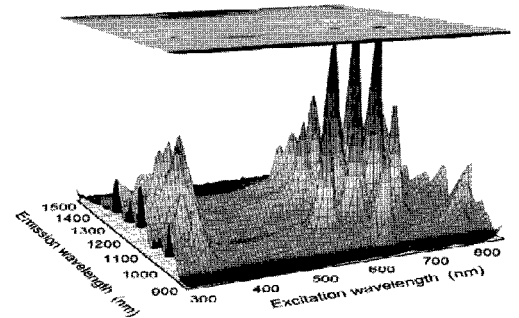
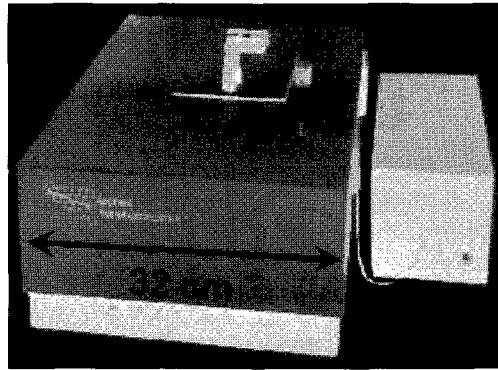
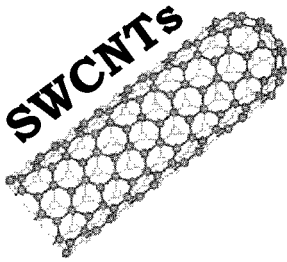
世界で唯一！

単層カーボンナノチューブ専用解析装置



NanoSpectralyzer

ナノスペクトライザー



単層カーボンナノチューブの、直径&カイラリティ (n, m) 解析に特化した専用機です。

- ◆近赤外の蛍光・吸収測定をする事により、直径・カイラリティだけでなく、分散性の評価が可能。
- ◆ワンクリックで測定開始、自動でデータ解析（測定：5秒、データ取得：1分）
- ◆高出力励起（～50mW） & 高感度検出器（InGaAs array）採用で、市場最高感度を達成！
- ◆非常に簡単な前処理 & 微量サンプル（200μL）に対応。
- ◆液体窒素不要・低消費電力・コンパクト設計で、設置場所を選びません。
- ◆流体セルによる反応プロセス中の測定や、可視光域（380～750nm）の吸光スペクトル、ラマン分光に対応したモデルもあります。

モデル名	NS1	NS2
励起光源	ダイオードレーザー（3波長）	ダイオードレーザー（3波長） ラマン分光用レーザー（2波長）
蛍光測定レンジ	880～1580nm	
吸光測定用光源	タンゲステン・ハロゲンランプ	
吸光測定レンジ	880～1580nm	400～1600nm
吸光測定解像度	4nm(近赤外域)	4nm(近赤外域)・1nm(可視光域)
ラマン分光レンジ	—	150～2900cm ⁻¹
ラマン分光解像度	—	3cm ⁻¹
本体サイズ (W×D×H:重量)	318×470×165 mm : 18 kg	318×470×195 mm : 22 kg

※仕様は予告なく変更される場合がございます。



日本カンタム・デザイン株式会社 先端技術部
 〒171-0014 東京都豊島区池袋2-40-13 池袋デュプレックスビズ3F
 Tel : 03-5954-8571 URL : <http://www.qd-japan.com/>

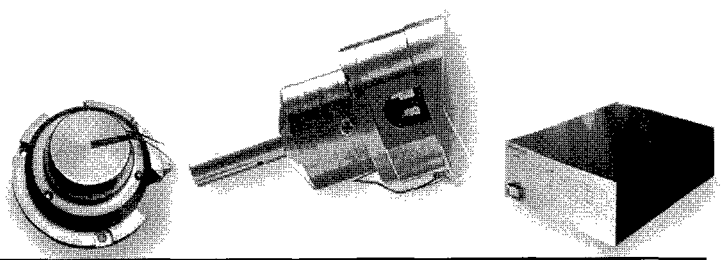
デモ測定 受付中！

NEW

SEM, FIB, 光学顕微鏡観察下での ナノ/マイクロ マニピュレーション・プロービングに最適 (大気中、真空中、低温環境に対応)

ナノ・マイクロ回転ステージ UP-200Rシリーズ

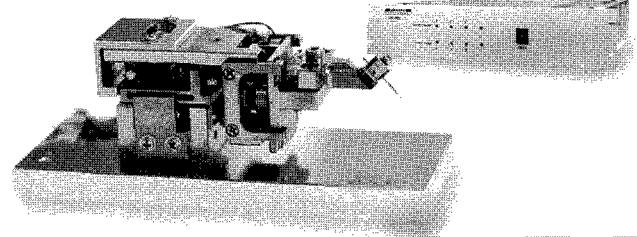
- 大気中、及び高真空中で微小回転動作と位置検出(オプション)のニーズに対応
- SEM, FIBへの組み込み可能
- 回転ステージのみ、及び、XYZ+回転(4軸)の選択可能



XYZ3軸 ナノマニピュレータ/プローバ = エンヨーダ付製品をまもなく販売開始! = UP-100U

- 簡単操作、粗動(数百nm動作)と微動(0.5nm以下)の切り替え式で素早い位置合わせが可能
- 低価格を実現! (価格はお問い合わせください。)
- 市販のSEM/FIB/光学顕微鏡に組み合わせ可能

- 大気中~超高真空まで、室温から極低温までの広範囲な動作環境
- マルチプロービングにも対応
- マニピュレーション、半導体ナノデバイスのIV測定、抵抗測定、EBIC測定 等幅広い用途に対応



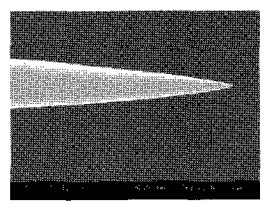
NEW

STM用プローブ、多探針接触検査用プローブ — ニッケルプローブは金、銀コート対応が可能です! —

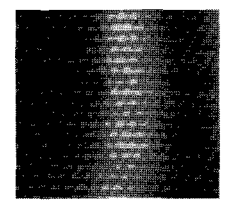
- STM用ニッケルプローブ、電解研磨白金イリジウムプローブ 汚染が少なく面倒な前処理不要、鋭い先端径により高い測定安定性を達成
- 接触測定用ニッケルプローブ、電解研磨白金イリジウムプローブ 低接触抵抗、接触の際に速やかな伝導性を得られWプローブより精度の高いV測定を実現

各プローブの仕様 >>

品名	NEW ニッケルプローブ		NEW 白金イリジウムプローブ※1	
	P-100Ni (P)	P-100Ni (S)	P-100PtIr (P)	P-100PtIr (S)
研磨方法	電解研磨			
用途	多探針接触検査用	STM用	多探針接触検査用	STM用
針先形状	円錐形			
線材・線形(mm dia.)	多結晶ニッケル0.25		多結晶白金イリジウム0.5	
全長(mm)	10			
先端径(nm)	50以下	30以下	50以下	30以下
傾斜角(両角)	10° ~ 15°		15° ~ 20°	
備考	低接触抵抗・マイルドな接触測定向け	面倒な針処理不要※2	低接触抵抗・マイルドな接触測定向け	面倒な針処理不要※2
販売単位	10本1組			



ニッケルプローブの針先部のSEM写真



ニッケルプローブによる金(111)のSTM観察例

品名	従来品 タングステンプローブ		従来品 PtIrコートタングステンプローブ	
	P-100W/P	P-100W/S	P-100W/PtIr	
研磨方法	電解研磨			
用途	多探針接触検査用	STM用	多探針接触検査用	
針先形状	円錐形			
線材・線形(mm dia.)	多結晶タングステン0.25			
全長(mm)	10			
先端径(nm)	100以下	50以下	100以下	
傾斜角(両角)	10° ~ 15°			
備考	接触抵抗を気にしない測定向け		低接触抵抗・マイルドな接触測定向け PtIr コーティング厚さ: 3nm	
販売単位	10本1組			

※1) STM用白金イリジウム機械研磨プローブも従来通り販売を継続しております。 ※2) 観察表面が活性な場合は脱ガスのための加熱を推奨いたします。

4. プローブ + FE-SEM・超高真空・極低温条件での走査型プローブ顕微鏡システム USM-1400-4P

- 2.5K~室温までの温度範囲で測定可能
- STMまたはAFM 選択可能 (各プローブ)



株式会社 マシナックス

代表取締役 佐野隆治

〒454-0856 名古屋市中川区小碓通 2-6

TEL 052-654-5021(代) FAX 052-654-5125

HP <http://www.mashinax.jp/>

メール mashinax@sf.starcat.ne.jp

菱田商店会社案内

オフィス家具

メーカー(既製品) オカムラ・コクヨ・プラス等
木製家具 好みにあわせて作ります

室内装飾

ブラインド 立川・日米
カーテン・カーペット スミノエ・サンゲツ・タジマ等
床仕上げ フリーアクセス・Pタイル・ロンリウム等
クロス ルノン・サンゲツ等
間仕切り 各種パーテーション

学校関連

黒板・ホワイトボード・掲示板
実験台・薬品棚・吊棚
既製品から特注品まで、もちろん取り付けます。

(有)菱田 商店

名古屋市緑区浦里4-207
Tel 891-8125
Fax 891-3957

CaHC

ライフサイエンスサポート企業へ。

株式会社「カーク」は、『創造と努力』『誠実と感謝』を企業理念とし、
科学・医学・産業の研究・開発の発展に寄与するため
試薬をはじめ、工業薬品、検査薬、分析機器の販売を通して顧客に貢献しています。
特に、バイオサイエンス・ライフサイエンスの分野において、
オンリーワン、ナンバーワンとしての存在を目指しています。

For Customer

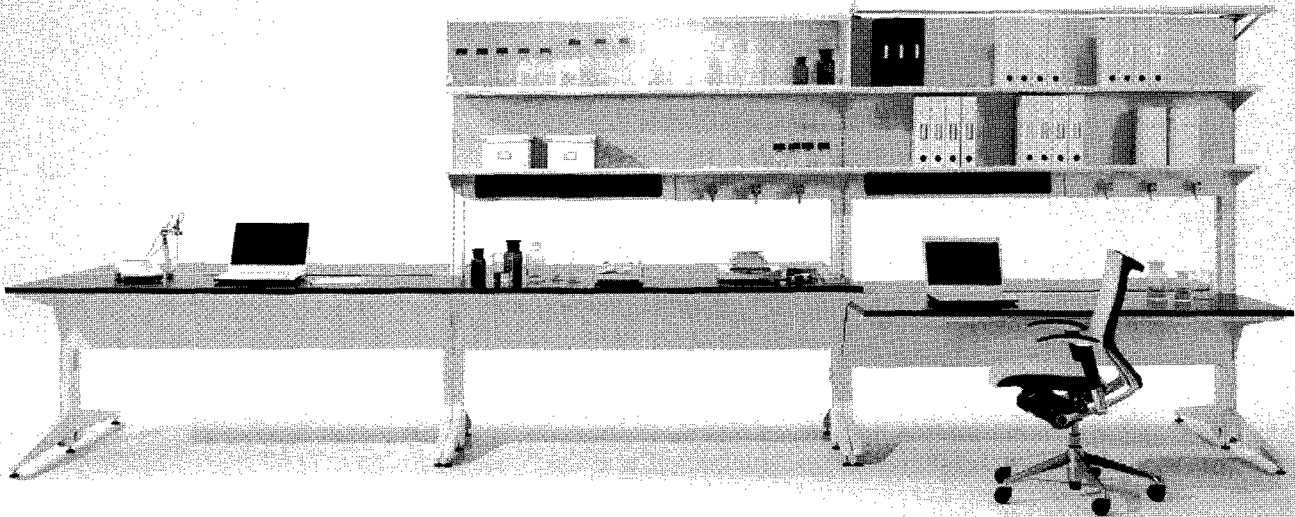


株式会社 カーク

〒460-0002 名古屋市中区丸の内 3-8-5
Tel 052-971-6533(代)
<http://www.cahc.co.jp>

愛知東営業所 0564-66-1580
岐阜営業所 058-268-8151
浜松営業所 053-431-6801
三重営業所 059-236-2531

研究者の創造性を刺激し、あらゆる実験・研究にフレキシブルに対応。
いま、研究施設に求められるもの——オカムラからの答えです。



RIFORMA

ラボ・システム[RIFORMA]

豊富なオプションパーツにより、用途や使用する機器に合わせて自由自在に組合せ・組替えが可能です。機能性と同時にスマートなデザインを追求、研究施設にこれまでにない洗練された雰囲気をつくります。

DESIGN

研究者が快適に実験・研究に集中できるシンプルでスマートなデザイン。

FUNCTION

高さ調整可能な天板、支柱を用いた配線機能など、隅々にまで使いやすさを追求。

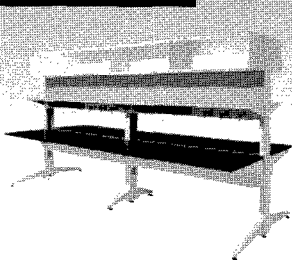
ABILITY

安全性や耐久性に加えて、点検もスムーズに行える高いメンテナンス性を確保。

FLEXIBILITY

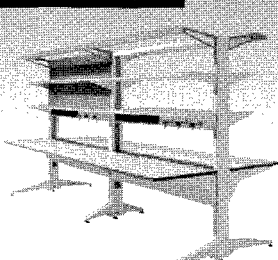
オプションを用いて自由自在にカスタマイズ可能。拡張性に優れ、組替えも簡単に行えます。

試薬ボックス・スタイル



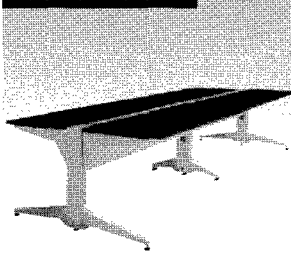
薬品や備品の
一時保管に最適

シェルフ・スタイル



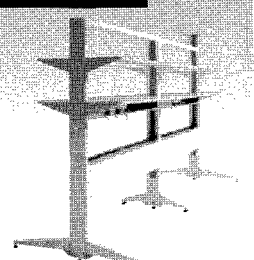
天板を広く使いつつ
十分な収容スペースを確保

フラット・スタイル



天板だけを広く
シンプルに活用

スタンド・スタイル



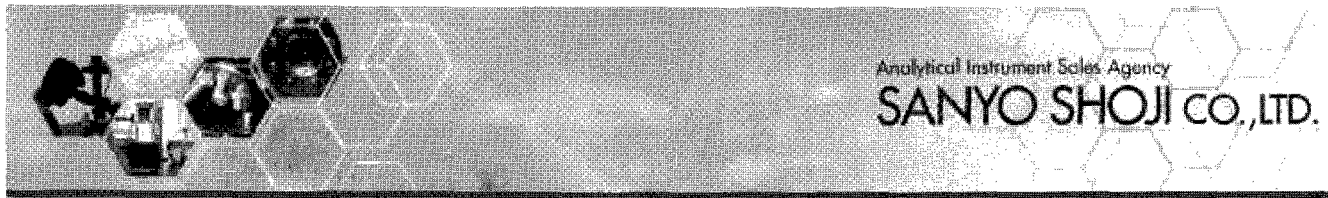
大型機器の配置など
天板を使用しないスタイルに

ホームページアドレス <http://www.okamura.co.jp/>

お問い合わせ・ご相談はフリーダイヤル **0120-81-9060** 月曜～金曜(祝日を除く) 9:00～18:00
お客様サービスセンターへ

よい品は結局おトクです

オカムラ
株式会社 岡村製作所



株式会社 三洋商事は
分析・試験装置のエキスパートです。

お客様の研究開発、品質管理、製造工程等、色々な分野におけるご要望に対し、総合的なご提案が出来るように努めております。
そして、新しい技術や内外の幅広い商品に関する知識情報を生かし、皆様の発展に貢献出来る事を希望しております。

●企業活動の基本方針

弊社の方針と致しまして“企業のコンプライアンスの遵守”
“地球環境に配慮した経営の推進” “地域社会に貢献し相互繁栄を考えた施策”
などを重視してまいります。

●お客様の満足度を第一に考えた営業活動

装置の導入目的、技術評価、コスト、納期、アフターサービス等
お客様のニーズに貢献できるよう、迅速な対応に努力し、
お客様との信頼関係を大切に致します。

●取扱商品の充実

新しい技術や内外の幅広い商品に関する情報収集と
共に知識の向上に努め、お客様の立場に立ったご相談相手として
お役に立てる事を目標にしております。

取扱品目

分析測定器 ・試験検査器 ・バイオ機器
理化学機器 ・実験用器具 ・実験室設備
環境計測測定機器 ・粉粒体測定装置
真空機器 ・その他専用機器

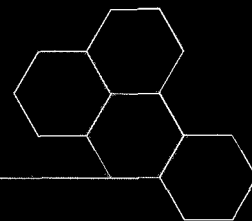
名古屋市中村区名駅三丁目28番12号

大名古屋ビル 〒450-0002

TEL 052-583-7070 FAX 052-583-7110

E-mail : nago@sanyo-shoji.co.jp

http : //www.sanyo-shoji.co.jp

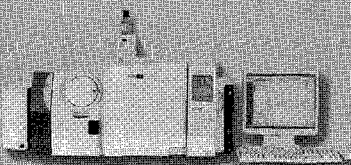


Best for Our Customers

～すべてはお客様のために～ を合言葉にナノテク新材料における最高のソリューションを提供します。

- ① 微量測定 ② 純度 ③ 直径 ④ 観察 ⑤ カイラリティ ⑥ 凝集分散

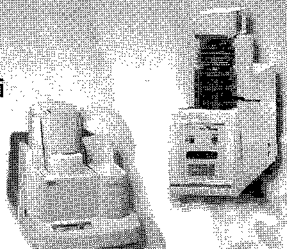
① 熱分解生成物・発生ガスの分析
 ガスクロマトグラフ質量分析計
 GCMS-QP2010 Plus



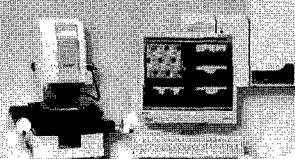
②③ 直径測定
 ②③ 結晶性と耐熱性の評価
 ラマン分光光度計
 Holo-Probe モニタリングシステム



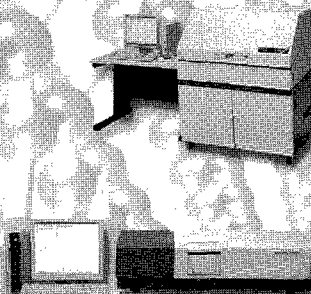
① 微量CNTの純度・熱特性評価
 ① CNTの結晶性と耐熱性の評価
 ミクロ熱重量測定装置
 TGA-50
 TG/DTA同時測定装置
 DTG-60/60H



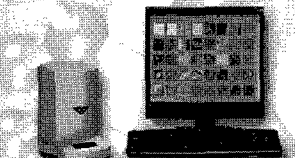
③④ あらゆるナノテク材料を観察・測定
 ナノサーチ顕微鏡
 SFT-3500



①② CNTの紫外可視近赤外吸収スペクトル測定
 紫外可視近赤外分光光度計
 SolidSpec-3700
 紫外可視近赤外分光光度計
 UV-3600



③④ 直径測定
 ③④ 精製前後の観察
 ③④ CNTとポリマーコンポジット試料の観察
 走査型プローブ顕微鏡
 SPM-9600



⑤ SWNTの近赤外PL
 3次元分布測定
 近赤外フォトルミネッセンス測定システム
 NIR-PL System



*こちらは特注製品となります

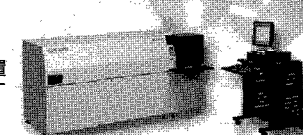
② CNTの密度測定
 乾式自動密度計
 アキュピックII 1340シリーズ



⑥ 分散・凝集過程評価
 ナノ粒子径分布測定装置
 SALD-7100



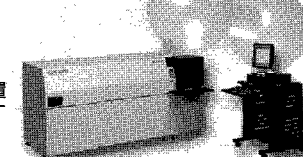
② 触媒元素の測定
 ツインシーケンシャル形ICP発光分析装置
 ICPS-8100



⑥ 独自のIG法による
 シングルナノ領域の粒子径評価
 シングルナノ粒子径測定装置
 IG-1000



⑥ 比表面積と吸着特性
 マイクロメリテックス
 高速比表面積/細孔分布測定装置
 アサップ2020シリーズ



nanotech
 SHIMADZU

Total solutions for the future of nanotechnology

株式会社 島津製作所

分析計測事業部 マーケティング部 プロモーションG
 〒604-8511 京都市中京区西ノ京錦原町1
 TEL075-823-1468 FAX075-823-1380 <http://www.an.shimadzu.co.jp>

NANORUPTOR® ~サンプル密閉式超音波分散装置~

———— バイオの技術をナノテクへ ————

本装置はカーボンナノチューブや燃料電池用触媒を始めとする
各種ナノ粒子を溶媒に分散させる用途に最適化されています。

実施例：燃料電池用触媒評価、カーボンナノチューブの分散
納入実績：各大学、自動車メーカー、光学機器メーカー、電子部品メーカー



NR-350

特長

- 分散に最適
各種ナノ粒子（カーボンナノチューブ、フラーレン等）の分散処理に最適。
- 密閉処理
溶媒の蒸発・揮散やコンタミがありません。
- 多検体同時処理
最大 24 試料を同時に処理できます。
- 再現性良好
回転機構の採用により均一な超音波照射が可能です。
- 低騒音
高性能消音箱により超音波の騒音が低く抑えられます。

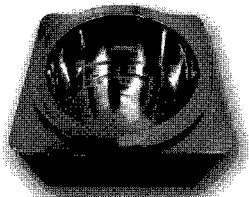
NR-350仕様表

品番	NR-350
品名	密閉式超音波分散装置 Nanoruptor
超音波周波数	20 kHz
超音波出力	~ 350 W 可変
電源	100 V、50/60 Hz、5.5 A
最低設置スペース概寸	400 (W) × 300 (D) × 680 (H) mm
発振ユニット概寸	400 (W) × 260 (D) × 160 (H) mm
処理ユニット概寸	170 (W) × 160 (D) × 270 (H) mm
消音箱概寸	400 (W) × 300 (D) × 520 (H) mm
NR-350 全体重量	36 Kg
ランタイマー	0 ~ 99 分 59 秒、デジタル
インターバルタイマー (ON)	0 ~ 99.99 秒、デジタル
インターバルタイマー (OFF)	0 ~ 99.99 秒、デジタル
処理本数	1 本 (50 mL)
付属品	消音箱、電源ケーブル、接続ケーブル、排水ポンプ、取り扱い説明書、ユーザー登録カード
備考	NR-350 は機器のみです。別途処理量に応じたアクセサリ（ギヤ・板 + チップ）をお買い求め下さい。

メーカー略号：TOS

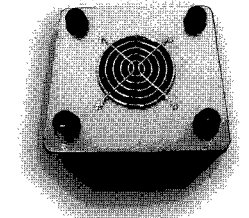
品名	品番	包装	希望販売価格
超音波密閉式分散装置 Nanoruptor®	NR-350	1 UNIT	¥1,950,000
50 mL チューブ用チップ	MM-50WS	1 SET	¥54,000
ギヤ板	NG350-50	1 PC	¥9,000
冷水循環器	CP-80R	1SET	¥264,000

デモ機をご用意しております！



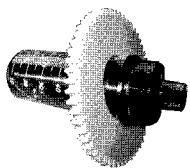
丸形超音波処理槽

丸形超音波処理槽の採用により分散の高効率化を実現。



冷却ファン

冷却ファン及び専用回路の採用により長時間運転が可能。



別売品

50 mL チューブ用チップ
ギヤ板
その他各種

販売



人と科学のステキな未来へ

コスモ・バイオ株式会社

〒135-0016 東京都江東区東陽2-2-20 東陽駅前ビル
URL: <http://www.cosmobio.co.jp>
TEL (03) 5632-9610 FAX (03) 5632-9619
営業部 栗原 mkurihar@cosmobio.co.jp
開発部 笹原 ksasahar@cosmobio.co.jp

製造



東湘電機株式会社

〒232-0027 神奈川県横浜市南区新川町5-29-2 新井ビル2F
TEL (045) 261-8388 FAX (045) 252-8935
技術部長 伊藤
e-mail: k-ito@bioruptor.jp

超遠心機による単層CNTの分離 (2)

※CNT: Carbon Nano Tube

CNTは炭素でできた円筒状の物質で、電極あるいは半導体材料などで「驚異の新素材」として注目を集めています。また、単層CNTには構造の違いにより金属としての性質を持つCNTと半導体としての性質を持つCNTが存在します。そして、その分離を超遠心機による密度勾配遠心法により行うことができます。

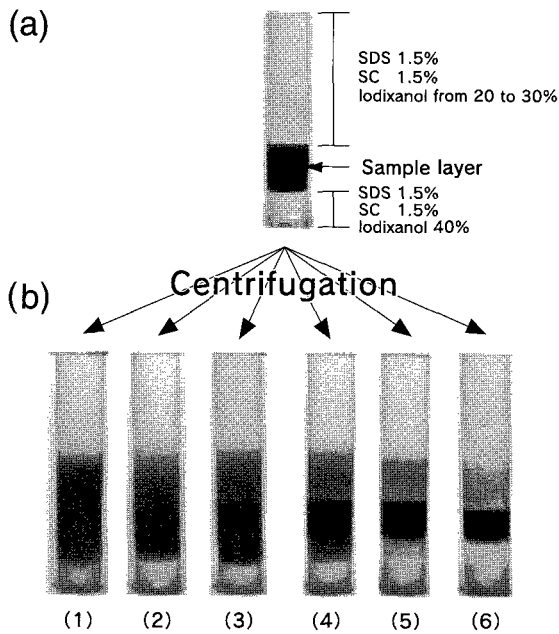


Fig.1. Pictures of centrifuge tubes (a) before and (b) after centrifugations in LV nanotubes. The concentration of iodixanol in a sample layer was 30%. The concentrations of surfactants in the centrifuge tube (except the sample layer) were set to be SDS 1.5%, SC 1.5%. Those concentrations in the sample layer were (1) SDS 1.5%, SC 1.5%, (2) DOC 0.25%, SDS 1.5%, SC 1.5%, (3) DOC 0.5%, SDS 1.5%, SC 1.5%, (4) DOC 0.5%, SDS 1.0%, SC 1.0%, (5) DOC 0.5%, SDS 0.5%, SC 0.5%, and (6) DOC 0.5%

ここでの実験例は試料に含まれる界面活性剤の組成により金属性CNTの分離状況が変化することを示しています。

(参考文献)

Yanagi, K.; Miyata, Y.; Kataura, H. Appl. Phys. Express **2008**, *1*, 034003-034005.

Yanagi, K.; Iitsuka, T.; Fujii, S.; Kataura, H. J. Phys. Chem. C **2008**, *112*, 18889-18894.

この分離を日立工機(株)製分離用超遠心機 CP-WXシリーズにて行うことができます。

また、遠心後の試料の分画にはDGF-U形フラクショネータを使用すると便利です。

皆様のご研究にお役立て下さい。

単層CNTの分離システム

(システム構成)

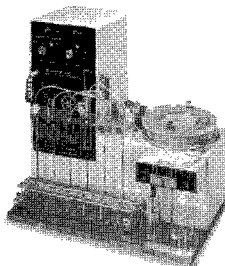
- ・日立工機(株)製
- (1) CP100WX形分離用超遠心機
- (2) P40ST形スイングロータ
- (3) DGF-U形フラクショネータ



(1) CP100WX



(2) P40ST



(3) DGF-U

遠心分離条件の例

- ・使用ロータ: P40ST(文献と同等のスイングロータ)
- ・回転速度: 40,000rpm(284,000 xg(max.))
- ・遠心管: 13PAチューブ
- ・時間: 約18時間
- ・密度勾配液: Iodixanol

【製造・販売・保守】

日立工機株式会社

勝田工場

〒312-8502 茨城県ひたちなか市武田1060

URL <http://www.hitachi-koki.co.jp/himac/>

首都圏地区 (甲種送付可)	東京都渋谷区千駄ヶ谷五丁目8-2 (イワオアネックスビル)	03-3226-7713
北海道地区	北海道札幌市厚別区厚別中央3条一丁目2-20	011-896-1748
東北地区	宮城県仙台市若林区卸町東三丁目3-36	022-288-0435
中部地区	愛知県名古屋市中区栄三丁目7-13 (コスモ栄ビル)	052-262-8221
関西地区 (甲種送付可送付)	兵庫県西宮市湊門大筋110-20	0798-23-4125
九州地区	福岡県福岡市東区松島四丁目8-5	092-622-4025

- このカタログに掲載した製品は、改善のため外観または仕様の一部を変更することがあります。
- 印刷の都合上、実際の色と異なる場合があります。
- 標準価格は仕様や構成により異なります。全て税別価格となります。

生命を構成するDNA。それは宇宙の誕生から現在まで途切れることなく、全ての生命に受け継がれてきました。しかし、もとをたどれば全宇宙に存在する虫も、動物も、そしてヒトも、全て同じものから創られているのです。

そこにはまだ、未知なる宇宙の神秘として医療・研究・開発者の前に立ちほだかり、

様々な難問を解かれることを待っています。

私たち「理科研」が、この問題へ向かう人々を真心でお手伝い出来るのは、設立当初から受け継がれてきた社訓、「誠意」が遺伝子として組み込まれているから。

理科研は、「バイオ研究」に欠かすことのできない機器・試薬の販売を通じ、

人類の幸せと豊かな社会の実現を願っています。

体内宇宙への挑戦。

理科研株式会社

- 本社 名古屋市守山区元郷二丁目107番地
〒463-8528 TEL 052-798-6151(代) FAX 052-798-6157
- 岡崎営業所 愛知県岡崎市明大寺町字西長峰50番
〒444-0864 TEL 0564-57-1751(代) FAX 0564-57-1757
- 福井営業所 福井県福井市開発3丁目3010
〒910-0842 TEL 0776-52-1651(代) FAX 0776-52-1653
- 岐阜営業所 岐阜県岐阜市岩地2丁目25番2号
〒500-8225 TEL 058-240-0721(代) FAX 058-240-1082
- 津営業所 三重県津市丸之内養正町20番地14号
〒514-0036 TEL 059-224-6661(代) FAX 059-224-6671
- 四日市営業所 三重県四日市市桜町2129番の1
〒512-1211 TEL 059-326-0231(代) FAX 059-326-3577
- 静岡営業所 静岡県駿河区広野3丁目29番8号
〒421-0121 TEL 054-256-3751(代) FAX 054-256-3755

- 東京支店 東京都文京区本郷七丁目2番1号
〒113-0033 TEL 03-3815-8951(代) FAX 03-3818-0889
- つくば営業所 茨城県つくば市高野台三丁目16-2
〒305-0074 TEL 029-856-2151(代) FAX 029-856-5071
- 柏営業所 千葉県柏市若柴197番地17
〒277-0871 TEL 04-7135-6651(代) FAX 04-7135-6751
- 神奈川営業所 横浜市緑区十日市場町901-31
〒226-0025 TEL 045-989-6551(代) FAX 045-989-6701
- 鶴見営業所 横浜市鶴見区朝日町一丁目49番地
〒230-0033 TEL 045-500-4551(代) FAX 045-500-4571
- 三島営業所 静岡県駿東郡長泉町下土狩217番地1
〒411-0943 TEL 055-980-1101(代) FAX 055-980-1105

<http://www.rikaken.co.jp>

溶液中の粒子のナノレベル微細化・分散に

BRANSON 超音波ホモジナイザー

ホーン先端部の振幅の安定性を、より高めた Advance タイプ になりました。

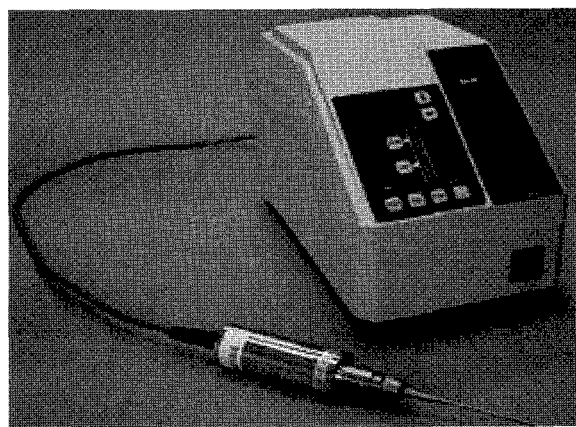
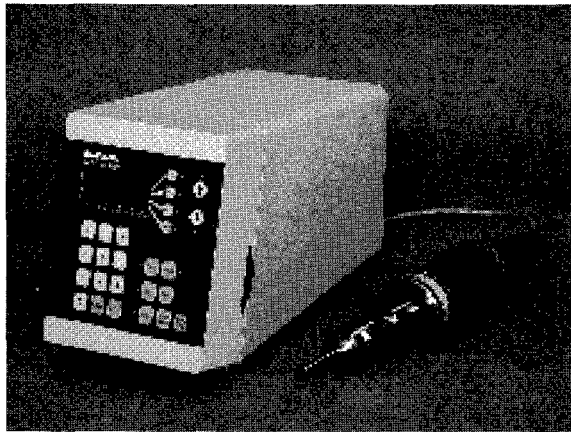
近年のナノテクノロジーの発展及び粉体関連技術の向上により、より微細な粒子に対する乳化分散処理の要望が増えてまいりました。

超音波ホモジナイザーを使用し、均質な乳化分散処理を行い、安定させることにより製品の機能は向上します。ブランソン社では 20kHz 機と、40kHz 機の 2 タイプを用意しております。

1 次粒子の凝集力にも拠りますが、20kHz 機では 100nm 程度までの分散力があります。40kHz 機は、さらに細かいレベルで分散ができる可能性があります。

20KHz 超音波ホモジナイザー
BRANSON SONIFIER シリーズ

高周波 40KHz 超音波ホモジナイザー
BRANSON SLpe シリーズ



ブランソン社の製品は、ホーン先端部の振幅の安定性が高く、強力なキャビテーションが得られ、効率良くまた、再現性の高い分散処理が行えます。

主なアプリケーション

分散

カーボンナノチューブ 有機顔料 無機顔料 セラミック セメント 感光体 記録材料
磁性粉 粉末冶金 酸化鉄 金属酸化物 シリカ アルミナ カーボンブラック
ポリマー ラテックス 製紙 ファンデーション
研磨剤 電池 フィラー 光触媒 触媒 ワクチン 体外診断薬 歯磨き粉 シャンプー
半導体 電子基盤 液晶 貴金属 金属 宝石 タイヤ 発酵菌類 その他

乳化

エマルジョン製剤 農薬 トナー ラテックス 界面活性剤 クリーム 乳液 クリーム 等

株式会社 **セントラル** 科学貿易

URL <http://www.cscjp.co.jp>

本社: 東京都台東区柳橋1-8-1

Tel (03) 5820-1507 Fax 5820-1515

大阪支店: 大阪市東淀川区西淡路 1-1-36 新大阪ビル

Tel (06) 6325-3171 Fax 6325-5180

福岡営業所: 福岡市博多区博多駅前 1-2-15 事務機ビル

Tel (092) 482-4000 Fax 482-3797

札幌出張所: 札幌市北区新琴似 11 条 13 丁目 9-3

Tel (011) 764-3611 Fax 764-3612

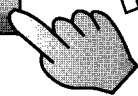
科学分析のご相談・ご依頼は UBE科学分析センターへ!

まずは、ホームページへ、どうぞ
<http://www.ube-ind.co.jp/usal>

検索サイトにて

UBE科学

カチッ+

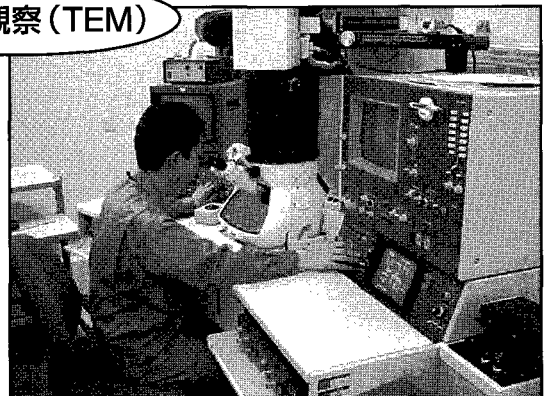


迅速に・精緻に・確実に

分析業務

- ☆組成分析と構造解析
- ☆形態観察と物性評価
- ☆表面・局所の超微小分析
- ☆超微量分析
- ☆安全性試験

形態観察 (TEM)

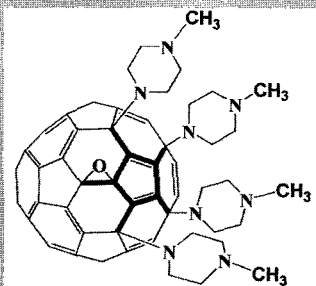


ご相談窓口	電話番号	FAX番号
東日本・関東地区	東京営業部 03-5419-6333	03-5419-6334
	千葉営業所 0436-23-5155	0436-23-5449
関西地区	大阪営業部 06-6346-2853	06-6346-1763
西日本地区	西部営業部 0836-31-6568	0836-31-6601

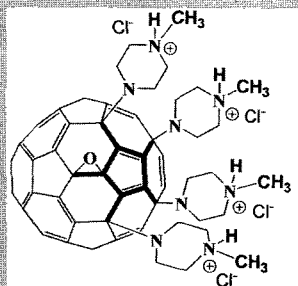
ユービーイー

株式会社 UBE科学分析センター

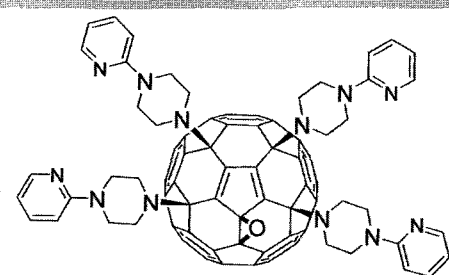
<http://www.ube-ind.co.jp/usal>



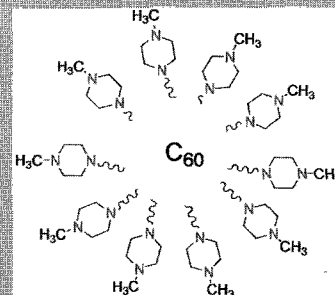
FBB-09



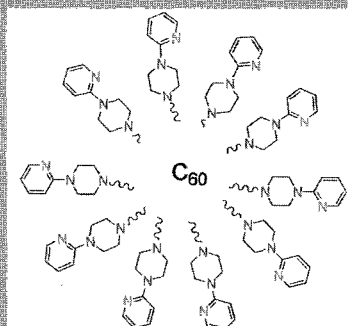
FBB-09-HCl



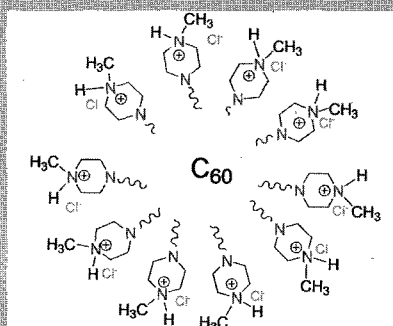
AMF-09-01



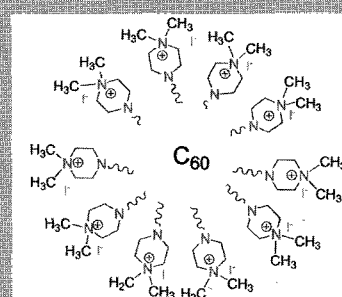
AMF-09-02



AMF-09-03



AMF-09-02-HCl



AMF-09-02-MeI

水溶性フラーレン誘導体は優れた生物学的特有を有し

新薬開発に期待されています

水溶性 C60 誘導体はヒト免疫不全ウイルスや C 型肝炎ウイルスの酵素を抑制し、C60 誘導体によっては癌の光治療にも抗増殖剤としても非常に有効であることは認められています。

“ラジカルスポンジ”効果により神経防護剤としても有効なものや、静菌性作用等があることも確認されています。

- 主な問題である、高水溶性 C60 誘導体を効率的に合成する方法について取り組み、水溶性 C60 誘導体を水溶性塩に変化させる効率的な方法が考案されました。
また新しい方法により、フラーレンケージにカチオン基の付いた新型高水溶性フラーレン誘導体の製造が促進されるものと確信しております。
- 従来はアニオン COO⁻基を有する水溶性フラーレンの研究が主流でしたが、上記の合成物に関する生物学的研究が進められた結果、この分野に関する大きな成果が得られました。
- 新型カチオン合成物はフラーレン誘導体の中でも最も水溶性が高く、200 mg/ml もの水溶性があります。

詳しいお問合せはこちら <http://atr-atr.co.jp>



株式会社 ATR

Advanced Technology Research

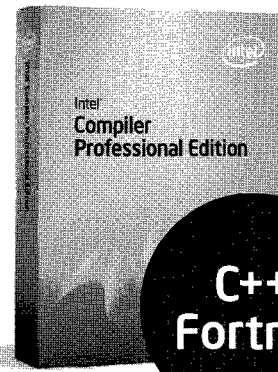
〒270-0021 千葉県松戸市小金原 7-10-25
TEL : 047-394-2112 FAX : 047-394-2100
Mail : sales@atr-atr.co.jp

シミュレーションを高速化

アプリケーションを高速化するコンパイラーです。

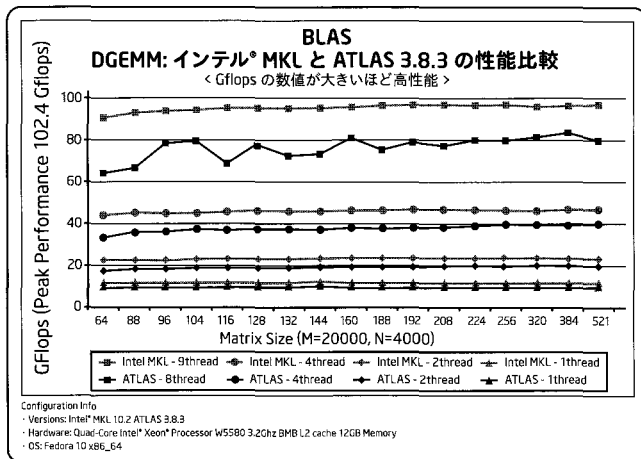
コンパイラーの自動最適化 / 並列化機能によりプロセッサの機能を最大限に生かし、高速に演算を行うことができます。

- ☑ インテル® Xeon® プロセッサ 5500 番台、インテル® Core™ i7 プロセッサに対応
- ☑ 次世代の 256 ビット命令セットに対応したインテル® AVX をサポート
- ☑ ISO 標準の Fortran 77/90/95 とより多くの Fortran 2003 規格に対応
- ☑ BLAS/LAPACK を並列化し、より高速になったインテル® MKL 最新版をバンドル



C++
Fortran

Windows*/Linux*/Mac OS*



他にも以下の性能向上が確認されています。

- ・インテル® Core™ i7 プロセッサにて DGEMM が最大 50% 向上
- ・インテル® Xeon® 7460 番台プロセッサにて DGETRF が 25% 向上

サイエンス・テクノロジー分野の研究、開発に最適！
 高速化で研究コストを削減！



お客様の声

「インテル® Fortran コンパイラーにより、アプリケーションが 24.5% から 31.5% ほど高速化されました。このパフォーマンスの改善は、劇的な変化をもたらしました。」

某大学天体物理学博士 殿

「非線形構造解析プログラムで計算時間の多くを占める行列の求解において、インテル® コンパイラーに含まれるインテル® MKL を用いることにより非常に高速化できました。今まで一昼夜かけて計算していたものが半日で行えることになり、非常に有効です。」

株式会社 計算力学研究センター 殿

インテル® コンパイラー 11.1 日本語版 好評発売中

ご購入に関するお問い合わせ先:

HPC システムズ株式会社
 www.hpc.co.jp
 TEL: 03-3599-3652

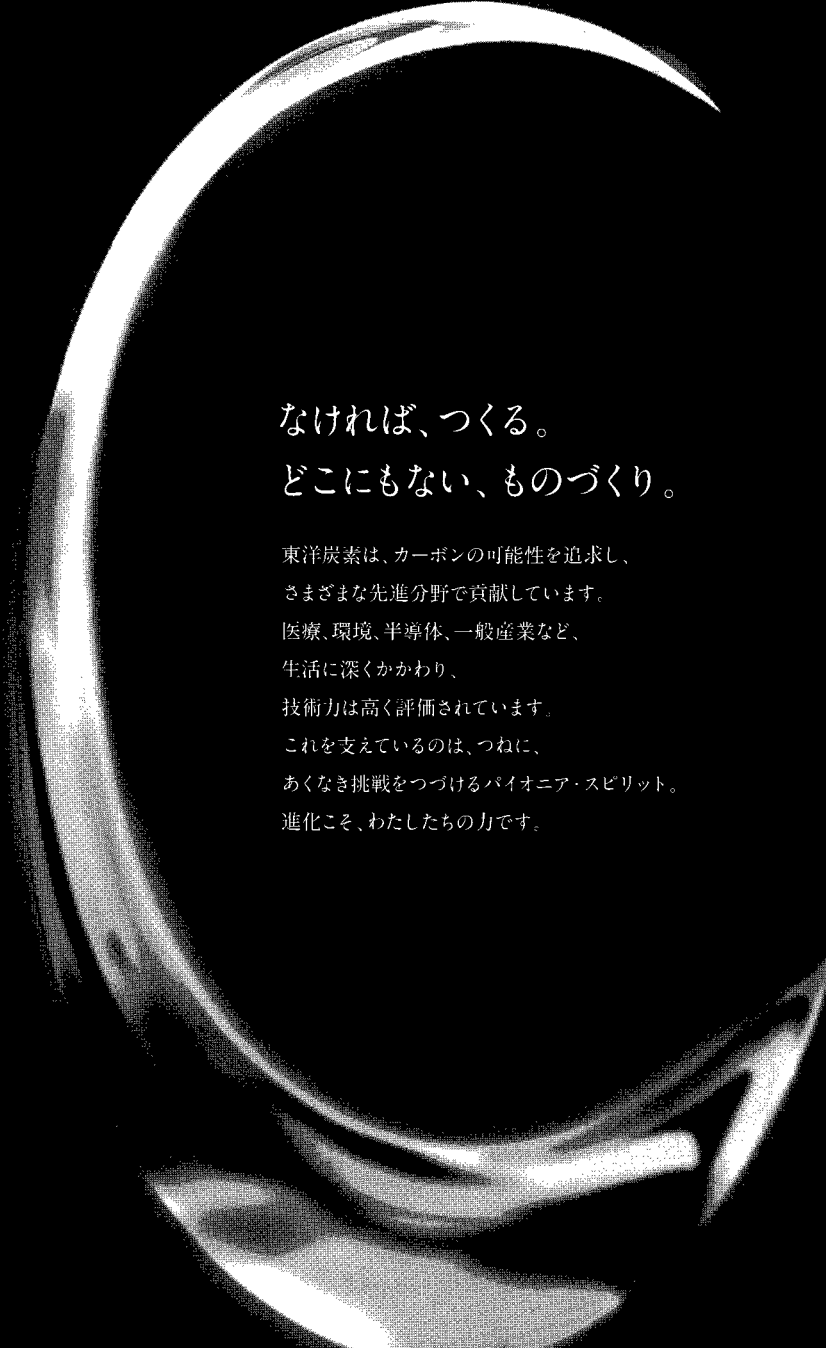
住商情報システム株式会社
 www.clubscs.com
 TEL: 03-5859-3011

HPC テクノロジーズ株式会社
 www.hpc-technologies.co.jp
 TEL: 03-6410-6070

株式会社 HPC ソリューションズ
 www.hpc-sol.co.jp
 TEL: 03-5640-7858

製品の詳細に関するお問い合わせ先: **XLSOFT** イケソフソフト株式会社 Tel: 03-5440-7875

www.xlsoft.com/intel



なければ、つくる。
どこにもない、ものづくり。

東洋炭素は、カーボンの可能性を追求し、
さまざまな先進分野で貢献しています。
医療、環境、半導体、一般産業など、
生活に深くかかわり、
技術力は高く評価されています。
これを支えているのは、つねに、
あくなき挑戦をつづけるパイオニア・スピリット。
進化こそ、わたしたちの力です。



TOYO TANSO
Inspiration for Innovation

東洋炭素株式会社

本社 〒530-0001 大阪市北区梅田3-3-10 梅田ダイビル10F Tel 06-6451-2114 Fax 06-6451-2186 www.toyotanso.co.jp

コンパクト&スマートな時代へ〈NEXTシリーズ〉

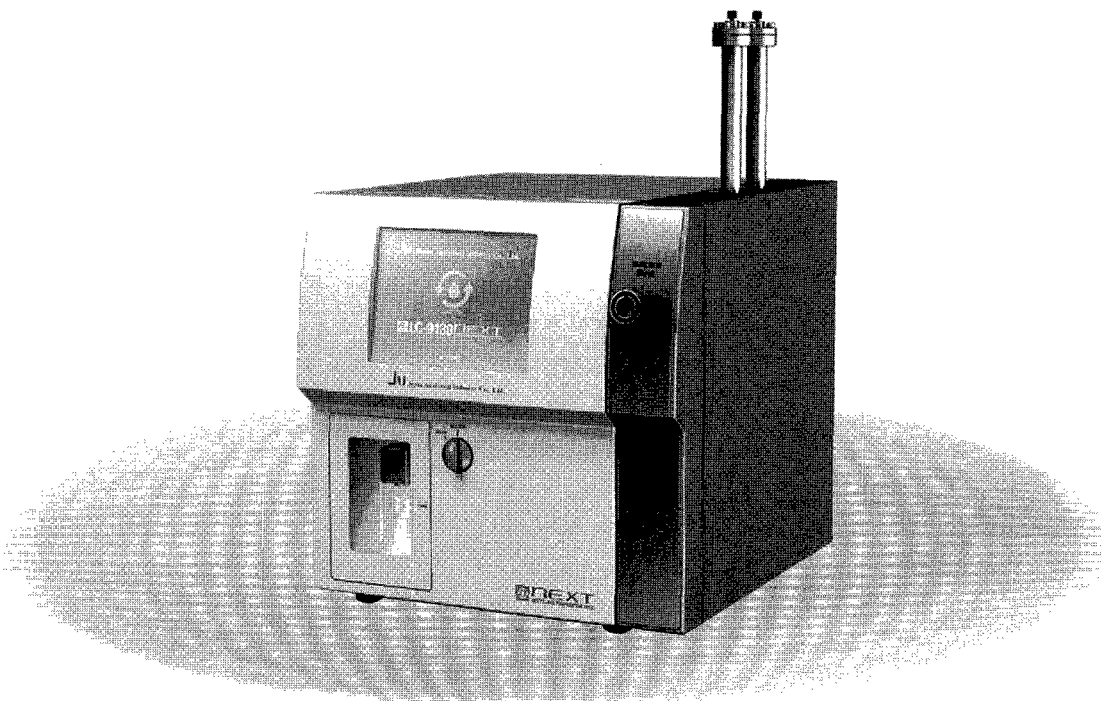
新発売!!

JAIのリサイクル分取HPLCは発売以来37年。
 おかげさまで2,500台を超える装置が国内外で活躍しています。

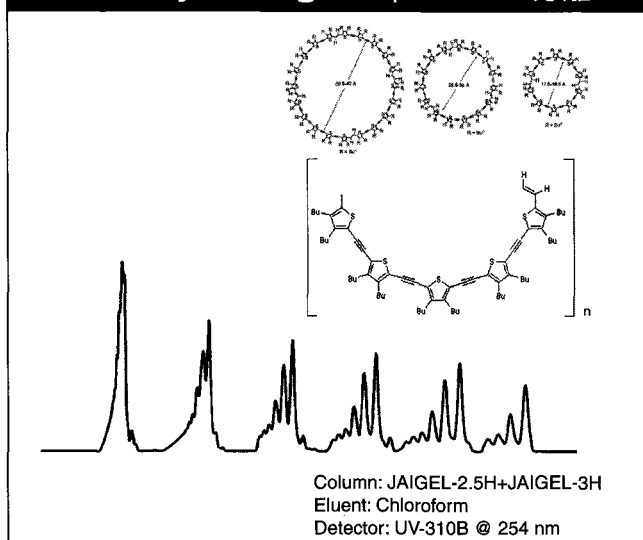
装いを新たにNEXTシリーズを発売!!

“高性能”・“使いやすさ”・“メンテナンス性能”を追求した究極の装置。

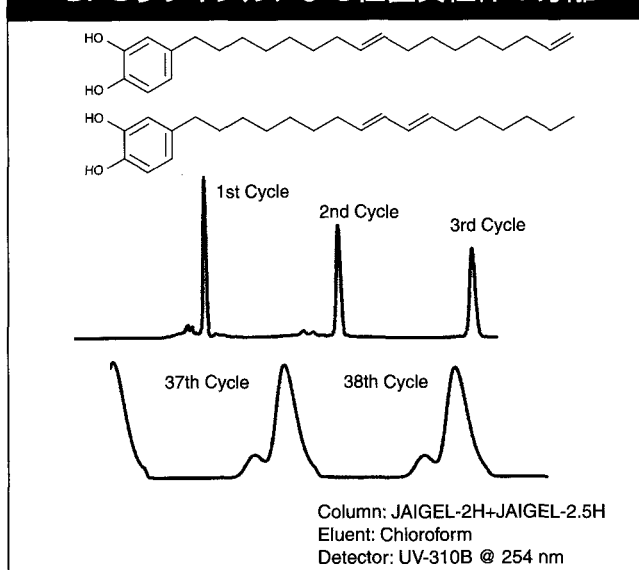
1/3ボディーサイズ(従来機比較)。NEXTを皆様のラボで是非ご採用ください。



GPCリサイクルによる Macrocylic Oligothiophenesの分離



GPCリサイクルによる位置異性体の分離



JAI 日本分析工業株式会社

- 本社・工場 〒190-1213 東京都西多摩郡瑞穂町武蔵208
- 大阪営業所 〒532-0002 大阪府大阪市淀川区東三国5-13-8-303
- 名古屋営業所 〒465-0025 愛知県名古屋市名東区上社3-609-3D

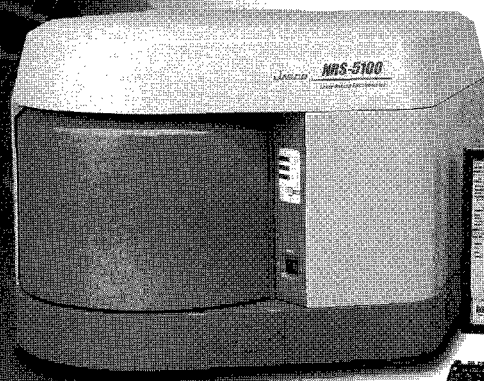
- TEL: 042-557-2331 FAX: 042-557-1892
- TEL: 06-6393-8511 FAX: 06-6393-8525
- TEL: 052-709-5400 FAX: 052-709-5403

URL : <http://www.jai.co.jp/> E-mail : sales@jai.co.jp

高分解から高速イメージングまで

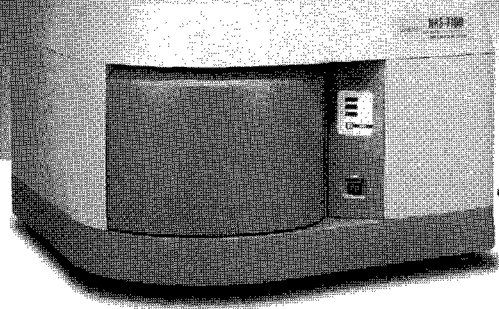
～次世代ハイパフォーマンス顕微ラマンシステム NRS series～

NRS-5000/7000シリーズは、顕微レーザーラマン分光光度計に要求される性能・機能を網羅し、さらにシステムの制御や光学調整等を自動化することにより、ラマンシステムの能力を維持し、安定して高度なデータを取得することができます。新開発のSPRIntSイメージングは、レーザー光をスキャンミラーにより試料上を走査して高速測定を行うVertiScan機能と高速データ取込機能及びZ自動ステージとの組み合わせによる3Dイメージングに対応しています。VertiScan機能は、共焦点性を損なうことなく測定することができ、高品質のスペクトルデータを取得することができます。



Laser Raman Spectrometer
レーザーラマン分光光度計

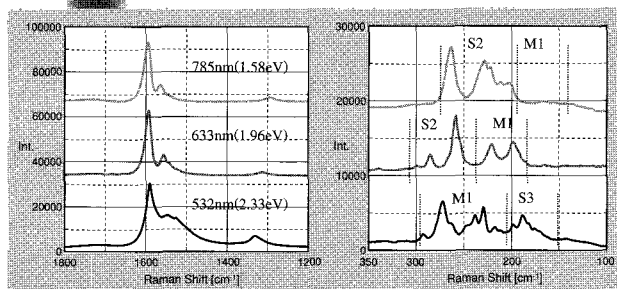
NRS-5000 series



Laser Raman Spectrometer
レーザーラマン分光光度計

NRS-7000 series

単層カーボンナノチューブ(SWNT)のラマンスペクトル(励起波長依存性)
(M1:resonance of metallic SWNT, S2,S3:resonance of semiconducting SWNT)



共鳴ラマン散乱効果で、特定の螺旋度およびチューブ径をもつSWNTを選択的に測定することができます。図のスペクトルでは、532nm励起で主に金属SWNT、633nmでは金属SWNTおよび半導体SWNT、785nm励起では主に半導体SWNTに共鳴していると考えられます。

NRS-5000/7000seriesの特長

- 異物分析から構造解析まで幅広く対応
- スペクトルクオリティにこだわったハイエンドモデル
- 新世代SPRIntSイメージングにより高速イメージング&3Dイメージング
- 1064nmレーザ+InGaAs検出器対応(デュアル検出器にも対応)
- 新機能DSF (Dual Spatial Filtration) で空間分解能がさらにアップ
- 段違いの操作性、顕微スペクトル測定プログラム
- 1クリックで蛍光除去、自動蛍光補正
- 誰でも楽々ラマン測定、ユーザアドバイス機能&フルオートシステム

JASCO は日本分光株式会社の登録商標です。

※記載されている製品の外觀は予告なく変更することがあります。

光と技術で未来を見つめる

日本分光

JASCO 日本分光株式会社

〒192-8537 東京都八王子市石川町2967-5
PHONE 042 (646) 4111 (代表)
FAX 042 (646) 4120
URL : <http://www.jasco.co.jp/>

北海道S-C 011(741)5285
北日本S-C 022(748)1040
筑波S-C 029(857)5721
東京S-C 03(3294)0341
西東京S-C 042(646)7001

神奈川S-C 045(989)1711
名古屋S-C 052(452)2671
大阪S-C 06(6312)9173
広島S-C 082(238)4011
九州S-C 092(588)1931

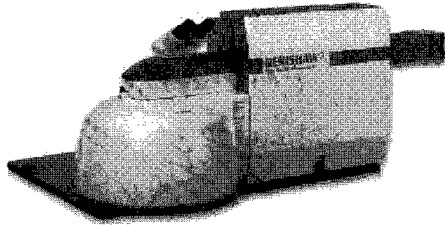




世界最先端のラマン分光装置

ユーザーの多様な研究・分析ニーズにフレキシブルに対応し、短時間で信頼性の高いラマン分析を提供します。

顕微レーザーラマン分光装置 inVia ラマンマイクロスコープ



inVia ラマンマイクロスコープ

明るい光学系で高性能なラマン分光システム

- ・弱いレーザーパワーで短時間で良質のラマンスペクトルが得られ、サンプルへのダメージも軽減できる

卓越したフレキシブルなラマンシステム

- ・極紫外から近赤外まで、複数の励起レーザーが搭載可能
- ・PL(フォトルミナッセンス)測定など、ユーザーの分析ニーズにフレキシブルに対応可能な拡張性

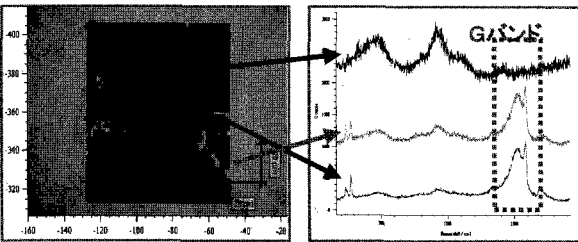
レーザー測長技術で培った高精度で再現性の高いシステム

- ・自社製XYZステージを開発し、より高速で再現性の高いマッピング測定が可能

StreamLinePlus:ハイスピードラマンイメージング機能

SWCNTの分析事例—観察不能なSWCNTの分析

シングルウォールCNTを水溶液で分散してスライドガラスに作成した試料で、光学顕微鏡ではCNTの存在が観察不能



Gバンドのラマンイメージ

ラマンスペクトル

- ・測定範囲: X:80 μm , Y:90 μm
- ・測定ステップ: 1.3 μm
- ・測定スペクトル数: 61 x 72=4,392
- ・測定時間: 362 秒

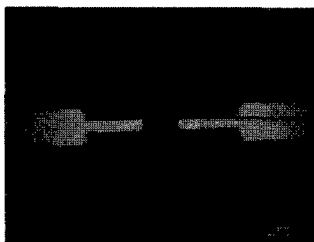
StreamLinePlus: 高速ラマンイメージング機能は、レニショー独自開発の画期的なマッピング測定法で、従来のポイントマッピングで1日以上要した測定が数分間で測定可能です。

- ・従来のポイントマッピング法と比較して100倍以上のスピードでハイスピードラマンイメージングが可能
- ・1 μm のマイクロ測定から数mmの広範囲なマクロ測定まで対応
- ・ポイントマッピングと同等なスペクトルデータ品質
- ・励起レーザーをライン状にしてサンプルにフォーカスするため、サンプルへのダメージを回避できる
- ・測定を行いながら同時に測定した点の解析と表示が可能

左図のように、StreamLineにより、観察不能なCNTの分布をラマンイメージにより短時間で可視化できます

超高分解能ハイスピードマッピング機能(2010年春リリース予定)

SWCNTの分析事例—電極間に架橋したSWCNTの分析



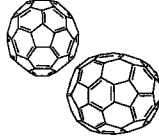
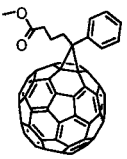
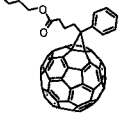
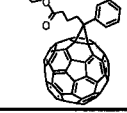
緑—Gバンドの強度分布

赤—RBM(265.2 cm^{-1})の強度分布

光(励起レーザー)の回折限界を超えた100ナノメートルオーダーの超高分解能ハイスピードマッピング機能を開発し、2010年春リリース予定です。



電極間に架橋したSWCNTを、100nmナノメートルオーダーの超高分解能で可視化されていることが確認できます

銘柄		分子構造	純度(HPLC面積%、代表値)	取扱数量
nanom purple フラーレンC60	ST		99	10g以上
	TL		99.5	5g以上
	SU		99.5/昇華精製品	2g以上
	SUH		99.9/昇華精製品	1g以上
nanom orange フラーレンC70	ST		97	1g以上
	SU		98/昇華精製品	0.5g以上
nanom mix 混合フラーレン	ST		C60、C70、その他高次フラーレンの混合物 ※微粒化品 (ST-F) もあります	50g以上
銘柄		分子構造	純度(HPLC面積%、代表値)	取扱数量
nanom spectra PCBM (phenyl C61-butyl acid methyl ester)	E100		99	1g以上
	E100H		99.5	1g以上
nanom spectra E200 PCBNB (phenyl C61-butyl acid n-butyl ester)			99	1g以上
nanom spectra E210 PCBIB (phenyl C61-butyl acid i-butyl ester)			99	1g以上
nanom spectra E110 C70PCBM (phenyl C71-butyl acid methyl ester)		 主成分	99 (異性体トータル) 位置異性体の混合物	0.5g以上
銘柄		分子構造	内容	取扱数量
nanom spectra D100 水酸化フラーレン		 (n = ca. 10)	C ₆₀ OH _n n=10を主成分とする混合物	2g以上
nanom spectra A100 水素化フラーレン		 (n = ca. 30)	C ₆₀ H _n n=30を主成分とする混合物	2g以上
nanom spectra G100			純度 (HPLC面積%, 代表値) 99	1g以上

銘柄、取扱数量等は予告無く変更する場合がございます。予めご了承下さい。

2009年12月1日現在

当社製品は、下記2社から購入いただけます。詳細は直接お問い合わせください。

・関東化学株式会社 試薬事業本部

〒103-0023 東京都中央区日本橋本町3-11-5 TEL:03-3663-7631 FAX:03-3667-8277

http://www.kanto.co.jp E-mail:reag-info@gms.kanto.co.jp

・第一実業株式会社 新事業推進室【担当: 鎧広(カギヒロ)】

〒102-0084 東京都千代田区二番町11-19 TEL:03-5214-8579 FAX:03-5214-8501

<本資料に関するお問い合わせ先>

フロンティアカーボン株式会社 営業販売センター【担当: 梶原】

〒806-0004 福岡県北九州市八幡西区黒崎城石1-1

TEL:093-643-4400 FAX:093-643-4401 <http://www.f-carbon.com>

※弊社へのお問い合わせはHPよりお願いいたします。